Online Partial Discharge Detection and Signal Analysis for High Voltage Cables

A DISSERTATION SUBMITTED TO THE

DEPARTMENT OF ELECTRONIC AND ELECTRICAL ENGINEERING

AND THE COMMITTEE FOR POSTGRADUATE STUDIES

OF THE UNIVERSITY OF STRATHCLYDE

IN PARTIAL FULFILLMENT OF THE REQUIREMENTS

FOR THE DEGREE OF

DOCTOR OF PHILOSOPHY

By

David Foo Ming Hui

2005

Text cut off in original

To my beloved Mum and brother, James Foo

Declaration

I declare that this Thesis embodies my own research work and that it is composed by myself. Where appropriate, I have made acknowledgement to the work of others.

David Foo Ming Hui

Acknowledgements

This project has been made successful with the aid and contributions by a number of individuals who have provided support through their resources, technical discussions, advices and moral support. In appreciation and gratitude, it gives me great honour to extend my sincere thanks to these people.

First of all, I would like to thank my two project supervisors, Prof. John Soraghan and Dr. W.H. Siew, for their endless support throughout the entire period of this project. Indeed, their guidance, input and motivation has steered this project towards the successful outcomes. To them, I would like express my sincere gratitude for their friendship and effort spent.

This project was very dependent on the provision of utility assets from ScottishPower Plc. To this, I would like thank Fraser McPherson for his kindness and his efforts through these years. Indeed without Fraser, many of the substation field visits would be impossible. I believed that in many occasions, his help was out of his own freewill. Hence, I am very grateful for his time and effort spent in this project.

I would also like to thank Diagnostic Monitoring Systems Ltd. in particular John Pearson, Owen Farish, Andy Sellars, and Tom Pahnke for the financial and technical support that enabled the completion of the new data acquisition hardware system.

My special thanks to Martin Stewart, who kindly aided me with his expertise in the field of hardware systems and electronics. His help in the technical discussions assisted me for the hardware preparations and the problems that I have encountered.

To Santiago Esteban, I would like to express my sincerest gratitude for teaching and guiding me in the software programming of my project. His patience

and sincerity has gone a long distance. I also thank him for being a supportive and understanding flatmate.

To the others in the SPD lab, Gavin Paterson, Stefan Martin, Christophe Lafon, Emmanuel Darakis, Kenny Hough, I thank them for being a great team that offered help and support whenever I needed it. A special thanks to Sheila Forbes for her help during my time in the University of Strathclyde.

To my spiritual brothers and sisters, Lee Ann Hodges, Pui Ee, Su Yin, Chin Thye, Patrick Shi, Joseph Chew, Chris Lim, Eileen, Willy, Lynn and others, I thank them for their prayers, support and friendship, which encouraged me to spur on and complete this Ph.D. I would like to thank also Pastor Winston and Sister Eunice for their guidance, prayers, and support during my stay here in Glasgow.

To all my family, especially my Mum and Dad, I would like to thank them for their endless support and love for me throughout all these years. Indeed I can say that without them I would not be who I am today. To my brother James, my one and only beloved brother, I thank him for being a kind and loving to me.

Finally, I would like to express my sincerest appreciation and thanks to God, who have shown blessed me with numerous miracles and blessings throughout this project, especially those times when I really needed a sunny day for the field trips.

Abstract

Partial Discharges are symptoms of insulation degradation that continually promotes the deterioration of the insulation condition, eventually leading to permanent failures. The PD event itself is not dangerous but it is the state of the discharge activity that can lead to unforeseen failures. Hence continuous monitoring of PD enables the prevention of these unforeseen failures that result in economic losses. High voltage equipment that has been installed more than forty years ago is highly susceptible to PD since it is reaching the insulation end life. For the case of underground cables, continuous PD monitoring will help avoid unplanned outages and the need for the immediate replacement of faulty cable sections that will incur large costs. Traditionally, PD diagnostics have been carried out through offline methods, whereby the cable specimen is removed from service during the diagnostic tests. On the other hand, online PD diagnostics are preferable since the services are not disrupted. However, there are some major challenges that come with the online approach. For instance, heavy noise interference, the detection and location of PD through the interpretation of measured signals.

Presented in this Thesis are presented novel contributions to the area of online PD detection for underground HV cables. The work encompasses aspects of physical data acquisition procedures and the post-processing signal processing algorithms.

A new online PD data acquisition unit equipped with pre-processing and signal conditioning is presented. The system has other features that take into account the difficulties of logistics as well as issues related to the regulations and protocols of the utility. The primary aim of this developed system is to produce a PD database that will be used for research purposes.

Since applied wavelets for the field of PD diagnostics have been popular amongst researchers, it was investigated further in this Thesis. Following from the data acquisition system, large data sizes required intensive processing. A new wavelet-based algorithm combined with the use of Higher Order Statistics is presented. This algorithm enables the simplification of data signals to highlight potential PD activity resulting in the reduction of manual examination of wavelet algorithms.

The conventional wavelet algorithms applied in the literature generally referred to a specific approach of the wavelet implementation i.e. the decimated approach. However, it was found that the non-decimated approach has several advantages with regards to PD signature detection and PD location. The application of both approaches and their comparisons is applied to simulated data as well as online field data.

Finally, the analysis of online PD data acquired from the new data acquisition system is presented. Several PD characterisation processes are applied and positive results were generated. Aspects relating to the physical environments of test site are also included. The challenges and experiences gathered in this research project are described.

Acronyms

2D	Two Dimensional
3D	Three Dimensional
BPF	Band-pass Filter
CBM	Condition Based Monitoring
CWT	Continuous Wavelet Transform
CT	Current Transformer
db	Daubechies
dB	Decibel
DWT	Discrete Wavelet Transform
EPR	Ethylene-Propylene Rubber
FIR	Finite Impulse Response
FT	Fourier Transform
FTP	File Transfer Protocol
GIS	Gas-Insulated Substation
GPS	Global Positioning System
HPF	High-pass Filter
HV	High Voltage
IDWT	Inverse Discrete Wavelet Transform
LPF	Low-pass Filter
LV	Low Voltage
MV	Medium Voltage

OWTS	Oscillating Wave Technique
PD	Partial Discharge
RF	Radio Frequency
RMU	Ring Main Unit
SNR	Signal to Noise Ratio
STFT	Short Time Fourier Transform
SURE	Stein's Unbiased Risk Estimator
SWT	Stationary Wavelet Transform
TDR	Time Domain Reflectometry
UHF	Ultra High Frequency
VHF	Very High Frequency
VLF	Very Low Frequency
WT	Wavelet Transforms
XLPE	Cross-linked Polyethylene

Contents

List of Figures

List of Tables

Chapter 1 : Introduction

1.1 Partial Discharge Diagnostics for Underground Cables

Recent growth in population and urbanisation has increased the demands of electricity supplies worldwide. Many important management and reliability issues have been prioritised in order to cope with the daily electricity requirements. Technology advancement from light industries to heavy industries in this competitive world has sparked a necessity of maintaining the supply of electricity without disruptions, as this would affect the vast businesses. Even domestic users are applying pressure on the utility companies to ensure continuous power supply to their homes. Hence, the pressure is increasing on the electricity distribution companies to ensure the reliability of their services. This means that unnecessary and unforeseen disruptions have to be minimised wherever possible. The main method of achieving this is to minimise electrical breakdowns from the high voltage equipment.

The majority of electrical breakdowns in the 21st century are likely to originate from insulation deteriorations. Much of the high voltage equipment that has been installed around the 1950's and 1960's is reaching the end of its operating life [Kreuger 1989]. Gas filled voids are common among such equipment, formed through continuous cyclic loading effects and also during the manufacturing processes. This is especially true for paper insulated oil impregnated cables. Insulation materials such as polyethylene and epoxy have been used widely because

of their good dielectric properties. When parts of the insulation are substituted with voids, the dielectric properties start to differ. These gas filled voids have lower electrical permittivity compared to the dielectrics. Hence, the electric field stress within the void is higher than in the dielectric. In general, a void has lower breakdown strength than the surrounding dielectric. A gas void will break down before the strength of the surrounding dielectric is reached. This phenomenon is known as Partial Discharge (PD).

The occurrence of PD is not classified as critically dangerous because it depends on the level of discharge activity within the insulation. However, the degradation of the insulation is further promoted through partial discharges and eventually leads to permanent breakdowns. For this reason, preventive measures are preferred, for example through continuous condition monitoring of high voltage equipment and substations.

In order to do this, the discharges must first be detected and located in order to accurately classify the level of discharge activity. There are several factors that will affect the level of discharge activity. The main factor is the physical properties of the defect, for instance: type of discharge - for example internal or surface discharge, corona or electrical trees. Other complex factors such as the size and orientation of the void and electric field stress will also affect the discharge activity [McAllister 1997, Bartnikas 2002].

PD diagnostics are performed either through offline or online methods. The offline diagnostics are more established and there have been several successful techniques used. However, offline techniques are performed whilst the cable circuit is removed from service and have to be energised separately through an external power source. Among these techniques are the 0.1 Hz Very Low Frequency (VLF) techniques [EaTech 2001, KEMA 2004] and the Oscillating Wave Test System (OWTS) technique [Gulski 2000]. The main advantage of this method is that the test cable will be isolated and the location of the discharge is performed relatively easily since there are fewer problems associated with signal interpretation and noise interference. Obviously, a disruption in service is required for the offline method, which could vary from several hours to several days. This is generally more

expensive and undesirable for economic reasons. Furthermore, the diagnostics will not exhibit actual characteristics of the PD activity during normal operating conditions.

For online diagnostics, the measurements are performed whilst the HV equipment is under normal operating conditions. This method is preferred mainly for economic reasons and to minimise power disruptions. Previously, the application of online diagnostics has not been widespread because of major challenges in data interpretation and dealing with high noise interference, which causes limitations in measurement sensitivity to levels above those required for accurate evaluation. Online diagnostics usually is performed by signal acquisition from sensors attached to the cables; this involves signal interpretation and some form of de-noising.

Recently, the research drive is to online PD diagnostics. Advancement in semiconductor and microprocessor technology has opened new avenues to deal with issues associated with online PD diagnostics. High-speed data acquisition devices, sensors, and microprocessors in the GigaHertz frequencies provide stronger processing power and noise mitigation capabilities. In addition, advanced signal processing techniques are more readily implemented through these technologies.

Commercial units available in the market mostly utilise computer-based systems that enable data acquisition and on-board data processing. Examples include the LDS-6 [LDIC], NetworkTrend [Webb 2002], and Partial Discharge Locator (PDL) [Baur 2005]. These units have high frequency sensors incorporated in the diagnostics toolkits. The PDL claims to have the ability to measure the apparent charge of the PD and to determine its location for MV cable joints. Other older online techniques would have required the cable surface to be accessible in order that sensors could be spread along the cable.

In reality access to underground cable networks is the major problem that hampers online PD diagnostics. Accessible points on the cables are limited and usually located at the terminations. Furthermore, live connections imply that the cable networks are interconnected so that signal interpretation becomes inherently complicated especially in the presence of noise interference.

In this thesis, we plan to address the issues associated with online PD diagnostics for underground HV cables particularly with signal acquisition and data interpretation.

1.2 Motivation for our Research

The motivation for our research in the area of online Partial Discharge detection and location for underground high voltage cables stems from several perspectives:

(i) Online PD diagnostics techniques are economical and efficient for underground cables. Data acquisition systems that operate under these conditions are limited and costly. The main driving force behind this research is the development of online PD diagnostic systems for high voltage underground cables.

(ii) Noise interference is a common problem for online PD diagnostics that impairs the detection and location of PD within the equipment. Most systems are operated offline for this reason. Field data from online high voltage equipment for research purposes are not available in the industry. Hence, priority is emphatically placed on the generation of field data.

(iii) In many situations, only single-ended diagnostic techniques can be performed under online conditions for underground HV cables. This is due to the physical accessibility to the equipment. We plan to investigate the feasibility of single-ended diagnostic systems for cables and to characterise the PD from such data.

(iv) Wavelet transforms have many forms of variations and have been applied in PD diagnostics but the investigation into online field data is limited. The development of wavelet-based algorithms and performance evaluation of current algorithm is investigated further in this research work.

In this thesis the problems associated with online PD detection and location through single-ended systems will be addressed. A new data acquisition system will be developed and novel digital signal processing algorithms for PD detection will be presented. Online field data from high voltage cable network will also presented and investigated.

1.3 Summary of Original Contributions

The research documented in this thesis includes original contributions to the field of Partial Discharge assessment for HV underground cables. These contributions are as follows:

(i) A new remote controlled PD data acquisition system (RPDAQ) is presented. This system enables the data acquisition from online cable systems. It includes features that enable signal conditioning during acquisition or post-processing and large storage capacity, addresses issues associated with logistics. A PD database is generated from this system.

(ii) A new kurtosis based wavelet transform algorithm for PD detection is presented. The algorithm identifies regions within the input signal that may contain PD activity. The algorithm utilises a novel 'Smart Sum' technique, which produces simplified signals for user interpretation.

The algorithm is applied to simulated data and field data obtained from the RPDAQ.

(iii) A method of PD location in cables for single-ended and double-ended systems that utilises the non-decimated Discrete Wavelet Transform is presented. The advantages and application of non-decimated Discrete Wavelet Transforms over conventional decimated Discrete Wavelet Transforms is analysed and demonstrated on simulated and field data from the RPDAQ.

1.4 Organisation of Thesis

The organisation of the thesis is as follows:

Chapter 2

In Chapter 2 the fundamentals of Partial Discharges in underground HV cables are presented. The different types of PD are described followed by their physical mechanisms and properties. The general theory of physical cable configuration and the characteristics of pulse propagation within the cable are also presented. These include the transmission line characteristics and the cable losses and the effects on PD signal due to such phenomena as attenuation and dispersion. Methods of PD detection are then covered where electrical and non-electrical methods are reviewed. Aspects of PD location in cables are dealt with, for instance the single-ended and double-ended methods where the procedure and interpretation of these methods are elaborated. Finally, a review of condition-based maintenance approaches is presented. This encapsulates the techniques that have been applied within this research field under offline and online conditions.

Chapter 3

Chapter 3 covers the relevant signal processing, wherein the various types of PD signal are discussed taking into account the aspects of pulse propagation and losses in the cable, and the uncertainties and errors that arises from these. Several knowledge rules of PD quantities are presented, and these include the basic quantities and the derived quantities that are generated through post-processing of PD data. These quantities are then used to aid the interpretation of PD and determine the severity of PD activity within the HV equipment. A review of signal processing techniques applied on PD diagnostics is then presented. Techniques employed by researchers such as digital filtering, fuzzy reasoning, neural networks and more are elaborated. Recently, wavelet transforms has emerged to be useful tool for PD processing. Hence, a section is dedicated to the understanding of wavelets and its applications. The different types of implementation, its application and how it has been applied to the field of PD analysis are presented.

Chapter 4

Chapter 4 describes the new remote controlled PD acquisition system (RPDAQ) that was developed in this research project. The difficulties and problems associated with online PD data acquisition are discussed. The requirements for online PD monitoring systems for optimal performances are also described. Then the new remote controlled PD acquisition unit is described. All the features and components of the system are elaborated stage by stage. Hardware description and software programmes are presented and a major operation procedure is included. Then the performance of this new system is evaluated through comparison with another prototype measurement system. The data acquired from field test are preliminarily examined with the current load profile and the various types of data acquired from the available data acquisition settings are presented. Finally, the limitations of the RPDAQ are discussed.

Chapter 5

In Chapter 5, issues related to the wavelet-based PD analysis are presented. The important aspects required for effective wavelet analysis and implementation is presented. For instance, the type of wavelet, the depth of the analysis and the natural tendency of the wavelet decomposed signals. The two approaches where wavelets are commonly used for PD detection - i.e. the multi-scale edge detection approach and the de-noising approach - are described. The advantages and disadvantages of each approach are elaborated. Then from among the several types of Wavelet Transform (WT) available, it is revealed that using non-decimated Discrete Wavelet Transform (DWT) yielded better performance compared to the decimated DWT. Robust PD signatures are generated through the non-decimated DWT and the effects are demonstrated when applied to PD location. These results are due to the shift-invariance property. The comparison of both wavelet implementation methods is performed and results from the analysis are presented. A new algorithm that combines this non-decimated DWT and higher-order-statistics is then presented. This algorithm can be applied to PD data to summarize segments of the signal (relative to phase) that may contain PD activity. It aids a user to pre-identify the useful part of the signal that will be analysed in detail. This algorithm is applied on simulated data and field data, and the results are presented.

Chapter 6

In this chapter, the signal processing and PD analysis techniques are applied to the field data acquired from the new RPDAQ acquisition system. The background of physical network configuration of the substation where the data acquisition was performed is described. This includes the cable joint details and the sensor devices used during the data acquisition process. The systematic approaches of locating PD's in a cable for a single-ended system and a double-ended system are presented. These approaches utilise the information of the cable joint locations because they are common locations of PD, according to the literature. Then the comparison of

unprocessed data and processed data for the set of measurements conducted for the pair of cables at the substation is presented. A noise analysis of the signals is performed and the result of the analysis is discussed. It was found that a signal structure within the set of signals contained information similar to PD. Hence, an attempt was made to characterise this signal structure. The result of the analysis is presented and the outcome from this analysis is discussed.

Chapter 7

Finally, Chapter 7 concludes with the summary of the contributions presented in this thesis and the conclusions drawn. Also presented is a discussion of the potential future research directions that may be employed in the area of detection and location of Partial Discharges in underground transmission cables.

Chapter 2 : Fundamentals of Partial Discharge in Underground Cables

2.1 Introduction

Much high voltage equipment is reaching the current end of its operational life at this present time. Equipment such as cables, transformers, motors, bushings, etc. are starting to cause problems since it was installed around the 50's and 60's. Insulation deterioration problems have prompted important developments in condition monitoring and early detection of potential breakdowns, in order to prevent unforeseen breakdowns. In many countries, industry and academics are collaborating to develop systematic and effective non-destructive diagnostic techniques and condition monitoring procedures to maintain the integrity of such high voltage equipment.

A common cause of insulation degradation is that due to Partial Discharges (PD). A partial discharge is considered as an effect arising from defective insulation. The danger of PD activity is that it promotes the further degradation of the insulation condition and eventually leads to permanent electrical breakdown. Hence, it has been a primary importance to monitor the level of PD activity. The theory of PD's involves the analysis of materials, electric fields, arcing characteristics, pulse wave propagation and attenuation, sensor spatial sensitivity, frequency response and calibration, noise and data interpretation [Paoletti 2001]. The expression "prevention is better than cure" has been adopted by the utilities and governments to avoid

catastrophic failures. The subject has been actively researched since the early 80's and significant advances have been made. However, researchers are still trying to develop methods of predicting the lifetime of insulation from measurements of the activity of partial discharges.

In this chapter, the fundamentals of partial discharge are presented. In section 2.2, the definitions and nomenclature of PD are described. The mechanisms and properties of PD are also presented here. Section 2.3 describes the models of cables and the different types of cables available including the dielectric properties of the cables. Methods of PD detection are presented in section 2.4. This includes the evolution of PD detection from the conventional methods to the more modern techniques. Basic and derived quantities for PD are presented in section 2.5. In section 2.6, the advantages and disadvantages or offline and online detection are presented and the conclusions drawn are presented in section 2.7.

2.2 Partial Discharge Definition

Partial Discharge (PD) is defined as a localised electrical discharge in the insulating medium, restricted to a part of the dielectric under test and only partially bridging the insulation between conductors [IEC 60270]. The discharge is caused by concentration of electrical stress localised in the insulation or its surface. PD's give rise to high frequency voltage and current pulses, which propagate along a cable returning through a ground path. Associated with these are electric and magnetic fields, which propagate in the surrounding insulation and dielectric material. Typical discharges have rise times in the order of ns and pulse duration of less than 1 μs [Boggs 1990a]. The order of magnitude of the discharges is small, usually measured in pC.

Partial discharge is commonly caused through field enhancement in the gaseous, solid or liquid insulation, or through voids or inclusions in the solid or impregnated insulation, or through sharp protrusions. Progressive deterioration caused by discharges in gas-filled voids [Mayoux 1995], has been known to be one

of the major factors limiting the life of cable, transformer and capacitor dielectrics. More emphasis has been given to power cables with regards to voids. Evidently, many new types of cables have been developed with better dielectric properties to cope with the issues of insulation deterioration and increasing the durability. Gaseous voids are usually formed during the manufacturing process or formed after a significant operation period [Bartnikas 2000]. Modern polymeric cables such as PE, XLPE, and EPR are screened thoroughly during the manufacturing process to eliminate the formation of voids [Peschke 1999]. For the oil impregnated paper insulated cables, the current and thermal loading of the cables often causes oil migration to occur which leads to formation of voids [Bungay 1982].

The various categories of PD are simplified into four types of physical discharges in [Kreuger 1989], i.e. surface discharges, internal discharges, electrical trees, and corona. PD is distinctively classified into internal discharges within a closed system or external discharges that occur outside the equipment [Weber 1986].

2.2.1 Internal Discharges

Voids or cavities, inclusions and electrical trees are the major sources of internal discharges. Inclusions can arise from dirt, paper or textile fibres and other foreign particles impregnated into the insulating material during manufacturing process. The low dielectric strength of such inclusions will cause internal discharges to occur. In gas-filled voids or cavities, the discharge properties and characteristics are governed by their orientation and size [McAllister 1997, Kreuger 1989]. Figure 2.1 illustrates several examples of internal voids and their orientation. A flat void situated perpendicular to the electric field has a stress value of

$$E_c = \varepsilon_d E_d \qquad (2.1)$$

where E_c is the stress in the void, ε_d is the dielectric constant of the insulating material and E_d is the stress in the dielectric. For a void that is long and parallel to the direction of the electric field, the stress is

$$E_c = E_d \qquad (2.2)$$

For spherical voids, the stress in the voids is [Kreuger 1989]:

$$E_c = \frac{3\varepsilon_d}{1+2\varepsilon_d} E_d \qquad (2.3)$$

which tends to $1.5E_d$, for large ε_d, where ε_d is the dielectric constant of the insulating material

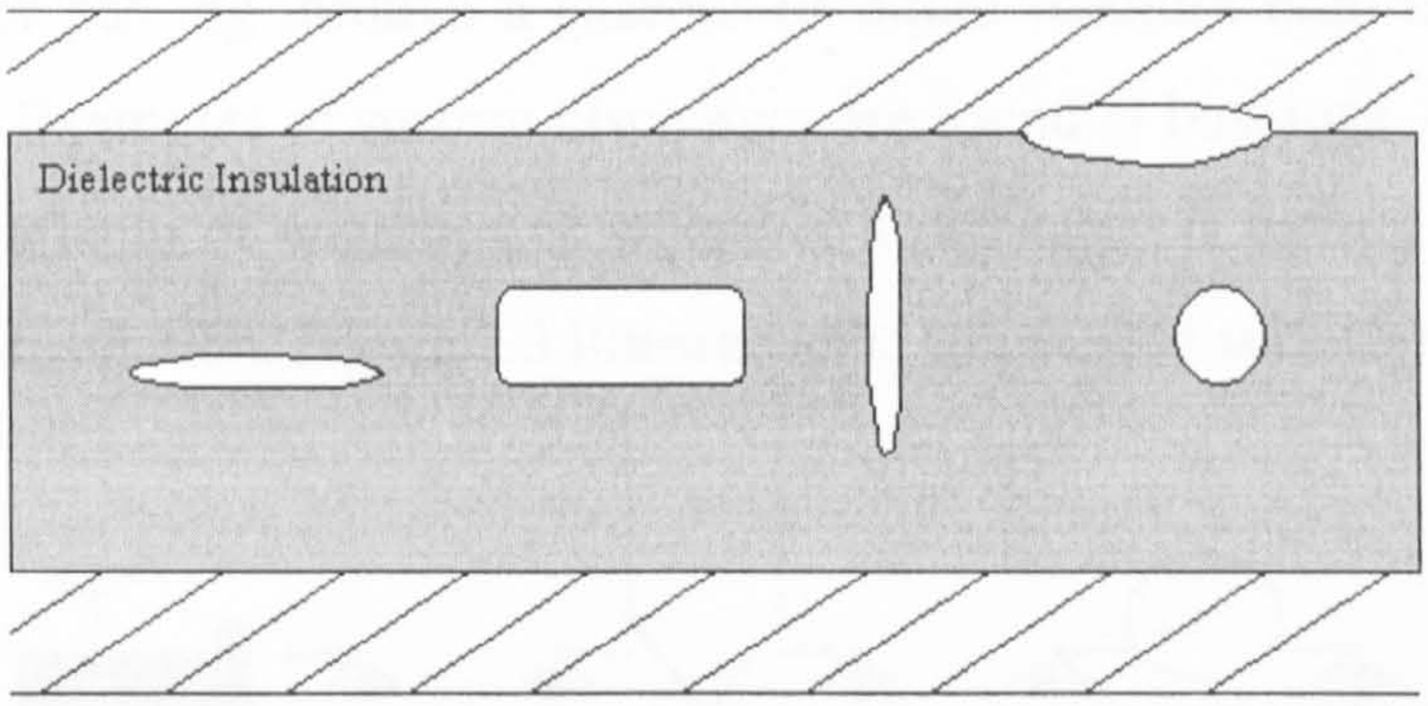

Figure 2.1: Internal discharges :-flat void, spherical void, long and parallel voids.

Another source of internal discharges originates from electrical trees as depicted in Figure 2.2. It starts from a defect in the insulation and the growth is rapid as the tree sets in. After some time, the branches and stems grow hollow. The discharges become clearly visible and grow in extremely short periods that may cause breakdowns [Baumgartner 1991]. Electrical trees can be caused by water trees, which are formed when moisture or water ingress into the insulation. The study of electrical trees and propagation of the trees are described in [Dissado 1997, Kaneiwa 2000].

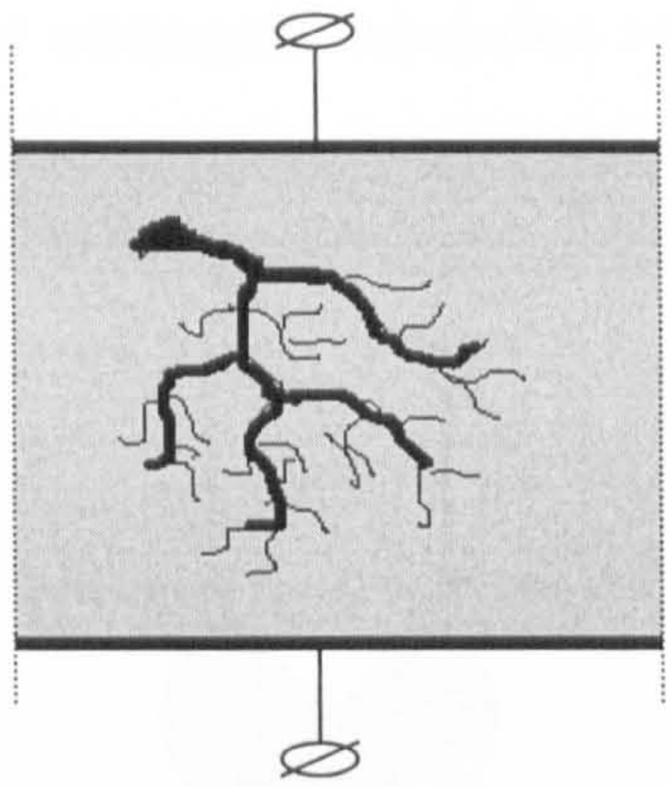

Figure 2.2: Electrical Tree

2.2.2 External Discharges

Surface discharges and corona are examples of external discharges that occur in high voltage systems. Surface discharges are partial discharges that may come from a conductor passing through a gaseous or liquid medium onto the surface of solid insulation. Examples of surface discharges are found at bushings, cable splices, terminations, overhang of windings or wherever a discharge is from a conductor in contact with the insulation. Figure 2.3 illustrates the location of surface discharges.

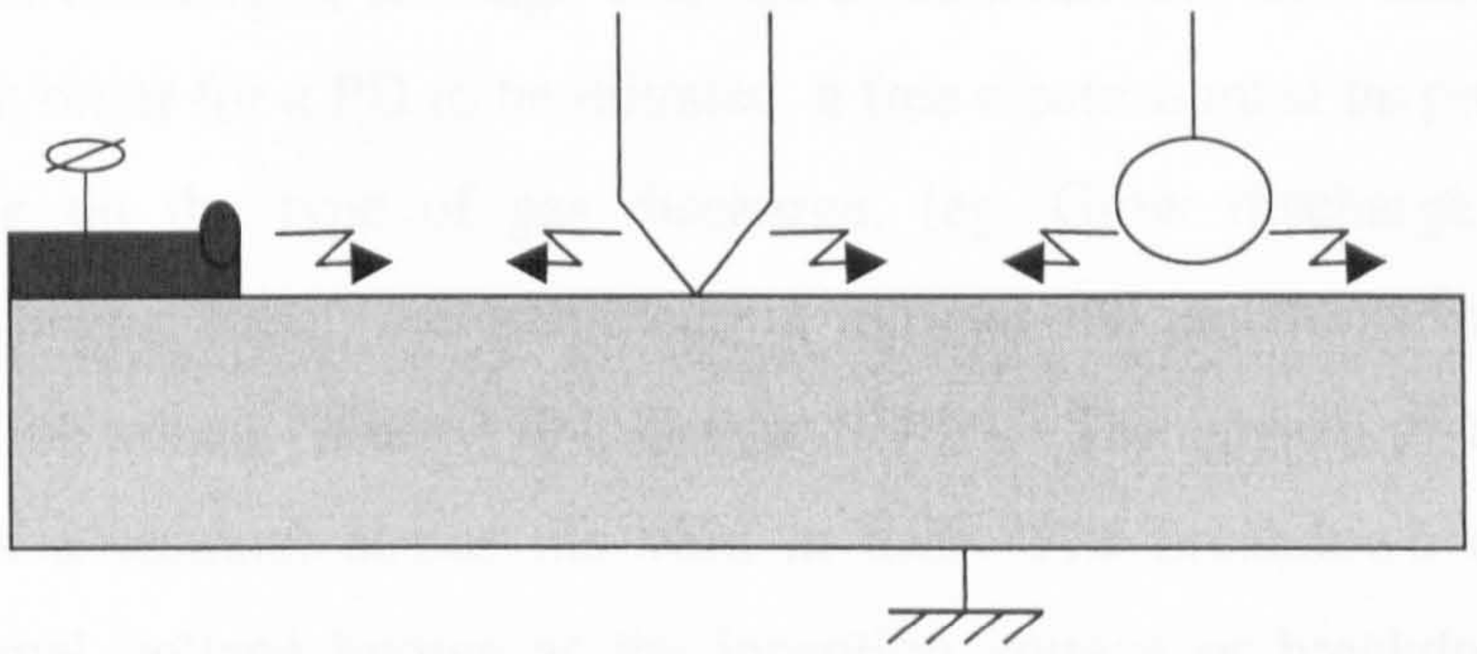

Figure 2.3: Surface discharges

Corona is a term used for discharges that occur with the breakdown of air and other gases at the tip of solid objects usually sharp points. For power cables, this can be caused by surface protrusions at the earth potentials, or even the wires. The enhanced electric field around the tip of the object causes a spark glow to occur appearing like a spark discharge. This is due to the partial breakdown of the surrounding air at the tip, as illustrated in Figure 2.4. Corona discharges in high

voltage networks usually indicate inadequate insulation and provide early warnings of possible flashovers [Trinh 1995].

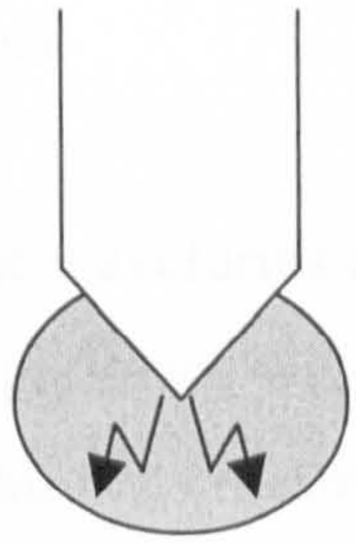

Figure 2.4: Corona at sharp edges

2.3 PD Physical Mechanism

There are many varieties of PD processes, which occur in high voltage electrical insulation. This variety is due to the vast range of insulating materials used and to the various voids or interface geometries. Generally, partial discharges can be considered as gas discharges, although electron avalanches may also occur in solids and in liquids. In order for a PD to be initiated, a free electron must be present in the void. Depending on the type of gas discharge, (eg. Glow discharge, Streamer, Townsend) [Bartnikas 2000], the free electron initiates the electron avalanche that travels towards the anode [Brunt 1994, Boggs 1990c]. The growth of the electron avalanche forms a channel across the void in time. The breakdown of the void requires a minimal voltage known as the inception voltage or breakdown voltage (U^+) whereby PD is observed. The value is often governed by the properties of the void [Morshuis 1993]. The magnitude of the induced charge is strongly dependent on the orientation of the void with respect to the applied field direction [McAllister 1997].

The behaviour of internal discharges can be described through the well-known "a-b-c" circuit [Kreuger 1989] represented as the electrical circuit depicted in Figure 2.5. The 'abc' circuit assumes that the dielectric components can be replaced with capacitances with:

C_a = The capacitance of the dielectric between the conductors

C_b' = The capacitance of the dielectric on each side of the void

C_c = The void capacitance

Figure 2.6 illustrates the voltage waveforms associated with the void and the dielectric with zero mean. The void capacitance will start to discharge as the voltage across the void increases until the breakdown criterion (inception voltage) is reached. The discharge in the void causes current impulses to occur that are concentrated in the regions of the rising or falling edge of the AC supply voltage and the PD reoccurs at every half cycle [Fouracre 2001]. However, the characteristic form of such discharge activity differs, depending on the type of void and PD [Robinson], [Brunt 1994]. This behaviour is repeated when the void voltage switches polarity and similar effects recur.

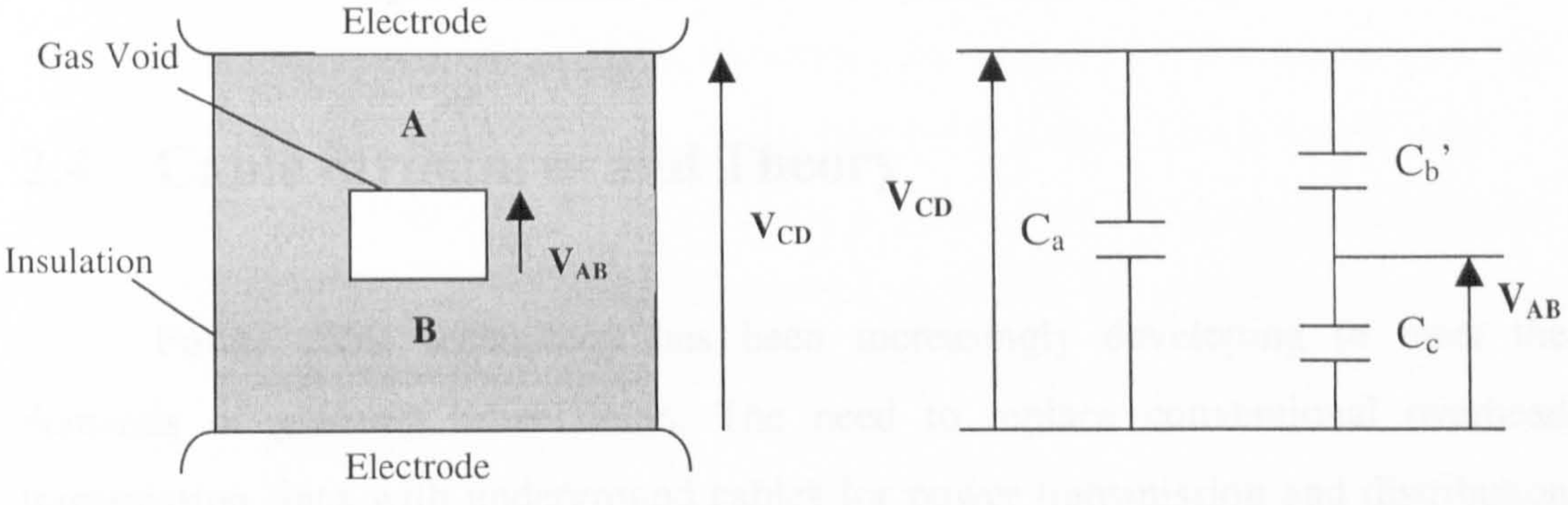

Figure 2.5: (a) Gas void in the insulation ; (b) Equivalent 'abc' circuit

After the discharge, some charges may remain in the void producing the final voltage known as the residue voltage, (V_r) [Kreuger 1989]. Each time a PD occurs in the rising edge of the signal, different time locations are manifested with reference to the AC supply signal with varying magnitudes. The repetition of discharges has a stochastic nature. This is due to the initiation time required to produce an electron avalanche required to produce the breakdown across the void. This is known as the statistical time lag [Bartnikas 2002]. Variations of the discharge frequency behave

with a stochastic nature. The stochastic behaviour in the distribution of the PD magnitudes and phases aids the determination of the type of discharges [Vonglahn 1995, Montanari 2000].

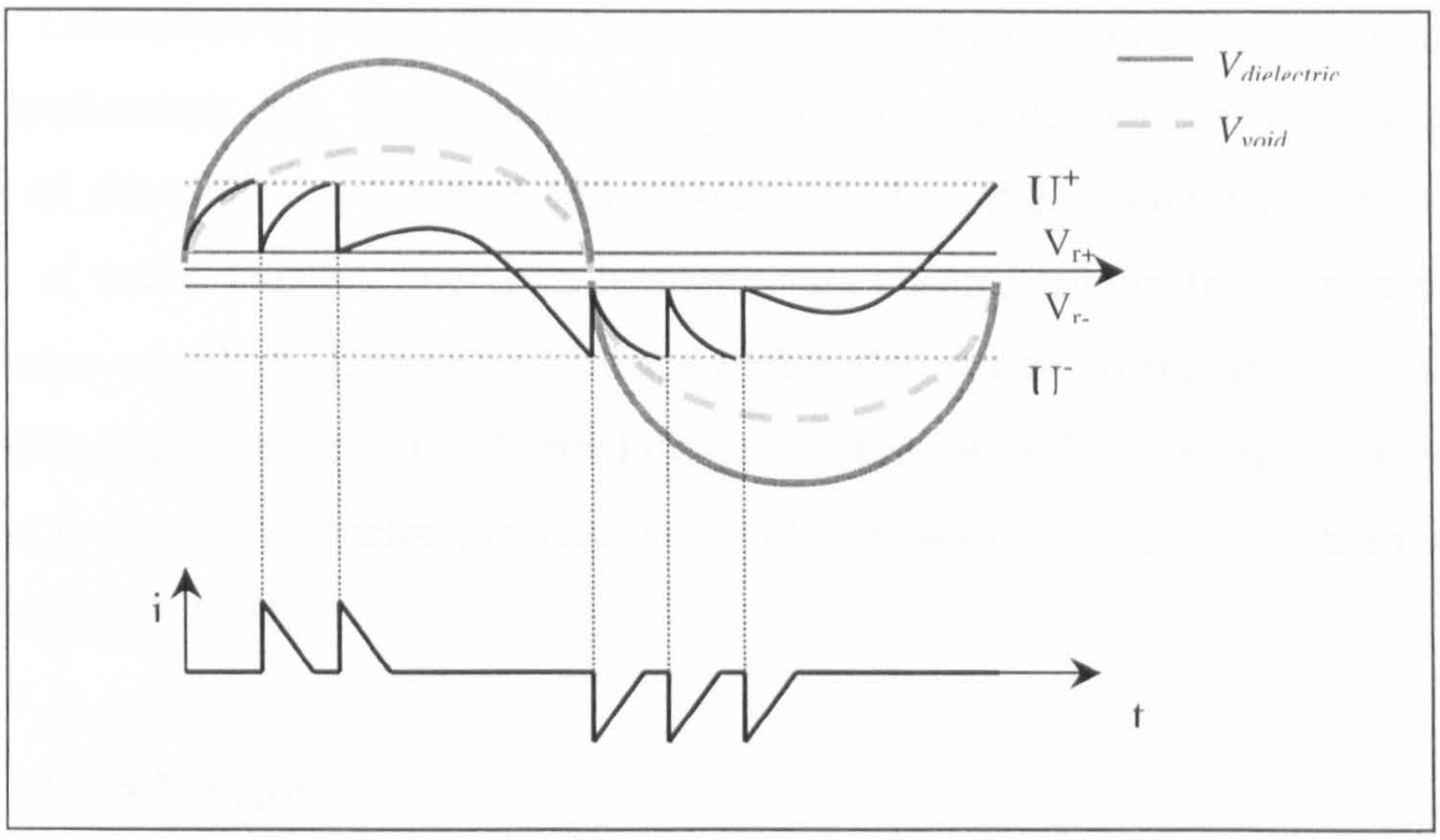

Figure 2.6: Recurrence of Discharges [Bartnikas 2000]

2.4 Cable Structures and Theory

Power cable technology has been increasingly developing to meet the demands of growing urbanization. The need to replace conventional overhead transmission lines with underground cables for power transmission and distribution has grown. In major cities, rapid growth of illumination under some circumstances is impossible to accommodate with the number and size of feeders required using the transmission line approach. As long ago as 1884 in New York City, an ordinance law was passed requiring the removal of the overhead line structures and their replacement by underground cables due to the dangers posed and to safety hazards [Meyer 1916].

Underground power cables come in different shapes and sizes depending on the specifications required. Some examples of these cables are the oil impregnated paper insulated cable, cross-linked polyethylene cable (XLPE), Ethylene-Propylene-

Rubber etc. These cables are differentiated by the dielectrics materials used as the insulation, and also the type of configurations employed [Gonen 1988]. Cables vary in diameter, type of conductor and number of cores; also load capacity, cyclic loading and thermal expansion.

Utilisation of power cables will also vary depending on the circumstances of each application. The main factor that governs the choice cables is the electrical rating of the cable i.e. voltage and current. [Cotton 1931]. Other factors such as choice of route, lengths, operating temperatures, climate, and critical stresses affect the choice of cables. Operating voltages define the insulation requirements and the maximum current defines the thermal ratings for the cable. The common components of a cable are its conductors, insulation, and the armour and sheath for high voltage cables [BICC 1948].

2.4.1 Conductor

Copper and aluminium are the common metals used for most conductors. The conductors are chosen based on their electrical conductivity, coefficient of expansion, breaking strength, heat resistance and cost. Aluminium is preferred over copper because of its lower costs. Figure 2.7(a) shows an example cross-section through PVC insulated 1kV cable with solid sector aluminium conductor and Figure 2.7(b) shows a stranded 4-core cable.

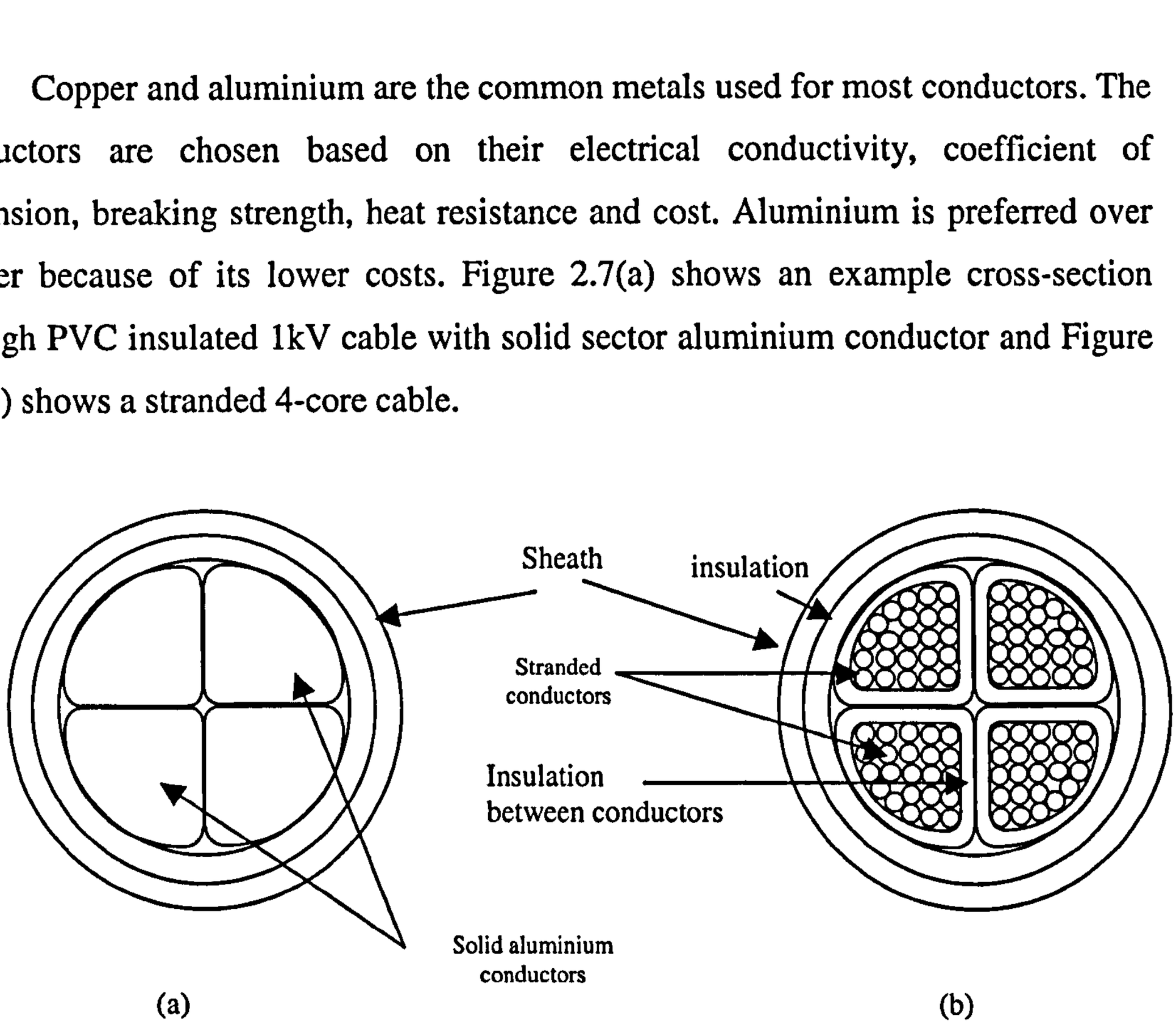

Figure 2.7: (a) PVC insulated solid aluminium conductor (b) Stranded 4 core cable

The application of solid conductors is beneficial for soldering and compression jointing but has a restricted flexibility. In the UK, solid conductors have extensively been used for the 600/1000V cables and 19/33kV cables with paper and polymeric insulation [Powers 1994].

2.4.2 Insulation

The vast majority of conventional power cables are insulated with either solid extruded dielectrics or liquid impregnated papers. The former now dominates the distribution power cable field, whilst the latter is still extensively used for high voltage transmission. Oil-impregnated paper insulations have been a popular cable for HV transmission. The liquid compound added to the paper was for the purpose of filling air gaps between sheets of the paper. This reduces the dielectric losses, reduces the chances of gap breakdowns, reduces moisture content and increases the flexibility of the cable [Bungay 1982].

In polymeric insulated cables, insulation types such as polyethylene (PE), cross-linked polyethylene (XLPE), ethylene propylene rubber (EPR) and poly vinyl-chloride (PVC) are common [Clegg 1993]. These may be classified into two different types of polymeric materials i.e. thermoplastic and thermoset materials. Thermoplastics are materials which are capable of softening by heating and hardening by cooling. The good example is the PE and XLPE, which have high dielectric breakdown strength and low dissipation factor [Bartnikas 2000]. Thermoset materials are insoluble and infusible. EPR is a thermoset material.

In HV cable configurations, a layer of semiconductor is usually placed between the conductor and the insulation. Imperfections in the surface contact produce small air gaps in the interface. Thus, to avoid surface discharges the semiconductor layer is added [Fouracre 2000]. Its primary purpose is to provide a smooth, continuous, conductive and isopotential interface between the conductor and insulation [Burns 1992].

2.4.3 Sheath and Armour

The sheath is the layer after the insulation. The sheath's main function is to provide a mechanical outer protection for the cable and cover for prevention of moisture ingression [Bartnikas 2000]. In oil-impregnated paper insulated cables, it also acts as a seal to prevent leakage of the oil compound in the cable. There are two types of sheath, metallic and non-metallic. Lead has been the material used for the longest time for sheaths in power cables [Powers 1994]. Another compound is aluminium, which is light, has more flexibility and has good mechanical properties.

Cable armour is the outermost layer of a cable. It functions to protect the cable in many aspects - such as from chemical corrosion, animal gnawing and sharp objects - and it has to withstand strong pressure forces especially for buried cables. Two universal types of armour are steel tapes and galvanized steel wires [Bungay 1982]. It also represents the ground return path for any external earth fault currents.

2.5 Transmission Line Equations

An approximation for a transmission line circuit model is the Distributed Parameter Line model, that has its circuit parameters distributed uniformly along the line. The electrical circuit representation of a line parameter of length Δz is illustrated in Figure 2.8. This is also known as the Pi-section model of the transmission line. A distributed parameter line is the product of cascading several Pi-sections together [Mathworks 2000]. The transmission line parameters are:

R , resistance of the conductors per unit length in Ω/m

L , inductance of the conductors per unit length in H/m

G , conductance of the dielectric media per unit length in S/m

C , capacitance of the conductors per unit length in F/m

The derivation of the line equations can be done by using Kircoff's Voltage and Current Law. The voltage equation around the perimeter of the circuit in Figure 2.8 can be written as:

$$\frac{\Delta V_s}{\Delta z} = -(R + j\omega L)I_s - \frac{1}{2}(R + j\omega L)\Delta I_s \qquad (2.4)$$

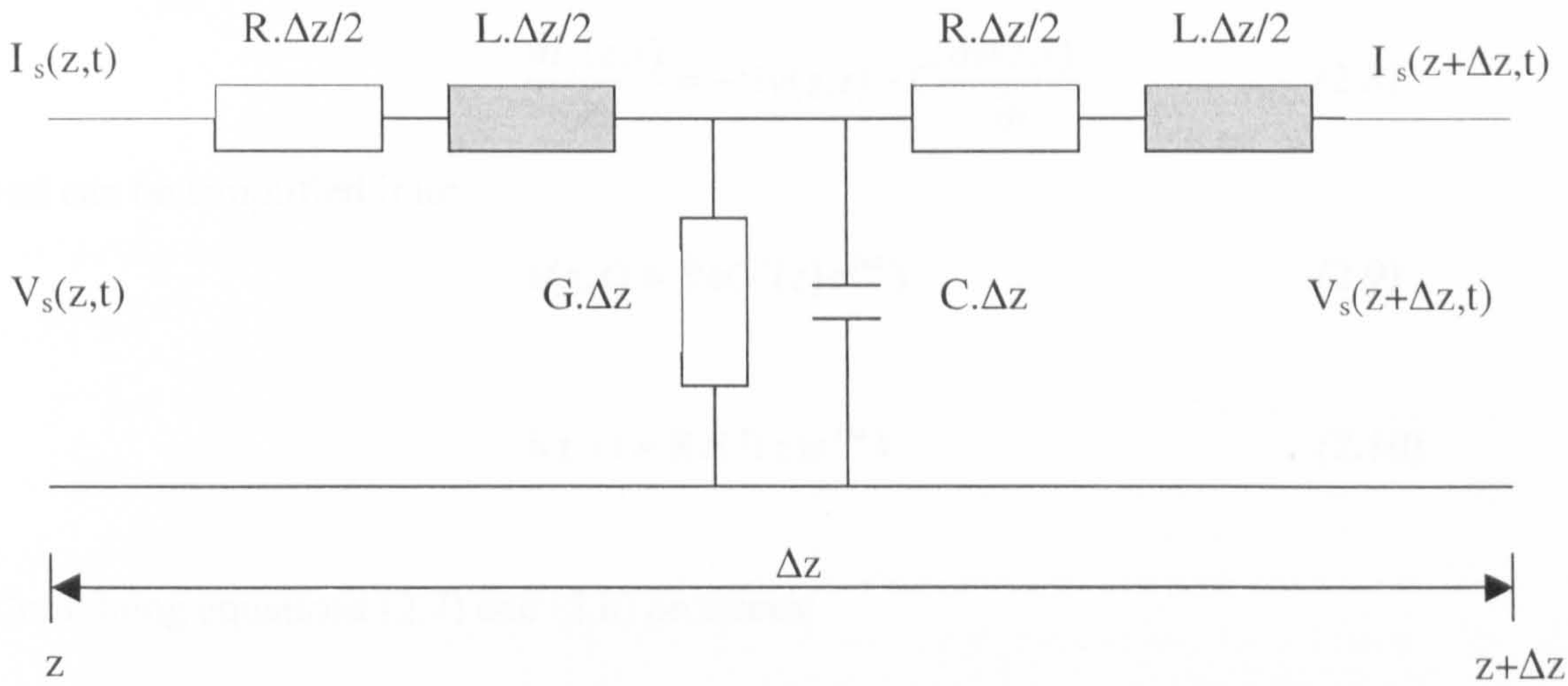

Figure 2.8: Equivalent circuit for a transmission line of length ΔZ

As Δz tends towards zero, ΔI_s also approaches zero, thus the second term vanishes leaving:

$$\frac{dV_s}{dz} = -(R + j\omega L)I_s \qquad (2.5)$$

By neglecting the second order effects, the voltage across the central branch can be approximated as V_s and the second equation is obtained:

$$\frac{dI_s}{dz} = -(G + j\omega C)V_s \qquad (2.6)$$

The equations above are known as the time harmonic transmission line equations [Hayt 1989]. The first order partial differentiation equations are known as the general transmission line equations as shown below:

$$\frac{\partial V_s(z,t)}{\partial z} = -R.i(z,t) - L\frac{\partial i(z,t)}{\partial t} \qquad (2.7)$$

$$\frac{\partial I_s(z,t)}{\partial z} = -Gv(z,t) - C\frac{\partial v(z,t)}{\partial t} \qquad (2.8)$$

and can be simplified into:

$$v(z,t) = \mathrm{Re}(V(z)e^{j\omega t}) \qquad (2.9)$$

$$i(z,t) = \mathrm{Re}(I(z)e^{j\omega t}) \qquad (2.10)$$

Combining equations (2.7) and (2.8) produces:

$$\frac{d^2V(z)}{dz^2} = \gamma^2 V(z) \qquad (2.11)$$

$$\frac{d^2I(z)}{dz^2} = \gamma^2 I(z) \qquad (2.12)$$

where γ is the propagation constant:

$$\gamma = \alpha + j\beta = \sqrt{(R + j\omega L)(G + j\omega C)} \qquad (2.13)$$

where:

α is the attenuation constant of the line with units of Neper/m.

β is the phase constant of the line with units rad/m.

Another important parameter is the characteristic impedance Z_o (Ω), which is derived by using the voltage line equation (2.5) divided by the current line equation (2.6), and is represented as:

$$Z_o = \sqrt{\frac{(R + j\omega L)}{(G + j\omega C)}} \qquad (2.14)$$

2.6 Attenuation and Dispersion

As a travelling wave moves along a transmission line, it suffers from the attenuation and dispersion/distortion phenomena. When the magnitude of a wave is decreased, it is known as the attenuation. When the wave changes shape i.e. becomes more elongated, its steepness is reduced, its irregularities are smoothed out or the voltage and current waves cease to be similar, then it is known as dispersion/distortion [Bewley 1951].

Attenuation is caused by energy losses and dispersion is induced by frequency-dependent variations in propagation velocity determined mainly by the inductance and capacitance. Losses are incurred by transient skin and proximity effects, dielectric losses or leakage over the insulators. High frequency losses are the result of the dielectric losses and the propagation of the radial displacement current through the resistance of the semi-conductive layers [Boggs 1996].

A lossless line is considered when the R and G = 0, (see equation 2.14). For a distortionless line, R/L = G/C must be satisfied [Bewley 1951].

2.6.1 Reflections at Terminations

A travelling wave may undergo reflections when it arrives at a termination of the transmission line. The reflections are governed by the value of load impedance connected at the end of the line. The reflection coefficient is given by:

$$\Gamma = \frac{Z_L - Z_O}{Z_L + Z_O} \qquad (2.15)$$

where:

Z_L is the load impedance at the termination

Z_O is the characteristic impedance

For a typical open circuit termination, a positive reflection of the incident waveform without any changes in the amplitude ($Z_L = \infty$) is expected. For a typical short circuit termination, a negative reflection of the incident waveform ($Z_L = 0$) is obtained. Matched impedances are used to avoid reflections i.e. ($Z_L = Z_0$).

2.7 How to Detect PD

Methods for PD detection are classified into non-electrical methods and electrical methods. In both instances, particular measuring devices and circuitry are used to detect the presence of PDs. These measurements can either be conducted offline or online. The difference between the terms is that offline methods are connections from the sensors or measuring devices and the measurements are performed whilst the measured equipment is switched off. For online methods, the connections and measurements are performed whilst the measured system is under normal operating conditions.

2.7.1 Non-Electrical Detection Methods

Non-electrical detection methods for discharge detection are such as chemical transformation, gas pressure, heat, acoustic and optical. Amongst the methods described, sound and light represent the ones of practical importance [Kreuger 1989]. For non-electrical methods, the main advantage is that noise disturbances will not affect the performance of the PD detection. One disadvantage of this method is that it

cannot be used for detecting the magnitudes of the discharges and is unable to characterize PD's. Often the case, non-electrical methods are tailored for specific applications and cannot be generalised for different equipment. Many times, the techniques are less sensitive, tedious, labour intensive and more costly than electrical methods, and in some cases not suitable for factory environments [Chan 1991].

Optical methods have the capability of achieving sensitivity up to 0.01pC through sophisticated devices. Photographic records can be taken without noise disturbances from discharges. However, this detection method can only be used for surface discharges and corona. Other disadvantages are high costs for development of photographs and the technique is usually performed in real time.

Acoustic methods have become somewhat popular among some of the researchers in this field. This method can be extended to locate discharges in a gas, both internally and at the surface of insulations. The advantages are low costs, high sensitivity and simplicity of application [Harrold 1993]. A good method is based on ultrasonic pulse-echo radar and is used for crack detection within the insulations [Lundgaard 1992a]. According to Lundgaard, acoustic methods are not suitable for PD detection in cables because of the reduced sensitivity with variations of distance from the discharge source [Lundgaard 1992b]. Furthermore, for underground cables the application of acoustic methods is limited since the cable is required to be submerged and surface may not be accessible. In [Tian 2003], VHF capacitive couplers have been successfully applied for offline detection of PD in joints and short lengths of cable. The disadvantage is that the method is only applicable to certain types of cables and the sheaths of the cables have to be removed to install the sensors.

2.7.2 Electrical Detection Methods

Partial discharges result in localised electrical disturbances that are modelled by considering a transient voltage collapse in a small volume of insulation. Electrical detection of PDs is done by measuring either by the voltage disturbances at the terminals of the equipment or by using sensitive, high frequency current devices

observing the current in the equipment conductors. The short duration of current pulses generated by PD's are of the order of a few *n*s [Boggs 1990a] and the optimum detection bandwidth ranges between 10 - 20 MHz [Kreuger 1993]. However, in solid dielectric cables the process of attenuation and dispersion alters the shape of the PD pulses depending on the relative distance from the source to the point of measurement. At the point of origin, attenuation or dispersion are at the minimum and the PD signal may be completely preserved [Boggs 1990b].

Discharge detection systems measure the PD levels, phase-resolved patterns and location of the discharges as a function of the applied voltage. Two principles for discharge detection process are [IEC 60270]:

1. Discharge detection by measuring the apparent charge magnitude of the PD pulses in *p*C or *n*C
2. High frequency measurement of the voltage magnitude of the PD pulses registered in μV and mV.

The first method involves measuring circuits, which function to detect the current impulses. The detection circuits may vary from detection impedance, RC circuits or RLC circuits [Kreuger 1989, Steiner 1991]. The method assumes that the test object is regarded as a capacitor, and the detection of the PD signals employs a coupling capacitor and the detector requires its input impedance with specific arrangements and a wide or narrow band-pass integrator [Cigre 2002]. The basic diagram of a detection circuit is depicted in Figure 2.9. The detection impedance, Z may be connected in series with the test object or in series with the coupling capacitor, C_k.

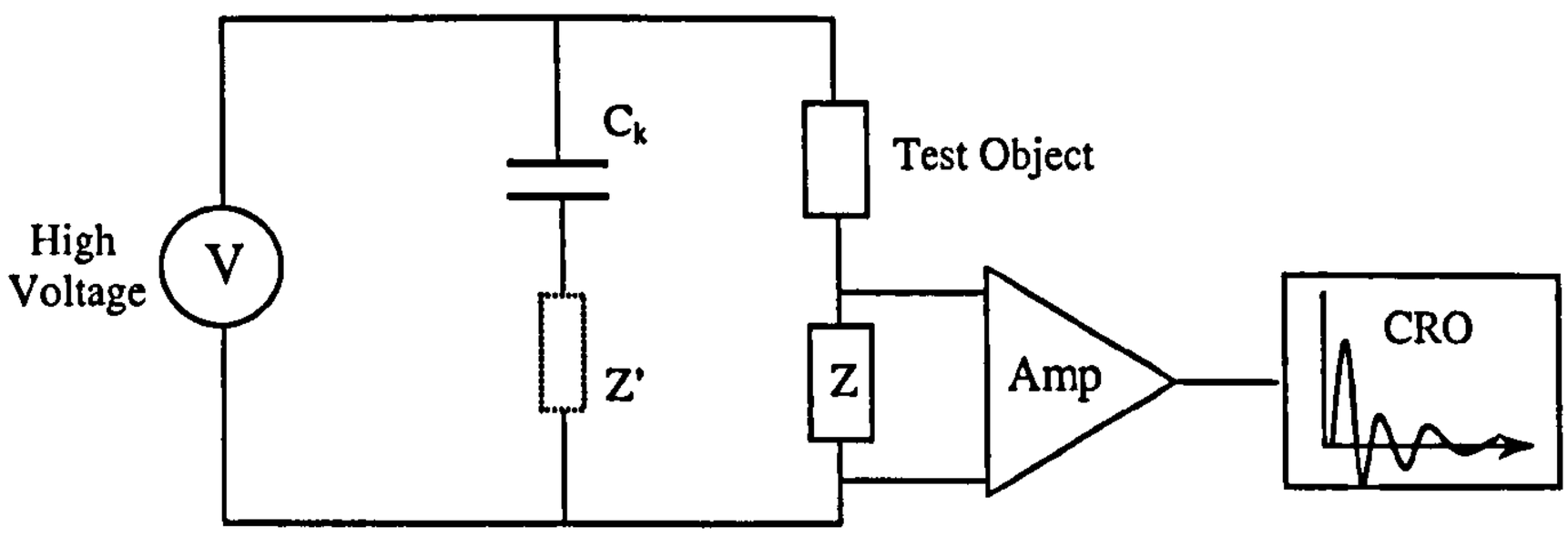

Figure 2.9: Basic circuit for electrical discharge detection

Another form of detection is performed by measuring the dielectric loss, which is quantified by the tan δ. The charge transfer in the void event produces a sudden change in the *tan δ* waveform as depicted in Figure 2.10. Energy dissipated from the PD can be measured using bridge circuits. The Schering Bridge is well known for loss tangent measurements with its circuit configuration shown in Figure 2.11.

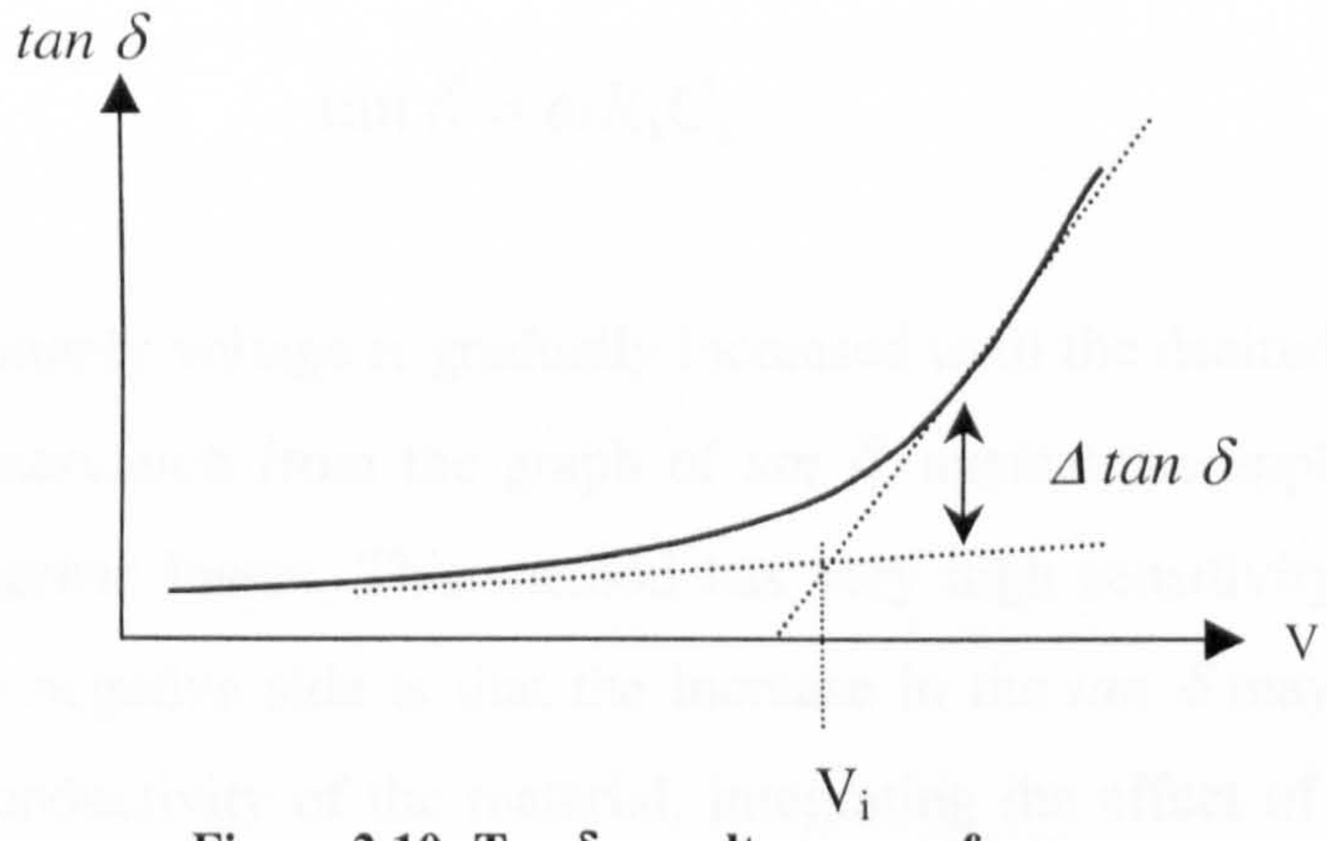

Figure 2.10: Tan δ vs voltage waveform

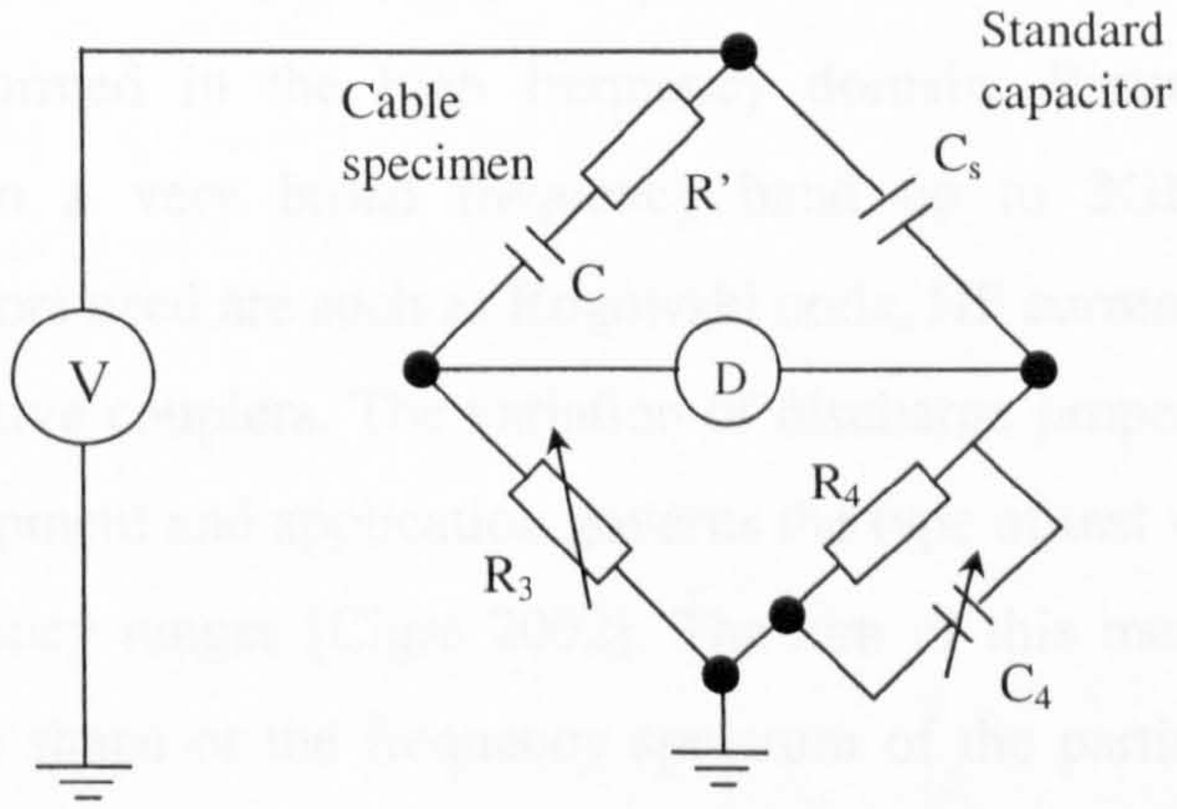

Figure 2.11: Basic Schering Bridge Circuit

The C_s represents a standard capacitor with negligible losses, R' and C represents the series equivalent circuit for the specimen, and R_3, R_4 and C_4 are balancing elements of the bridge. When the bridge is balanced, the voltage drop across Cs (phase and magnitude) equals that across the specimen, as the null detector is reduced to zero. Hence, the product of the of the impedance terms at opposite arms must be equal:

$$Z_3 Z_s = Z Z_4 \qquad (2.16)$$

After inserting the relevant components into equation 2.16, and equating the real and imaginary terms (more information in [Bartnikas 2000]), the dissipation factor for the series equivalent circuit of the cable insulation is given by

$$\tan \delta = \omega R_4 C_4 \qquad (2.17)$$

Then the supply voltage is gradually increased until the desired test voltage is achieved. The observation from the graph of *tan* δ against the applied voltage, V indicates the dielectric losses. This method has very high sensitivity for discharge detection, but the negative side is that the increase in the *tan* δ may be due to the increase in the conductivity of the material, integrating the effect of PD activity as well [Fouracre 2000].

In the second method, signal acquisition of the specimen under test conditions is performed in the high frequency domain. Partial discharges may contain energies in a very broad frequency band up to 3GHz. The detection instruments or sensors used are such as Rogowski coils, HF current transformers, and inductive or capacitive couplers. The variation of discharge properties due to type of discharge, test equipment and application governs the type of test voltage applied and the different frequency ranges [Cigre 2002]. The aim of this method is to measure and to quantify the shape or the frequency spectrum of the partial discharge pulses under on-site conditions. The two approaches to this method are conducted under offline conditions or online conditions. Offline techniques are performed whilst the specimen is de-energized during the test period, while online techniques are conducted whilst the specimen is fully energized. Each approach has its pros and cons, which will be discussed in the next section.

Recent advances in technology has produced state-of-the-art equipment and electronic devices, in effect this has significantly improved the quality of detection capabilities in this research field. The major contribution is evident in the increase of

powerful microprocessors and data acquisition systems, advancing the capabilities in data storage and processing power.

However, a major problem with this technique is noise interference. These disturbances can originate from switching circuits, radio interferences, imperfections in cables and connections, and higher harmonics of the test voltages [IEC 60270]. The danger is that sometimes the PD can be masked under the noise levels, which makes detection difficult. Thus, applications of digital signal processing are now being developed and used to enhance the detection of PD's. The various signal processing algorithms applied to date to PD diagnostics will be reviewed in Chapter 3.

2.8 How To Locate PD's – Signals Point of View

Emphasis has been given towards the location of PD's since the 1920's [Kreuger 1989]. The process of PD location is somewhat more difficult compared to detection. Being able to quantify and locate the PD along a cable is advantageous since condition-based monitoring procedures and necessary risk assessments can be carried out on the equipment. The general concept of locating a PD within a cable is either through scanning probe methods [Morin 1999] - whereby the cable is scanned for its entire length for PD activity (less feasible) - or Time Domain Reflectometry (TDR) based methods. The limitation of the scanning probe method is that the entire surface of the cable has to be fully exposed for scanning purposes. The TDR is the preferred method since the application of the concept is simple yet effective. Nominally, the TDR method is performed by signal acquisition from one end of a cable or from two ends of cable.

2.8.1 Single Ended Location

The travelling wave method, or the time domain reflectometry (TDR) method, is commonly used in radar applications and determining distances. Reflections of the incident pulses are used to determine the origin of the source. The

concept is applied for cable fault locations, which functions the same with PD location. When a discharge occurs, the discharge current impulse travels through the conductor and the sheath of the cable and propagates towards both ends of the cable [Ahmed 1998]. The main reflection of the incident pulse occurs at the termination of the cables. This is better illustrated with the Bewley Lattice Diagram [Bewley 1951] shown in Figure 2.12.

The PD pulse will propagate towards both ends of the cables starting at x_1 distance away from the measurement end. Reflections take place at the measurement and far ends of the cable. After a period of time, the first reflection from the far end will arrive to the measurement end of the cable. The process continues until the reflected signal eventually becomes negligible. The second and third reflections are usually very small because they travel double the distance along the cable.

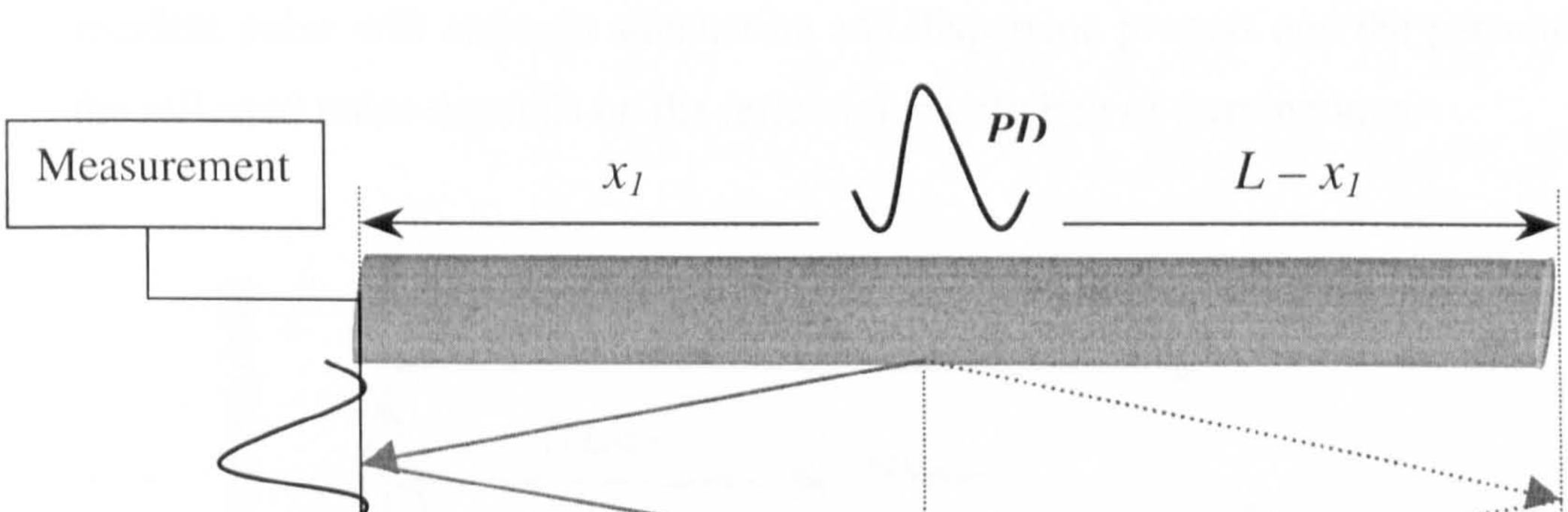

Figure 2.12: Bewley lattice diagram for PD event

Figure 2.13Figure 2.13 illustrates examples of expected PD pulses measured from one end of the cable. With the time between the incident pulse and the first reflected pulse (reflection time, T_r), it is sufficient to deduce the origin of the PD. The reflection time is given by:

$$T_r = \frac{2(L - x_1)}{v} \qquad (2.18)$$

where v is the velocity of propagation in the cable, and L is the length of cable. By simple manipulation of equation 2.18, the origin of the PD source from the measured end is given by:

$$x_1 = L - \frac{v.T_r}{2} \qquad (2.19)$$

In real cable systems, reflections are likely to occur because of mismatch of impedances at the end of the cable and some in cable joints [Clegg 1993]. The incident pulse will undergo attenuation and dispersion process and the percentage of the reflected pulse depends on the reflection coefficient of terminations.

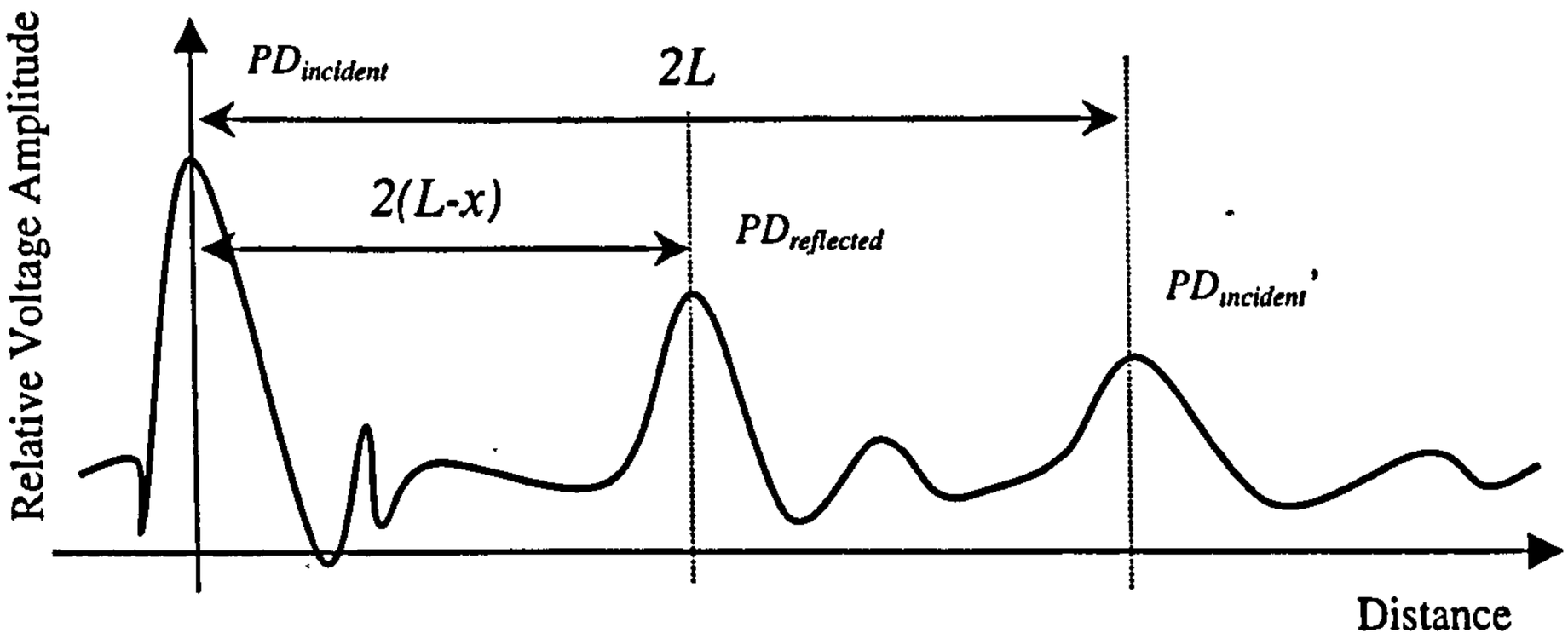

Figure 2.13: Measured PD signals

2.8.2 Double Ended Location

The difference between this method and the single ended method is that measurements are performed at both ends of the cables. Double-ended location methods are usually performed for online diagnostics of cables. Reflections of the incident pulses are not of particular importance. However, the measurements must be done simultaneously and synchronised to determine the PD location. Depending on

the length of the cables, typical time of flights of pulses to propagate from one end to the other is within regions of μs. Hence, any time difference between the start time of the acquisitions will cause errors to occur. In [Kezunovic 1996], Global Positioning System (GPS) satellite receiver and a digital fault recorder was used to locate faults in the cable through synchronisation of samples. This has been extended to partial discharge diagnostics for multiple branched cables [Steennis 2001]. Although the GPS services are more readily available now, the cost of the service is still relatively high. Furthermore, when using the GPS synchronisation, both ends (or every sensor location) have to be within the line of sight of two satellites if locations are known and four if not [Wielen 2004].

An interesting method was introduced by Shim et. al. using double ended measurements utilising synchronising pulses known as timing pulses [Shim 1999]. These timing pulses were injected from one end of the cable. PD can appear in any random location, causing ambiguity in determining the point in time where it occurred ($t=0$). The timing pulses provide a reference point to correlate the measurements acquired from both ends of the cable. The mathematical description is described in [Shim 2001], together with test results. The method is also extendable to cases whereby more than one discharge occurs.

Every method comes with its disadvantage; in the case of timing pulses, this method was not applicable to scenarios whereby only one end of the cable is accessible. In the UK, some HV systems have completely enclosed Ring Main Units (RMU) at one end of the cable circuit, which prohibit any possibility of access points. Based on previous experiences, high noise levels in the cables exceeding the amplitudes of the injected timing pulses causes problems with the registration process [Shim 2001]. In the Netherlands, double-ended methods are extensively used for online PD location since their cable systems are mainly accessible at the Ring Main Units (RMU) [Wielen 2003a].

There are some limitations to the TDR method, which have been described in [Du 1997]. When a PD occurs at the far end of the cable from the measuring end, the reflection times becomes very small which in turn produces a superposition of the

incident and the reflected PD. Thus, evaluation of the time delay then becomes a problem.

2.9 Condition Based Maintenance

Many utilities are emphasizing Condition Based Maintenance (CBM), which is preventive maintenance depending on the actual conditions of the high voltage equipment. New asset management strategies are being developed to provide efficient handling of risks of equipment failures. A risk based asset management approach is used to target assets that are suspicious and have high risks of permanent failures. This encapsulates the technical aspects of condition assessment, which includes the type of defect and its location [Cigre 2002]. For EDF Energy Networks (England), several key criteria necessary for effective condition-based asset management program are identification of critical plant and equipment, direct monitoring and maintenance of critical plants, establishment of early warning systems, generation of a condition-based table of assets based on age, type and health [Walton 2003]. For Scottish Power, scheduled diagnostics for plant and equipment are carried out periodically by employing third parties to perform tests to screen out potential dangers arising from them, mainly EA Technology (UK) and KEMA (Netherlands). Nevertheless, partial discharge testing is one of the common procedures conducted to detect early signs of insulation deterioration. Especially aged high voltage equipment such as transformers, cables, bushings, motors, and gas-insulated substations systems that are susceptible to PD activity. In general, the detection and location of PD's is performed either using offline diagnostic methods or online diagnostic methods.

2.9.1 Offline Location Techniques

During offline diagnostics, the normal operating voltage on the cable is switched off. The circuit breakers are de-activated or set to open circuit mode to isolate the test cable and other parts of the network connected to it. In practice, there are several methods of conducting the offline diagnostics. Each method requires the test cable to be energised separately with an external HV power supply. The different techniques of offline diagnostics are generally categorised from the method of energizing the cable and the frequency characteristics of the supply voltage. Ideally, the test cables should have similar conditions to its normal operating conditions. However, to energise the cable at 50 Hz (or 60 Hz) at high voltages, large supply trucks are required and only can produce very short periods of power for this purpose. Practically, this is not advantageous and is very costly. Other sought alternatives are methods such as DC testing methods, the very low frequency (VLF) or the 0.1 Hz method, and the Oscillating Wave Test System (OWTS).

In all methods, the general procedure is to gradually increase the supply voltages from a value well below the inception voltage until discharges are detected [IEC 60270]. Since the cables have been taken offline before the energising, the supply voltage can vary from 1Uo up to 3Uo. Higher stress is required to initiate the first PD that will cause the chain of PD's to occur. This is one of the reasons why offline techniques can be dangerous. In the process of trying to locate the PD, higher stress applied to the cables may cause other weaker points in the cable to breakdown.

Noise levels in offline diagnostics are often much less than noise interferences during operating conditions. Since the test cable is isolated, good signal to noise ratios are achieved unless a source of AM broadcast is situated close to the test site.

The DC method has found to be studied to be disadvantageous because of the continuous stress that is exerted on the cable throughout the testing. Many countries that have applied DC testing on their cables, and majority had found that breakdown of the cable occurs not long after the test [TF21.05 2002].

On the other hand, the VLF method has been quite popular in the industry. Many diagnostic service providers such as KEMA, EATechnology, UltraPower Technology, Detroit Edison, Baur Equipments [Baur 2005] etc. utilise this method [Hassani 2002]. Through this method, the test cable is energised at supply voltage of 0.1Hz. The inception and extinction voltages can be successfully determined and PD's can be located. However, the results from this method cannot be directly extrapolated to normal power frequency conditions [Hotboll 1997]. The partial discharge behaviour varies because of the characteristics of the cable. The electrical field distribution of the cable undergoes a transition from capacitive to resistive when the supply voltage is varied from normal AC conditions to DC conditions [Kreuger 1995].

The Oscillating Wave Test System (OWTS) applies oscillating voltage wave of several tens of cycles duration and frequency that ranges between 50 Hz and 1000 Hz [Gulski 1998, Turner], which is similar to the power frequency during operating voltage. The test cable is charged up to operating voltage for few seconds duration using a DC source. The system uses a solid-state switch with fast closure time to create a series resonant circuit from the test object and air-cored conductor. Oscillation of the circuit is determined by resonant frequency ($f = 1/[2\pi\sqrt{LC}]$) of the inductance of the air core. During this time, the PD that occurs are recorded and diagnosed. Location of the PD is then performed using the TDR method.

2.9.2 Online Location Techniques

The process of locating the source of PD's in cable through online techniques is relatively more complicated than offline techniques. The main difference is that the diagnostics are conducted whilst the cable is under normal operating conditions. Hence, the main implications are higher noise interferences and increased complexities for the interpretation of data signals. Since all the other parts of circuit are connected to the test cable, noise originating from the other electrical devices is

coupled into the measuring devices. Transients originating outside from the test cable have to be recognised in the data interpretation process.

The common practice for online diagnostics is to acquire data from the cables through a measuring system and process the signals. Signal processing is applied to the data signals to extract useful information pertaining to PD activity. Both single-ended and double-ended location techniques are employed to locate the PD's within the cable wherever applicable, subjected to the substation configuration and regulations. For single-ended systems, the localisation process is heavily dependent on the reflection from the far end of the cable, compared to the double-ended system, which only requires the direct PD pulse. The double-ended system will either be conducted through the synchronisation of the measurements through GPS, atom-clocks or by injecting timing pulses into the cables [Wielen 2004, Shim 1999].

Recently, [Matthieu 2003] has introduced an enhancement for the single-ended TDR technique by using a manual transponder device, which is an active device using match filtering. This active device functions to magnify the reflection of the PD from the far end of the cable. The reflected signal is re-transmitted into the cable to enable successful identification of the reflected pulses from the measured signals (at the measuring end). The transponder utilises the concept of match filtering, whereby the PD signature is required to be known before the device can be operated. However, this method is limited by the connectivity of the device onto the cable circuit. Where terminations are completely enclosed, this method cannot be applied. Furthermore, there is the element of uncertainty with regards to the variations of PD signatures from cable to cable.

The challenges of locating PD through online conditions are certainly great, because of the high levels of complexity to the problem. There are not many researchers that claim to have successful technology in location of PD's in cables. However, there are several companies that have units that enable online diagnostics of PDs, and have the capability of PD location.

2.10 Conclusion

In this chapter, the phenomena of Partial Discharges for cables were reviewed. Physical properties and characteristics of cables were discussed in order to provide better comprehension of PDs, including the variations of PD types. Typical pulse propagation within the cable was presented by accounting for the attenuation and dispersion, including the voltage and current characteristics of cables.

The major points addressed in this chapter are the process of detection and location of PD within cables. Offline and online PD diagnostic detection and location techniques were reviewed. The advantages and the shortcomings of using those techniques were discussed. From the literatures, the trend has been to enhance online PD detection systems because of economic and non-economic benefits. The older and the newer PD diagnostic technology were discussed. With the advance in technology and measuring systems, modern diagnostic techniques are becoming more powerful and more easily implemented.

Chapter 3 : PD Data Interpretation and Signal Processing Techniques

3.1 Introduction

One major part of online PD diagnostics will rely on the application of signal processing techniques. These techniques are used to deal with noise interference and data interpretation, which represents the major challenges associated with online PD diagnostics. In order to fully maximise the effectiveness of signal processing algorithms, prior understanding of the PD signal properties is required. In this chapter, the aim is to provide a better understanding of the signal wave shapes and characteristics of PD signals as well as the signal processing tools that have been developed and applied in this field by the worldwide research communities.

The typical PD signals, characteristics and wave shapes are described in Section 3.2. Signals originating from narrowband and wideband sensors are illustrated. The effect and consequences from the attenuation and dispersion phenomena of the signal propagating in a cable is also discussed. In Section 3.3, knowledge rules pertaining to PD analysis is described. Statistical approaches and the measurable quantities are provided. In Section 3.4, the signal processing algorithms and techniques applied to PD diagnostics are reviewed. Older and recent techniques that have been applied by other researchers are discussed. The wavelet-based techniques will be explored in depth because its applications published in the literature. Section 5 describes the theory of wavelet transform algorithms, the types

of implementation methods and its applications within the PD diagnostic field. Finally, the conclusions are provided in Section 3.6.

3.2 Partial Discharge Signals

Electrically measured PD signals obtained from sensor devices used in monitoring of HV systems will have a number of variations. The variation in waveform shape and amplitudes often depends on the type of equipment monitored, the type of defect and the time of measurements. In Figure 3.1, several PD waveforms generated from experimental measurements is illustrated. The diagram illustrates the effects of discharge strength from different sources of gas voids [Okubo 2002]. Here the variations of the discharge pulse shapes, its duration of the pulse and the characteristics of the decay are used to identify the types of gas discharges. PD activity also changes as the current load conditions changes and it causes variations in the signal amplitudes [Wester 2003]. The waveform obtained from the measuring terminal is not the actual representation of the PD waveform at the point of origin due to attenuation and dispersion effects [Boggs 1996]. In addition, noise from electromagnetic interferences whether coupled conductively or radiatively and different type of sensors used will govern the final shape of the signal [Ma 2002]. Sensors systems will have their own frequency responses, which could modify the true PD signal.

3.2.1 Types of signals

The shape of the measured signal will be governed by the system response of the PD detectors and the measuring system. These PD detectors can be narrow band or wide band measuring detectors, which result in generalised PD wave shapes depicted in Figure 3.2. The wide band signal is similar to an exponentially decayed impulse that is overdamped, while the narrow band signal has more oscillatory decayed signal that is underdamped. The Gaussian model of a PD pulse is another model that can be used for the wideband signal [Zu 1997].

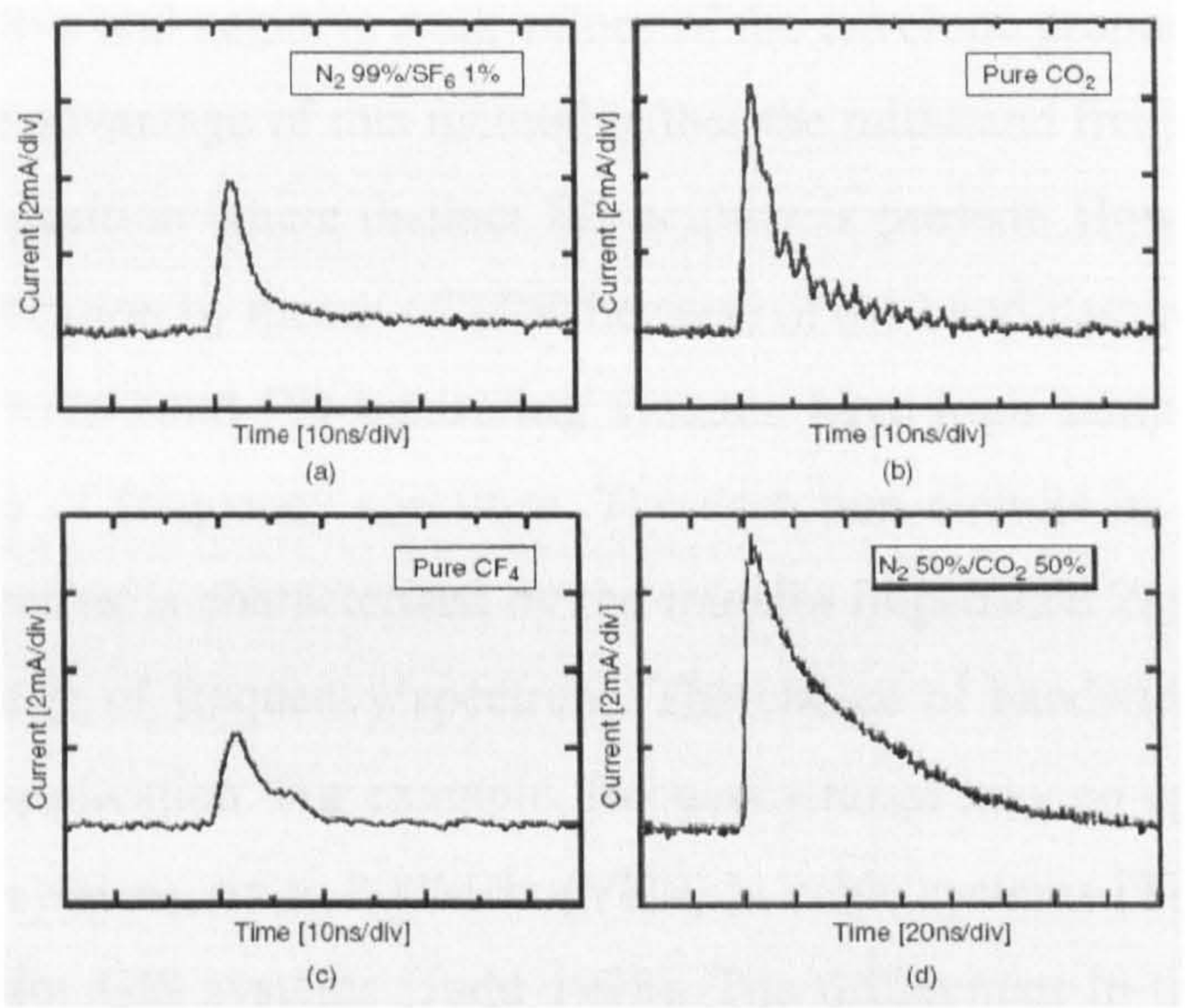

Figure 3.1: PD current pulse waveforms: (a) N_2 99%/$SF_6$1%, (b) pure CO_2, (c) pure CF4, (d) N_2 50%/CO_2 50% [Okubo 2002]

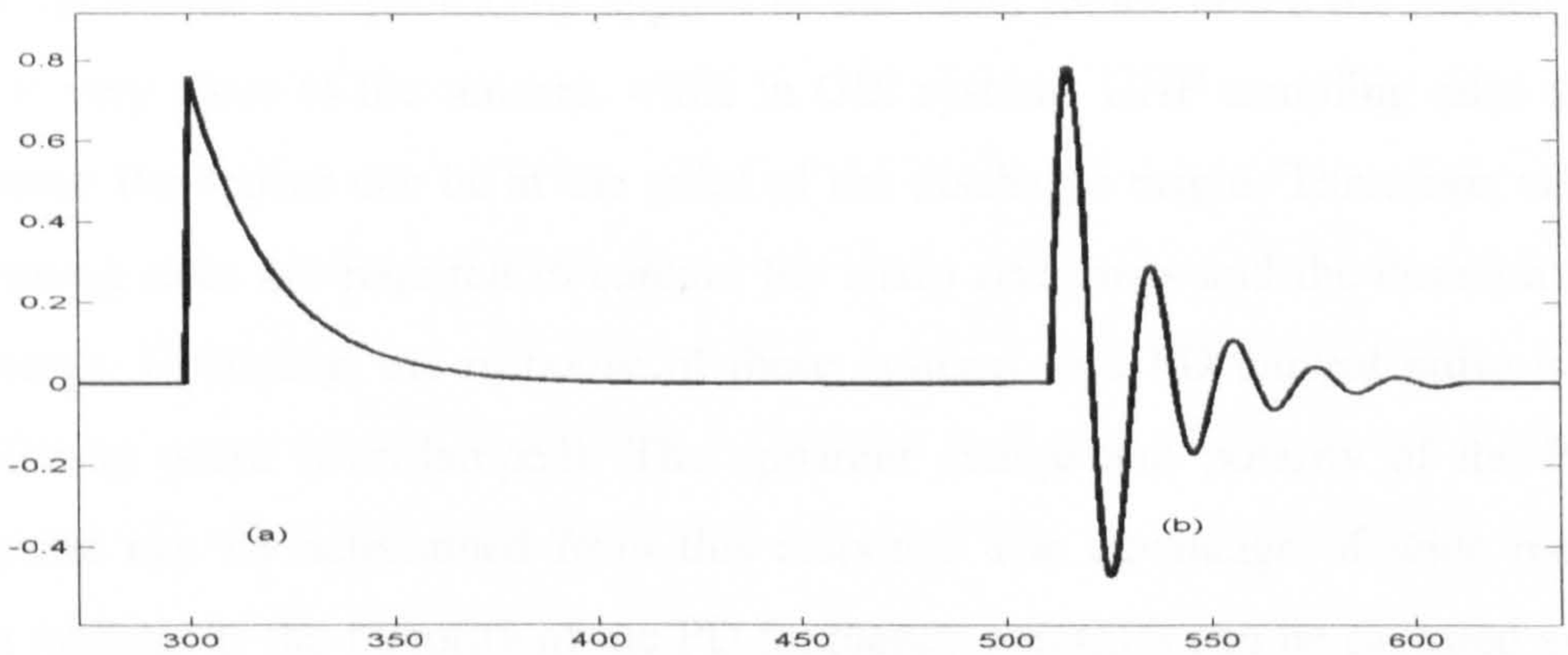

Figure 3.2: PD wave shapes (a) Wide band detection systems (b) Narrow band detetion systems

Narrow band measuring systems are characterised by a small bandwidth Δf and a mid-band frequency f_m, which can be varied over a wide frequency range [BS 60270]. This system is similar to a band-pass filter with a variable bandwidth. The recommended stop-band value of the frequency spectrum should be at least 20 dB below the pass-band value. The application of narrow band detection is to isolate bandwidths of the frequency spectrum that contains strong PD frequency spectrum.

The output response of a PD current pulse occurring in the system is a transient oscillation with positive and negative peak values of the envelope proportional to the apparent charge. The advantage of this method is that the mid-band frequency can be tweaked to the best position where distinct PD activity is present. However, it may be less accurate for location by means of TDR because of the band-pass response.

Conversely, wide band PD measuring systems have high sampling rates to capture a wide range of frequency spectrum. The detection circuits in combination with the coupling devices is characterised by the transfer impedance $Z(f)$ with fixed values within the range of frequency spectrum. The choice of bandwidth may vary from application to application. For example, frequency range may go up to 10 MHz (HF) in transformer systems, up to 200MHz (VHF) in cable systems [Tian 2003], or up to 2GHz (UHF) for GIS systems [Judd 1998]. The differences in the frequency used takes into account the distance between the discharge and the measuring sensor. In the transformer case, 10 MHz is sufficient for measuring the discharge signals. The VHF technique are specifically applied to the cable joints, hence the discharge distance is very close to the sensors, while in GIS systems UHF sampling rates are used because the sensor can be at the point of the discharge origin. Therefore, very high sampling rates are required to capture the sharp rise times and the duration of the discharge. Generally, the response of these systems to a PD current pulse is a non-oscillating pulse (overdamped). The apparent charge and polarity of the PD current pulse can be determined from this response The advantage of wide band detection systems is the majority of the PD frequency spectrum can be captured and the measured signal provides a better representation of the actual PD source. There is an increasing trend to higher frequency bandwidth monitoring and it is an important specification in the PD description. Subsequently, applying TDR techniques on these signals will produce more accurate results compared to the narrow band method. The drawback is that with higher frequency resolutions, data sizes increase and there may be an increase in the noise interference, depending on the noise levels present at the measurement site.

3.2.2 PD Propagation and Cable Effects

Previously, in section 2.5 the definition of the attenuation and dispersion effects in the cable were presented. In this section, the consequences of these phenomena are taken into account. The method of quantifying the measured pulses and the error in the location is further elaborated.

3.2.2.1 Quantifying Pulses in Signals

The PD pulses are usually measured in voltage form. The apparent charge of the discharge is calculated using the voltage signals. In most cases, a calibration is required to determine the apparent charge of the PD signal and the minimum discharge level specified by the IEC [IEC 1981]. Calibration is performed by injection of a known pulse from one end of the cable and measuring the signal at the other end. This is usually carried out on the measurement system and the cable by injecting a step pulse. The losses of the step pulse will provide the attenuation and dispersion characteristics of the cable. Due to the varying pulse shapes and sizes, it is crucial that a fixed standard of quantifying a pulse be employed. The IEEE standard definition for 2-state pulse is illustrated in Figure 3.3 [Paulter 2002]. In general, PD pulses will have 3-states sequence and it is common to either note the location of the pulse (relative to the phase) after the transition occurrence time or at the peak of the epoch.

3.3.3 Errors in PD Location

When a PD occurs within the cable, it will propagate towards the ends of the cables [Ahmed 1998]. The amplitude of a PD pulse propagating towards the ends of the cables will decrease due to the resistance and dielectric losses. Generally, the origin of the PD pulse will affect the PD location process because of the pulse propagating distance from the origin to the measurement system. This applies to both

the single-ended or double-ended location methods. The effect of the attenuation and dispersion causes the point of reference within the PD pulse to vary and errors are produced when synthesising these pulses. An example is illustrated in Figure 3.4 a single-ended approach; where the location process is performed by evaluating the difference between the incident and the reflected pulse. The time taken for the incident pulse from the base to the 50% reference level is t_1 and t_2 respectively. The value of t_2 will be larger t_1 because of the attenuation and dispersion occurring. There are several methods of performing these measurements such as the level crossing method, generalised cross-correlators, and more sophisticated sub-space and nonlinear maximum likelihood techniques. Steiner et. al summarises the varieties of time delay estimators that can be used to locate PD in cables for instance generalised cross-correlators, level crossing method, and match filtering method [Steiner 1992]. The simplest method for time delay estimation is the level crossing where the reference point is predetermined by an amplitude threshold.

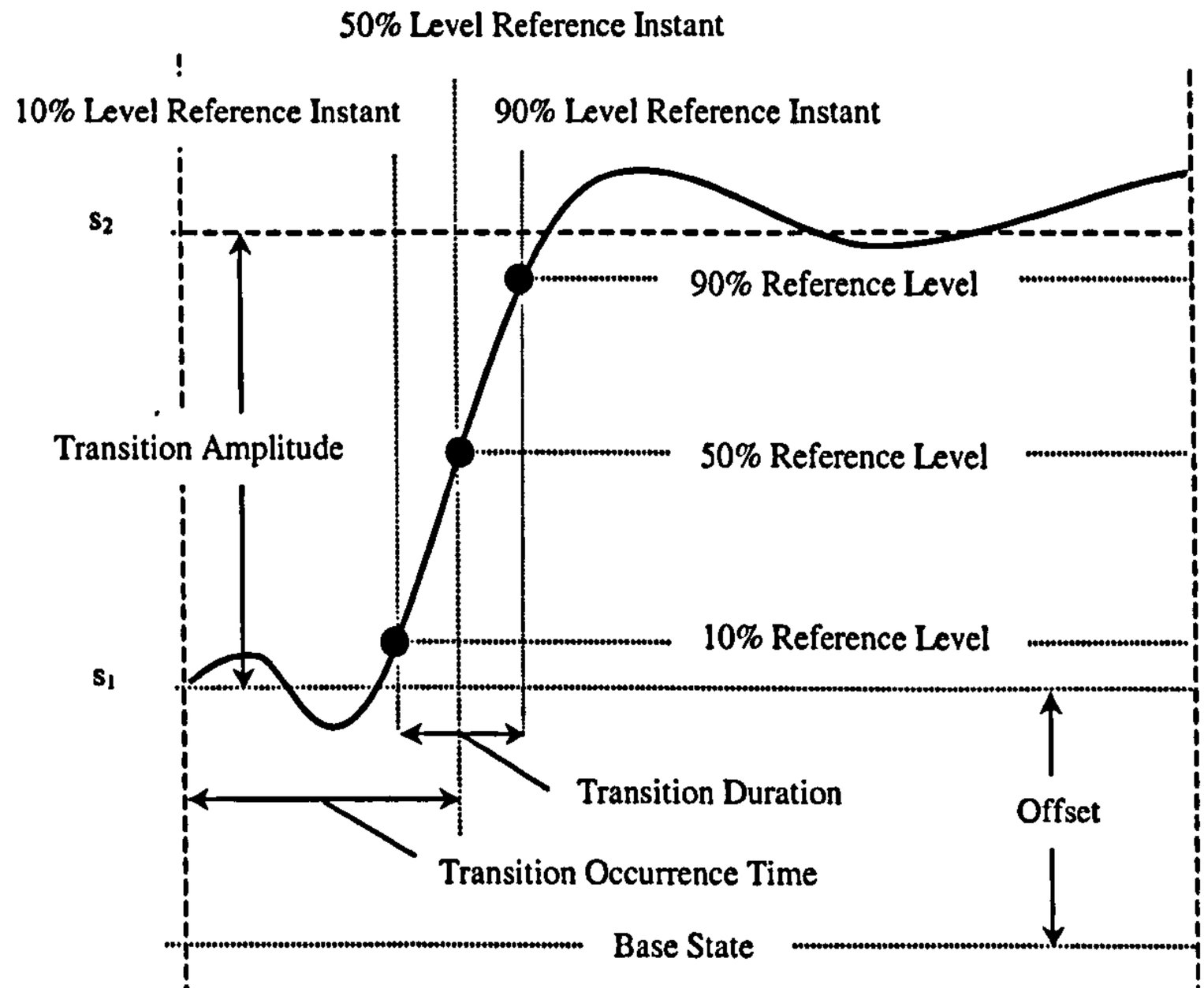

Figure 3.3: Step-like waveform for a positive going transition from state s_1 to state s_2 [Paulter 2002]

In the time domain, the high frequency content of the reflected pulse will be attenuated [Kreuger 1993, Boggs 1996]. The pulse width of the reflected pulse is wider and the height of the pulse is reduced. It will also have a longer rise time compared to the incident pulse and the maximum point of the main pulse epoch will deviate. Hence, the evaluation of the distances will contain errors when using the maxima point. In a cable fault location technique, the reference point is made at the time the pulse is initiated i.e. at the relative zero crossing of the pulse [Navaneethan 2001].

Another cause of errors is pulse superposition that may occur for reflected PD pulses when the pulses originate from the far end of the cable. However, this is typical for only single-ended systems. The pulse that originates from the far end of the cable will have reflections closer to the incident pulse. It is also known as the blind length of the cable [Kreuger 1993]. If superposition occurs in PD pulses with oscillatory natures, locating the reflected pulse may not be possible. This depends on the PD signal structure for instance its time duration and the pulse shape whether oscillatory or non-oscillatory. Oscillatory pulses will tend to have a longer duration than non-oscillatory pulses, hence more likely to be superimposed.

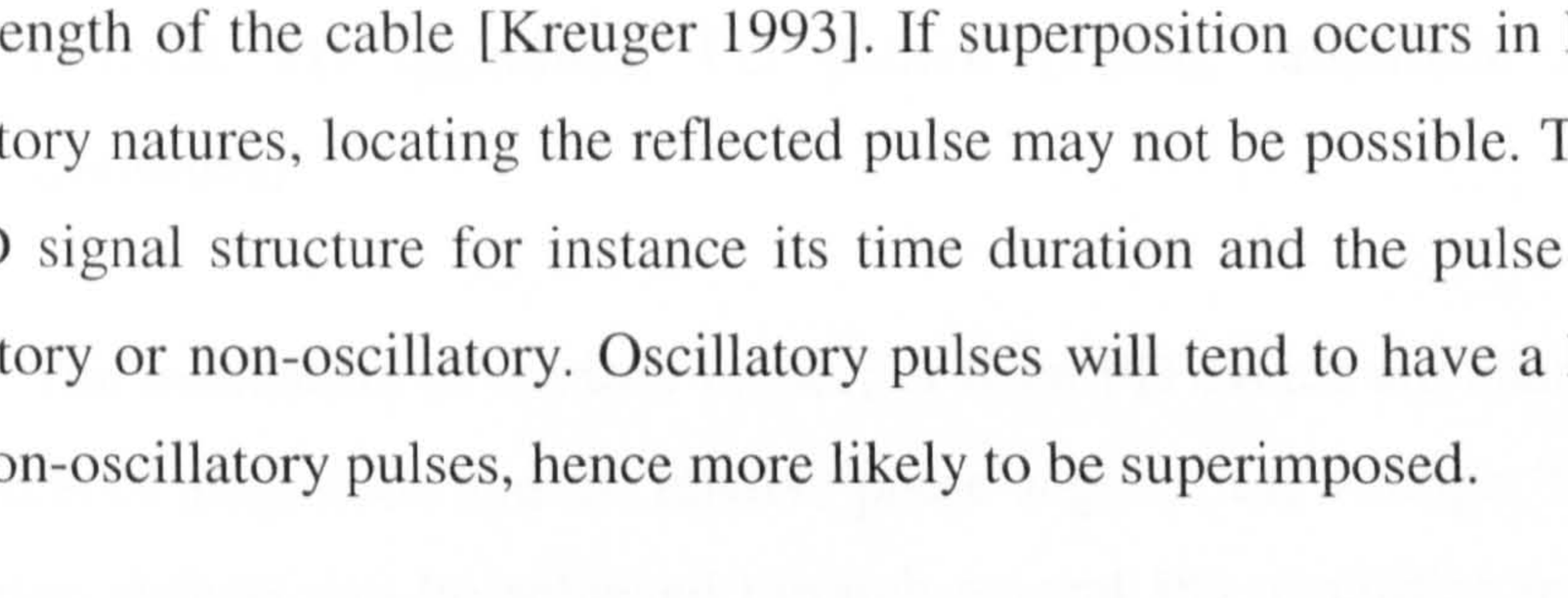

Figure 3.4: Pulse distortion of incident and reflected PD pulse

3.3 Knowledge Rules for Data Interpretation

3.3.1 Partial Discharge Quantities

Partial discharges occur repetitively within the power frequency cycle for both positive and negative half of the voltage cycle. Factors that affect the rate of discharges are the type of discharges, the size of the voids and orientations [McAllister 1997], number of discharge sources, the type of cable and its temperature. These discharge characteristics can be quantified systematically and can be divided into two main groups:

- Basic PD Quantities (according to IEC 60270 [IEC 1981])
- Derived PD quantities, PD pattern (Phase, amplitude related derived quantities)

The evaluation of random properties from PD events are characterised by the variations of magnitude and the relative phase angle of the voltage. The diagnosis on insulation defects can be achieved through several PD quantities indicating the PD recurrence and classical methods of evaluating PD [Cigre 2002]. Recent advances in computer-aided systems and data capturing equipment, facilitates the opportunity to store large amount of data and the capability of post processing. Complete high resolution and long durations of data recordings are acquired such that thorough analysis and further diagnostics of insulating systems may be performed. Basic quantities and derived PD quantities can be reproduced from the data. Pattern recognition algorithms are also developed through the large volumes of data.

3.3.1.1 Basic Quantities

PD signals are processed using the frequency domain or the time domain. The results of the processing are the quantities that are determined are summarized in Table 3.1. The exact definition of each parameter is available from the IEC 60270

[IEC 1981]. These are the parameters that are usually observed during the diagnostics of the cable. In cases where voltage signals are measured, the parameters have to be correctly interpreted and converted; usually requiring the cable and the instruments to be first calibrated.

Parameter	Units
Discharge magnitude, q_i	[pC], [nC], [μC]
PD pulse amplitude	μV and mV
Discharge phase, ϕ_I	[ms]
PD intensity (repetition rate), N	-
Time between successive PD pulses, Δt	[s]
Inception voltage, V_i	[kV]
Residue voltage, V_r	[kV]
PD pulse shape	V(t)
PD pulse spectrum	DBm

Table 3.1: List of Basic PD Quantities

A combination of one or more of these quantities is used to produce more complex quantities used as diagnostic tools. The derived quantities are usually in two-dimensional or three-dimensional formats, which can be in time functions, histograms or patterns of PD.

3.3.1.2 Derived Quantities

The PD characteristics are known to be complex and depending on a wide range of conditions at the discharge environment, for example the thermal or the electrical stress conditions. The derived quantities are often associated with observing a particular PD quantity over a period of time or a function of the applied electric field. The outcome of this are usually illustrated in 2-dimensional or 3-dimensional phase resolved patterns. For instance, the N-ϕ-q patterns where the PD

pulse intensity is taken against the discharge phase and the apparent charge quantity, depicted in Figure 3.5. It has been found that different phase resolved patterns can be used to differentiate the types of PD sources for example corona discharge, void discharge and surface discharges [Hudon 1995, Heitz 1999]. Other examples of derived quantities the inception voltage conditions (PD type dependent), changes in electrical or thermal loads over monitored period. However, these will only indicate the temporary characteristics of PD and does not indicate the direct relation to the insulation degradation.

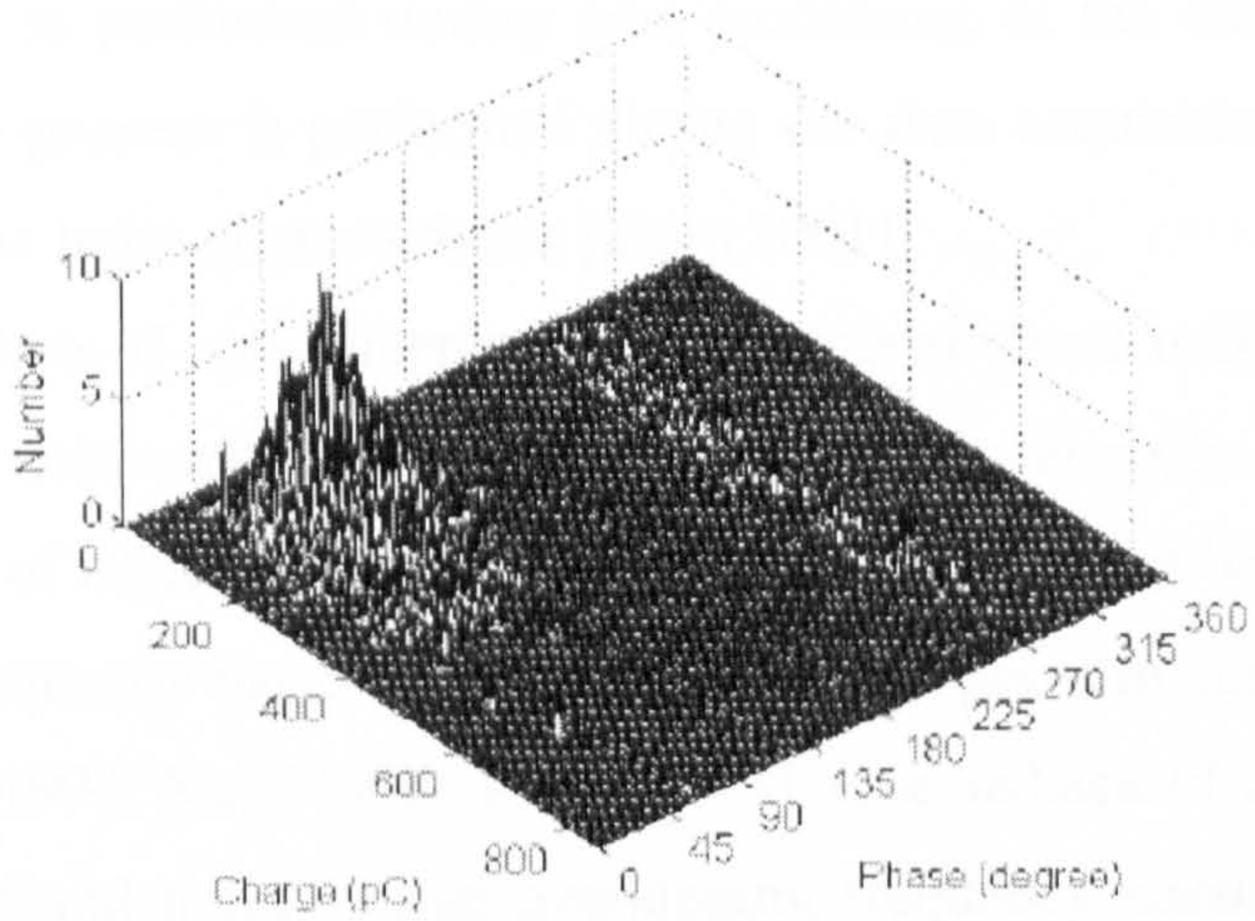

Figure 3.5: Example of N-ϕ-q plot generated from liquid nitrogen through a plane electrode [Swaffield 2004]

In some instances, experimental procedures are specially designed to generate some derived quantities within high voltage laboratories. Kim et.al utilised the N-ϕ-q patterns to observe the PD characteristics of aging dielectric insulation [Kim 2004]. These patterns can also commonly combined with fuzzy based or neural network based signal-processing techniques to classify the type of PD activity [Candela 2000, Salama 2000, Contin 2002, Tu 2002].

3.4 Applied Signal Processing for PD Diagnostics

The major signal processing challenges for PD diagnostics come from the online diagnostics where the noise interference is significantly higher. The noise

interference may completely mask the small amplitudes of the PD pulses and hamper PD detection. Another challenge for online diagnostics is to isolate the pulses originating within the cable. Signals originating beyond the cable are regarded as noise. Since the connections are live, there will be external sources of signals propagating into the cable and measured into the measuring devices.

Various techniques of signal processing have been applied to counter these challenges and in this section they will be presented. Noise reduction methods were classified into the open-loop or the close-loop approach, where in the former the noise reduction is performed during post processing of the data and the latter the noise reduction process is performed during the data acquisition period with prior knowledge to the noise characteristics [Shim 2001].

One source of noise interference is the narrowband noise. Common sources of narrowband noise are radio interference usually local radio channels within the area. Rejection of narrowband noise using digital notch filters has been implemented to reject the frequency bands within the frequency spectrum containing narrowband noise [Nagesh 1994, Kopf 1995, Werle 2002]. One setback of using notch filters to remove narrowband noise is that overlapping frequency bands of the PD will be removed during the process. In cases where many bands of narrowband noise are present, then much of the PD spectral characteristics may be removed. Digital filters can also be used to enhance PD signals by band-pass filtering, where known PD spectral characteristics can be selected for processing [Steiner 1992].

Match filtering has also been applied for PD detection enhancement. Match filters are designed specifically to filter out spatial components of a signal that is similar to the match filter characteristics, whereby the SNR at the output is maximized [Ifeachor 1999]. However, the PD signal has to be known prior to the usage of match filters. The PD signals can be simulated in the high voltage laboratories and the results generated are used to design the match filters. In some instances, a match filter bank is applied to the signals to address the variations of the PD pulse undergoing attenuation and dispersion along the cable [Veen 2003]. The cable must firstly be calibrated, in order to determine the loss parameters. The matched filter bank is created based on the PD pulse originating from the cable joint

locations. This is because PD has high probability of occurring from them [Cigre 2002]. This method has been successfully applied by using double-ended data acquisition method through accessible points at the cable terminations [Wielen 2004]. The match filter technique was also implemented in a device known as the transponder [Matthieu 2003], as described in Section 2.5.

The variations of stochastic PD properties for instance the type of PD, repetition rate and amplitudes over time generate different PD signatures. These PD signatures can be used to determine the type of PD occurring within the equipment. PD pattern analysis and classification is performed based on the knowledge of PD signatures through various advanced signal-processing techniques. Majority of these techniques involve the application of fuzzy reasoning and neural networks. These techniques may include a combination of other signal processing techniques to form hybrid algorithms that are used for pattern recognition. For instance, applying fuzzy reasoning, neural networks and wavelets [Carminati 2001], neural networks and wavelets [Tu 2002, Smith 2002]. PD pattern recognition can be performed by pulse height observation over a period of time [Contin 2002, Cavallini 2003]. The outcome of which may be intensity histograms, phase resolved patterns or time domain signals. Different types of PD will exhibit certain characteristics and can be determined from these results. In another approach, the statistical and fractal parameters were utilised through a neural network for PD recognition [Candela 2000].

Several important factors associated with PD pattern recognition are that large volumes of data are usually required to train the algorithms to work effectively and that known sources of PD are required. Laboratory simulations can produce PD signatures that are used as approximations for field data, Hence, in order to accurately classify field data effectively, experimental procedures have to be thoroughly examined and the parameters have to be as identical to the cable if possible.

3.5 Wavelet-based Algorithms for PD Analysis

3.5.1 Introduction to Wavelet Transforms

The Wavelet Transform (WT) was evolved from the realisation of the limitations of the Fourier Transform (FT). As the FT performed the analysis of the signal in the frequency domain, time localisation of the frequency was not permissible. Hence, the analysis of time-frequency components was unavailable with the FT method. Modifications were made to the Fourier method, to enable a means of localisation of both time and frequency through the Short-Time-Fourier-Transform (STFT) introduced by Gabor in 1946 [Polikar 1998]. Windowing is introduced to the conventional FT to map the signal into a two dimensional map in time and frequency function. This provides a limited precision of both domains, depending on the size of the window. However, the STFT was bounded by Heisenberg's Uncertainty Principle, which states that,

$$\Delta f \cdot T \geq 1 \qquad (3.1)$$

where Δf and T represent the resolutions in frequency and time respectively. When a window size is chosen, this window remains the same for all frequencies. If good time localisation is present, frequency resolution is less accurate and vice versa. This limitation is significantly disadvantageous for analysing non-stationary signals, especially transient type signals.

Hence, logically WT was introduced in replacement of the STFT. It has similarities with the FT and the STFT, by which instead of having the signal weighted by a series of sines and cosines, the signal values are weighted by wavelet functions. A wavelet is a waveform that has a finite duration and is localized with an average value of zero [Misitti 2000]. All wavelet functions are derived from a basic (mother) wavelet. The WT breaks up the signal into scaled and shifted versions of the original or mother wavelet. At low scales, a high frequency resolution is obtained with a wide selection of time base. The opposite is achieved for high scales where good time localization is achieved.

Wavelets have their unique properties that are attractive for analysing signals. Applications of wavelets include detection of events, transients, regularity of a signal, compression, de-noising and more. Analysing wavelets are classified to their family of wavelets, which have properties such as singularity, regularity, time and frequency localization, orthogonal, and compactly supported wavelets [Mallat 1989, Daubechies 1994]. Figure 3.6 illustrates several examples of wavelet functions.

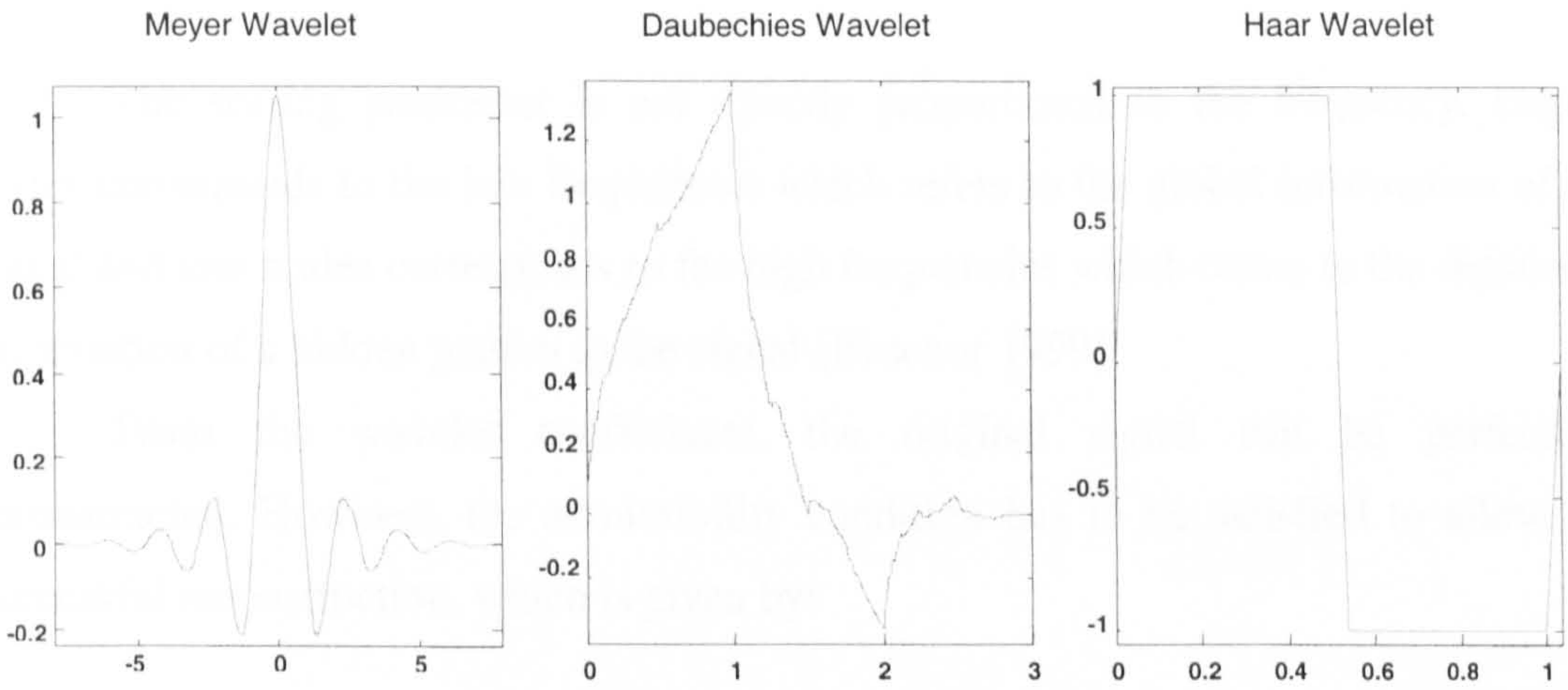

Figure 3.6 : Meyer Wavelet , Daubechies Wavelet, Haar Wavelet [Misiti 2000]

3.5.2 Types of Wavelet Transform and Implementation

3.5.2.2 Continuous Wavelet Transform

The family of wavelet functions are derived from the mother wavelet, $\Psi(t) \in L^2(\Re)$, by performing scaling and shifting operations on the $\Psi(t)$ given by:

$$\psi_{\tau,s} = \frac{1}{\sqrt{s}}\psi\left(\frac{t-\tau}{s}\right) \tag{3.2}$$

where s and $\tau \in \Re$ ($s > 0$) are the scaling factor and shifting factor.

The Continuous Wavelet Transform (CWT) produces wavelet coefficients from the product of the scaled and shifted versions of the mother wavelet convolved

with the signal. The wavelet coefficients are decomposed into frequency scales, which are weighted by the similarities or correlation of the wavelet function and the input signal. The CWT is defined as:

$$CWT_x^{\psi}(\tau,s) = \Psi_x^{\psi}(\tau,s) = \frac{1}{\sqrt{s}}\int_{-\infty}^{+\infty} x(t).\psi^*\left(\frac{t-\tau}{s}\right)dt \qquad (3.3)$$

The scaling parameter is not directly proportional to the frequency. High scales corresponds to the low frequencies which refers to the global information of a signal and low scales corresponds to the high frequencies which refers to the detailed information of a hidden pattern in the signal [Ifeachor 1999].

From the wavelet coefficients, the original signal can be perfectly reconstructed. However, the admissibility condition has to be satisfied to allow a successful reconstruction, which is given by:

$$C_{\psi} = \int_{-\infty}^{+\infty} \frac{\left|\Psi(\omega)^2\right|}{\omega}\partial\omega < \infty \qquad (3.4)$$

where $\Psi(\omega)$ is the FT of $\Psi(t)$. Equation 3.4 implies that $\Psi(0) = 0$ and that,

$$\int_{-\infty}^{+\infty}\psi(t)dt = 0 \qquad (3.5)$$

Thus, for equation 3.5 to be satisfied the wavelet must be oscillatory and will exhibit band-pass behaviour. The reconstruction process is performed by using the equation below:

$$x(t) = \frac{1}{c_{\psi}^2}\int_s\int_{\tau}\Psi_x^{\psi}(\tau,s)\frac{1}{s^2}\psi\left(\frac{t-\tau}{s}\right)d\tau.ds \qquad (3.6)$$

3.5.2.3 Discrete Wavelet Transform

The CWT has a high level of redundancy and is impractical for large samples. Discretisation has been applied to the CWT to improve the performance of the transform, reduces the complexity and the computation time yielding the Discrete

Wavelet Transform (DWT). The DWT implement method is relatively easier and more efficient compared to the CWT. Equation 3.3 can be discretised by replacing s with s_o^j and τ with $k\tau_0$ which produces:

$$\psi_{j,k}(t) = s_o^{-j/2}\psi\left(s_o^{-j}t - k\tau_0\right) \tag{3.7}$$

For scales and shift parameters that are chosen in the powers of two are called dyadic scales and translations. Thus, the wavelet transform becomes:

$$\psi_{j,k}(t) = 2^{-j/2}\psi\left(2^{-j}t - k\right) \tag{3.8}$$

If the $\psi(j,k)$ constitutes an orthonormal basis, then the DWT is defined as:

$$x(t) = c_\psi \sum_j \sum_k \Psi_x^{\psi\ j,k} \psi_{j,k}(t) \tag{3.9}$$

The implementation of the DWT was efficiently introduced by Mallat by using the dyadic filtering schemes [Mallat 1989]. Mallat's algorithm is also known as the classical two-channel subband coder [Strang 1996, Vetterli 1995]. For this reason, the DWT is commonly referred to the decimated DWT. The algorithm is illustrated in Figure 3.7 for a two level decomposition.

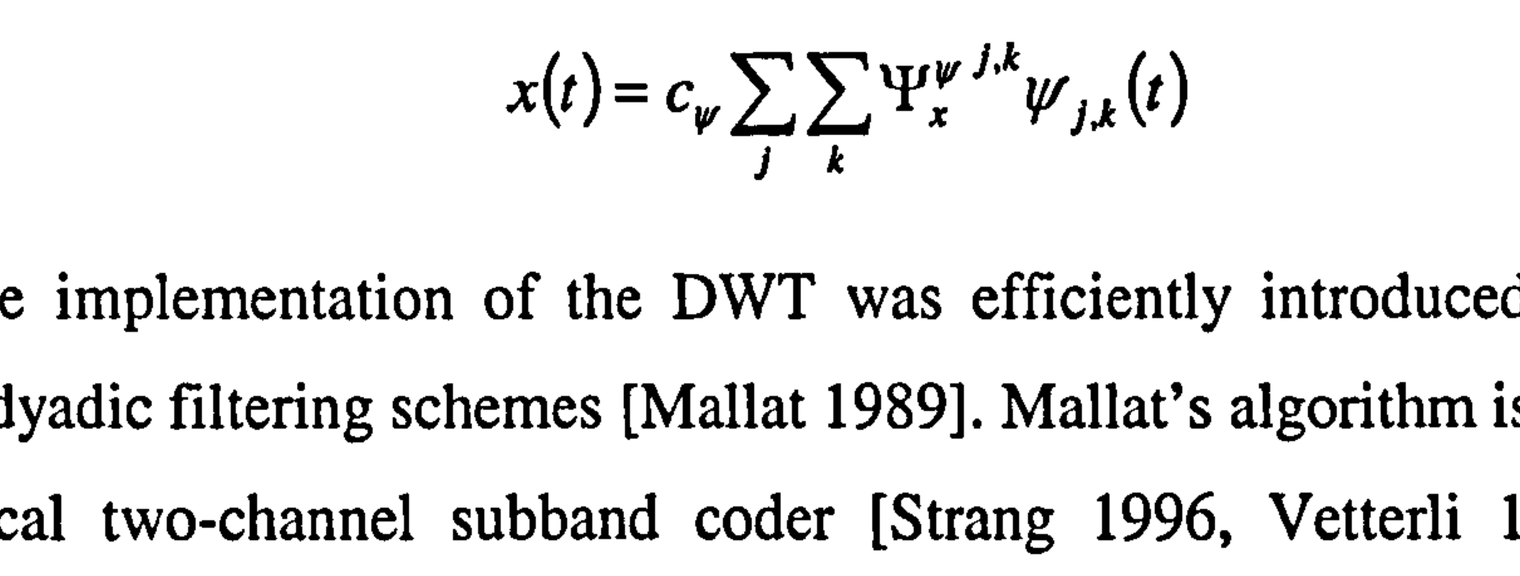

Figure 3.7: Wavelet decomposition for decimated DWT

The original signal, x[n], convolved with a high-pass filter, *G*, and a low-pass filter, *H* , of which the outputs are decimated by a factor of two. This outputs of this process yields the detail (D_k) and approximation (A_k) scales respectively, where k is the depth level of the decomposition. The decimation process produces filter coefficients that are half of the original length. The advantages of a dyadic decomposition with the decimation process is utilised because the same set of filter coefficients can be used repetitively [Ramchandran 1996]. At the next level, the output from the low-pass filter or the approximation scale is used as the substitute for the input signal. The same filtering process is carried out on the new input signal, A_k, to produce the D_{k+1} and A_{k+1}. This process is iterated until the desired or maximum level of decomposition is reached.

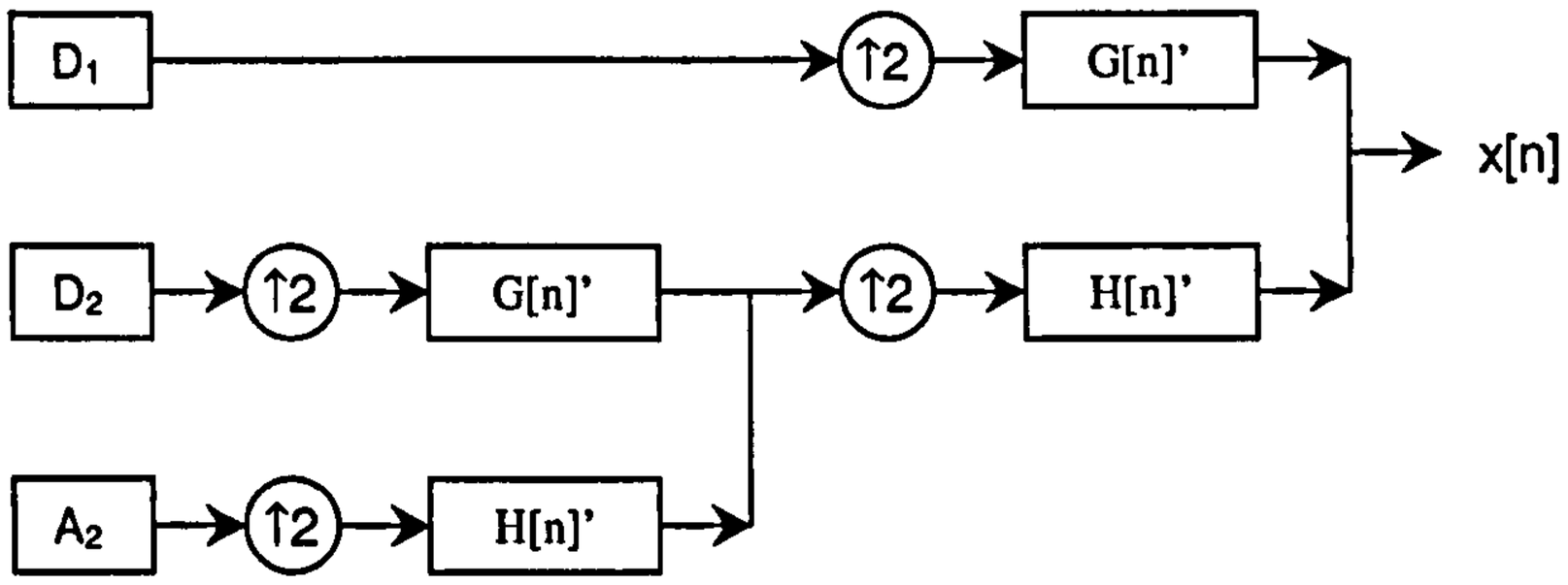

Figure 3.8: Wavelet reconstruction for decimated DWT

From the wavelet decomposition scales, the reconstruction process known as the Inverse Discrete Wavelet Transform (IDWT) is illustrated in Figure 3.8. In the same manner, the signal is reconstructed level-by-level, starting from the lowest scale. The approximation (A_k) and detail (D_k) scale are first interpolated by a factor of two, then convolved with the inverse filter G[n]' and H[n]' to form the original decomposed signal, A_{k-1}. This is iteratively repeated until the original signal is produced. The decimation process introduced at the decomposition process will cause aliasing effects. Thus, to achieve a perfect reconstruction of the signal, the filter coefficients for the decomposition and reconstruction has to be closely related. Effectively, quadrature mirror filters are employed to achieve this [Vetterli 2001].

3.5.2.4 Stationary Wavelet Transform

The Stationary Wavelet Transform (SWT) is also known as Non-Decimated Discrete Wavelet Transform, which is the redundant version of the decimated DWT. The filter bank technique is also applied for SWT implementation with some modifications. The wavelet filters used are essentially similar to the DWT with the difference that the decimation and interpolation processes are removed [Nason 1995, Mallat 1992]. Hence, the wavelet filters are updated at each level of the wavelet decomposition and reconstruction process. The block diagram representation of the wavelet decomposition is illustrated in Figure 3.9.

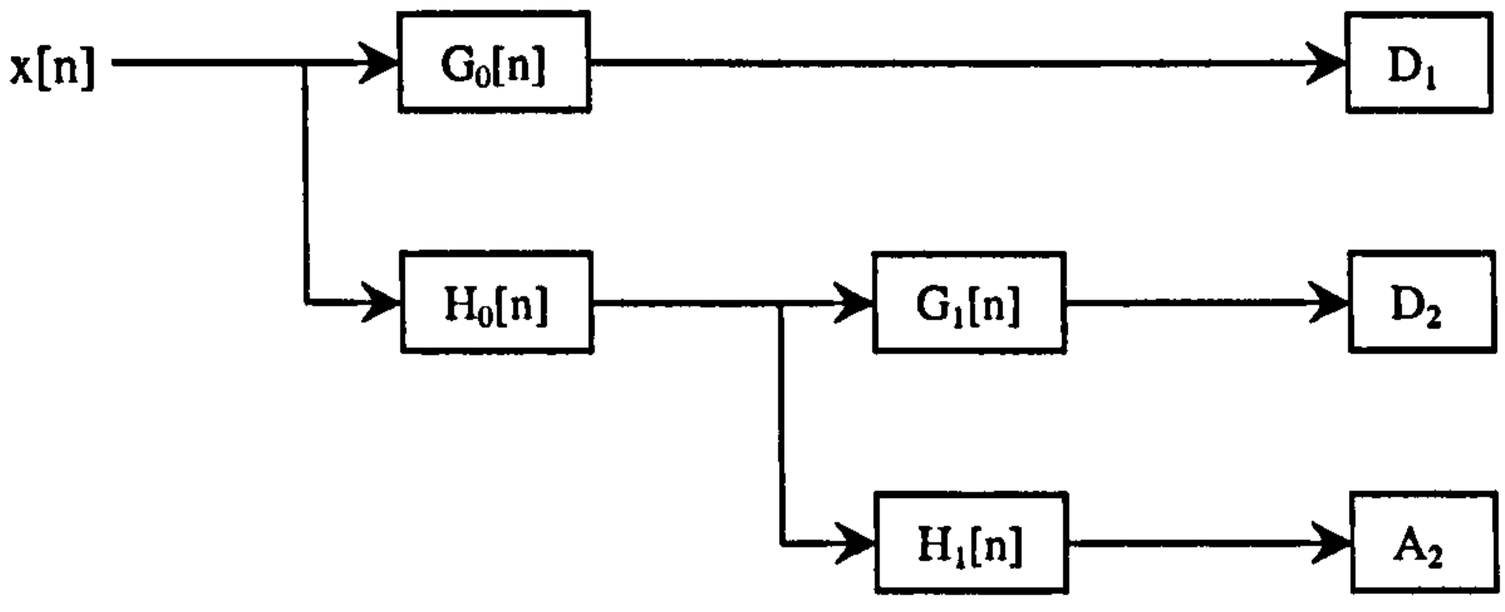

Figure 3.9: Wavelet Decomposition for SWT

At the first level, the original signal, x[n], convolved with a high-pass filter, G_0, and a low-pass filter, H_0, produces the detail and approximation scale D_1 and A_1 respectively. In the next level, the wavelet filters are modified by zero interpolation i.e. a zero is added between each filter coefficients to form the new filters. In other references, the filters are noted in a different manner where $2^{(k-1)}$ zeros are added between each filter coefficient of the original filter [Pesquet 1995, Guo 1995, Coifman 1996]. Then, with the approximation of the previous level used as the new input signal the decomposition is repeated. This is iterated until the desired or maximum level of decomposition is reached.

For the reconstruction stage, the detail and approximation scales are convolved with the reconstruction filters respectively and added together to form the approximation scale at the next level. The reconstruction filters are obtained

similarly with the conventional DWT approach i.e. by using the quad-mirror filter technique. The difference is at the k^{th} level the filter has $2^{(k-1)}$ zeros inserted between each of the original reconstruction filter coefficients. The filtering and adding process is iterated until the new reconstructed signal is obtained. An example of a two level reconstruction process is illustrated in Figure 3.10.

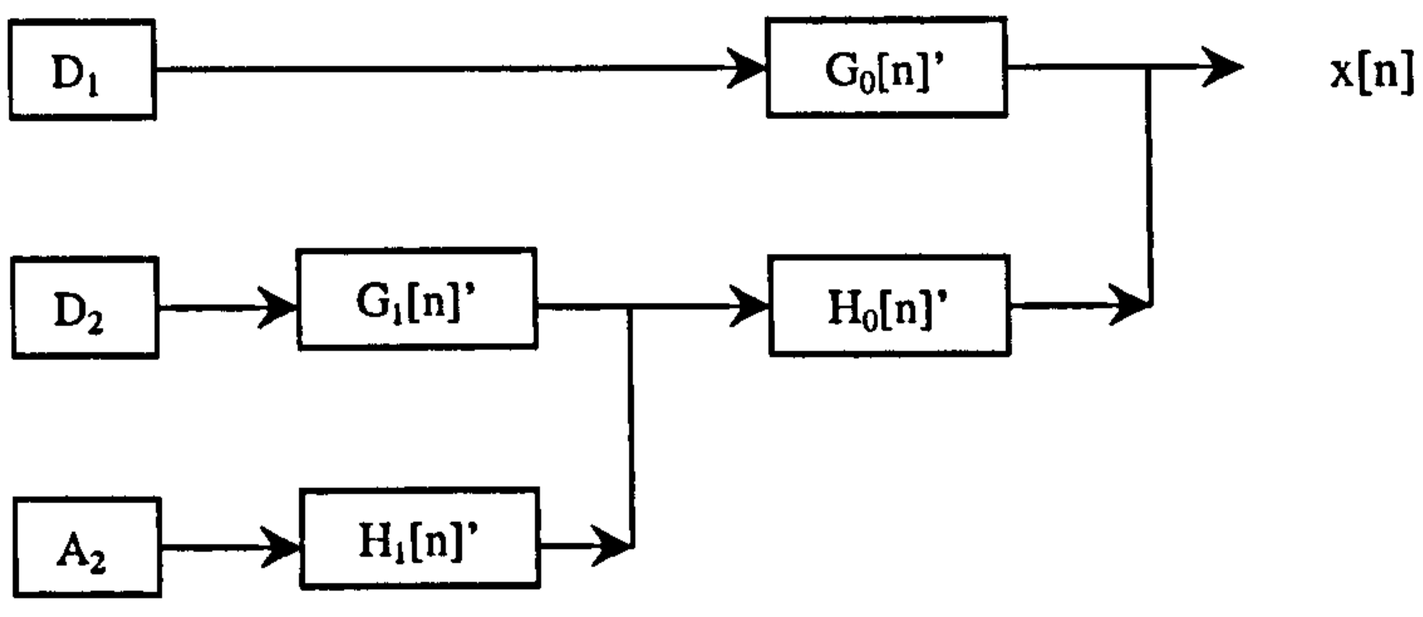

Figure 3.10: Wavelet reconstruction for SWT

3.5.3 Wavelet De-Noising

The "important" part of a signal can be recovered or enhanced by suppressing the unwanted signal levels or noise through wavelet de-noising. Wavelet de-noising is performed by applying thresholds on the wavelet decomposition to remove or reduce elements that contain characteristics of noise. The basic procedure for wavelet denoising is to compute the wavelet decomposition of the signal, applying the selected threshold, and the de-noising procedure is complete after the threshold wavelet coefficients are reconstructed through the inverse wavelet transform [Donoho 1995a]. Thresholds types are divided to hard and soft thresholding, or *VisuShrink* and *SureShrink* respectively [Donoho 1995b]. The differences between both the threshold methods are illustrated through Figure 3.11. The outputs of which, are as follows [Strang 1996]:

$$Y(t) = \begin{cases} x(t), & |x(t)| > \delta \\ 0, & |x(t)| \le \delta \end{cases} \text{ Hard Thresholding}$$

$$Y(t) = \begin{cases} sign(x(t))(|x(t)| - \delta), & |x(t)| > \delta \\ 0, & |x(t)| \leq \delta \end{cases} \quad \text{Soft Thresholding}$$

Hard thresholding is described as the process of setting to zero the absolute values that are lower than the threshold. Soft thresholding is similar to hard thresholding except with an addition of shrinking the non-zero values above the threshold value towards zero, as shown in Figure 3.11(c). Hard thresholding method creates discontinuities at borders of the zeroed values whilst soft thresholding does not. Donoho claims that soft thresholding provides a visually more pleasing estimate than hard thresholding [Donoho 1994], but asymptotically the optimal thresholds give similar results. However, in some instances it may be beneficial to use hard thresholding to retain the original peak within a signal.

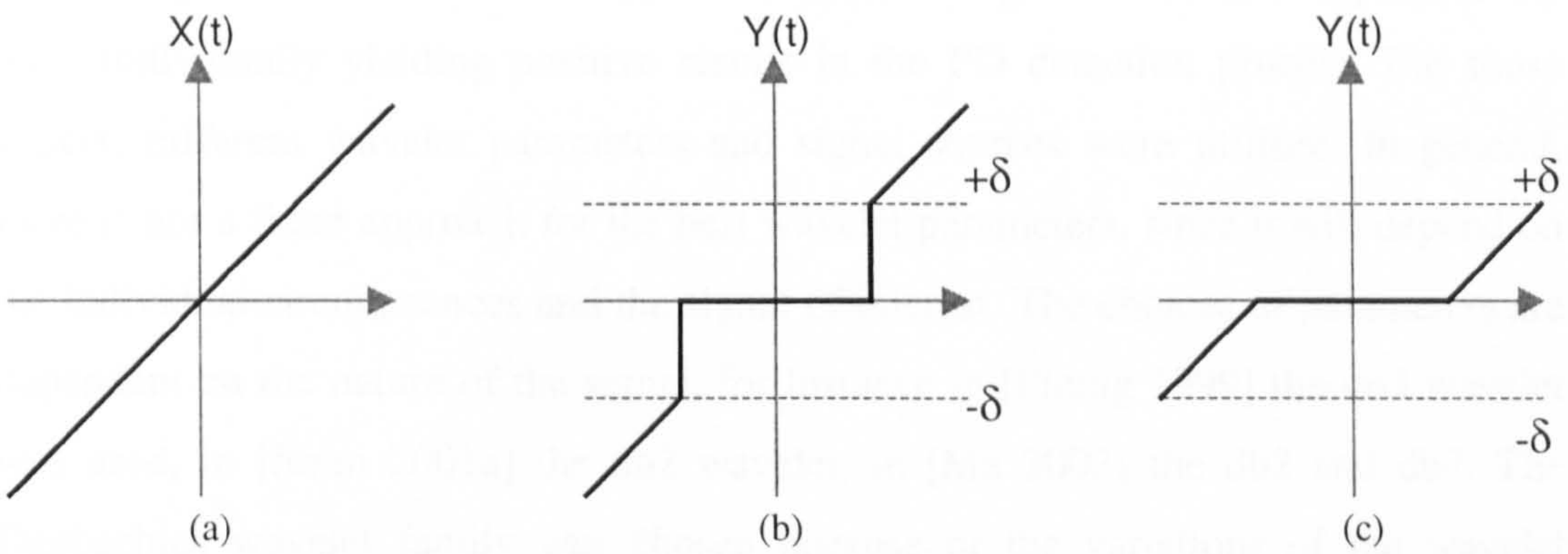

Figure 3.11: Types of threshold (a) Original signal (b) Hard thresholding (c) Soft thresholding with value of δ.

The next important point is the threshold selection rules. The performances of each thresholding rule depend on the statistical properties of the sample signal. Hence, the advantages and disadvantages of the rules are evaluated individually depending on case. Since Donoho and Johnstone, there are other variations of threshold selection algorithms, which are improved versions through additions or combinations with other algorithms, for example, Non-Negative Garrote [Gao 1998], Generalised Cross Validation [Jansen 1997], Stein's Unbiased Risk Estimate (SURE)

[Donoho 1995b], Bayesian Approach [Abramovich 1998], Minimax [Krim 2000], Fixed Threshold, or a combination or more [Misiti 2000].

3.5.4 Applied Wavelets to PD diagnostics

In the past decade, wavelet-based algorithms has emerged as an important tool for PD diagnostics and have been applied to diagnostics for various high voltage equipment. The major application of these wavelet-based techniques is for the purpose of signal de-noising. This was because the performance of the de-noising was found to be effective and enhanced the PD detection process. Many researchers have successfully applied difference wavelet-based algorithms to reduce the noise levels in the signal [Hu 1998, Phung 1999, Shim 2001a, Ma 2002, Satish 2003]. In these analysis, different wavelet types and thresholding methods were applied to the data, individually yielding positive results in the PD detection process. For those papers, different wavelet parameters and signal sources were utilised. In general, there is not a fixed approach for the best wavelet parameters, since it will depend on the individual circumstances and the signal of interest. The choices of parameters are dependent on the nature of the signal, for instance in [Phung 1999] the db3 wavelet was used, in [Shim 2001a] the db2 wavelet, in [Ma 2002] the db2 and db7. The Daubechies wavelet family was chosen because of the variations of the wavelet shapes that range from less oscillatory characteristics (db2) to higher oscillatory characteristics. In [Satish 2003], their signals were analysed and compared with the range of db family wavelets ranging from db 12, 15, 16, and 30. One common platform that these researchers have is that the type of wavelet transform utilised was the decimated DWT because of its efficient implementation method.

Other than signal de-noising, wavelet-based algorithms was also applied for other purposes such as data compression, PD classification, PD location in transformers. The acquisition of PD data often produces large data sizes due to the high sampling frequencies used. Ma et. al. found that PD data size can be compressed to 10% of its original size [Ma 2001]. This was performed by discarding

information that is conveyed within the wavelet scales based on the hard thresholding technique. However, by performing this most of the high frequency details were discarded and issues relating to the original PD signal resolution had arisen. Wavelet analysis was used for classification of multi-sourced PD's in [Lalitha 2000]. This was feasible because different sources of PD had different signal structures, which yielded PD wavelet signatures that could be distinguished. PD location was successfully applied to transformers using the UHF technique in [Yang 2003]. This is relatively different with power cables because in the transformers, PD reflection was not required. Essentially the PD location process is similar to the double-ended system used for cables as described in Section 2.8.2.

3.6 Conclusion

In this chapter, the issues pertaining to PD signals and their characteristic, and the aspects of PD signal processing were presented. Typical errors in PD location for power cables were discussed and methods of quantifying PD were presented. This included the standard basic quantities and also the derived quantities, which are commonly used to produce 2D or 3D graphical results that aid the PD interpretation procedures.

Various applied signal-processing techniques were also reviewed. Among these techniques was application of digital filtering for noise reduction and signal enhancement, for instance FIR filters, match filters and adaptive filters. Fuzzy reasoning combined with neural networks was shown to effective for PD classification.

Wavelet-based algorithms represented a major part of this chapter because of its emergence as an important diagnostic tool for PDs. The basic theory of wavelet transforms was included to provide a clear distinction of the difference in types. This will be used later in this thesis in chapter 5, where the advantages of using the non-decimated wavelet transform will be described. The application of wavelet analysis is widespread and was found to have positive results in the literature. Based on this,

the pattern of PD diagnostics is predicted to converge into hybrid algorithms that will consist of wavelets, fuzzy reasoning, higher order statistics, and neural networks.

Chapter 4 : Remote Access PD Data Acquisition (RPDAQ) System Design

4.1 Introduction

In order to address the issue of lack of field data [Shim 2001], the need was present for a new method of data acquisition. A permanent means of robust data acquisition was produced. Previously, data acquisition was carried out on field trials basis, whereby the equipment used for data acquisition consisted of separate hardware components and had to be brought to site each time. Measurements were conducted on the power cables under energised conditions. The entire process was time consuming and several problems were experienced.

The objective of this chapter is to present a new partial discharge measuring system developed in this project. In section 4.2, the problems and challenges associated with online PD data acquisition are presented. Main issues here are the protocols and safety procedures for field trials to the requirements of hardware systems. In section 4.3, the requirements for a PD data acquisition instrument is described. Section 4.4 presents the new PD acquisition unit developed. The features and description of the new PD acquisition unit (RPDAQ) is elaborated, together with the hardware architecture details and the overall system processes. The performance of the new PD acquisition unit is evaluated in Section 4.5, whereby a comparison of the developed device and the original prototype measurements are performed. The problems and limitations encountered by the new device will also be presented. Finally the conclusions are presented in section 4.6.

4.2 Problems associated with Online PD data acquisition

An agreement has to be made with the collaborating power utility company prior to the data acquisition. To achieve a successful agreement, conditions of the stringent health and safety issues have to be met. Making online connections for HV systems are serious issues and usually requires thorough evaluations before it is allowed. If allowed, connections are performed by skilled and authorised personnel. Risk assessments procedures are conducted during each site visit. This includes the protection issues of the connecting equipment, training and competence of the visiting personnel to the substation. In addition, hardware components used, the methods of connections, and its operating conditions has to qualify the integrity criteria set by the utility. This will vary from utility to utility.

The first criterion is emphasized on operating conditions during faults. If a fault should occur from the data acquisition equipment, it must not set off the cable systems protection alarm in the substation. The connection configuration depends on the layout of the protection sensors. Secondly, the data acquisition unit also has to be properly isolated from the cable circuit in any circumstances of faults, whether occurring from the cables or the data acquisition equipment.

A general rule is that at least one authorised personnel is present and closely monitoring every action that is made. This means that an engineer is required during each substation visit; including relevant protocols and paperwork. In many cases, valuable engineers time that is sacrificed.

In overall, the process of performing PD data acquisition is very time consuming and troublesome. Especially when most of these substations are remotely located, and access is restricted. Hence, it is clear that to address the need of field data for research purposes, a robust method of data acquisition is of high importance.

4.3 Requirements for PD data acquisition instrument

PD data acquisition instruments will vary depending on the type of application, for example if only for data acquisition or self contained diagnostics units. There are many companies that offer PD diagnostic services and equipment for the high voltage industry such as [Lemke], [EATech 2001], [ERA 2004], [Kema 2004], and many others. Each of these companies has developed techniques to diagnose high voltage equipment for partial discharge activity. However, the issues of online PD monitoring and diagnostics are still not addressed. Although several companies have produced equipment for online diagnostics [Russworm 2000], the challenges are still the performance of the equipment and its cost.

In each of these companies, a means of PD data acquisition has to be developed. The equipment will meet the specifications of the [IEC 60270], and have unique features. To address the problem of data acquisition, instead of purchasing these commercial products, a new data acquisition unit was proposed. The reason why the system was created rather than bought was because of the limitations of the readily available systems in the market. Some of the issues related to it were the means of protection for the system against faults, some technical features, and the safety feature. The system we required will be installed permanently at substation site in the open. Hence it would require safety features against theft and severe weather conditions. Ideally, the unit must have the capability of remote control and access to minimise site visits. The proposed unit must be capable of performing data acquisition using the wideband technique or narrowband technique. High sampling rates are required to sufficiently capture the properties of the PD. Other important features are large storage facilities, noise reduction features, and signal enhancement capabilities. In overall, the data acquisition system must be flexible and robust.

4.4 New Partial Discharge Acquisition Unit

4.4.1 Technical specification and unique features

A new partial discharge acquisition unit has been developed to address the issues of field data and the access issues associated with it. The unit utilises filter concepts, such as high-pass and band-pass filters, which have produced good results [Shim 2000]. In addition, several enhancements were added by exploiting the advances of technology in modern communications and digitised equipment to produce a new partial discharge acquisition unit. The key features of the system are as follows:

- Fully remote controlled system; allows user to operate system either on-site or remotely
- High sampling rates up to 100MS/sec with adequate amplitude resolution of 14 bits.
- Signal conditioning features that offers choices of noise reduction and PD signal enhancements in hardware and potentially extendable in software.
- Large storage capacity and robustness in retrieval of data.
- Flexible and robust; PC-based system which can be customised according to preferences.

4.4.2 Hardware Architecture

The remote controlled partial discharge acquisition unit (RPDAQ) was developed to facilitate easier acquisition of PD data. At this stage, the main objective of the RPDAQ is to facilitate online field data. In future, enhancements will be added to produce an independent system for PD detection and location for HV underground cables. The block diagram of the RPDAQ is depicted in Figure 4.1.

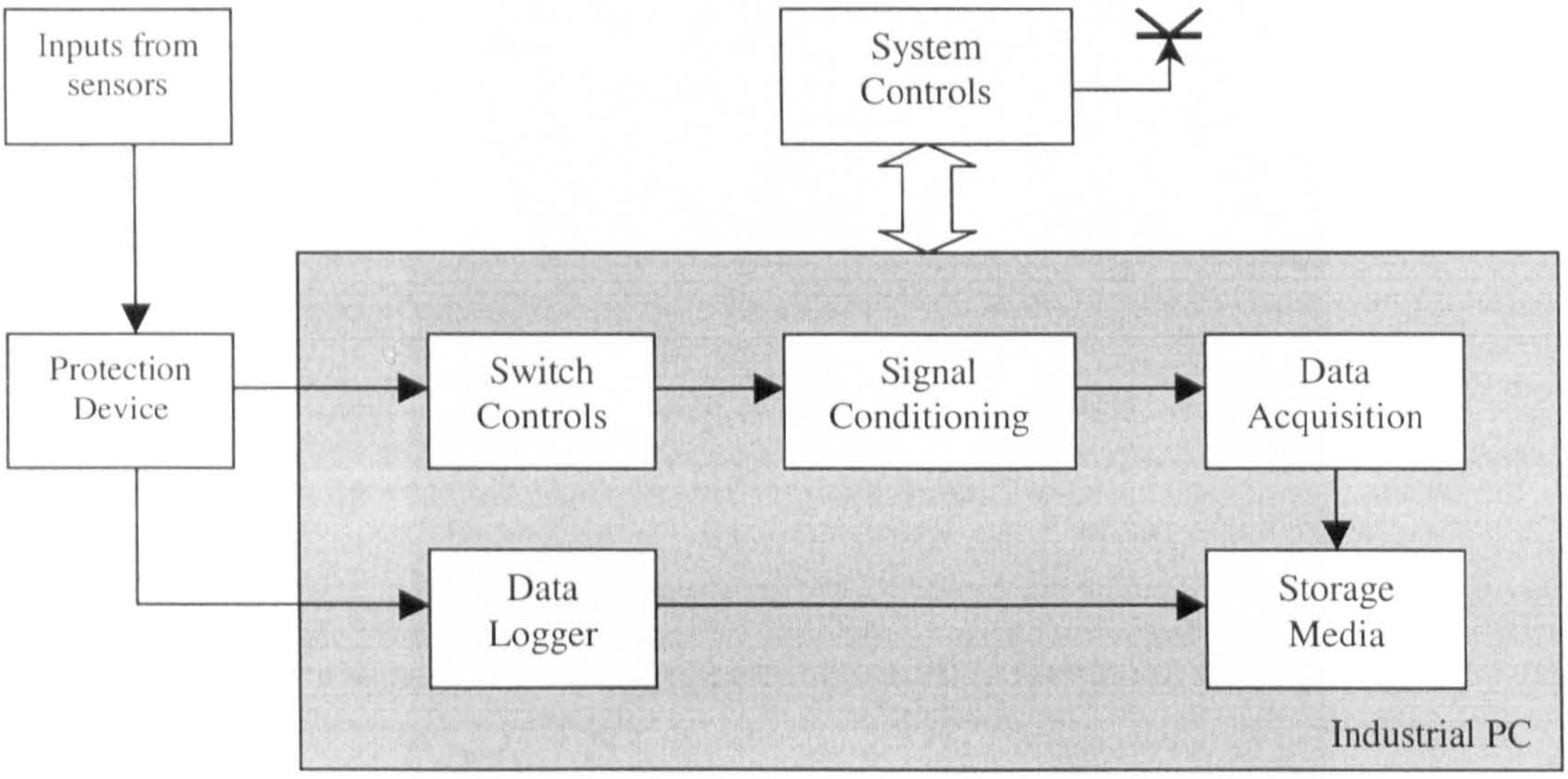

Figure 4.1 Block diagram for RPDAQ

The RPDAQ is a PC-based system that is fully equipped with remote control features. This allows a user to operate the system either on-site or remotely. Figure 4.2 depicts the picture of the RPDAQ during on-site testing. A laptop is used as the user interface to control and monitor the signal acquisition in progress. Remote control access is performed either through a network connection or a modem connection. These are the advantages of using a PC-based system i.e. the flexibility and the capability to customise the data acquisition parameters and analysis. Specified acquisition parameters are stored in fixed text files, and are uploaded to the RPDAQ. The acquired data can be accumulated for days or weeks, depending on the user defined frequency and quantity of data acquisition.

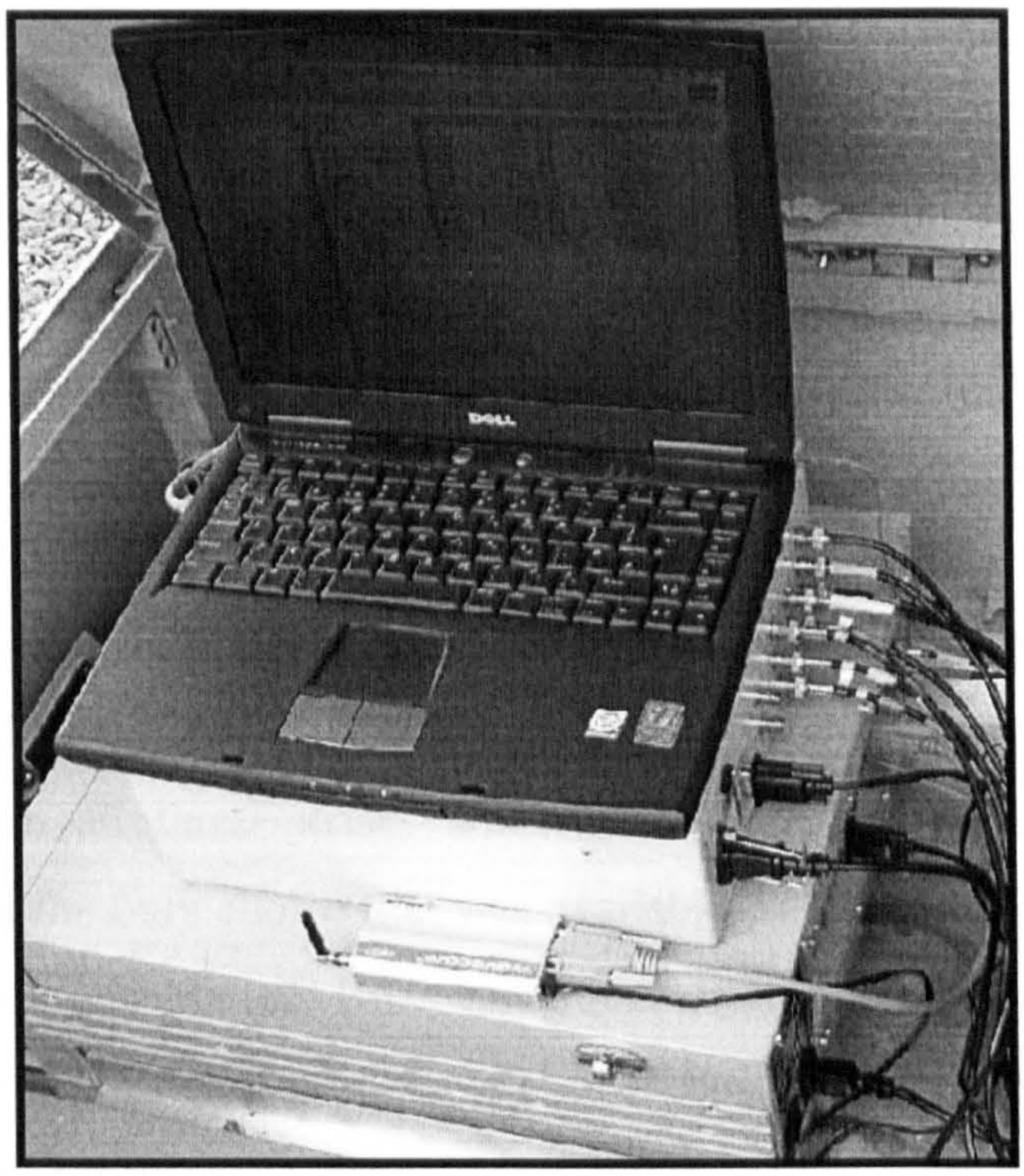

Figure 4.2: Picture of RPDAQ during On-site testing

4.4.2.1 Inputs from sensors

Sensors usually either capacitive coupled or inductively coupled to measure signals from HV equipment. The advantages of using inductive couplers over capacitive couplers for online are clearly described in [Wielen 2003a]. Inductive coupling method using current transformer (CT) was the preferred method for the RPDAQ. In cases of HV underground cables, limited access points will govern the connection configuration to the RPDAQ. Phung et. al. [Phung 1999], made the CT connections to the sheath of the cable, whilst Matthieu [Matthieu 2003], made connections to the earth line of the cable. In both cases, the types of cables used were 1-phase cables and accessible points were available.

However, when working with 33kV networks in Scotland, most of the cable types are 3-phase cables that share a common earth [ScottishPower 2003]. If the CT connections were made to the earth, the signal amplitudes are too small and will be superimposed from all three phases, which complicates the interpretation of data especially PD detection.

An alternative was to use the CT readily installed at the substation. These CT are used for protection purposes and conforms to the British Standards [BS3938 1973]. It usually has low frequency responses up to 100kHz since it was designed for protection monitoring purposes. Although the CT was not designed for high frequency responses, they were also not designed to have a band limit. Hence, high frequency components are still measurable from these CT through its stray capacitances. This stray capacitance will become dominant at frequencies above the self-resonant frequency of the CT. For the CT used in the present work, no data was available, which would allow any quantitative assessment of this capacitive coupling. The CT outputs from all three phases are connected to the protection device. Nevertheless this was the only choice that was available for this project. Alternative sensor connections were prohibited. However, the performance of the RPDAQ will be more reliable and precise with alternative high frequency inductive couplers can be used in replacement for this CT.

4.4.2.2 Protection Device

The collaborating power utility required a protection device as the interface between the sensors and the data acquisition unit. In general, the design of the protection device will vary and is custom built according to their specific requirements. The primary function of the protection device is to isolate the cable circuit and the data acquisition system in any case of fault from the RPDAQ or a surge over-voltage occurring in the cable circuit. It was designed to protect the alarm system of the utility company rather than the RPDAQ itself. If any fault should occur from the RPDAQ system, triggering the alarm system of the utility is prevented. The CT at the substation is connected a measurement device for the alarm system. It has very low impedance. The RPDAQ is connected in parallel to this measurement device. Therefore the RPDAQ is required to have high input impedance. Hence, the failsafe mode was required to be open circuit; otherwise the alarm will be triggered if the CT output is short-circuited. A block diagram that represents the connection between the RPDAQ and to the CT is depicted in Figure A1 (see Appendix A).

Figure 4.3 depicts the picture of the protection box, with all the co-axial connections made. The box is situated within the switchyard cabinet, where the accessible points to the CT are situated. The circuit diagram for the protection device is depicted in Figure 4.4.

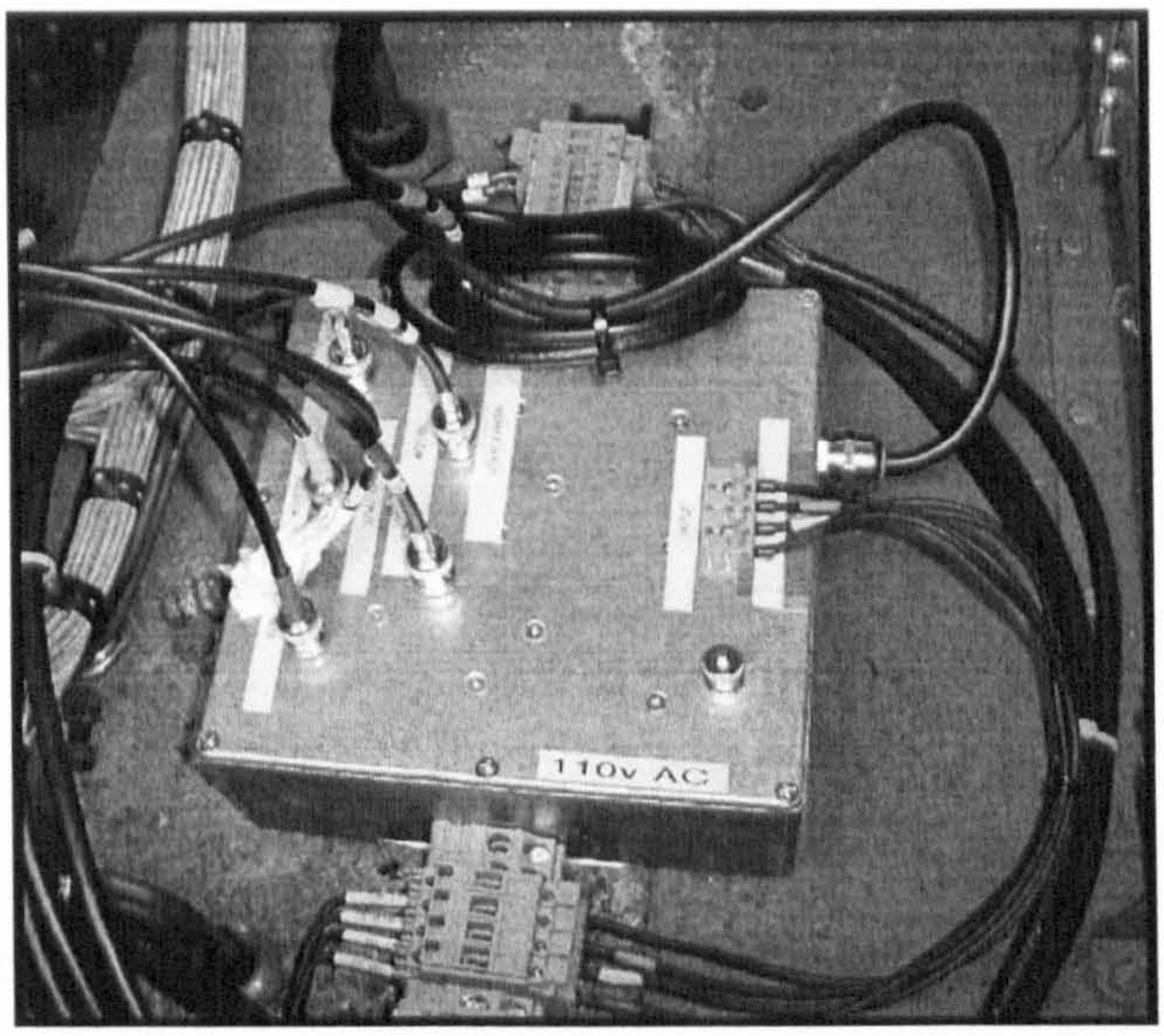

Figure 4.3: Picture of Protection Box at site, with connections made

The protection device has an input impedance of 1kΩ and inverting amplifier circuit has unity gain and bandwidth up to 60 MHz. In a case of a surge over-voltage the op-amp of the amplifier circuit will blow. A limiting factor to the system is that the protection device can only be blown once. After one surge, the protection device no longer function to protect the remaining circuitry connected to it. However, there is a fuse included before the protection circuitry to disconnect the data acquisition device from the CT sensors if a surge occurs.

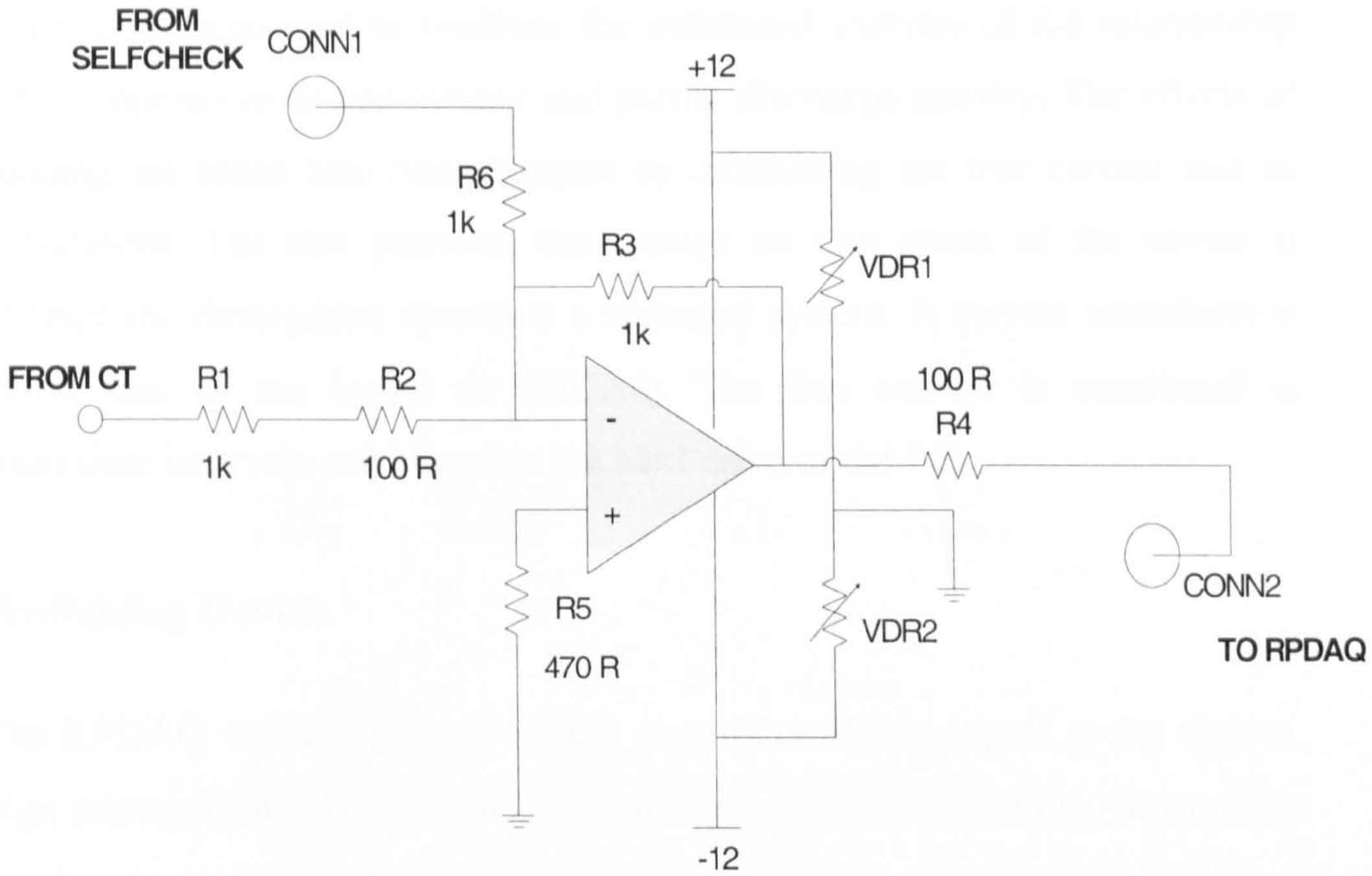

Figure 4.4: Circuit diagram for protection device

In order to check if the protection device is still functioning remotely, a "self-check" system was developed. The self-check operation is performed before each data acquisition is initiated, to ensure the integrity of the protection device. A burst of pulses is transmitted from the signal-conditioning unit into the inputs of the inverting amplifier. If the op-amp has failed, the output of the signal will not be inverted; hence the failure of the op-amp can be detected by the observation of the self-check signals.

4.4.2.3 Data Logger

Partial discharge activity is related to the ambient temperature of the operating cable [Dervos 1990]. The temperature is related to the load conditions of line current. When the line current increases, the amount of heat dissipated to the insulation also increases. However the exact measurement of ambient temperature of the entire length of the underground cable is usually not feasible. Hence, a current

data logger was incorporated to facilitate the estimated analysis of the relationship between the temperature or line current and partial discharge activity. The effects of current loading are taken into consideration by monitoring the line current and its loading conditions. For this purpose, the current on one phase of the circuit is sufficient since the three-phase system is a balanced system. A current transducer is connected to one of the inputs to RPDAQ. The line current is monitored at programmed time intervals and stored in the hard drive of the PC.

4.4.2.4 Switching Device

The RPDAQ was designed to accept maximum of two inputs to the system. This design strategy was chosen mainly because of economic reasons. Since there were three input sources to the system, a switching device was required. Software controlled switches were included such that up to two channels of acquisition can be selected simultaneously. For single-phase measurements, the switch is programmed to select one of the three phase inputs. Any two out of the three combinations for phase inputs can be selected for the dual phase measurements. This is performed depending on the choices of the user.

The mechanisms used for this purpose were high frequency relays that were only switched in during an acquisition process. The relays have a high isolation between contacts of 3kV, which was over the estimated amplitude of surge over-voltages. In a case where a surge travels beyond the protection circuit, the relays can withstand and protect the internal circuitry of the RPDAQ. This indirectly minimises the risk sustained from possible multiple series of surge over-voltages in the cable. The chosen input signals are then sent to signal-conditioning unit.

4.4.2.5 Signal-Conditioning Unit

The signal-conditioning unit comprises of pairs of anti-aliasing filters, amplifiers, high-pass filters and band-pass filters for the two channels. The individual components on both channels can be activated independently. If required, the filters

can be bypassed. Figure 4.5 depicts the block diagram for the signal-conditioning unit.

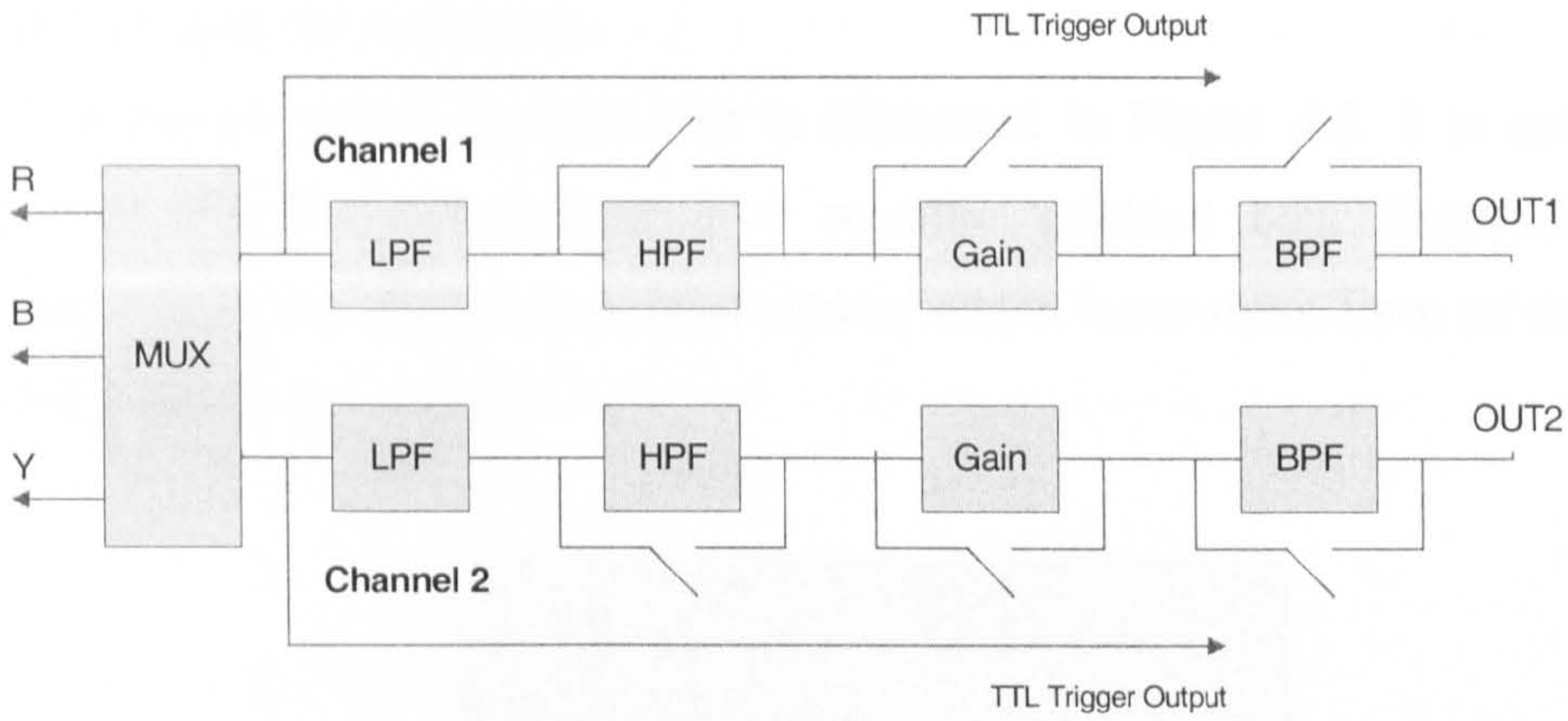

Figure 4.5: Block Diagram for signal-conditioning unit

The high-pass filter is designed specifically for the removal of the 50Hz frequency of the power signal. The aim is to provide better amplitude resolutions to the PD signals. The amplifier has preset gain or attenuation values and those values are set at 1x, ±10x, and ±100x respectively. Modification on the resistor values in the hardware components will allow the change of the preset values. Finally, followed by a band-pass filter that has a variable centre frequency and bandwidth up to 60MHz. The Sallen-Key filter design methods were utilised for both the high-pass filter and the band-pass filter.

In our RPDAQ, the purpose of this signal-conditioning unit is to provide a means of noise reduction in addition to enhancing the PD signals. The aim is to provide a choice of narrowband or wideband detection methods. In the former, certain bandwidths of the signal with strong PD activity can be extracted through the band-pass filter. Wideband detection method is achieved when the band-pass filter is switched off.

The self-check sequence is also initiated from this unit. A train of square pulses are generated for duration of 2 ms. The self-check signal is passed through the protection device and through all the components of the signal-conditioning unit. Any defect of in any circuit components will be detected by observing different of

the amplitude and the polarity of the signal in comparison to the default self-check signal. The default self-check signal is obtained with before the RPDAQ is commissioned into the substation.

The picture of the physical unit is illustrated in Figure 4.6. It is externally connected to the PC and housed in a metallic shielded box. Extruded BNC connections allow the usage of co-axial cables, which have some form of shielding from radio noise to the system.

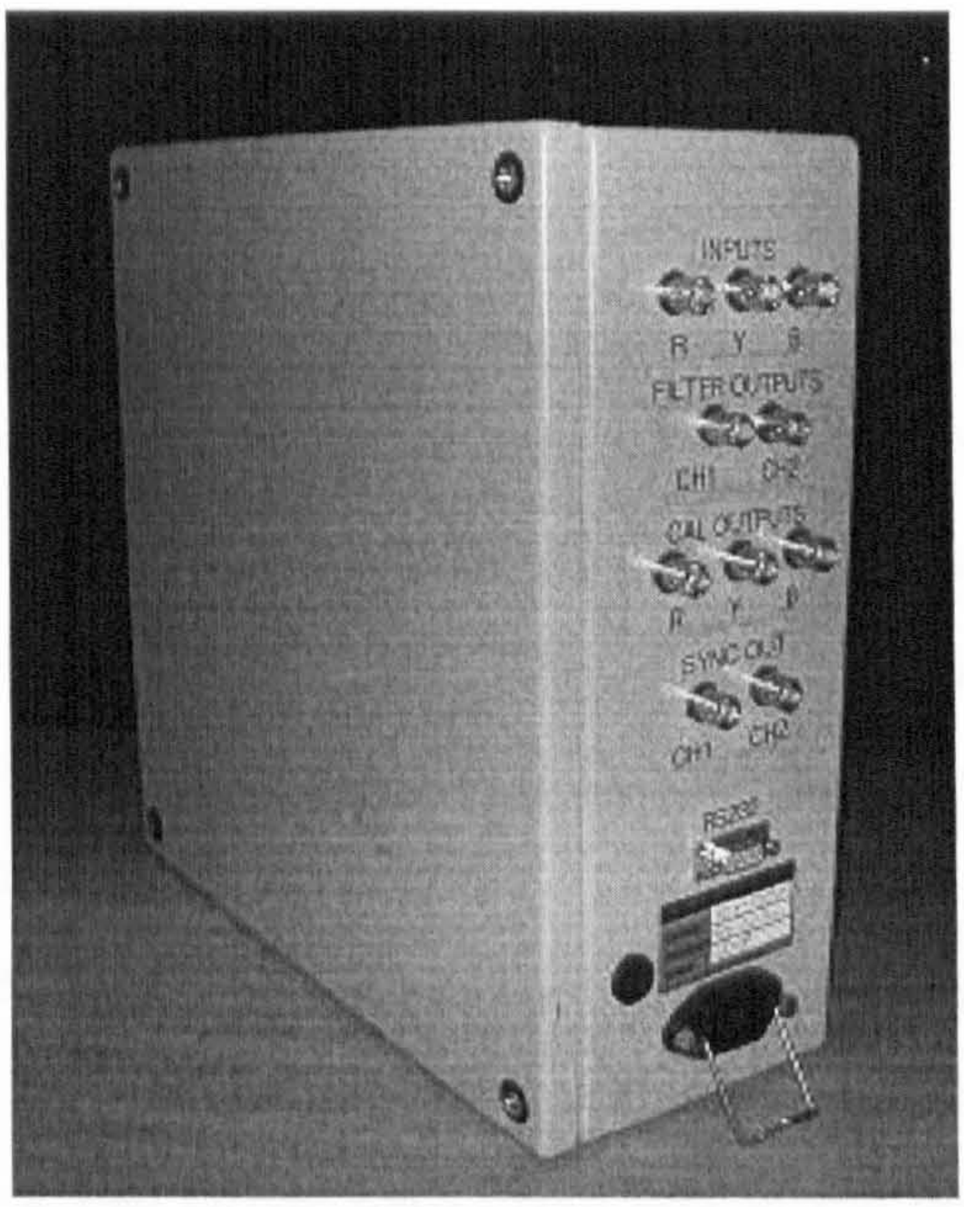

Figure 4.6: Picture of signal-conditioning unit

4.4.2.6 Data Acquisition

The next component is the data acquisition block, which comprises a high-speed analogue-to-digital converted card within the PC. The card has two channel inputs with sampling rates up to 100 MSamples/s (single channel) and 50 MSamples/s (dual channel). The amplitude resolution of the card is 14-bits and it has 8 MByte of on-board memory. This card was chosen for cost optimisation. If a four channel input card was chosen, the cost of the card would have been doubled. The chosen specifications are sufficient and adequate for capturing PD properties and data analysis. Based on previous experience [Shim 2000a], high sampling rates are required together with good amplitude resolution. The advantage of using high

sampling rates is that there is better time resolution in the signals when applied for time domain reflectometry (TDR) applications. However, one limitation of the card whilst sampling at high sampling rates is the maximum continuous acquired data is limited by the fixed amount memory. When the memory buffer is filled, the data is transferred into the storage section. If continuous data is required, the sampling rates can be adjusted to low sampling rates for instance, 1,2,5, and 10 MSamples/s. These settings are utilised for statistics analysis, for example the trend or characteristics of the PD over short period of time.

4.4.2.7 Storage Media

The acquired data is transferred to a storage media every time the memory buffer is full or during each separate cycles of data acquisition. These files are stored in systematic file formats, for easy recognition. Files and folder management are performed with correlation to the date and time of acquisition. This is further elaborated in the next section. Log files are also generated for a history of acquisition and feedback results from the acquisition process.

The storage media is mainly comprised of a hard drive unit. With the current technology, there are many new hard drive units with increased storage capacity up to 500 Gbytes. In our case, a 140 Gbyte hard drive was at the optimum price range and value for money. Stored in removable casing, the hard drive can be swapped whenever it was necessary. The process of retrieval was designed for easy access. An authorised personnel of the utility company is able to perform the taskby himself. This avoids unnecessary paperwork and logistics.

4.4.2.8 System Controls

The RPDAQ is highly flexible in its system controls. A user can operate the system either on-site or remotely from any PC in the world. A standard GSM modem is used as the means of remote communications. The GSM modem is capable of establishing a connection speed up to 14.4kbps under normal data call mode.

However, the practical nominal speed that it can establish is within 3kbps. The GSM service provider usually governs the data transfer rate. Higher speeds are available through GPRS packages offered by the service providers. These packages provide higher data transfer rates up to 2Mbps, at a higher subscription cost. In our case, the speed is relatively slow, but it is sufficient for the purpose of system control. The actual acquired data is not transferred back to the base of operations. Only acquisition parameters, programs, and important files are transferred to the RPDAQ. If a user wishes to view certain result of acquisition (or processing), the log files, system file contents and the compressed version of the data signals can be retrieved.

The data signals can be customised and compressed into a visual aid, for example a JPEG file. The JPEG file is retrieved for inspection purposes from the RPDAQ. This allows the user to check if the acquisition parameters were satisfactory.

The system is also equipped with adequate security protocols. Using layers of TCP/IP protocols, the remote user must first establish a dial-up connection. The right phone number (data), user name and password is required before a connection is established. Furthermore, if the correct details are provided, the usual protocol for the RPDAQ is that it will return the call to a pre-set phone number. This callback feature is activated for security purposes, and can be de-activated with additional passwords and relevant parameters. Therefore, the flexibility of remote accessibilities to the system is not compromised by its security.

4.4.3 Software Operations

The RPDAQ system parameters and data acquisition board settings are controlled by software. These parameters are stored in "daq" files. The "daq" files is a text file that contains a specific set of RPDAQ board and system parameters. For individual data acquisitions, their corresponding system parameters are stored in separate daq files. Each time the acquisition parameters change, the relevant daq file containing the parameters is retrieved. The daq files are generated by using specific software ("header-generator"); designed to create, modify, view the daq files. The

header-generator is a graphical user interfaced that has many drag/drop objects for parameter selection. This is to minimise the possibilities of errors occurring from manual creation or tweaking of the daq files. Figure 4.7 depicts the header-generator software for the RPDAQ.

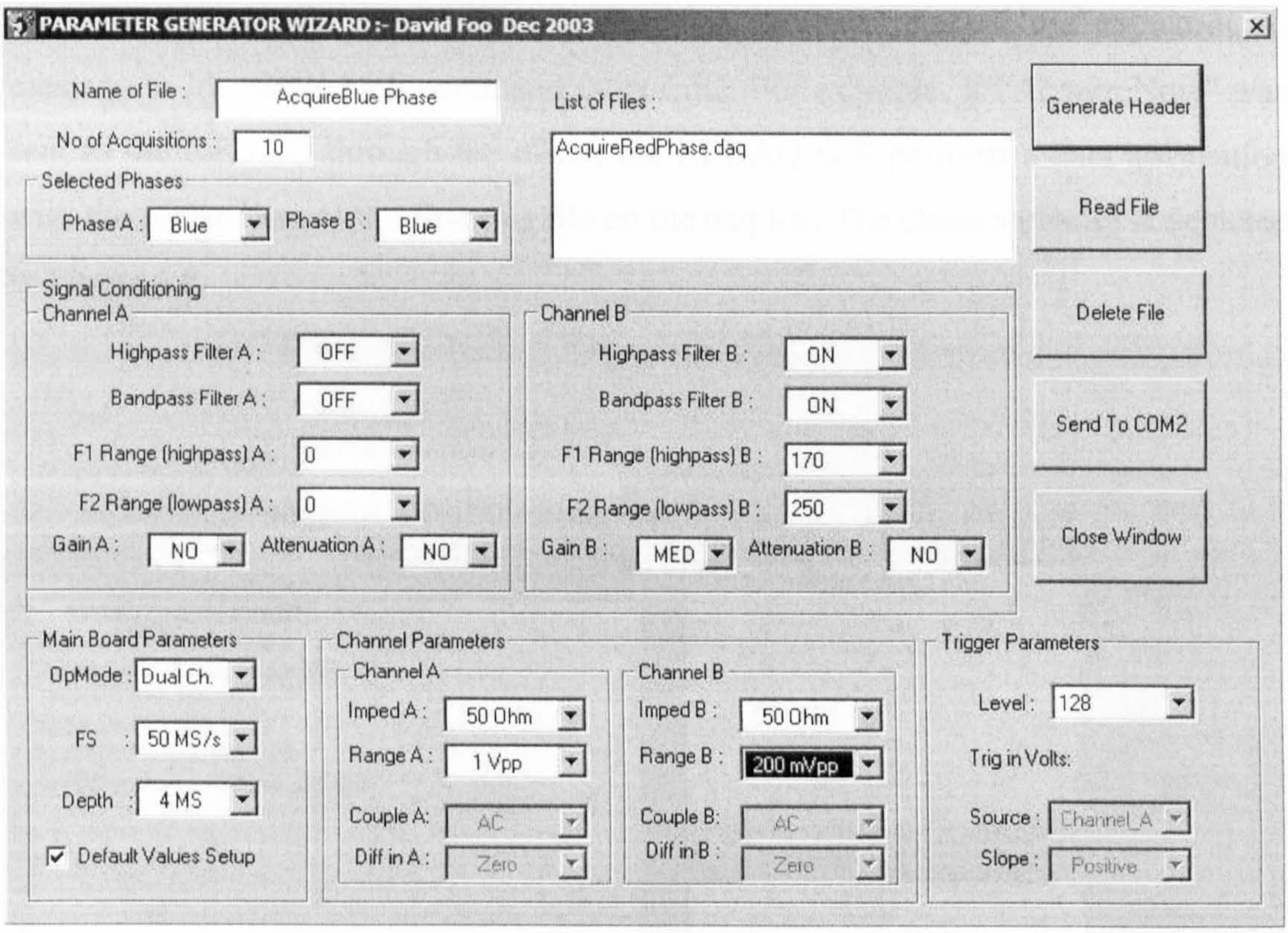

Figure 4.7: Header-Generator software for RPDAQ

The generated daq files are uploaded into the RPDAQ through file-transfer protocol (FTP) using the client software. At the RPDAQ, the server software is switched on 24-hours listening on a port for an incoming call. The call is initiated from the remote computer that uses the client software. The client software is the interface that enables a user to monitor the status of the RPDAQ, check, upload, modify and delete the daq files within the RPDAQ. At the server side, the daq files are listed in the order of their names. Hence, the file that resides at the top of the list is the first to be initiated by the RPDAQ. Once the file has been opened and initiated, the daq file is changed into a different filename. This effectively changes the type of

the file and denotes that the operation has been completed on that file. This is used for verification and checking purposes.

Besides this, the client software is also used to initiate commands to the RPDAQ. These commands correspond to specific actions that the RPDAQ is to perform. The commands will be elaborated in the next section. The client software operated in the command line mode i.e. the server compares the keywords in message to identify which command to execute. For example, if "AcquireNow" was sent to the RPDAQ through the client, the RPDAQ will perform a data acquisition with the parameters of the first daq file on the daq list. The client software is depicted in Figure 4.8.

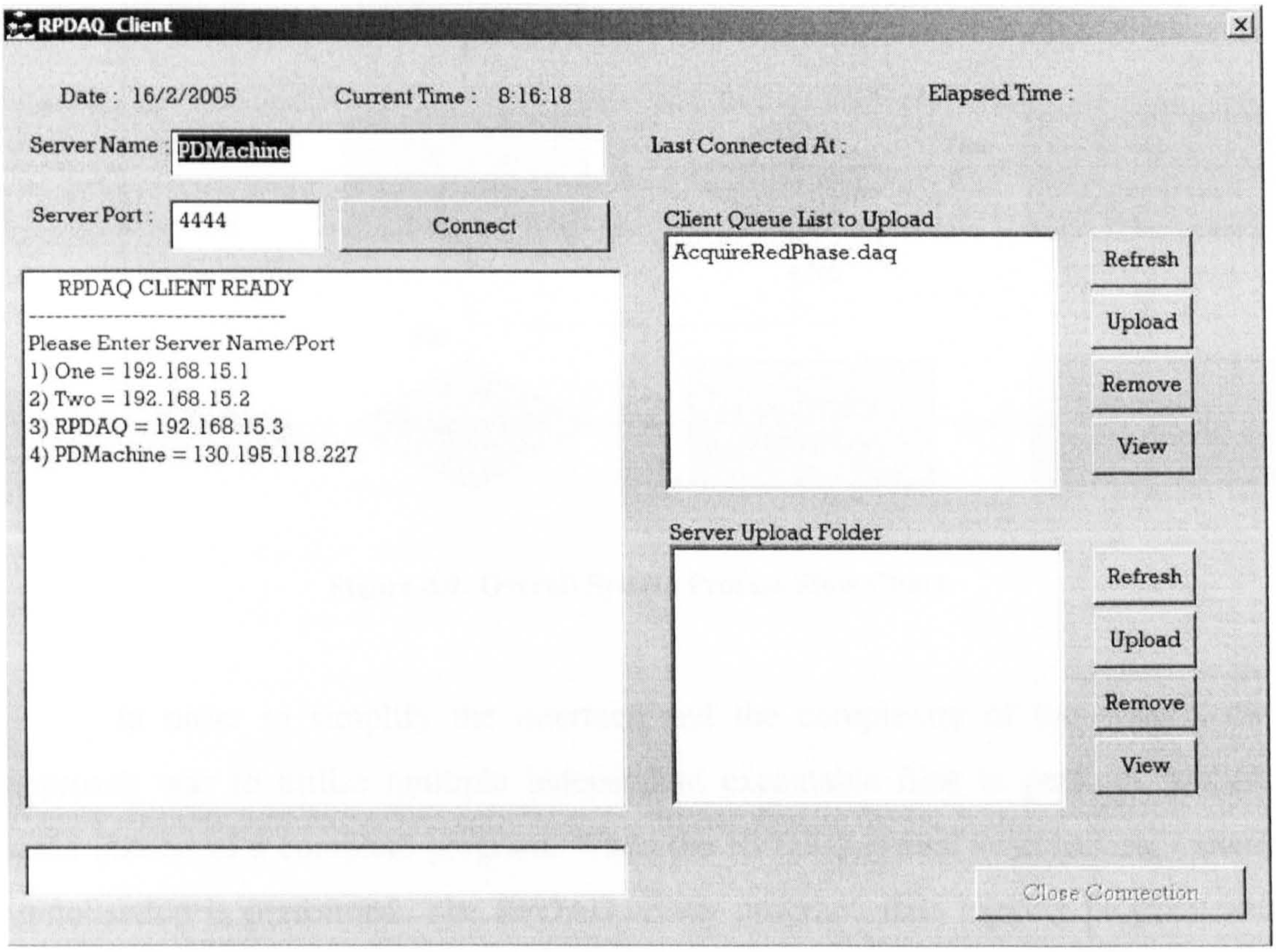

Figure 4.8: RPDAQ client software

4.4.4 Overall System Process

The RPDAQ operates as a server, which is permanently switched on. The system allows users to make connections to the RPDAQ remotely or on-site via a network connection. Commands are sent from a remote user to the RPDAQ through the GSM modem connection. These commands are processed and executed by the RPDAQ. The flow chart of the overall system is presented in Figure 4.9.

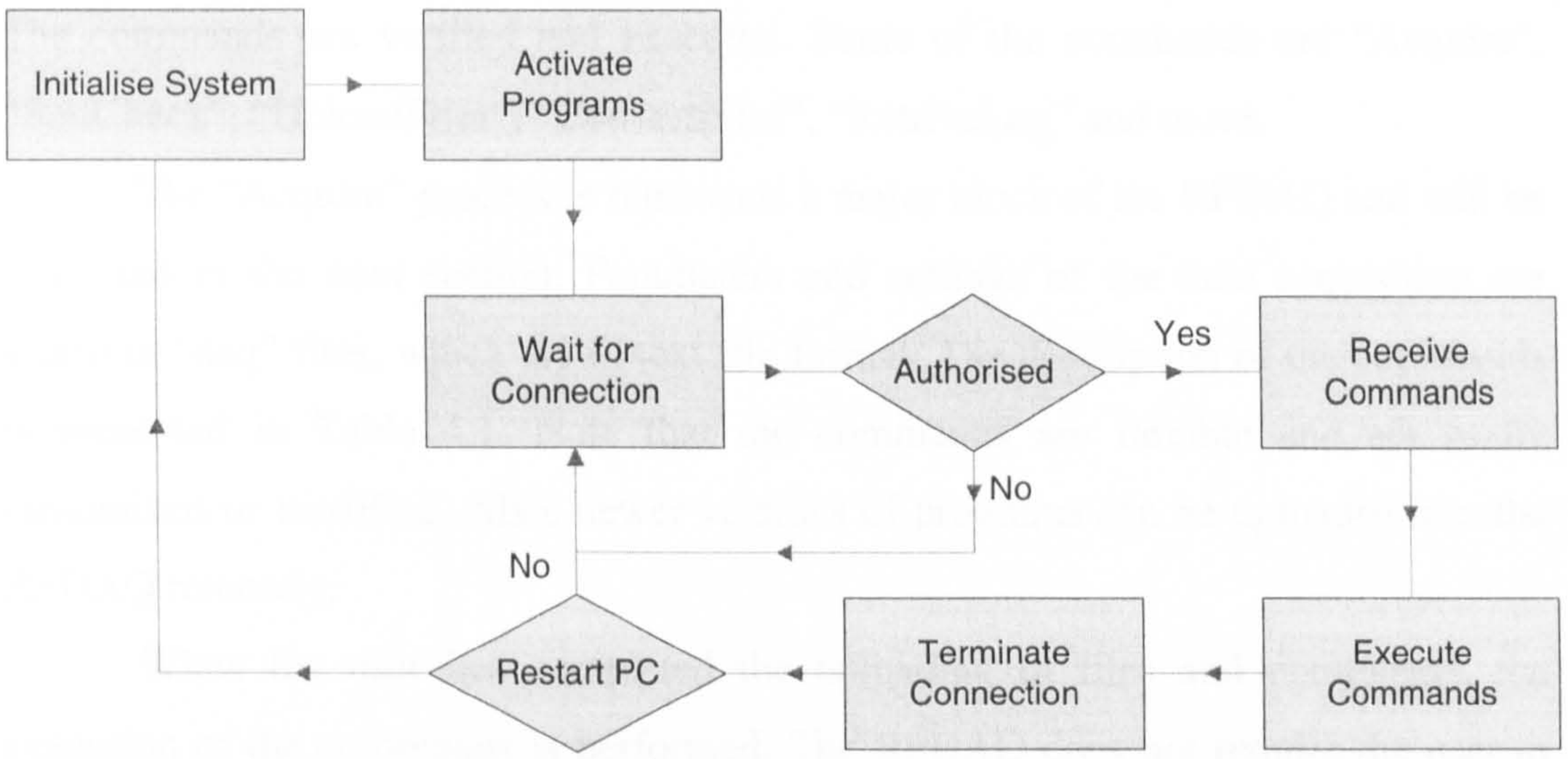

Figure 4.9: Overall System Process Flow Chart

In order to simplify the interface and the complexity of the system, the approach was to utilise multiple independent executable files to perform specific tasks instead of a complete program. When the RPDAQ is first switched on, system initialisation is performed. The RPDAQ server program, data logging program and scheduled data acquisitions are activated. The server program functions to accept connections from remote users and to decipher the commands sent to the RPDAQ. This is the main program that controls and performs the execution of data acquisition process. The data logging process is independent of from the server program; it only controls the acquisition of the data logger. For instance, data acquisition for all three phases of the cable can be performed under hourly basis for one week; to monitor the

PD activity at different current loadings. The scheduled data acquisitions are performed at fixed time intervals through timer software.

Once the programs are activated, the RPDAQ waits for dial up connection from a remote user. When a connection is received, the security parameters are verified. The callback sequence is initiated automatically, i.e. the RPDAQ returns the call to the specific preset phone number. The option is available to bypass the callback sequence by supplying a special username and password. Upon authorisation of the call, the RPDAQ then awaits for the commands from the user. The commands are verified and executed. Some of the commands are "Acquire", "SelfCheck", "UploadFiles", "ConvertFiles", "RetriveLog" and more.

The "Acquire" process is represents a major block of the RPDAQ and will be discussed in the next section. Parameters and settings of the data acquisition are stored in "daq" files, which are in text file format. The description of the commands is presented in Table 4.1. Note that the commands are flexible and are easily customized or modified. Also, newer versions of programs can be uploaded into the RPDAQ remotely.

When the user has completed the uploading of files and commands, the execution of the commands is performed. The RPDAQ does not require the user to stay connected for the data acquisition procedure; hence the connection may be terminated at this point. In some instances, the user may choose to restart the RPDAQ for refresh its memory. Being a Windows based PC system, restarting the system is advantageous; especially when the scheduled data acquisitions are performed very frequently. Otherwise the system may become unstable and connections may be refused. If the RPDAQ is not restarted, it will return to the wait for connection state for the next connection.

Command Name	Description
Acquire	Performs data acquisition, uses the parameters from the "daq" files. The command can either perform acquisition for all the "daq" files uploaded into the RPDAQ or individually.
SelfCheck	This command initiates the switching relays, generates the self-check signal for testing the hardware components in the protection device and signal-conditioning unit.
UploadFiles	The "daq" files are uploaded from a remote computer to the RPDAQ through this command. A list of "daq" files is refreshed each time this command is initiated.
ConvertFiles	This command allows the selection of data files for conversion into JPEG images. When the JPEG files are generated it is sent to the remote user.
RetrieveLog	The log files of the data acquisition and errors are sent back to the remote user through this command.
RangeTest	The optimum range for data acquisition is checked with this command. The input range is varied from the maximum setting to the best range setting.

Table 4.1: List and description of commands for RPDAQ

4.4.4 Data Acquisition Process –"Acquire"

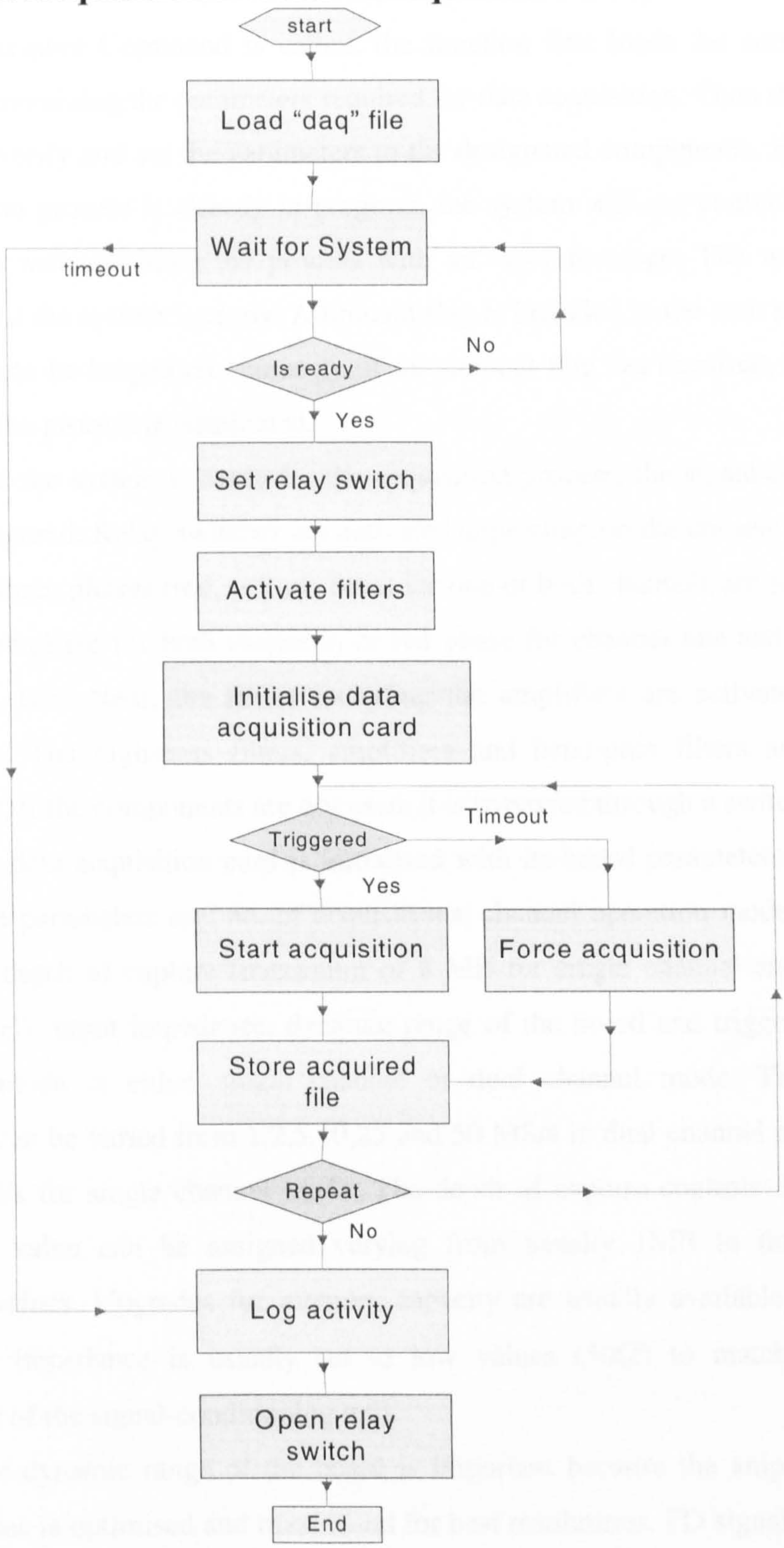

Figure 4.10: Process flowchart for "Acquire" command

The process flow chart of the Acquire command is depicted in Figure 4.10. When the Acquire Command is called, the function first loads the corresponding "daq" files containing the parameters required for data acquisition. Then the RPDAQ attempts to verify and set the parameters to the designated components. However, if an acquisition process is already in progress, the system will not continue with the process and will terminate the process with an error message. The wait state is invoked, until the system is ready. A timeout flag is included in the wait state to stop the program to be looped continuously. If the timeout flag has occurred, the error is logged and the process is terminated.

Once the system is ready for the acquisition process, the signal-conditioning unit is configured. Relay switches are activated depending on the chosen parameters. Any of the three phases (red, yellow, blue) for one or both channels are selected. For example, red phase for both channels, or red phase for channel one and blue phase for channel two. Next, the filters including the amplifiers are activated (refer to Figure 4.5). The high-pass filters, amplifiers and band-pass filters are activated accordingly. If the components are not used, it is bypassed through a switch.

The data acquisition card is initialised with its board parameters in the next state. These parameters are: no. of acquisitions, channel operation modes, sampling frequency, depth of capture (maximum of 8 MB for single channel and 4 MB for dual channel), input impedance, dynamic range of the board and trigger level. The operation mode is either single channel or dual channel mode. The sampling frequency can be varied from 1,2,5,10,25 and 50 MS/s in dual channel mode and up to 100 MS/s for single channel mode. The depth of capture controls the length of data. Any value can be assigned varying from usually 1MB to the maximum allocated values. Upgrades for memory capacity are usually available if required. The input impedance is usually set to low values (50Ω) to match the output impedance of the signal-conditioning unit.

The dynamic range of the board is important because the amplitude of the signal pulses is optimised and maximised for best resolutions. PD signals are usually of small amplitudes; hence optimised range settings will provide better resolutions to PD signal.

Triggering is usually performed on the measuring phase. By default, the trigger is set for rising edges on channel one. However, the value of the trigger setting has to be adjusted accordingly. The trigger is set at the zero crossing of the positive half of the 50 Hz power frequency. There is an option available for external triggering if required. Both the range settings and trigger settings are tested each time the RPDAQ is deployed to a cable network. The nominal characteristics of the individual cable networks are recorded before the optimum parameters are decided. It is also used for comparison purposes and data analysis.

Next the data acquisition process is started. If the signal is triggered, the captured signal is stored into the hard drive of the system. If the signal is not triggered, the system waits for a short period of time before a timeout is produced. Once the trigger timeout it invoked, the capture is forced. The log file will contain the information of the triggering process. The captured signals are stored into filenames systematically and for easier identification. Folders are created on the basis of the dates of the data acquisitions. Each folder will contain files stored in *.SIG formats (default format). The file format is binary numbers stored in 32-bit integer formats. The naming of files is done as such that the phase, sampling frequency and range information can be identified from the observation of filenames. An example filename is "r64a1.sig", from this the first alphabet denotes the phase of the cable (r,b,y), the next number denotes the sampling rate, followed by the range setting, channel, and no. of acquisition. The data acquisition process is repeated until the desired iterations are achieved.

Finally, the log files are generated from the acquisition and stored together with the data files. Then the relay switches are opened so that the RPDAQ is not connected to the protection device. This is such that the risk of damage to the RPDAQ is minimised.

4.5 Performance of PD Acquisition Unit

Before the RPDAQ was installed at the substation, several preliminary field trials were conducted using pre-prototype devices. The aim of the field trials was to gain familiarisation with the substation environments and the nominal signal conditions. From these preliminary field trials, several important points were discovered.

4.5.1 Pre-prototype Field Trials

The pre-prototype field trials were carried out with a few measurement devices. The configuration of the devices is depicted in Figure 4.11. Each filter component in the block diagram is self-contained devices. The low-pass filter functions as the anti-aliasing filter with the cut-off frequency at 25 MHz. The sampling rate used was 50 MS/s, for both channels. The high-pass filter was used to remove the 50 Hz power frequency. The band-pass filter had preset gains, windowed of 300kHz, up to 20 MHz. However, the resolution of the oscilloscope was 8-bits.

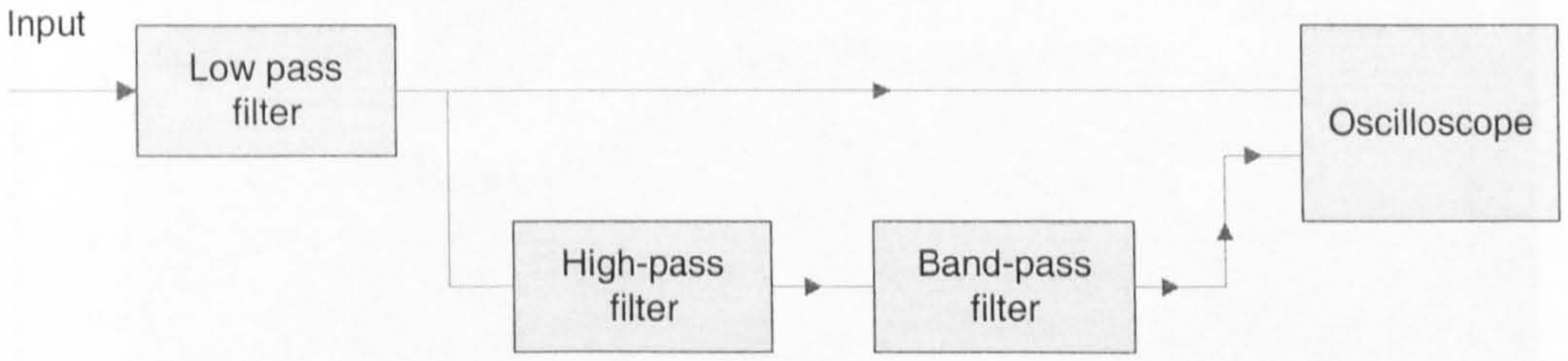

Figure 4.11: Block diagram of pre-prototype measurement devices

One observation from these signals was the quantisation error was high due to the high sampling rates used combined with the 8-bit resolution. Hence, this setup was performed at a lower sampling rate (25MS/s). This field trial was mainly to determine the voltage output range of a typical measured signal for all three phases and signal and noise characteristics.

4.5.2 Full system Field Trials

4.5.2.1 Current load profile

The amplitude of the measured signals was found to vary with the time of the day with respect to the current loading. The current loading of the power cables is governed by the usage and demand of electricity supply. The maximum demand of electricity usually is dependent on the seasons; the highest demand is typically during winter. Hence, this should be accounted for in the analysis of PD because the PD activity is affected by the change in temperature and current loading. The daily load profile will also vary depending on whether it is a weekday or weekend. The effects of thermal loading may provide useful information with relations to PD activity. Figure 4.12 depicts the typical daily load profile pattern for 2002/2003.

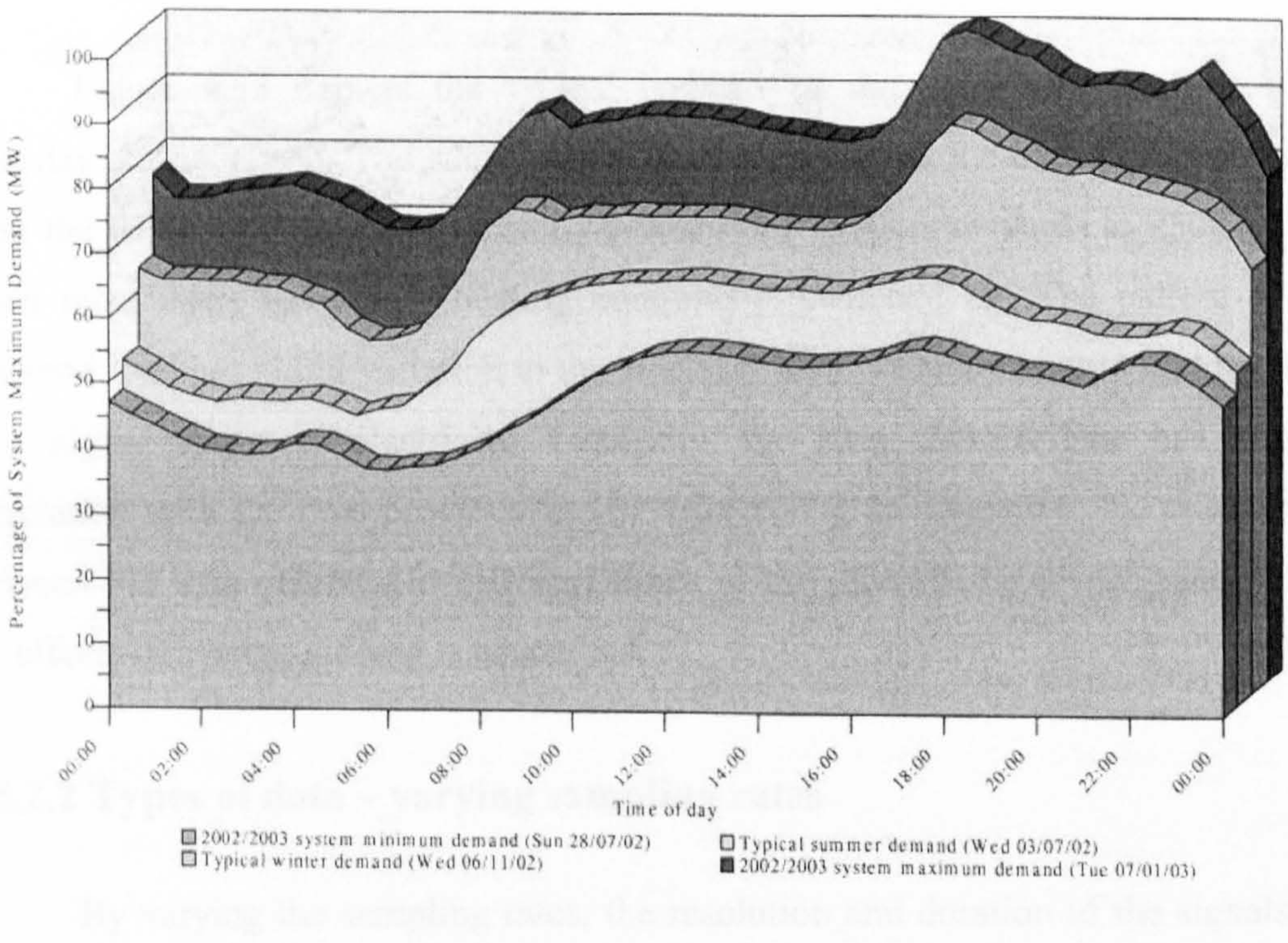

Figure 4.12 : Daily Load profiles: Maximum, minimum and typical patterns for summer and winter 2002/2003 [SP Dist 2003]

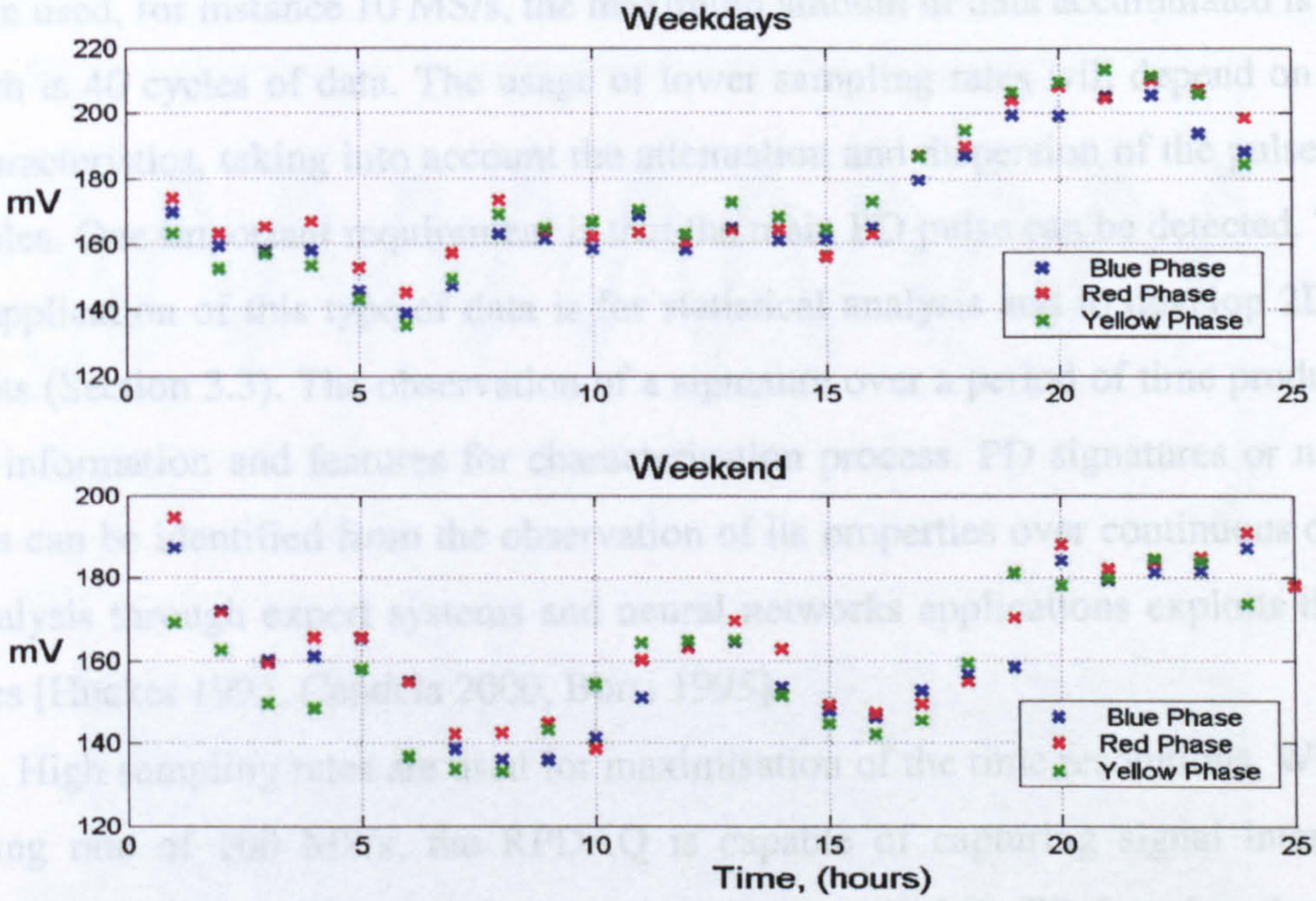

Figure 4.13: Daily load profile during weekday and weekend measured from RPDAQ

Figure 4.13 depicts the typical patterns of the daily load profiles for a weekday and weekend. The same pattern is observed from the data that is obtained from the RPDAQ. Usage of electricity peaks from 1800hrs onwards to 2300hrs, i.e. when most users have their heating equipments switched on. The pattern of the weekend load has slight variation to the weekday load, whereby around midday there is a higher usage of electricity. Generally, the load characteristic has a good correlation with the data provided in [SP Dist 2003]. In chapter 6, the comparison between PD data obtained at different times of the day will be investigated, where the effects of current loading is accounted.

4.5.2.2 Types of data – varying sampling rates

By varying the sampling rates, the resolution and duration of the signals can be adjusted. Low sampling rates facilitates longer durations of data whilst high sampling rates provides data with good time resolution. The sampling rates are governed by the application of the data for analysis purposes. When lower sampling

rates are used, for instance 10 MS/s, the maximum amount of data accumulated is 0.8 s, which is 40 cycles of data. The usage of lower sampling rates will depend on the PD characteristics, taking into account the attenuation and dispersion of the pulses in the cables. One important requirement is that the main PD pulse can be detected. The main application of this type of data is for statistical analysis and to develop 2D or 3D plots (Section 3.3). The observation of a signature over a period of time produces useful information and features for characterisation process. PD signatures or noise sources can be identified from the observation of its properties over continuous data. PD analysis through expert systems and neural networks applications exploits these features [Hucker 1995, Candela 2000, Borsi 1995].

High sampling rates are used for maximisation of the time resolutions. With a sampling rate of 100 MS/s, the RPDAQ is capable of capturing signal intervals within 10ns duration. This is advantageous when applied to PD location through TDR methods. Depending on the length of cable, reflections are in the order of μs; this effectively provides a better representation for the signals. The higher the sampling rates the better the time resolution, at the expense of increased noise interference and shorter duration of data (governed by the memory buffer size).

A general idea of the types of measurement conducted with the RPDAQ is illustrated in Figure 4.14, where (a) is a typical measurement containing the phase voltage and (b) is the measurement performed with the 50 Hz frequency removed. Type (a) is useful for providing phase information relating to the PD pulses and type (b) provides good amplitude resolution for the pulses because the settings are matched to the dynamic range of the signal. For both cases, high or low sampling rates may be used. Another combination of signal measurement is using dual phases of the cable. This type of measurement provides correlation between the signals from two phases. It is also used to isolate pulses that are stronger within phases. However, one physical drawback is that the RPDAQ can only measure 2 phases simultaneously out of the three phases of the cable.

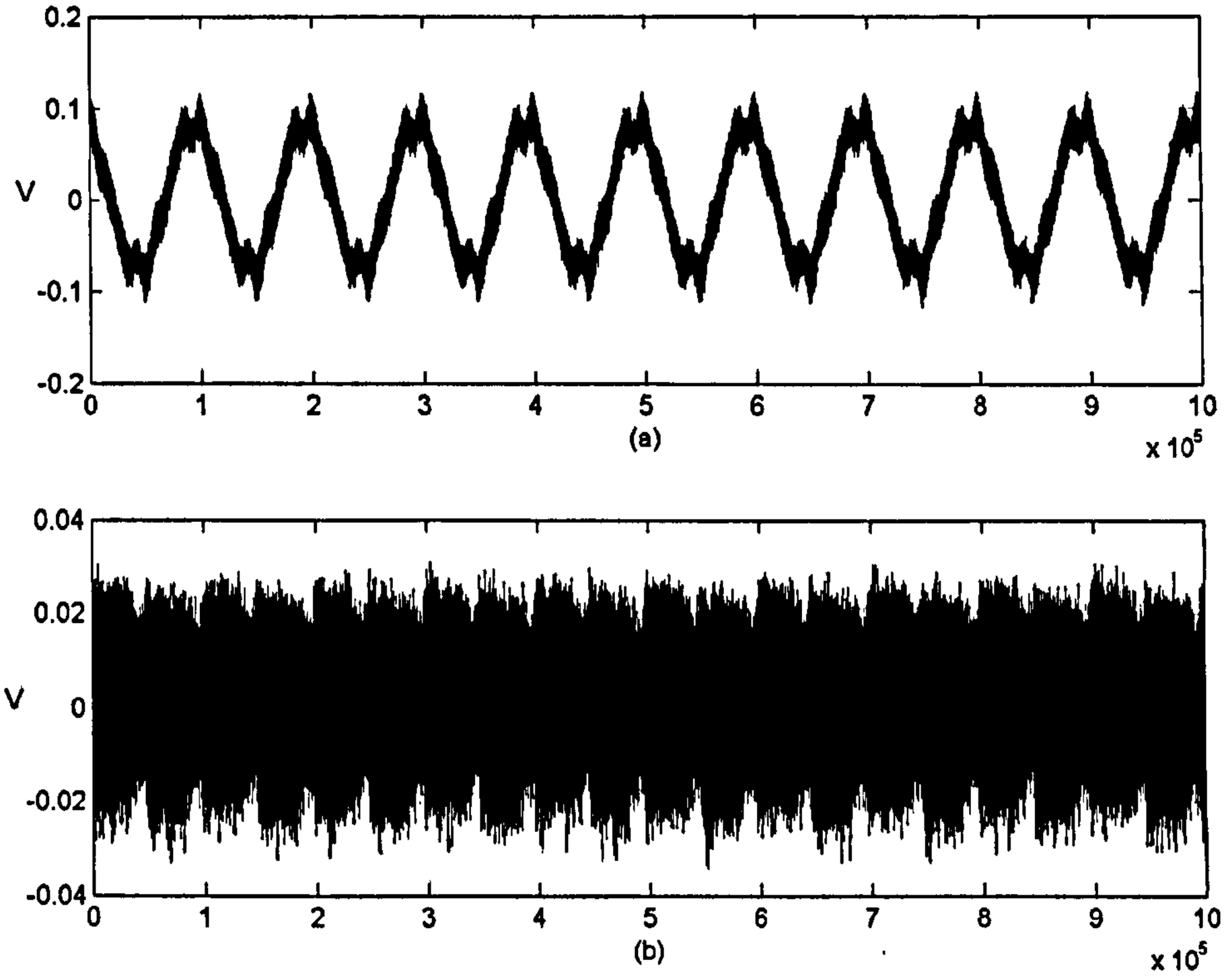

Figure 4.14: Typical examples of measured signal from the RPDAQ

Finally, there is the single phase measurements usually conducted at the maximum sampling rate i.e. 100 MS/s that provides 80 ms of signal duration. This type of data is used to analyse individual components within the signal in the time and frequency domain. PD type signatures are analysed and checked for reflections.

4.5.2.3 Comparison to pre-prototype data

The measurements were carried out with the prototype measurement configuration and with the RPDAQ separately to determine the difference between measurements. These measurements were conducted at different time instances; hence there will be variations in signals. The comparison was performed initially to correlate the measured signals and determine the system response of the measurement system. The results depicted in Figure 4.15 is an overview of the signal for a complete 50 Hz cycle; where the top traces are the signal containing the raw

signal and the bottom traces are measured through the high-pass filter removing the 50 Hz.

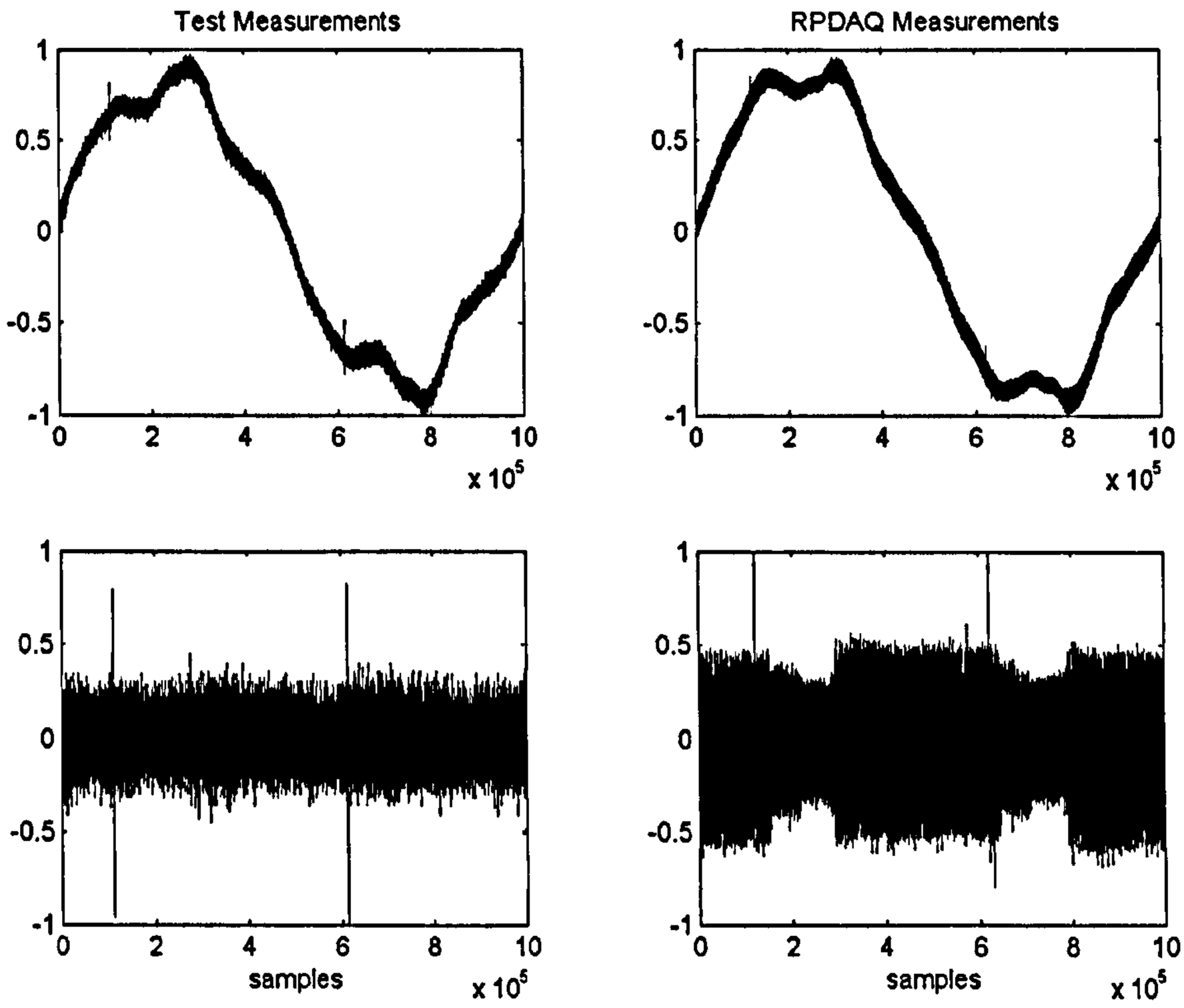

Figure 4.15: Comparing measurements from prototype setup and RPDAQ

A zoomed version of the signal is depicted in Figure 4.16. The main transient structure had high correlations in both traces. However, the RPDAQ signal had better defined transient noise compared to the other. This difference is due to the higher resolution of the RPDAQ and the sampling rate used. The exact calibration of the RPDAQ measurements was not possible to achieve because a test measurement system with identical specifications as the RPDAQ was not available. In general, the measurements from the RPDAQ were found to be fairly accurate in terms of amplitude and shape of measured signals and the frequency content.

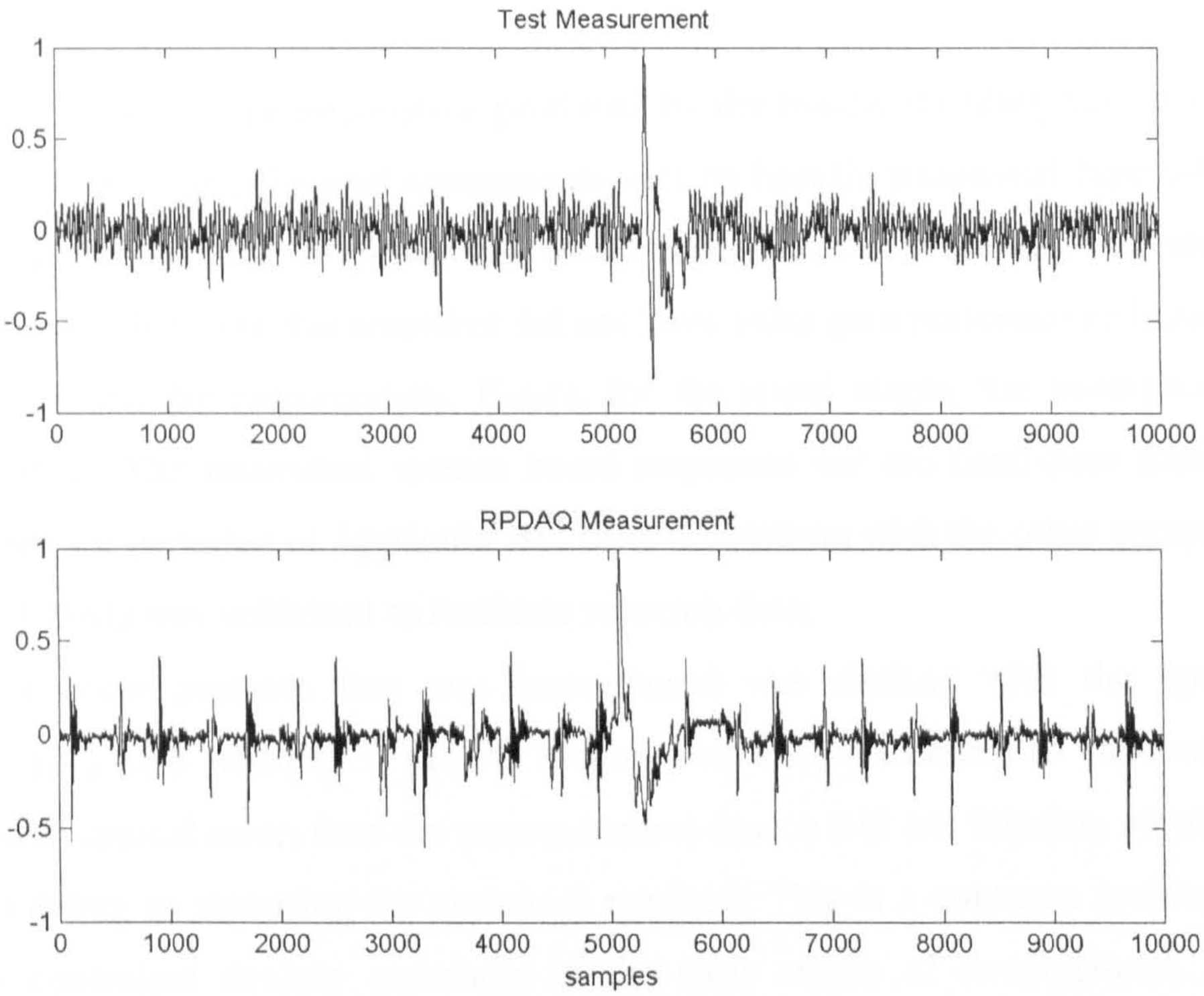

Figure 4.16: Zoomed version of PD structure for test measurement setup and RPDAQ

4.5.3 Problems and Limitations of the system

One problem that was encountered was related to the band-pass filter of the RPDAQ. The band-pass filter was designed by cascading series of high-pass filters and low-pass filters. The Sallen-Key filter techniques were used in the filter design. The high-pass filter forms the lower cut-off frequency whilst the low-pass filter produces the higher cut-off frequency. During the design stages, the overall performances of the filters were accepted. Simulation results indicated that the filter performance corresponds to the desired specifications. However, when the band-pass filter was constructed on PCB, the problem was changing the cut-off frequencies of the filter. The minimum allowable bandwidth was within 60 MHz. Although the cut-off frequencies were set to produce low bandwidths, the output of the band-pass filter produced unexpected results. The wide bandwidth of the filter was inappropriate for

usage since the performance was beyond the capability of the other acquisition components.

Furthermore, the attenuation produced by the band-pass filter was within the region of –20dB. Small signal components will be heavily attenuated especially PD signal components. The amplifier that was produced was capable of producing gain of 100 times. However, the amplifier did not have unity gain performance because of the high bandwidth requirements. Hence, for the initial stages, the band-pass filter was omitted. The individual system board responses for the band-pass filters and amplifiers are included in Appendix B1. Data acquisition with the other components of the RPDAQ was sufficient to facilitate research data.

Another problem that was encountered was dealing with the operation system. In a case whereby if the PC system was out of memory or encountered a Windows® critical error, then the remote control device will not function normally. A manual debug or restarting the system is required. This is a common problem with remote controlled devices especially in the early stages of development. Hence, precautionary measures were taken to avoid the cases of encountering errors as such. Restarting the PC after a period of time and checking of software codes ensures the reliability of the remote system.

4.6 Conclusion

In this chapter, a PD data acquisition system called the Remote Partial Discharge Acquisition Unit (RPDAQ) was presented. The primary objective of the RPDAQ is to facilitate online field data for research purposes. The RPDAQ has satisfied the safety requirements of the collaborating utility company. Logistic and preparation issues related to site visits are minimised through the RPDAQ. The initial installation at designated site allows a user to fully control and manage the acquisition system. This reduces the work required at site and performs the task more efficiently. Retrieval of the storage media is also performed relatively easier and

faster because a quick replacement of a second storage media or also known as a "hot-swap" is permissible.

The main hardware configurations and software operations were presented in this chapter. Preliminary data from the test site was presented along with the data from the completely installed RPDAQ. A comparison was performed to identify the performance of the RPDAQ. The results indicated that the RPDAQ has produced satisfactory data.

Several problems that arose from the system were highlighted and identified. Despite the limitations of the band-pass filter from the signal-conditioning unit, the RPDAQ was still capable of achieving its primary objective. In the next two chapters, the emphasis will be towards data analysis and interpretation techniques. The data acquired from the RPDAQ will be investigated.

Chapter 5 : Wavelet-based PD Analysis

5.1 Introduction

During the course of this research, the wavelet-based techniques emerged as important and useful tool for PD analysis. The provision of good time and spectral information from wavelet transforms has significant advantages and impact on non-stationary signals such as Partial Discharges. There are many published journals and conference papers on the applications of wavelets for PD diagnostics for HV equipment. Within HV cable diagnostics, wavelets have been primarily used for de-noising purposes [Shim 2001a, Phung 1999], which enhanced the PD detection process. Another application is data compression for PD signals [Ma 2001].

Wavelets techniques have been used in many applications as described in Section 3.5.4. Also there are several methods and variations the implementation. The type of implementation, selection of filters and properties of wavelets will vary depending on the choice of the user. Each technique and wavelet family will have their advantages and drawbacks. This will also depend on the purpose of the application.

The commonly referred wavelet technique is the decimated Discrete Wavelet Transform i.e. DWT. This is because of the simplicity and efficiency of the method of implementation. The method utilises the filter bank approach described in Section 3.5. The advantage of this method is obvious, whilst the drawback of it have not been clearly emphasized.

In this chapter, wavelet-based techniques for PD data analysis is presented. Issues of wavelet-based techniques are explored in more depth. The drawbacks of the conventional wavelet approach will be discussed. The emphasis is given towards the

analysis of the time domain characteristics for individual datasets instead of statistical methods. Firstly, the general approaches to PD detection through wavelet transform are introduced. Two approaches presented are the wavelet de-noising method and the edge detection method. Both approaches are described in detail and the important factors for implementation are described in Section 5.2. In the next section, the types of wavelet implementation are investigated. A distinct comparison of the non-redundant DWT method (DWT-A) is made with the redundant non-decimated discrete wavelet transform (DWT-B) is presented in Section 5.3. The performances of both methods are investigated with simulated data and online field data acquired from the RPDAQ described in the previous chapter. In Section 5.4, a new wavelet PD detection algorithm based on kurtosis presented. The efficacy of PD detection process has been improved through this new algorithm because it minimises the requirement for data interpretation for the user. The investigation of the advantages and drawbacks are presented and the algorithm was applied to simulated data and several field data. Finally, the conclusions are drawn up in Section 5.5.

5.2 Why Wavelet-based PD Detection

The major difficulties of analysing online field data are noise interference reduction and signal extraction processes. In Chapter 3, various signal processing tools and techniques for PD analysis were reviewed. The conventional method for PD analysis is performed from the time domain or frequency domain analysis. However, noise interference present hampers effective characterisation of PD's within both the time and frequency domain. In the past decade, wavelet analysis has emerged as a superior signal-processing tool for PD analysis. Its time-frequency resolution has a better representation of information for non-stationary PD signals and effective signal extraction within a noisy environment. Hence, wavelet-based approaches are appealing for this purpose. However, there are many variations of

wavelet implementations. Figure 5.1, illustrates a self-explanatory flow diagram of a general approach to PD analysis.

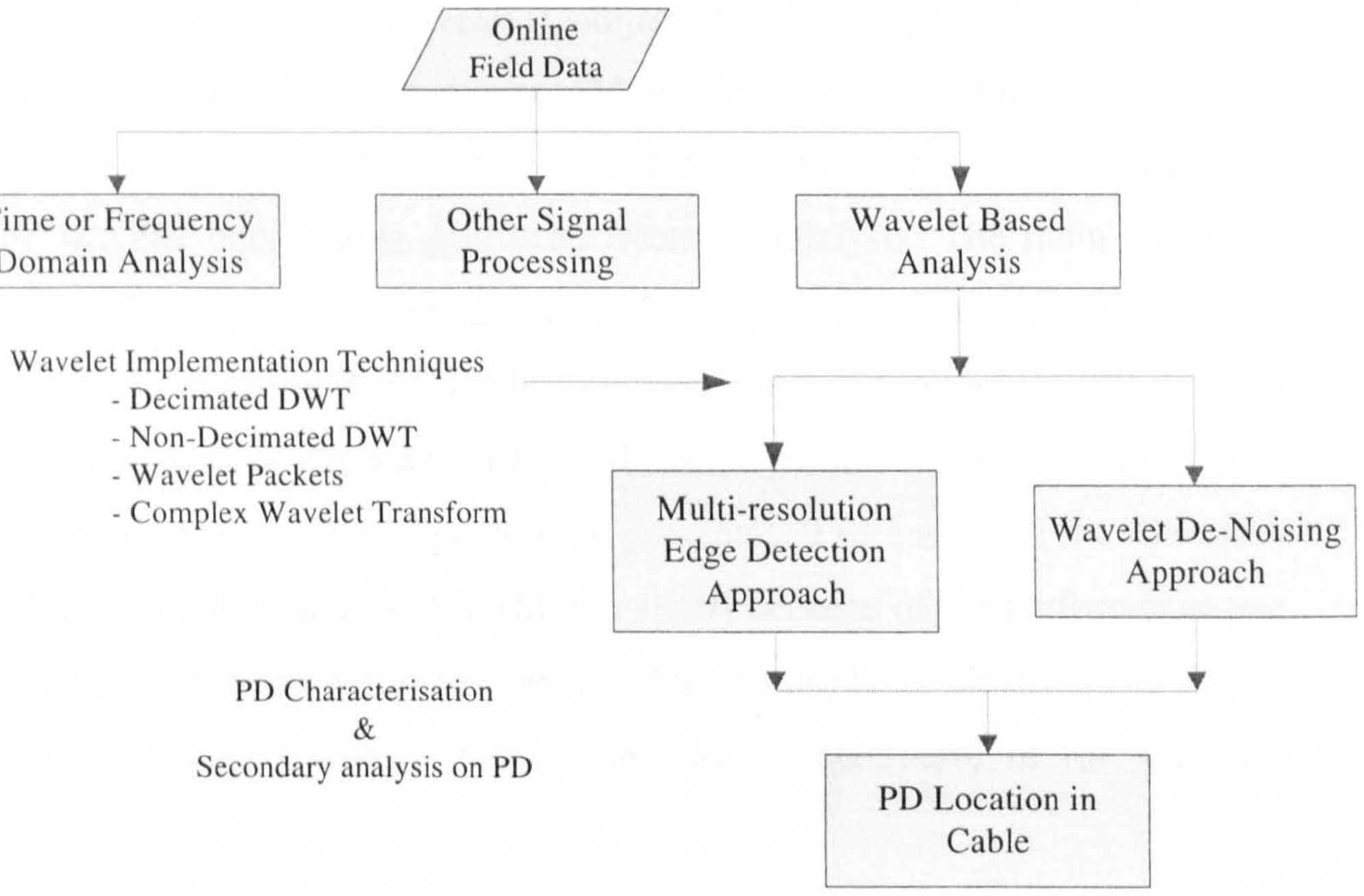

Figure 5.1: Flow Diagram of general approach to PD analysis

5.2.1 Important Factors for Wavelet Implementation

Prior understanding of wavelet properties is necessary in order to maximise the efficiency and outcome of the analysis. Several important factors for wavelet implementation can be simplified into three categories:

5.2.1.1 Choice of wavelet

Choosing the right and the optimum wavelet from a wide selection of wavelet families is important to produce accurate and desired results. Several popular ones are the Daubechies, Morlets, Coiflets, Symlets, and more have been used in the power-engineering field [Pillay 1996, Hamid 2002, Ece 2004]. In each wavelet family, there are different wavelet variations depending on the properties of the wavelet such as the regularity, number of vanishing moments, compactly support and

others. More information of the wavelet properties can be found in [Mallat 1989a, Daubechies 1994, Misiti 1997]. However, in regards to applications for detection of transient like discharges (or singularity detection), the rule of thumb is rather straightforward. The choice of a wavelet is subjected to the shape of the discharge (or system response from the detection device) [Mallat 1989, Shim 2000, Ma 2002]. The wavelet with the best correlation with the shape of the discharge will maximise the result in the wavelet coefficients generated from the analysis. The main aim is to identify PD wavelet signatures from the wavelet analysis. Generally, if the discharge is assumed to be an impulse, then wavelet signature produced in the wavelet analysis is the impulse response of the wavelet filter. In some instances, the wavelet may be chosen because of the wavelet signature it generates. For instance, the Gaussian wavelet and its derivatives are used in [Mallat 1989] because of the performance and effectiveness in the interpretation the results. This example is illustrated in Figure 5.2, where the wavelet signature shape takes the 1st derivative of the Gaussian function.

5.2.1.2 Level of Decomposition

The maximum level of wavelet decomposition is governed by the equation: $\log_2(N)$, where N is the signal size [Misiti 2000]. The relationship between the frequency of the signal and the wavelet scales is inversely proportional. The important characteristics to note in the wavelet decomposition is that the low detail levels will usually be corrupted with the noise interferences, and the extreme high detail scales will contain very low frequency bandwidths. Choosing the maximal level of wavelet decompositions may not necessarily be good because at both extreme ends, there will be redundant scales [Mallat 1992]. Hence, choosing the optimum level is important to avoid extra computation efforts. This can be done through trial and errors until the highest scales (low frequency regions) start to exhibit very low frequency components.

5.2.1.3 Deviation of Local Maxima

In an event of a transient or PD, one-wavelet maximum will be produced in each wavelet scale. The peak of each wavelet signature produced is known as the local maxima. This forms a maxima line when observed across the wavelet decomposition scales. However, as it reaches the higher scales (low frequency), the wavelet signature tends to undergo "dispersion", which causes the broadening of the pulse and altering the position of the maxima point. The maxima line tends to deviate/curve away from the actual time value whereby the discharge had occurred. If the higher scales were included in the process of edge detection, this may result in significant errors. Hence, some of the higher scales are redundant and often neglected in the analysis [Mallat 1992].

5.2.2 The Approaches to PD Detection

Transient like signals such as PDs are non-stationary, which ideally are Dirac impulses and most of the time contains a wide frequency spectrum. Multi-scale approaches will exhibit more information when used to extract useful information from these signals.

Wavelet-based techniques have been widely used in the literature for discharge analysis, in particular discharge detection. The upper hand of wavelets compared to the Fourier techniques is distinctly shown in the performance of discharge localisation. Wavelets have achieved good performances by exploiting the multi-scale properties, which have good time-frequency localisation. Two approaches that are used for discharge detection through wavelets are the multi-scale edge detection method and the de-noising of the signals method. Both methods are described in this section.

5.2.2.1 Multi-scale Edge Detection Method

The most important features for analysing the properties of transient signals are the points of sharp variations. The wavelet transform is a good candidate that is

closely related to multi-scale edge detection. The wavelet transform edge detection is similar to the Canny edge detector [Canny 1986], which is to observe the local maxima of the wavelet transform modulus. The local maxima of the wavelet transform provide useful information of the transient. In general, wavelet signatures produced from transient events will form the wavelet modulus maxima. Synchronization of the wavelet modulus maxima across the wavelet decomposition will confirm the presence of the transient within the signal.

Using the second criteria discussed in Section 5.2.1, a good wavelet candidate is a non-orthogonal wavelet $\psi(x)$ depicted in Figure 5.2. This wavelet has unique wavelet signatures that are prominent and easy to distinguish. The mother wavelet itself is the first derivative of the cubic spline function $\phi(x)$. The generated wavelet signature from $\phi(x)$ has an extrema that corresponds to the zero crossings or inflection point of the mother wavelet signature (see Figure 5.3). This wavelet signature is easy to detect and useful in the development of the multi-scale edge detection algorithm.

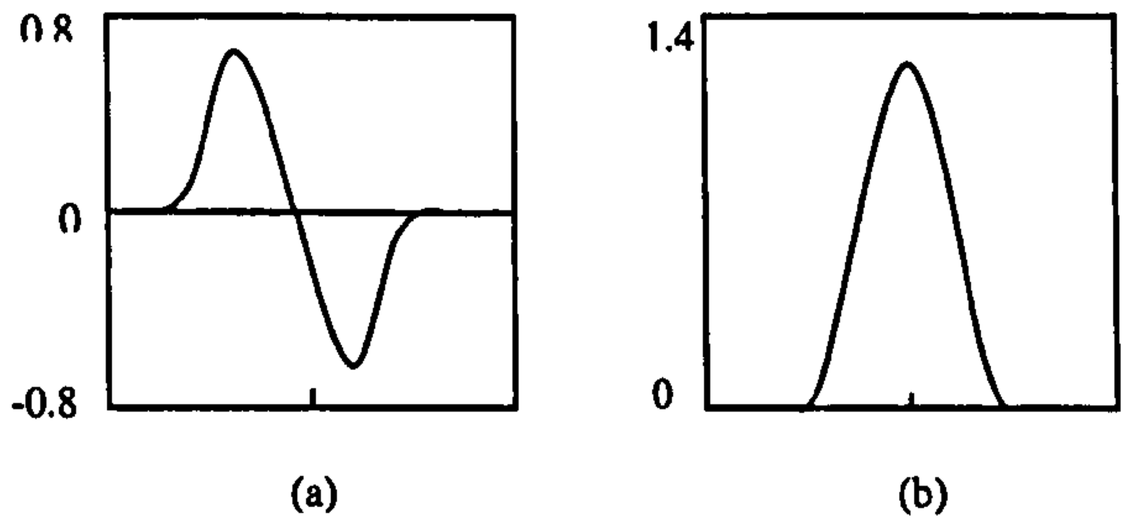

Figure 5.2: Mother wavelet ψ (x) in (a), and cubic spline function, ϕ(x) in (b)

Example for Multi-scale Edge Detection Method

In this example, the sample signal used is an exponential decaying pulse. The sample signal and the wavelet decomposition with the cubic spline wavelet are depicted in Figure 5.3. For this example, noise was excluded in order to provide a clear understanding of the edge detection method. The three important criteria for wavelets mentioned previously were taken into account. The level of decomposition

was stretched to the maximum i.e. 7 levels (for illustration purposes), where a_n and d_n (n = 1,2, … N) are the approximation and detail scales.

In this case, the higher scales (low frequency) produce wavelet signatures that are smoothened. If noise were added to the signal, the first few lower detail scales will contain high amount of noise. The noise level dictates the possibility of detecting the wavelet signature. Hence, the usual procedure is to neglect the first few detail scales to discard the noisy signals and the extreme end of the higher detail scales to avoid inaccurate evaluations [Mallat 1989].

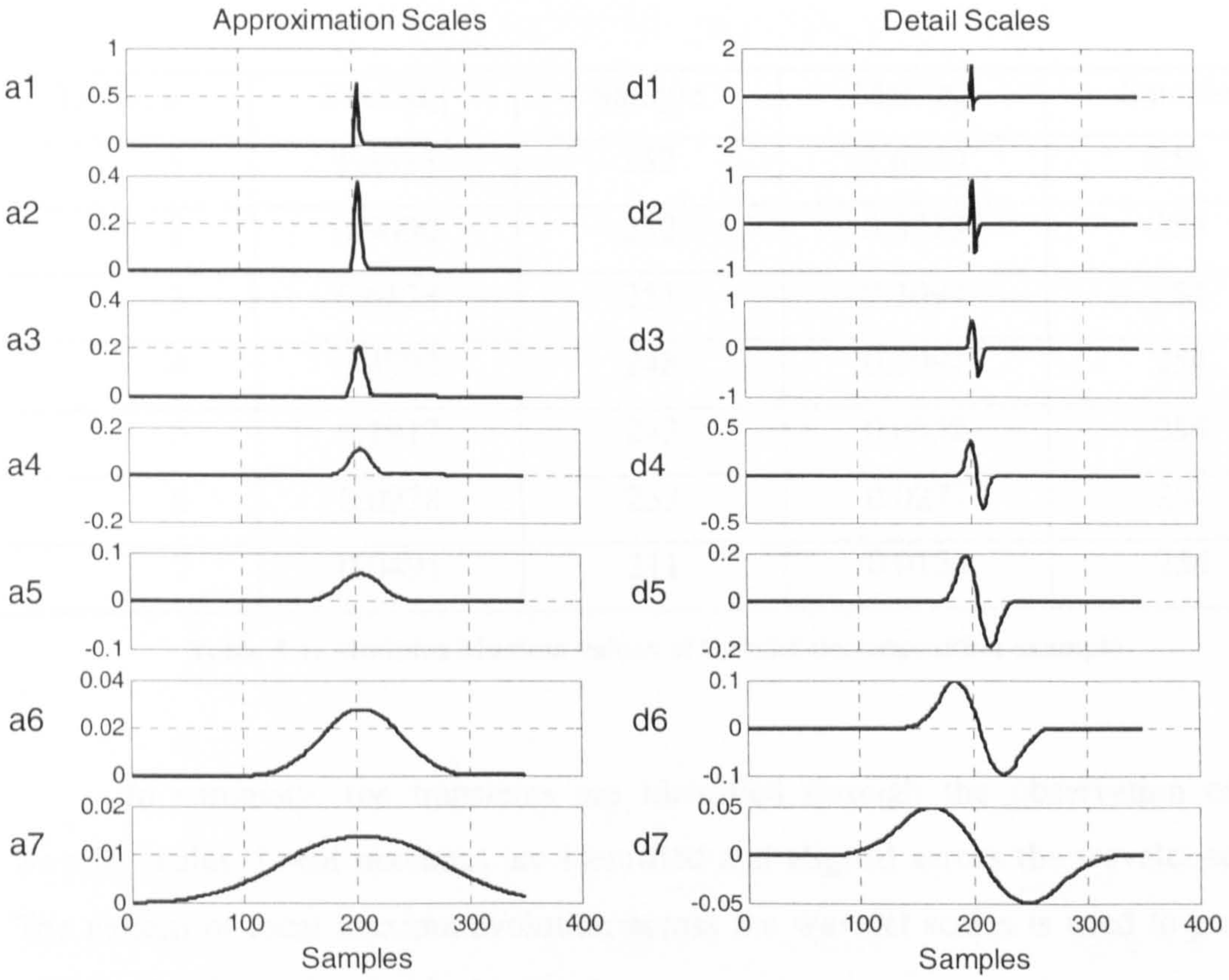

Figure 5.3: Example of wavelet decomposition

The evolution of the wavelet transform modulus maxima across the scales generates specific patterns can be used to distinguish the type of transient present. It can be used to characterize the transients or singularities. The measure of the decay across the wavelet decomposition allows the classification of the type of transient. This is illustrated in [Mallat 1992] with an example, whereby a series of different types of edges produces different types of modulus maxima patterns that conform to exponential decay shapes.

Table 5.1 indicates the values of the wavelet modulus maxima and the relative location in samples unit. The modulus maxima in both approximation and detail scales have an exponential decay feature. As the scales approaches higher levels, the location of the modulus maxima tends to deviates away from the actual location of the input pulse, caused by the smoothening of the pulses. This is obvious for the detail scales, but the approximation scales do not show deviations because noise is not present. In reality, it is common practice to discard the low frequency scales for localisation purpose.

Level, *n*	Max $\|d_n\|$	Sample	Max $\|a_n\|$	Sample
1	1.3333	252	0.6330	253
2	0.9030	252	0.3719	253
3	0.6128	251	0.2094	254
4	0.3592	248	0.1091	254
5	0.1917	243	0.0552	254
6	0.0978	233	0.0277	254
7	0.0491	211	0.0138	254

Table 5.1: Modulus Maxima values of wavelet decomposition example

In summary, the transients are identified through the observation of the wavelet scales. Local maximas are identified and aligned across the wavelet scales. The pattern of local maxima evolution across the wavelet scales is used to provide additional information for the transient.

5.2.2.2 Wavelet De-Noising Approach

The other approach is by using wavelet de-noising. First, the appropriate wavelet is applied to the signal to produce the wavelet decomposition. Next, wavelet thresholding is carried out with the selected threshold method and the "cleaned" signal is reconstructed. The detection of discharges is performed from the analysis of the new reconstructed signal. The difference between this method and the multi-scale

approach is that the PD analysis is performed on the new signal only. The main purpose of de-noising is to enhance the visibility of the discharges.

The drawbacks of this method is that peaks that occur in the new reconstructed signal may not necessarily be discharge sources, and can be mistaken to be a false discharges. The de-noising procedure also reduces a portion of the information portrayed from the discharge source because of the signal clipping through the thresholding process. This is especially in cases where high noise levels are present; the performance of the de-noising process will be weak.

Wavelet de-noising has become the basis of signal-processing block in the power-engineering applications. Excessive noise interferences can be significantly reduced, hence making it a powerful tool. This is evident from the amount of literature published with variations of different applications [Wilkinson 1996, Pillay 1996, Santoso 1997, Lai 1998]. Several authors have reported their successes in noise reduction for PD analysis [Ma 2002, Shim 2001a, Phung 1999].

The key to wavelet de-noising is the selection of the thresholds. The application of thresholds in de-noising in general will depend on individual cases. The main factors that affect threshold selection are the nature of the noise and the properties of the signal. There are many thresholding techniques that have been developed over the years and often involve high depths of signal processing. Some examples are SUREshrink [Donoho 1994, 1995b], Minimax [Sardy 2000], Non-Negative Garrote [Gao 1998], Fixed Thresholding [Donoho 1994], etc. In [Ma 2002], a modified version of the Fixed Threshold method was presented. Instead of having a fixed threshold for all the wavelet scales, the threshold was computed at each wavelet scale through the same method for the Fixed Threshold with an addition of scaling the local noise power.

5.3 Which optimal Wavelet Technique?

5.3.1 Implementation of Wavelet Transforms

In Chapter 3, the methods of implementing wavelet transforms were presented including the conventional Discrete Wavelet Transform (DWT) methods. For notation purposes the Decimated DWT will be noted as DWT-A and the Stationary Wavelet Transform, (or Non-Decimated DWT) will be noted as DWT-B. There are major differences that result from these two approaches for PD analysis. These include the generation of robust PD signatures in the wavelet decomposition, better and accurate results from de-noising process. The result of which, produces a better diagnostic method for the detection and location of PD in the cables. The DWT-B approach will produce more accurate PD wavelet signatures compared to the DWT-A approach because of the preserved shift invariant property; but the drawback is that the computation complexity is increased. This is confirmed by the illustration of the comparison of both methods on a simulated PD signal, presented in the next section.

5.3.2 Significance of Shift invariant properties

Figure 5.4 illustrates the results obtained for a shift invariant and non-shift invariant system. The second input signal is the exact duplicate of input signal 1, with a delay of 200 samples. The output for the DWT-A approach indicates that the wavelet signatures generated vary, but the DWT-B result depicts the same version of the output from input signal 1, delayed by 200 samples. The DWT-B approach is known to be shift invariant.

Signals exhibiting similar features but slightly different alignment in time or frequency might generate fewer signatures in comparison to each other. Characterisation of PD signatures plays an important role in the data interpretation process. Origin of PD from the same source will have variations in amplitudes and frequency because of the stochastic nature. Hence, it is important that the generated

PD signatures are shift invariant to provide consistency and robustness in the classification of PD's. Furthermore, if multiple discharges are present, consistency in the generated PD signatures can be used to differentiate them.

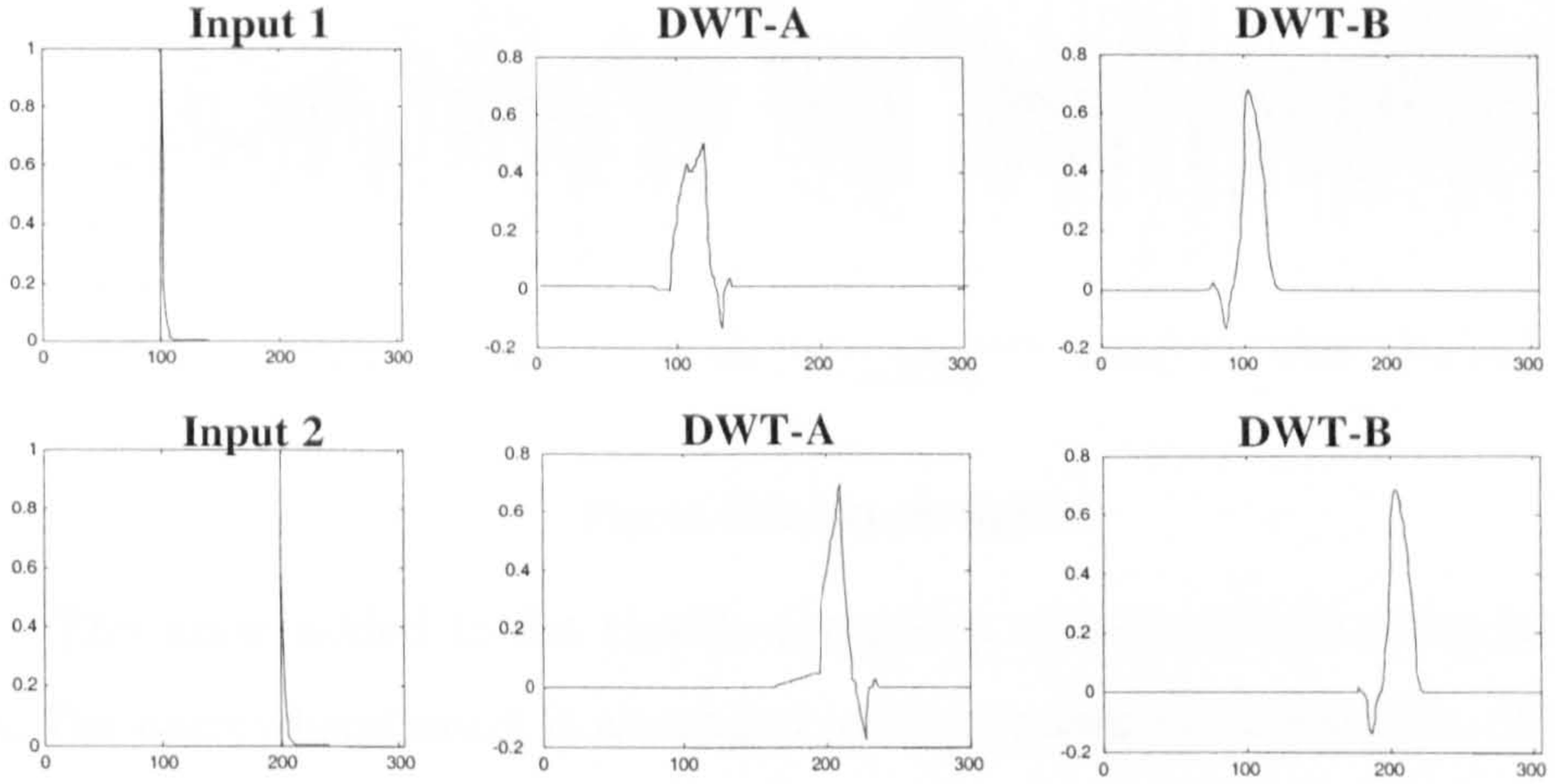

Figure 5.4: Example for shift invariant property

Discharge pulses often undergo reflection at cable terminations, which produce reflected discharge pulses that are reduced in amplitudes and dispersed. The shift invariant properties of wavelet processes can produce better results in efforts to locate the origin through TDR methods.

5.3.3 Performance of Decimated and Non-Decimated DWT

5.3.3.1 PD Detection and Its Wavelet Signature

The main objective in this example is to demonstrate the accuracy and performance of both the wavelet approaches when applied to TDR signals. All the generation of signal models and analysis were performed using Matlab. The original signal and the noise added signal is illustrated in Figure 5.5. The signal examples are deliberately chosen to be easy for the purpose of demonstrating the performances of the DWT approaches. The PD signal was assumed to be an exponential decay pulse i.e. an over-damped signal. With a 200-sample delay, a smoothened and attenuated version of the incident pulse is added to imitate a positive reflection from the termination.

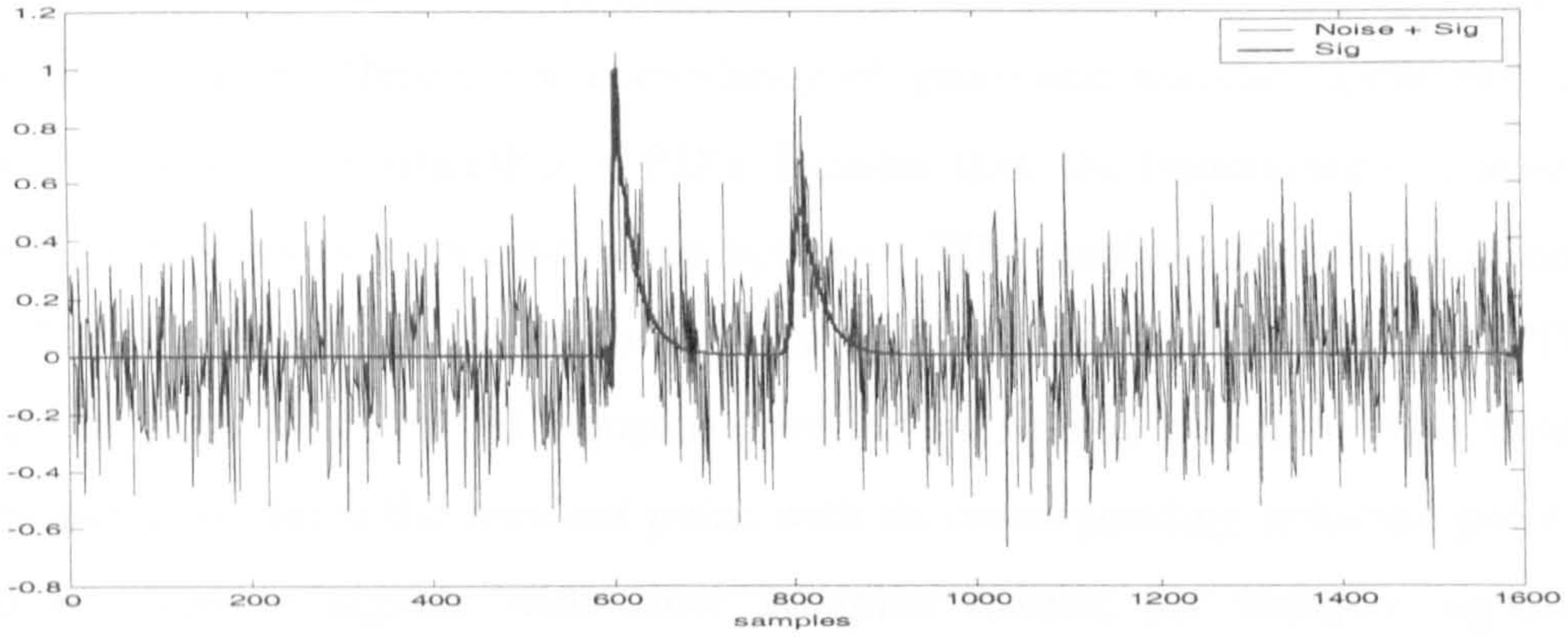

Figure 5.5: Sample signal

The noise added to the signals comprises of narrowband noise and random noise. The narrowband noise is simulated radio frequencies at 200 kHz, 600 kHz and 800 kHz. The overall signal to noise ratio (SNR) was set to –3 dB. The important points of this simulation are:

- Attenuation of the pulse along the cable is very small, almost negligible.
- Pulse dispersion does not occur.
- Reflection only occurs at one end of the cable
- Noise added to simulation is identical to noise in real environments.

The wavelet analysis was carried out on this signal, and the results of the DWT-A and DWT-B are depicted in Figure 5.6 and Figure 5.7 respectively. The wavelet filter used for this analysis is Daubechies-2, with 7-stage decomposition. For the DWT-A, the wavelet signatures generated for the first PD incident (around abscissa 600) are not similar throughout the detail scales. In the DWT-B, the wavelet signatures generated are more consistent throughout the detail scales. Furthermore, if we observe the reflection of the PD pulse (abscissa 800), in the DWT-A case the wavelet signatures are inconsistent throughout the detail scales and also comparing to the incident pulse. However, for the DWT-B more consistent wavelet signatures are generated.

Wavelets are used in certain instances to derive feature vectors or for statistical classification. Hence, the consistency of generated wavelet signatures is important for accurate classification of PD's. Besides that, the importance of robust PD wavelet signatures is portrayed when applying TDR analysis for PD location purposes. PD reflections will undergo attenuation and dispersion, causing the PD wave-shape to vary. If robust PD signatures are not generated, problems may arise when attempting to match the incident pulse with its corresponding reflected pulse. This will be seen in signals with more complex nature; for instance signals comprising more than one PD sources arriving at the measured end and measured within close proximity.

The TDR analysis is performed by measuring the time duration of the reflected pulse with the first pulse. In the wavelet domain, the same measurement of the time duration of the first generated PD signature and the second one is performed. Only certain scales are suitable for this purpose, and it is usually the wavelet scales that contain minimum noise yet with its spatial features preserved. In this case, the detail scale 5, (D5), is chosen and depicted in Figure 5.8.

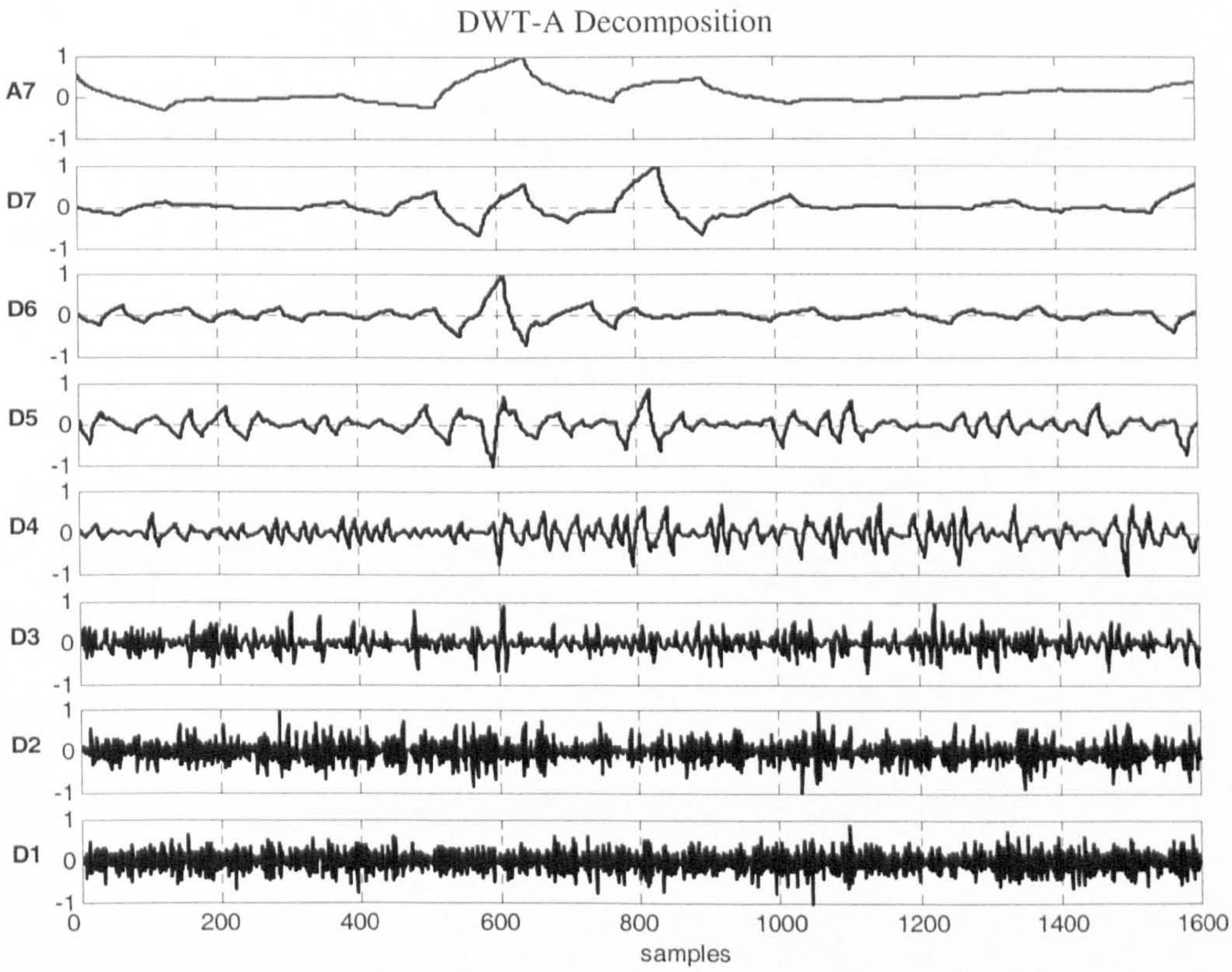

Figure 5.6: Normalised wavelet decomposition using DWT-A approach

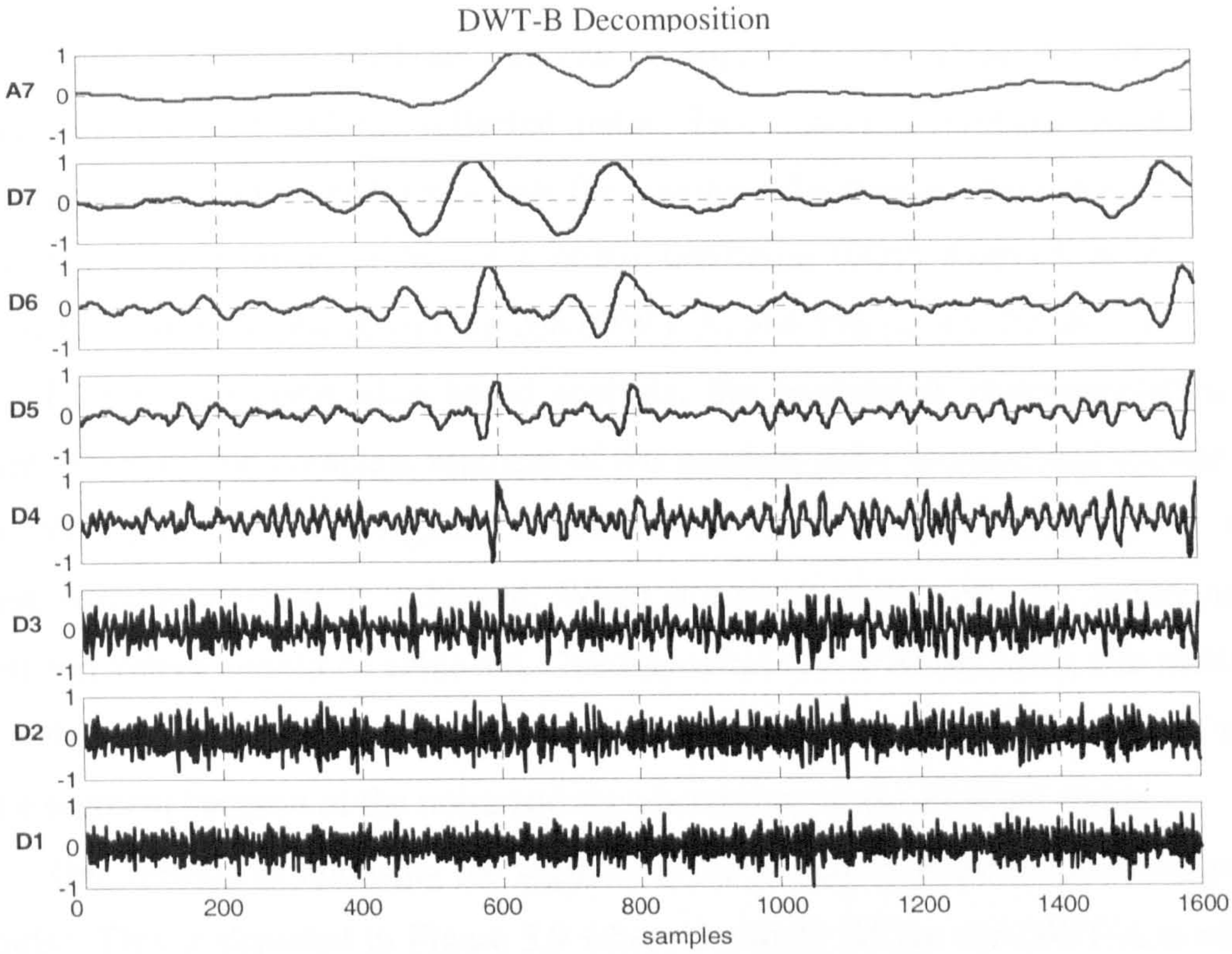

Figure 5.7: Normalised Wavelet Decomposition for DWT-B approach

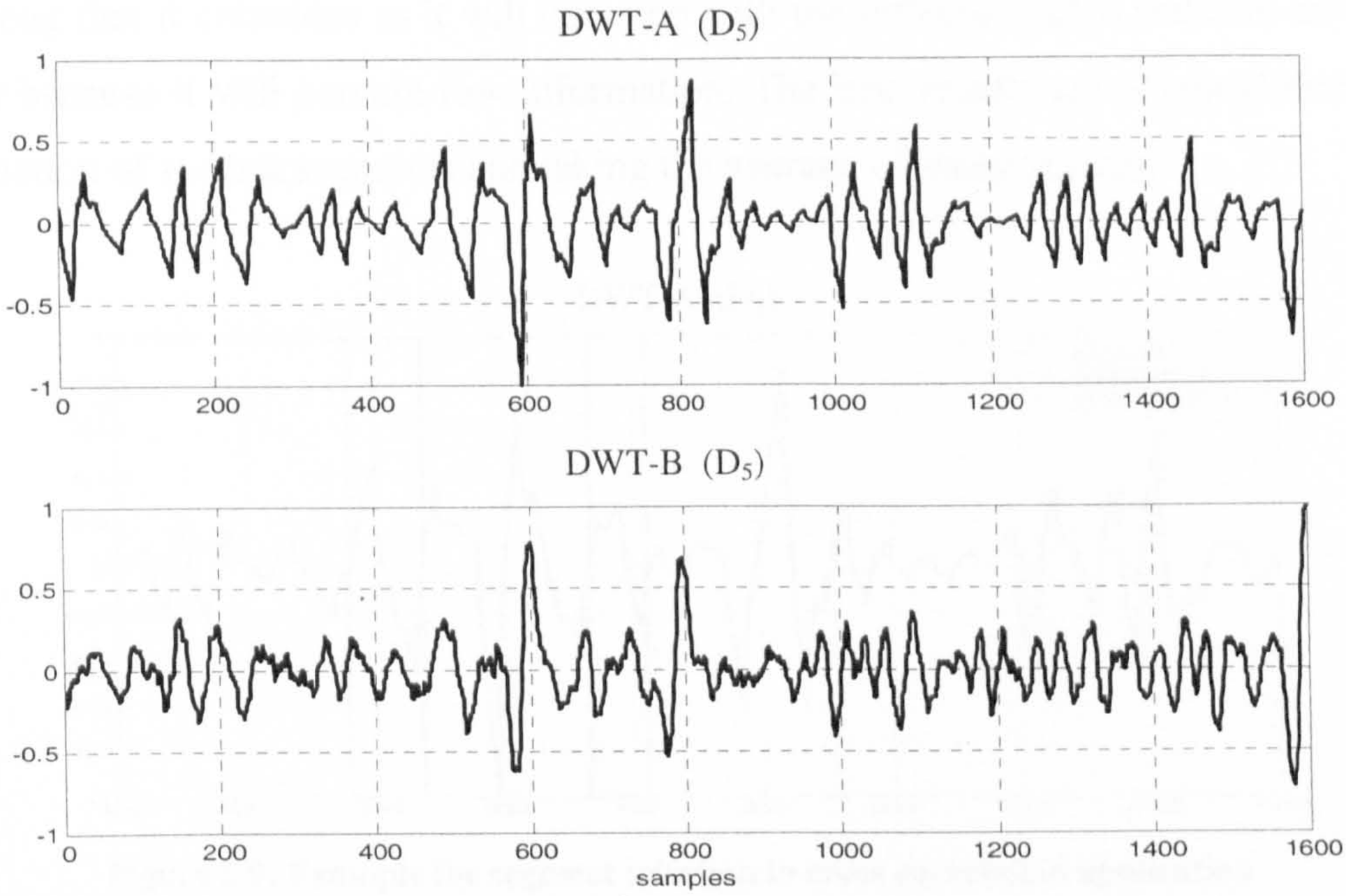

Figure 5.8: Detail scale 5, (D5) for DWT-A and DWT-B

There are several methods that can be applied to determine the delay time between the incident and the reflected pulse. Two common methods are directly choosing a prominent point for example the maximum/minimum point and matching it with the second pulse, or to use a cross-correlation based analysis. In the first method, the results for the delays are 208 (DWT-A) and 198 (DWT-B) samples.

In the cross-correlation based analysis, the segmented cross-correlation is applied, whereby the complete segment of the incident pulse is taken and applied to the whole signal. When the segment is at the exact location of the incident pulse, the highest correlation value is achieved. When it arrives at the reflected pulse, high correlation values should be achieved. One important factor whilst using this method is how the segments are determined. It may be difficult to determine the start and end for the segment because of the noise and the uncertainty of the incident shape.

One method of choosing the segment is the selection of the zero crossings of the pulse. This is depicted in Figure 5.9 where the scale D5 for the DWT-A is used. The two examples of segments are provided. The length of the segment should not be too long that it coincides as it will coincide with the reflected pulse and also not too short because it will contain low information. The best results are obtained through evaluation of several segments and taking the average of many signals.

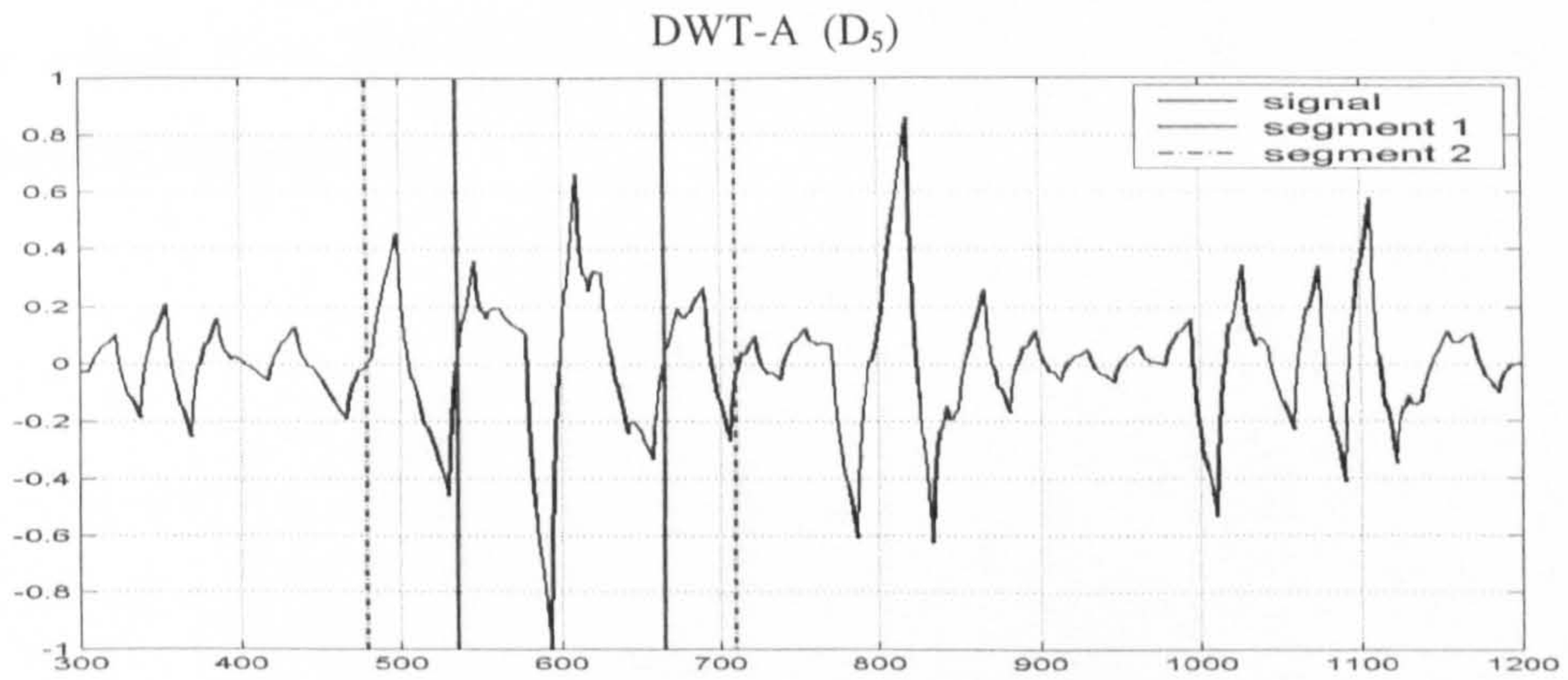

Figure 5.9: Example for segment selection in cross correlation application

For this case, the choice was made on approximating the start of the pulse until the duration of the pulse is complete. In reality, the accuracy of this method will depend on the selected segment. Best results are obtained by clearly identifying the shape of the PD signature. Here, the results are 193 and 197 for the DWT-A and DWT-B respectively.

The process of determining the reflected pulse for the DWT-B method is relatively easier and more accurate than DWT-A. The consistent wavelet signatures generated within the noisy environment indicates the benefits of using DWT-B. Although in this case the results do not show great differences, the implications for the actual PD location may be critical. The resolution used for this simulation was the no. of samples as the measure of time difference. The actual resolution of the distance in meters for every 10 samples is given by:

$$0.5 \times 10 samples \times \frac{\nu}{F_s} \qquad (5.1)$$

where ν is the velocity of propagation, and F_s the sampling rate. Hence, every 10 samples of signal will correspond to 16.7m in the actual distance of the cable ($\nu = 1.67 \times 10^8$ ms^{-1}, F_s = 50 MHz). From the consultation with a utility manager, PD location within 10 meters of the actual PD origin is considered good, especially through online diagnostics.

5.3.3.2 Wavelet De-Noising

The performance of wavelet de-noising is generally evaluated by measuring the closeness of the de-noised signal with the original signal. The quality of the de-noising will depend on the accuracy of removing the noise whilst restoring the original waveform. In many cases, the signal of interest is rarely known; hence the performance cannot be directly measured. Using knowledge rules from the de-noised signal or signal structure is one reasonable method to evaluate this.

Here the decimated DWT and non-decimated DWT application of wavelet de-noising is compared. The evaluation is performed by comparing the original known signal with the de-noised signal i.e. using the cross-correlation method. The sample signals used are the exponential decay pulse and the decaying sinusoid wave (Figure 3.2). These signal structures represent non-oscillatory transients and oscillatory transients. The best wavelet thresholding method was pre-identified and found to be the Heuristic Stein's Unbiased Risk Estimator (SURE) Thresholding [Donoho 1994]. The comparisons were performed for a range of SNRs; the result of which is tabulated in Table 5.2. The values in the table represent the normalised cross correlation values of the original signal and the de-noised signal. Hence, higher values of the correlation factor indicate that the de-noised signal is closer to the shape of the original signal.

	Exponential Decay		Oscillatory	
SNR	DWT-A	DWT-B	DWT-A	DWT-B
-3 db	0.8235	0.8477	0.6989	0.8067
-5 db	0.8229	0.8439	0.5233	0.7255
-10 db	0.7942	0.8252	0.6089	0.5911
-15 db	0.5255	0.6487	0.4311	0.4900

Table 5.2: Results of comparing de-noised signal through the normalised cross correlated values of the de-noised signal and the original signal for the exponential decay pulse and the decaying sinusoidal pulse.

For the exponential decay pulse, the performance of the de-noising was better for the DWT-B. For the decaying sinusoidal wave, the performance of the de-noising was better for the DWT-B compared to the DWT-A. The wave shape of the de-noised signal is more accurate to the original wave shape for the DWT-B. In overall, as the SNR decreases the performance of the de-noising becomes poorer. From –10 db onwards, the de-noised signal starts to contain false signal structures, as depicted in Figure 5.10. Transient structures arising from high noise levels are produced whilst the original signal structure becomes less precise. Hence, the correlation results between the original signal and the de-noised signal become less accurate. In some cases, visual observation of the signal is the best way to identify the quality of the de-noised signals.

These results also highlight the drawback of using the wavelet de-noising approach for transient detection i.e. when low SNR is present, false transients will appear. If this was performed on the full wavelet decomposition scales, the accuracy of transient detection will be higher.

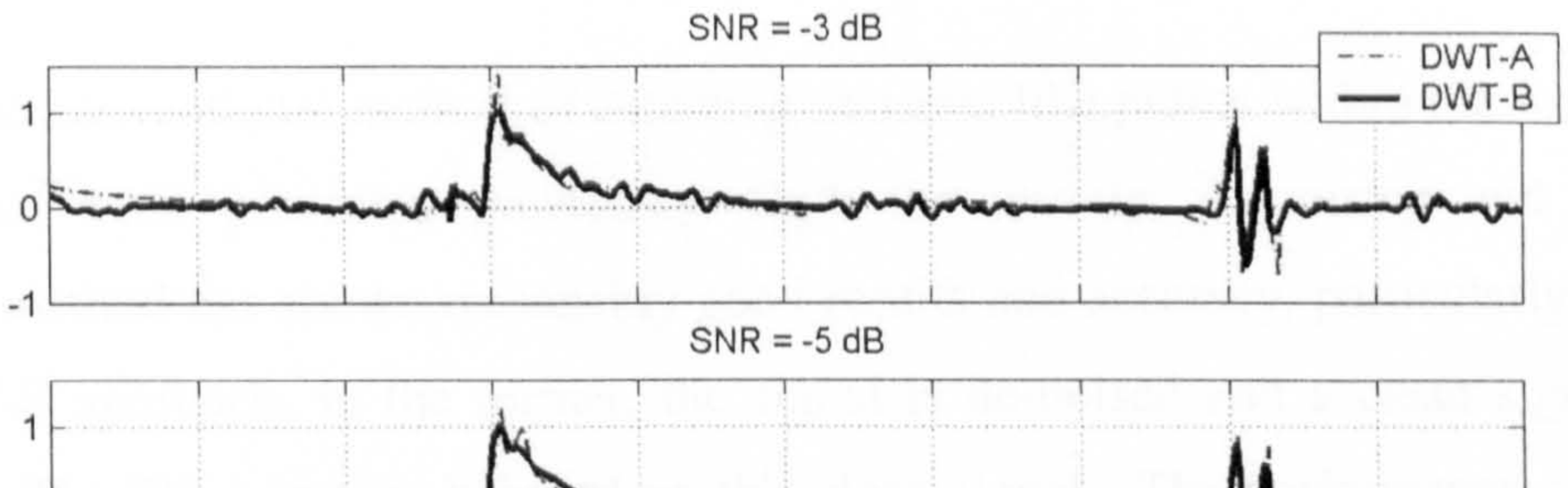

Figure 5.10: De-noised signals for the DWT-A and DWT-B using the HeurSURE thresholding method for various SNRs

5.4 Novel Kurtosis Based Wavelet PD Detection Algorithm

PD signals are categorised to have similar characteristics to transients. Its distinct signal structure that is different from noise characteristics produce large coefficients in the wavelet decomposition. This generates a distribution that is non-Gaussian. In contrast to noise samples, a Gaussian distribution is obtained when the signal is observed for a sufficiently long time [Ravier 1998]. The combination of the narrowband noise and random noise will generate a distribution close to a Gaussian distribution. Hence, the discrimination between PD's and noise can be deduced from a Gaussianity measure. Higher Order Statistics (HOS) are traditionally used to carry out this characterisation process through obtaining the kurtosis, which is the normalised fourth order cumulant. The kurtosis of a signal y can be evaluated as [Nikias 1993]:

$$\gamma_y = E\{y^4\} - 3(E\{y^2\})^2 \qquad (5.2)$$

The conventional method of detecting transient like pulses within the wavelet domain has been presented previously. Both the wavelet de-noising and edge detection method has shown reasonably good results and accuracy, particularly with the DWT-B approach. In the former, the signal is de-noised and a clean signal is produced. The PD detection is based on this clean signal. The performance of this technique is limited when there is poor signal-noise-ratio (SNR), or when the threshold parameters are not suitable. The latter technique has more reliable results because the PD detection is based on a multi-scale decomposition, based on the knowledge rules of PD characteristics and the wavelet criteria mentioned previous sections. However, this technique is also subjected to poor performances with very low SNR.

Generally, the wavelet-based algorithms are performed using Simulink from Matlab software platform because the enhanced graphical interfaces. The main disadvantage is that, the process time is increased and generally more tedious

especially when dealing with large data samples especially for computers that have low specifications. Low memory capacity and the processor capability will form limitations that will affect the performance of the user's controls. Hence, efficient methods of using these techniques will require relatively good processors and memory specifications to generate cost effective and valuable results. Implementation of the wavelet algorithms can be significantly improved by using other programming languages such as C/C++, Pascal, Oberon and others. However, the drawback of this is more complex programming is required for producing good graphical outputs. Hence, there will be minimal graphical user interfaces for data interpretation.

In reality, the PD detection process is complicated because of variations in PD amplitudes, shapes and features for each cycle of the power signal. In addition, noise interference present will also hamper the PD detection process. When dealing with raw field data, the computation complexities of the wavelet algorithms are increased significantly due to the large PD databases that are caused by using high sampling rates. This is especially for the DWT-B approach, which uses the redundancy concept of the wavelet transform. On the other hand, high sampling rates are necessary for maintaining the high frequency spectrum and good spatial resolution of PD pulses.

Often large sizes of data are divided into smaller sizes for file management and data analysis. This generally reduces the computation complexity and optimises the resolution of wavelet analysis. The new segmented data is processed using the relevant choice of wavelet-based transforms, and are conditioned individually. Under usual circumstances, a user will have to manually select the segments of the data that may portray useful PD information within the cable. Each segment is individually analysed using wavelet analysis and visually inspected for the existence of a PD signature until the complete signal has been covered. This process can be tedious and cumbersome especially for large PD data size. When these useful segments are selected, secondary analysis is conducted to isolate and identify potential PD activity.

In this section, novel kurtosis based wavelet PD detection algorithm is presented. Although, the technical aspects of this algorithm are not new on its own,

the combination of these algorithms produces a powerful tool for PD detection. The method of synthesising the obtained results is simplified and more efficient compared to the manual identification of PD activity. The main advantage of this algorithm is the flexibility under operation. This new algorithm also functions as a semi-automated PD detector, which highlights regions within a signal that may contain PD activity.

5.4.1 The Algorithm Description

The flow chart of this new algorithm is depicted in Figure 5.11. The raw signal is first segmented with sufficiently long segment size for effective characterisation of the noise levels. This is to guarantee the performance of the proposed algorithm. The concept behind this is to isolate segments of the signal containing mainly noise and selecting segments of data with useful information. Next, the segmented data are analysed using the wavelet transform i.e. using the DWT-B. A suitable wavelet filter and the maximum level for the wavelet analysis are chosen. In the previous section, a manual inspection of the wavelet scales was used for PD detection. In Figure 5.11, this manual inspection process is replaced with the application of decision rules generated by the evaluation of the kurtosis of each wavelet scale and performing signal processing.

Each scale in the wavelet decomposition is treated as individual signals. For a signal that contains mainly noise, the measure of kurtosis tends to be close to zero. If a PD or transient event is present, the kurtosis is a finite and distinct value. Kurtosis values in the wavelet scales will indicate if it contains useful signal structure. When the kurtosis values across the wavelet scales are tabulated, the distribution of the kurtosis values will indicate the existence of a potential PD or only noise. Preliminary results are obtained from the classification process, which is done by the observation of the generated pattern of the kurtosis values across the wavelet-decomposed scales.

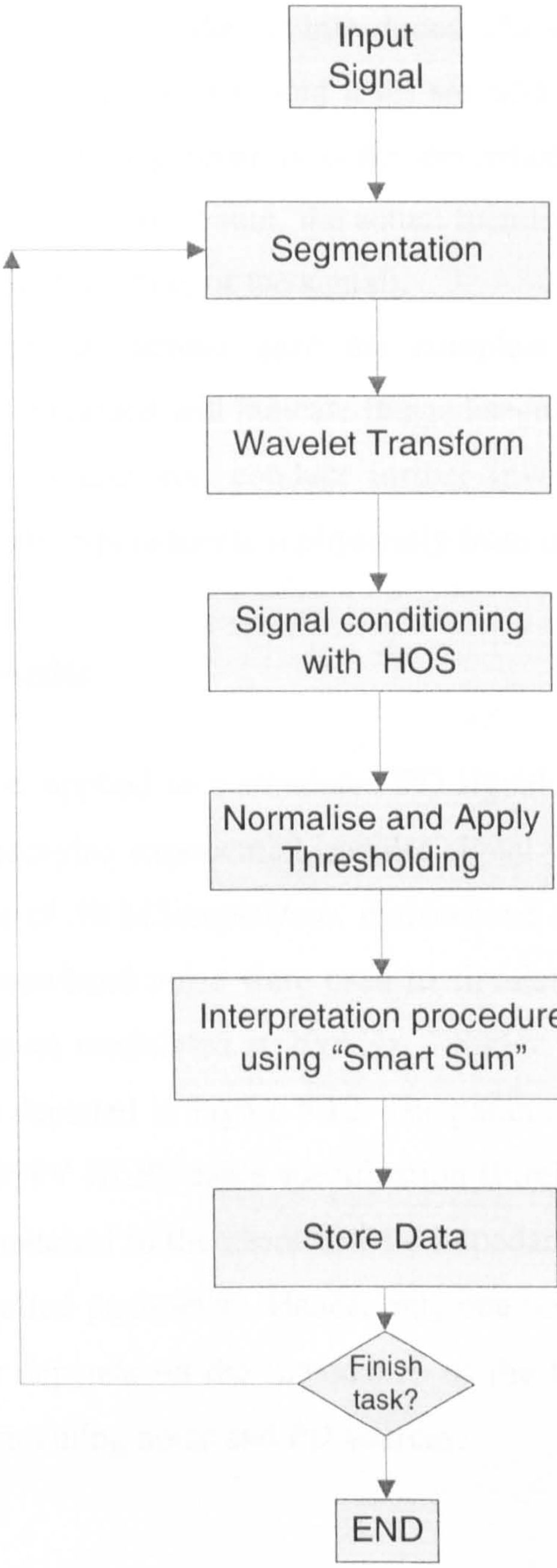

Figure 5.11: New wavelet-based on HOS PD detection algorithm

Next, the wavelet decomposition scales are normalised and thresholding is applied to them to produce a simplified binary format signal. In theory, the sum of all wavelet scales will produce the highest pulse peak at the instance where the transient has occurred. However, this is not necessary true especially when noise interference

is present. Here, a "smart sum" procedure is introduced whereby only wavelet scales that have kurtosis levels beyond the threshold level are added; i.e. only scales with prominent signal structures. This process is better described by using an example analysis. From the results of the smart sum, the actual location of the transient event can be identified (relative to the phase of the signal).

This entire process is iterated until the complete raw signal has been analysed. The final results obtained will indicate flagged segments from the complete signal. From the results, a user can conduct further investigation to verify the presence of the PD's and attempt to locate it physically from the flagged segments.

5.4.2 Simulation Results

The algorithm was applied to a simulated PD signal created in Simulink. A PD signal comprised a decaying exponential impulse signal with pulse width of 200 *n*s. With a sampling rate of 50 MSamples/sec, narrowband and random noise were added to the signal. Narrowband noise were used to simulate the RF interferences; and consisted of sine waves modulated at 200kHz, 700kHz, 800kHz and 1.2 MHz. The simulation model is depicted in Figure 5.12. The parameters of the cable are set according to the Pirelli 33kV XLPE cable specification [Pirelli 1996]. In this model, one end of the cable is matched to the characteristic impedance and the other can be varied depending on required parameters. Hence, only one reflection is produced and the reflection parameter depends on the impedance of the load. The results of the simulation are signals containing noise and PD sources.

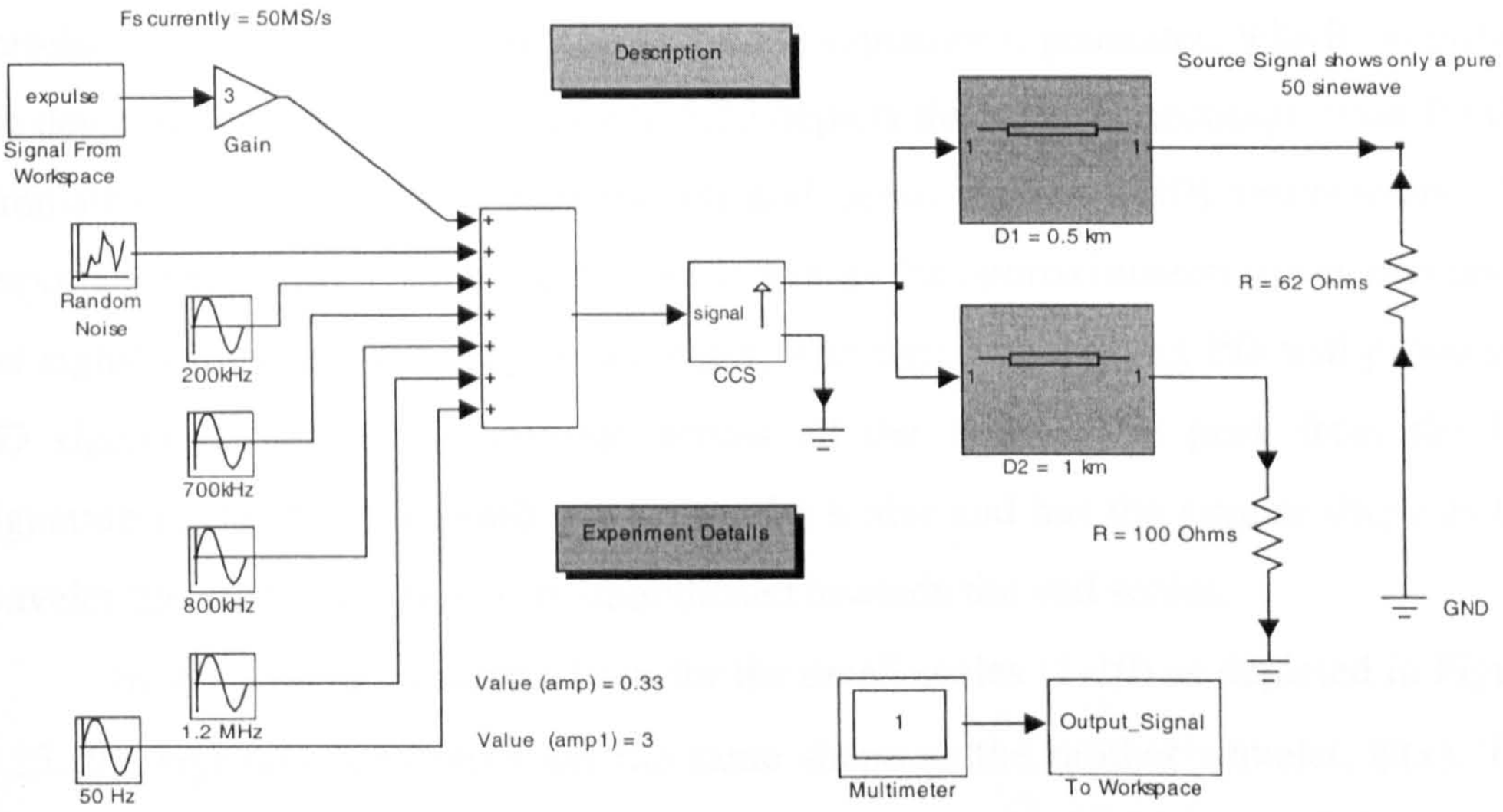

Figure 5.12: Simulink model for PD simulation in cable

The overall signal-to-noise ratio was -15dB. The simulated signal is separated into two segments for illustration purposes; segment-A with the simulated PD model and segment-B with pure noise without PD. Figure 5.13 depicts the normalised versions of the corresponding segments. The PD event is located approximately at 0.08 of the abscissa in Figure 5.13(a).

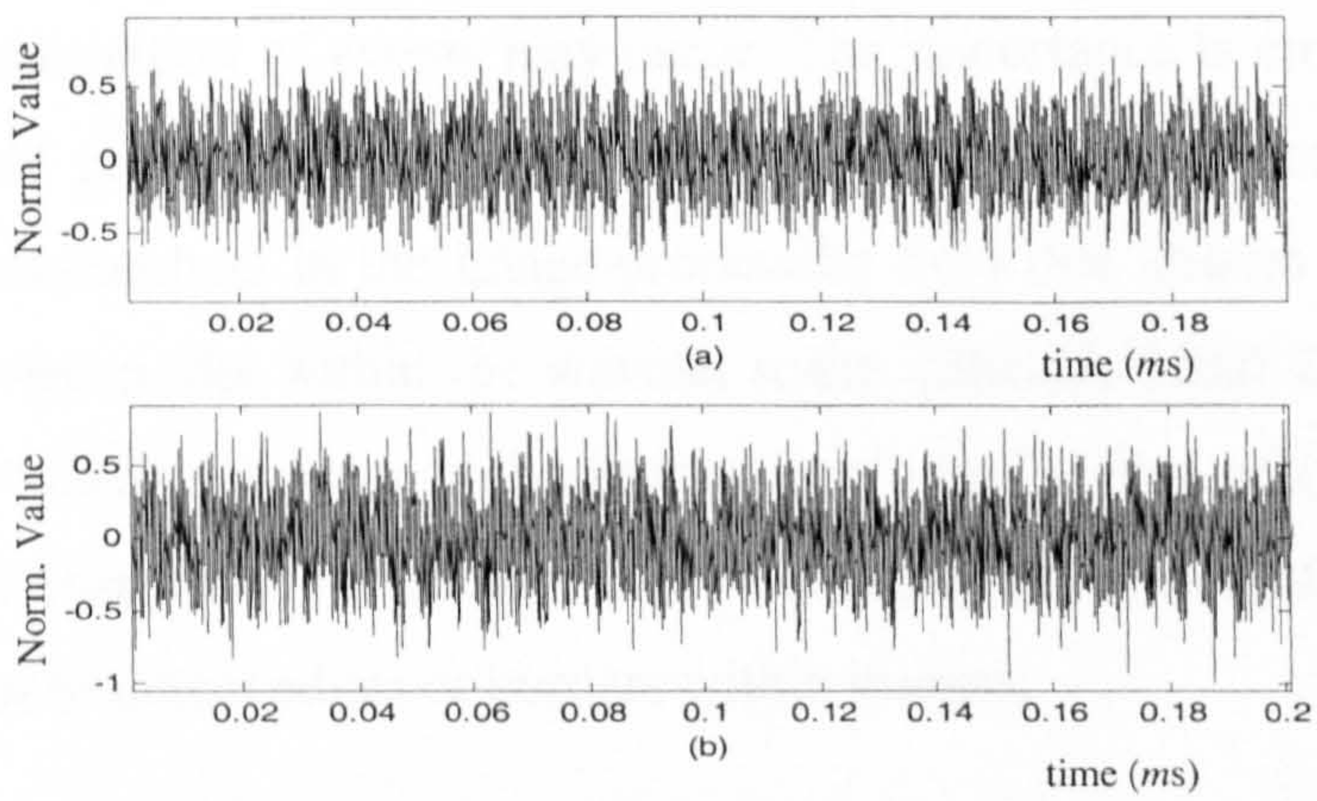

Figure 5.13: (a) Simulated PD signal (b) Pure noisy signal

The wavelet decomposition was carried out on the signals by using the cubic spline wavelet depicted in Figure 5.2. This wavelet was chosen because of its good correlation to the transient signals and the PD signature it generates, which simplifies the detection process. Figure 5.14 and 5.15 depicts the wavelet decomposition for the simulated PD signal for approximation and detail scales (1-10) respectively. An important observation from Figure 5.14 is that as the approximation scales increases, the signal information conveyed decreases. The signal containing PD will produce a PD signature that is synchronised across all the scales. The peak from the PD signature is clearly distinguishable across the scales and has the similar shape as the wavelet function. However, it is smoothened towards the end scales.

In the wavelet decomposition for the detail scales (1-10) as depicted in Figure 5.15, the signature generated has the same shape as the mother wavelet, $\psi(x)$. The detail scales contain mainly the high frequency components of the signal. Hence, the PD signatures generated within the first few scales cannot clearly be distinguished, since it mainly contains the high frequency noise components from the signal. It is common practice in signal processing to discard the first few scales (D_1-D_3) [Mallat 1990], depending on the usefulness of the information conveyed in these scales.

In Figure 5.16 and 5.17, the wavelet approximation and detail scales of the noisy signals are illustrated. There are some indications of peaks in the scales but there is no distinct indication of an event in the wavelet scales. However, in computer vision, the peaks in each scale will still be accounted for. The result of this is that false information of events may occur. The importance is emphasised on the identification of peaks that are events in the signal. There are several algorithms developed by researchers in the image-processing field that utilises fuzzy reasoning to isolate relevant peaks within the wavelet scales [SheikhAkbari 2005, Setaredhan 1998]. These techniques have high computation complexities and work best with step functions instead of oscillatory and non-oscillatory transients. The primary application was to detect edges or borders within images.

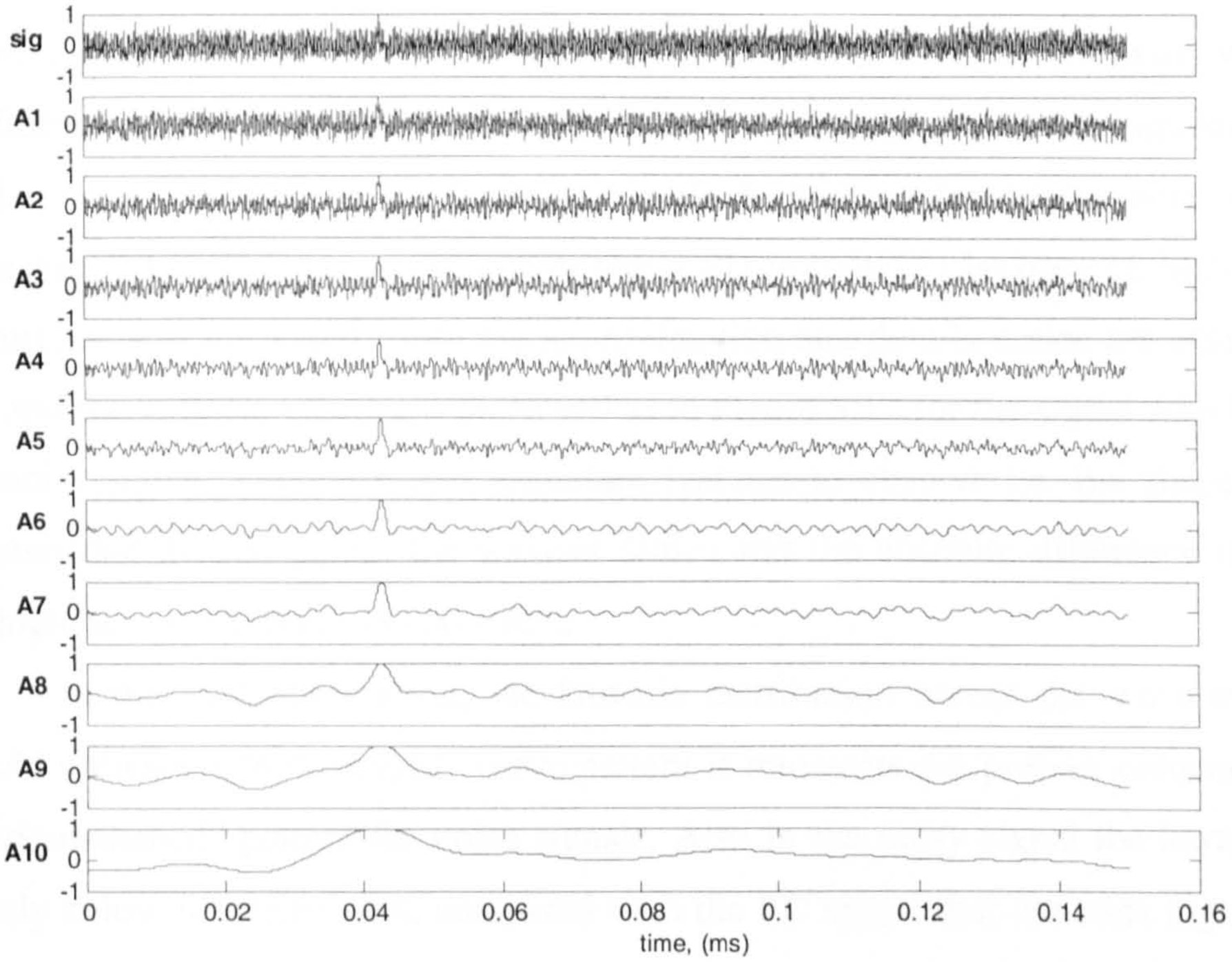

Figure 5.14: Wavelet approximation scales for signal containing PD

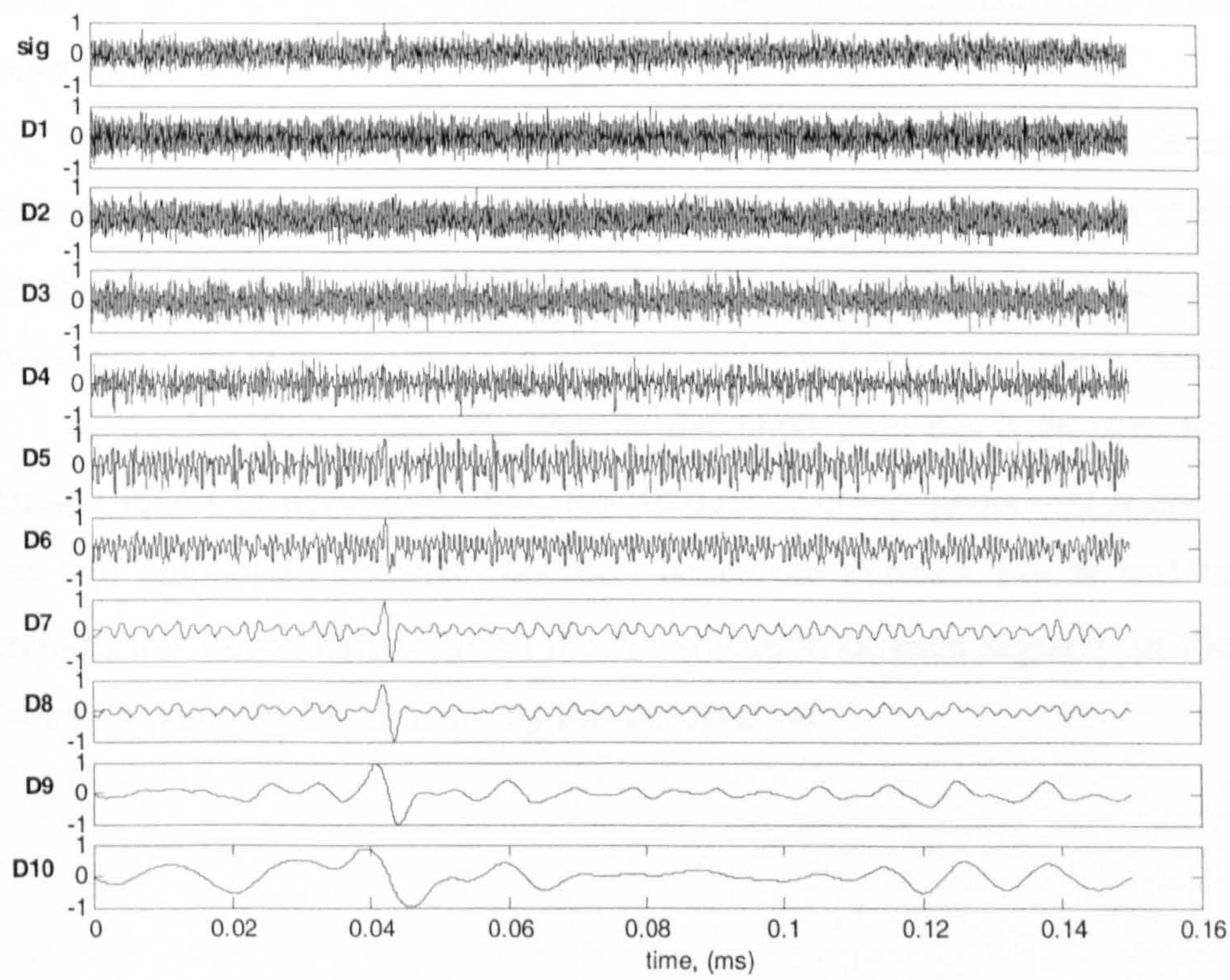

Figure 5.15: Wavelet detail scales for signal containing PD

After obtaining the wavelet decomposition, the kurtosis of each wavelet scales is evaluated to produce the measure of Gaussianity. In reality, if a signal is

approximately Gaussian, the kurtosis will not exhibit a zero value, but exists within a confidence interval [Ravier 1998]. The average values obtained from simulated and field results showed that the kurtosis value had an upper boundary value of 4 for Gaussian distributed scales. In cases where a PD is found to be present, high values of kurtosis was measured. Both the approximation and details scales are utilised for this and the kurtosis values are displayed as in Figure 5.17 for the signal with PD and the noise signal. There are two important features to observe i.e. the shape of the kurtosis distribution across the wavelet scales and the absolute difference between the highest value and the lowest value.

In the first observation, the kurtosis distribution across the wavelet scales should indicate a "bell-shaped" curve pattern if transients are present compared to a "random-shaped" pattern for noise signals. Also in the noisy signal the kurtosis are mainly below the value of 4, compared with the PD signal that contains high values of kurtosis. The approximation (A_5-A_{10}) and detail scales (D_8-D_{11}) of the PD signal indicate the presence of non-Gaussian signal components is distributed across these wavelet scales.

From the redundancy and deviation of wavelet maxima issues described in section 5.2.1, a range of scales around the first and last few scales in the wavelet decomposition are neglected. Noise mainly resides in the first few scales, hence the observation of the kurtosis values from these scales will have minimum values.

At the last few scales, the wavelet decomposition has been stretched to the maximum levels of decompositions, low frequency components that reside in these scales will emphasize Gaussian features; hence the kurtosis values will be small. Therefore, this observation enables the classification of each segment of the signal; i.e. whether potential PD or noise by this observation.

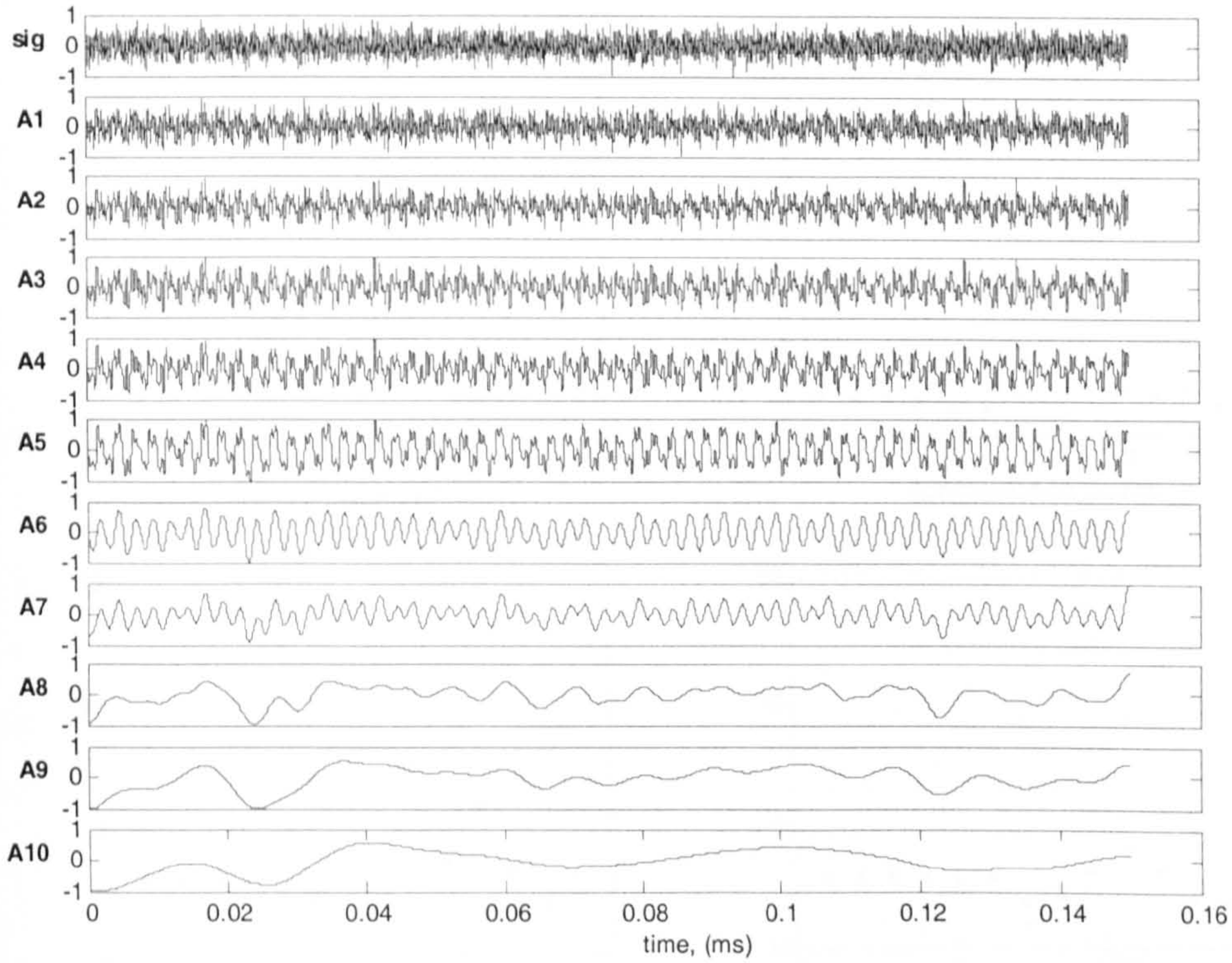

Figure 5.16: Wavelet approximation scales for signal with no PD

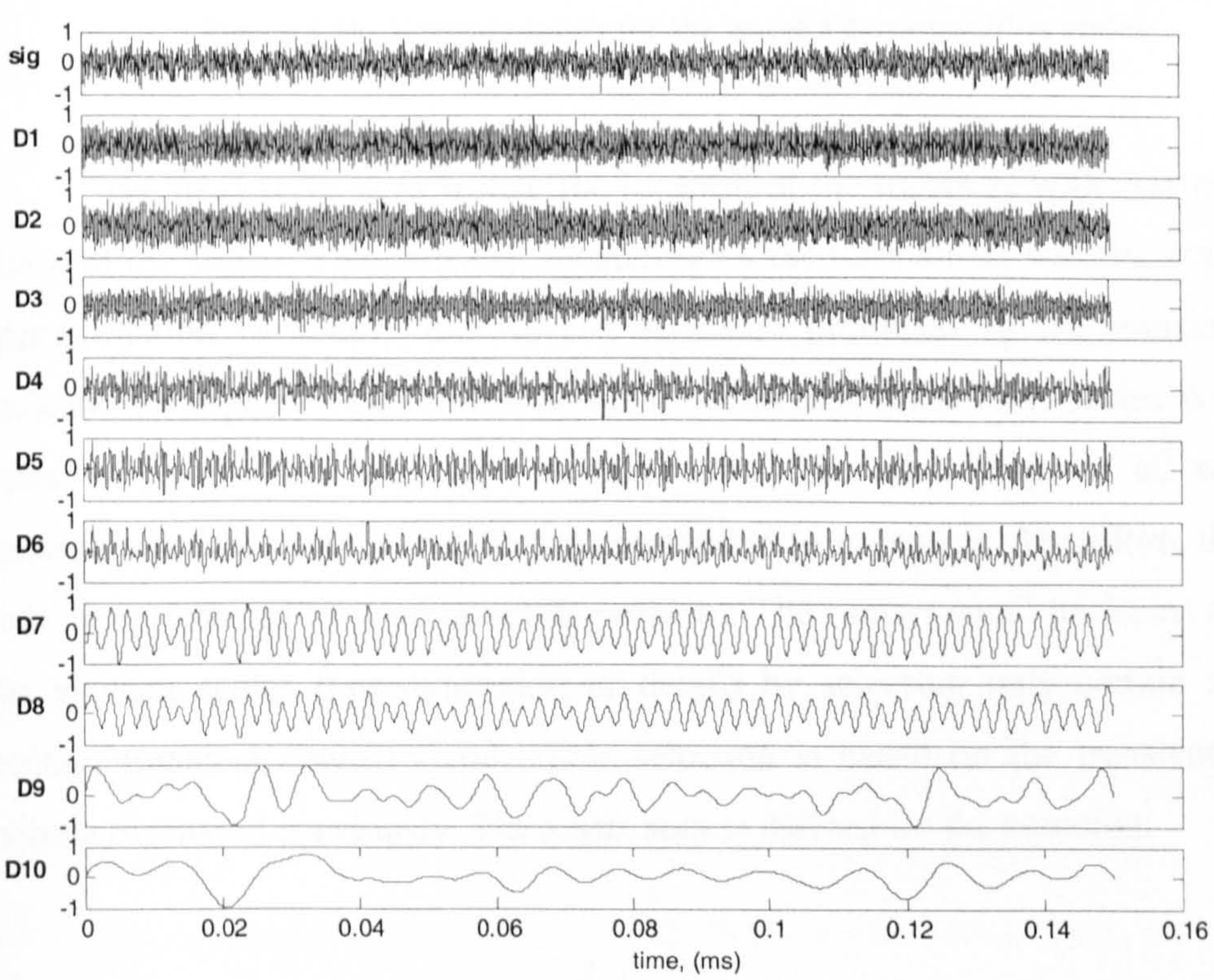

Figure 5.17: Wavelet detail scales for signal with no PD

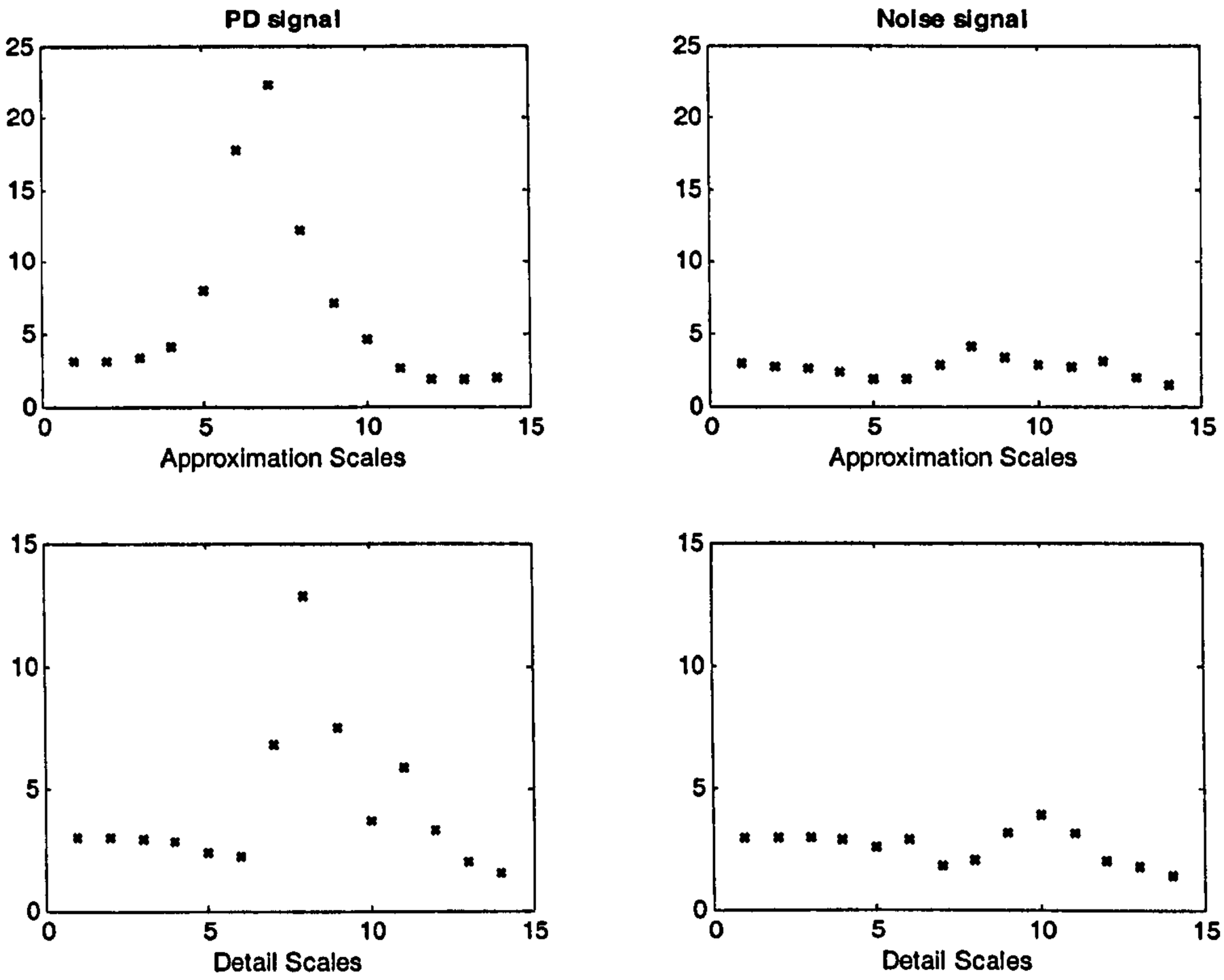

Figure 5.18: Kurtosis values for the wavelet decomposition scales

The next stage is to isolate the location of the transient with reference to the phase of the signal. Theoretically, by adding all the normalised wavelet scales (either approximation or detail), the wavelet signature produced by the transient should indicate the highest value at the point of occurrence. However, scales with mainly noise will cause the results to be inaccurate. The summation of all scales may generate maximal values that do not correspond to transients. Therefore, the "smart-sum" is introduced to overcome this problem. The "smart-sum" performs addition to the wavelet scales (approximation or detail) by selecting only certain scales that contain transient characteristics. This selection is based on the transient detection criteria discussed previously. The smart sum is defined by the equation:

$$S = \sum_{n=1}^{J} \delta_n \cdot \mathrm{X}_n \bullet \mathrm{B}_n \qquad (5.3)$$

for n = 1,2,.... J, where δ_n is the individual hard limit threshold for each wavelet scale, X_n is either the set of approximation, (A_n) or detail scales (D_n), B_n is the selection multiplier (1 or 0). The hard limit threshold, δ_n, is determined by using a percentage of the normalised wavelet scale, for example 75%. Any values below this threshold is set to 0 and above this value is set to 1. The multiplier, B_n, is obtained from the kurtosis values of the wavelet scale. This means that only wavelet scales that have high kurtosis values and above the threshold are selected. Hence, if the scale comprises of noise then that signal is neglected. From the simulated experiments with various types of noise and distribution, the nominal value for the kurtosis was found to be approximately 4. Therefore, from this analysis the threshold was set to this value. Estimators can be used to determine a more accurate threshold for the kurtosis. However, under the criteria of kurtosis-based characteristics this experimental value was sufficient to perform the task.

The smart sum output is illustrated in Figure 5.19 and 5.20. The smart sum has the form of a simple binary signal with three values, (-1.0,1). The evaluation process is repeated for all the segments in the signal. Finally, the smart sum is used to indicate whether segments of the signal contain potential PD activity or noise. The important segments are flagged and secondary analysis is further conducted for PD detection and location. However, the interpretation process for the smart sum by computer algorithms have to be determined by using a set of knowledge rules to produce accurate interpretation of the data. These rules are as shown:

Rule 1: Ratio of maximum value of the smart sum and the total scales used
Rule 2: Difference of peak values and the threshold values
Rule 3: Number of consecutive kurtosis values above the threshold value.

When a transient like signal is present, the sum of scales will produce a high value at the proximity of the event. The first rule observes the maximum value of the smart sum compared to the number of scales used for the addition procedure. For instance, if the maximum value is 5 and the number of scales used is 6, the ratio will

indicate high value of 83.3% (5/6). The high ratio values indicate high probability that the result occurs because of a transient event and likewise for low ratio values.

The second rule observes the difference of the peak value of the kurtosis distribution with the threshold value. From this, if the values are not distinctly more than the threshold value, the signal has not prominent non-Gaussian features and the kurtosis distribution is highly probably caused by false events that are a weak transient representative.

The third rule relates to the wavelet signatures within the wavelet scales. As mentioned previously in Section 5.2, transients will produce wavelet signatures across all scales. In some instances, there may be scales that will not produce strong prominent wavelet signature depending on the strength of the noise within the scales, especially narrowband noise that might have stronger wavelet coefficients in certain scales. In other instances, a noisy signal structures (noise events not originating from PD) may display high kurtosis values in random scales. Therefore, the sequence and consecutiveness of the kurtosis values satisfying the threshold are observed. The consecutive values correspond to the likelihood that the event is a transient; In other words by observing the "bell-shape" pattern as depicted in Figure 5.18.

In Figure 5.19, the summing techniques were applied to the wavelet approximation scales for the signal and the noise. If the top two axes are observed, the summed values both indicate distinct peaks at around abscissa 0.05. The results of both are reasonably good. However, the purpose of the algorithm was for semi-automated PD detection purposes. This is clearly illustrated by the summed signals from the noise. In the smart-sum process the maximum value is 1, which is a very low value, compared to the conventional summing method that has high values of 9. In this case, the machine will have difficulties interpreting the signals obtained from the conventional summing method because of the similar amplitudes of signals generated. The smart-sum algorithm clearly distinguishes the signal and the noise.

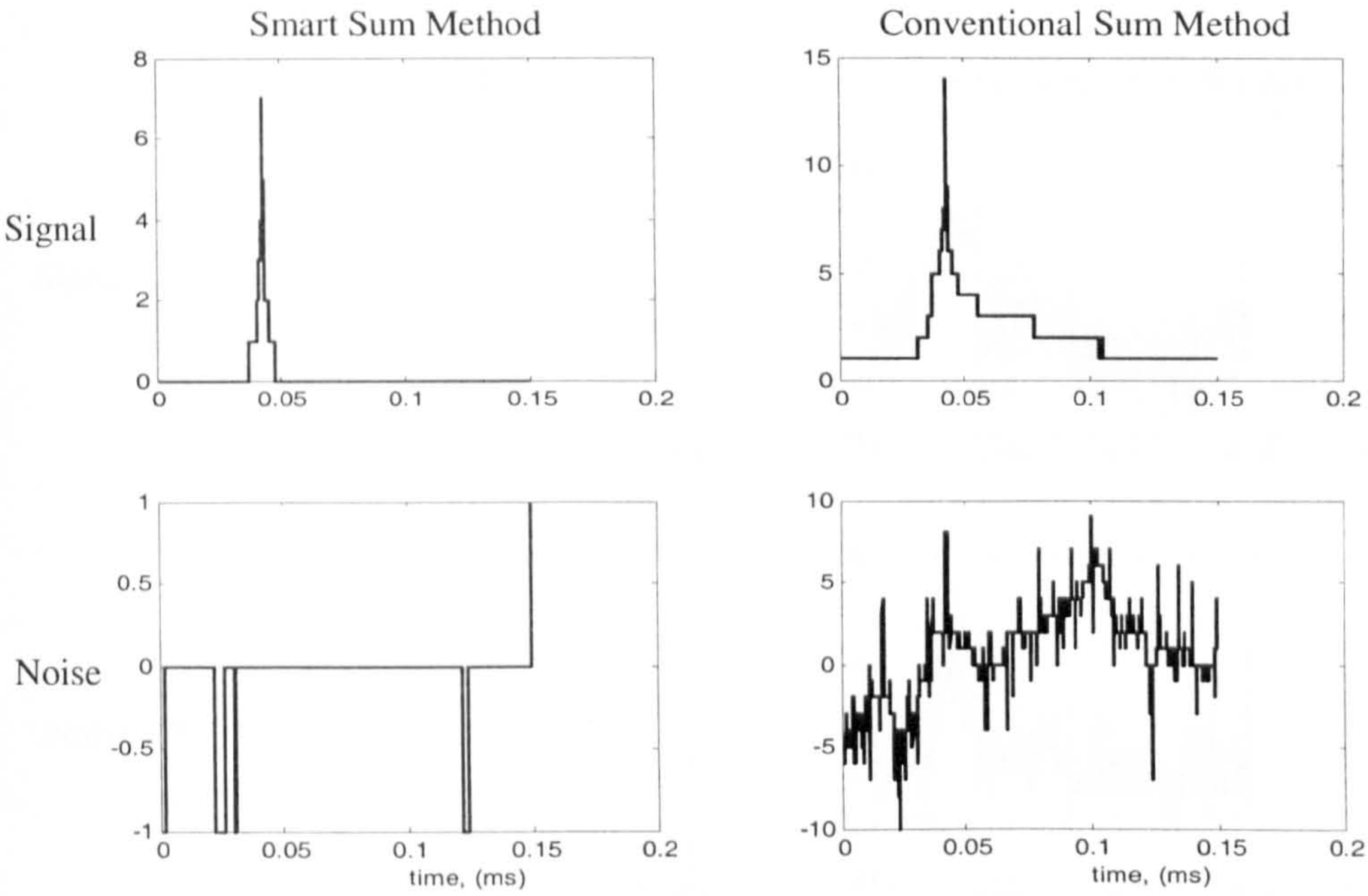

Figure 5.19: Smart sum for wavelet approximation scales

The identical process was applied for Figure 5.20, where the summing methods were performed on the wavelet detail scales instead for the same set of signal and noise. Again the smart-sum method clearly distinguishes the signal and noise. In this case, the values obtained are lower than the values in the approximation scales because of the added noise i.e. only a few scales are used for the smart sum. The conventional method does not work well because it generates similar characteristics for both signal and noise. Hence, this new algorithm has potential to be a useful tool for a semi-automated PD detection.

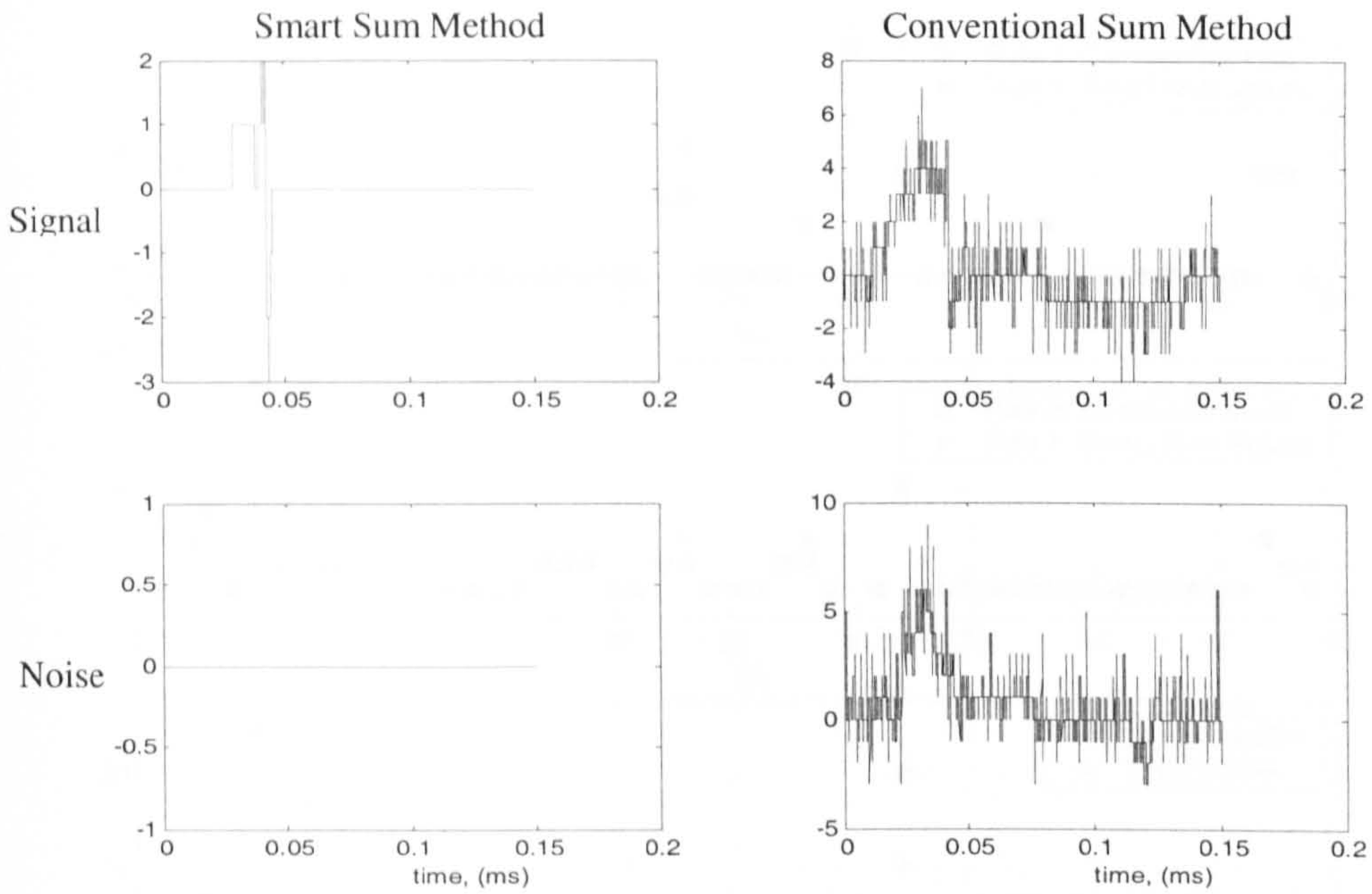

Figure 5.20: Smart sum for wavelet detail scales

5.4.3 Results on Field Data

This algorithm was tested on field data obtained from a 33kV cable network. The sampling rate used for this signal was 50 MS/s; hence the size of this dataset was $1x10^6$ samples (one 50 Hz cycle). Firstly, the signal was divided into fifty segments of 20000 samples each. These segments were processed and the results of which is shown in Figure 5.21. In Figure 5.21(a), the smart sum values (see *Rule 1*) and the consecutive wavelet scales above the kurtosis threshold (see *Rule 3*) is shown for the approximation scale. Figure 5.21(b) also provides the same information as Figure 5.21(a) but for the detail scales. Figure 5.21(c) shows the range of the kurtosis (see *Rule 2*) of the wavelet scales for each segment. For simplicity, we will only concentrate on one half of the 50 Hz cycle i.e. from segment 1 to 25. Segments 5 and 7 have prominent kurtosis value range that suggest that transient activity is likely. In addition the maximum smart sum values are high and also with high ratios of the maximum smart-sum value to the maximum sequence.

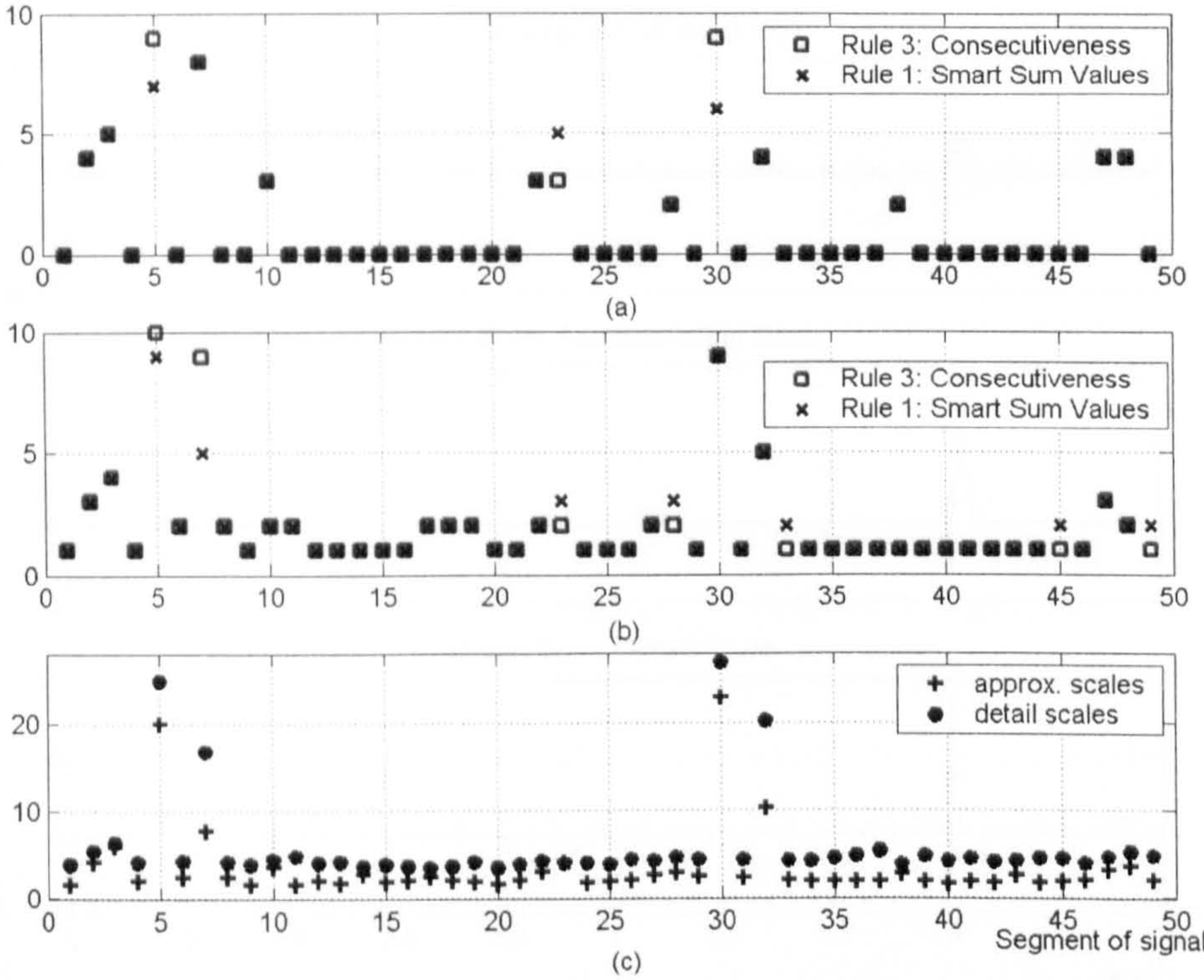

Figure 5.21: New Algorithm results for 33kV field data where the x-axis denotes the segmented parts of the whole 50Hz sample signal (a) Rule 1 and 3 for approximation scales, (b) Rule 1 and 3 for detail scales, (c) Rule 2 for both approximation and detail scales

In actual case, a prominent transient was present in segment 5 of the signal. This is illustrated in Figure 5.22, where the top trace is the original segment of the signal and the other two are smart-sum signals. Here, clean signals were produced within the smart-sum for both the approximation and detail scales. Also note that the shape of the smart-sum represents a simplified approximation of the original transient structure.

However, for segment 7 prominent transient signals was not the case. Here, the signal structures had less amplitudes and noise is comparable to the size of the transients (as illustrated in Figure 5.23). There were more than one instances of transient in this case; both with low amplitudes and detected by the algorithm. The structure of this signal was different to the one in segment 5 in amplitude and shape.

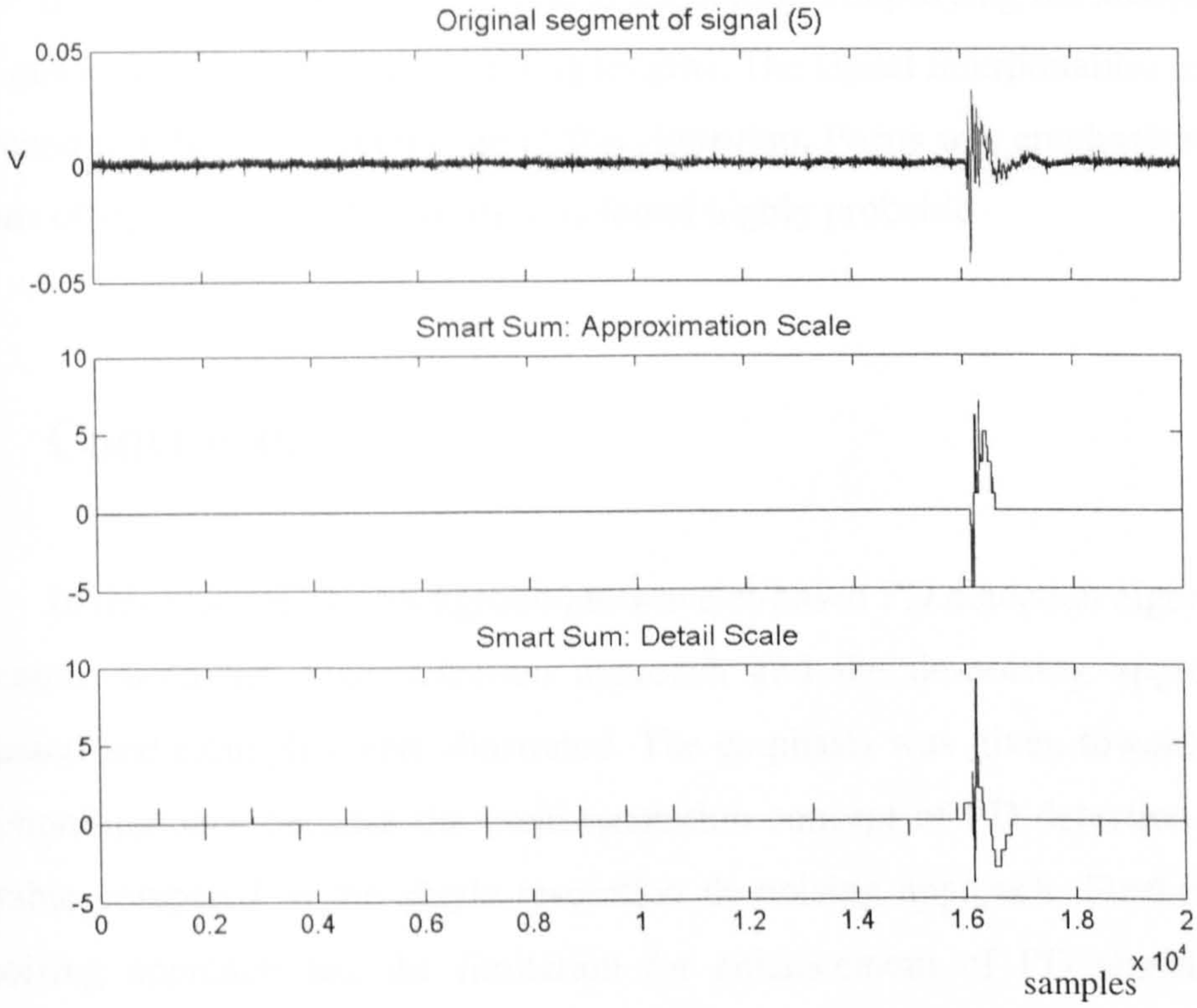

Figure 5.22: Smart-sum result for segment 5 of signal

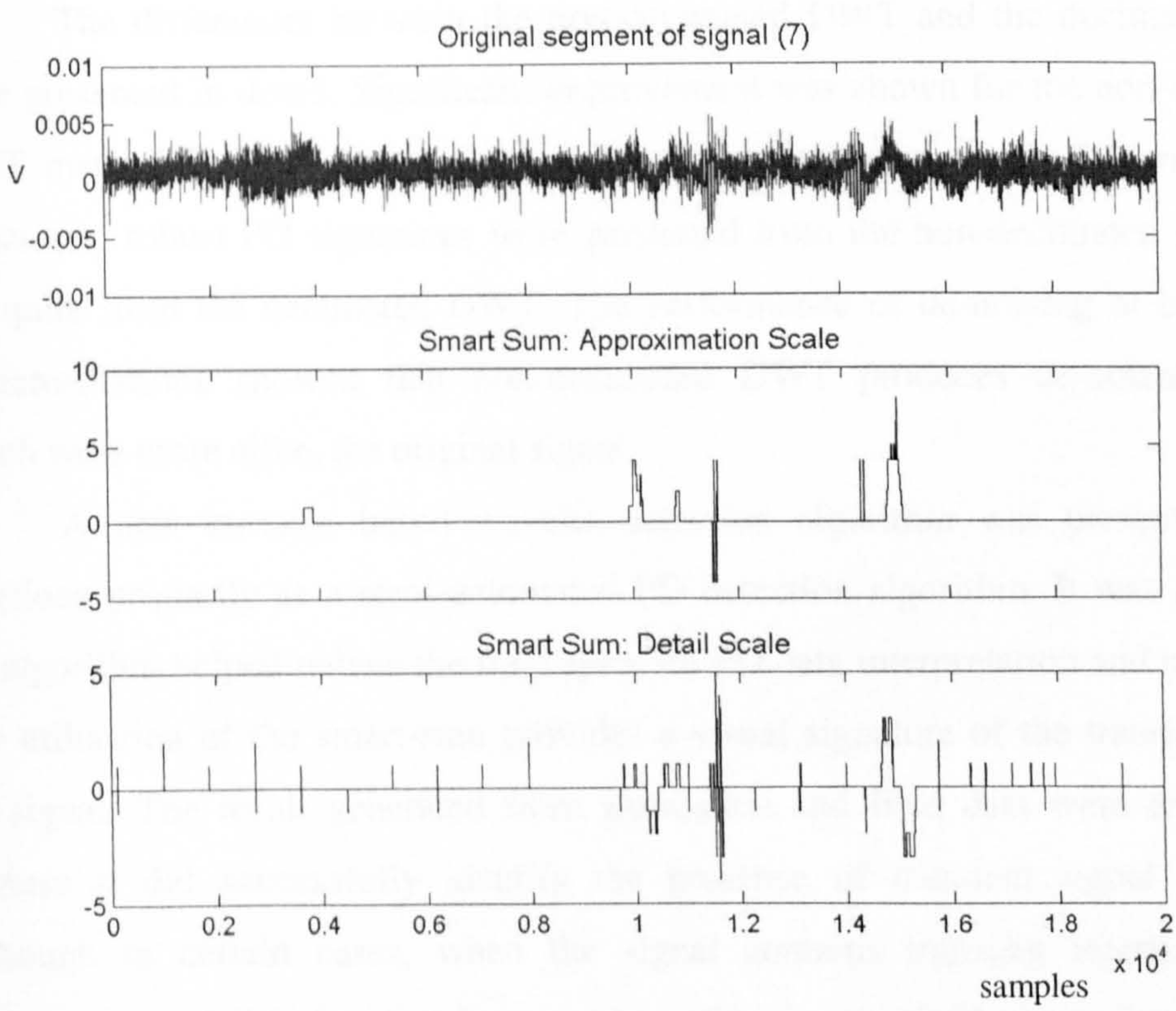

Figure 5.23: Smart-sum result for segment 7 of signal

In overall, this algorithm provided a means of simplifying the analysis of large quantity of datasets that have long lengths. The signal interpretation time was shortened significantly with the aid of this algorithm. Focus was emphasized on the regions of signal where PD activity was found highly probable.

5.5 Conclusions

In this chapter, the background to wavelet-based PD detection algorithms was presented. Both the edge detection approach and the de-noising approach were discussed and examples were illustrated. The emphasis was given towards the edge detection approach because the multi-resolution concept of PD detection was more desirable compared to the single resolution de-noising approach. Furthermore, the de-noising approach has the limitation for enhancement of PD signal for TDR applications, especially for highly noisy signals.

The differences between the non-decimated DWT and the decimated DWT were presented in detail. Significant improvement was shown for the non-decimated DWT method for PD detection through edge detection approach. In terms of PD signatures, robust PD signatures were generated from the non-decimated DWT and not quite from the decimated DWT. The performance of de-noising of both DWT implementations showed that non-decimated DWT produces de-noised signals, which were more alike, the original signal.

A new kurtosis based wavelet detection algorithm was presented which functions primarily as a semi-automated PD detection algorithm. It was found that the algorithm helped reduce the time spent on PD data interpretation and processing. The utilisation of the smart-sum provides a visual signature of the transient within the signal. The result generated from simulation and field data were encouraging because it did successfully identify the presence of transient signal structures. Although in certain cases, when the signal contains transient interference this algorithm may fail to function because the entire signal would trigger the smart-sum process. This will apply to the signals that are presented in the next chapter. Those

signals are the same signals that were measured from Subtation A (Cable-1 and Cable-2), but at a different time instance.

Chapter 6 : Interpreting Online HV Field Data

6.1 Introduction

In the past two chapters, the data acquisition system for field data measurements and wavelet-based signal processing techniques were presented. In this chapter, the outcome of the previous two chapters is merged; where field data will be analysed. This chapter aims to address the issues related to data analysis procedures and to present results of the analysis. This is emphasised on the various signal-processing techniques developed, in conjunction with the wavelet-based algorithms to produce important data analysis and interpretation procedures. The investigation is performed in-depth and results and analysis will be provided. Aspects of efficiency of the algorithms will also be covered for the algorithms with high computation complexities.

However, before that prior knowledge and understanding to the physical cable network configuration is required. Hence, the network configuration, background and brief history of the test site is discussed in Section 6.2. In Section 6.3, the signal interpretation procedures for detection and location are presented. This covers the single-ended and the double-ended approaches. Next, the acquired data from the test site is provided in Section 6.4. The signals acquired from the set of power cables at the substation is analysed and compared. The noise interference analysis was conducted in order to differentiate signal from noise. Difficulties with signal interpretation are also discussed in this section. Section 6.5 then provides the results of all the data analysis conducted on the variety of field data signals. The

trends and characteristics of the PD are highlighted in this section. Finally, the conclusions are presented in Section 6.6.

6.2 Substation A - B 33 kV Network Configuration

In this project, the emphasis was placed towards the single-ended PD detection and location techniques. The developed data acquisition system was used to gather data from a selected 33kV network. The particular cable network (Substation A - B) was chosen because of its history of frequent breakdowns. The cable network works under a dual cabling system, whereby two parallel sets of cables were laid from Substation A - Substation B. This was to ensure that if a breakdown does occur on one set of cables, the other functions as backup for the network. When both cables are under normal operating conditions, the load current is shared equally between both sets of cables (Cable-1 (W1) and Cable-2 (W2)). The utility company found that whenever, either one set of cables is taken offline for repairs or maintenance, the other corresponding set of cables tends to have a fault not long after the event. This is likely to occur because the backup cable has to sustain double its normal current loading of the cable, which enhances the stress conditions on the cable. A picture of the substation switchyard is shown in Figure 6.1 and the section of network configuration for the Substation A – B network is illustrated in Figure 6.2.

At the Substation A end, the cables are divided into 2 circuits i.e. Cable-1 and Cable-2. The cables originate from connections are made to the 33kV bus bars known as the Substation A Grid. There are many other 33kV cable networks connected to this bus bar (see Appendix C1). The cable lengths are approximately 1.7 km, running towards Substation B. At Substation B, the cables are connected to a step-down transformer, which converts the voltage to 11kV distribution network.

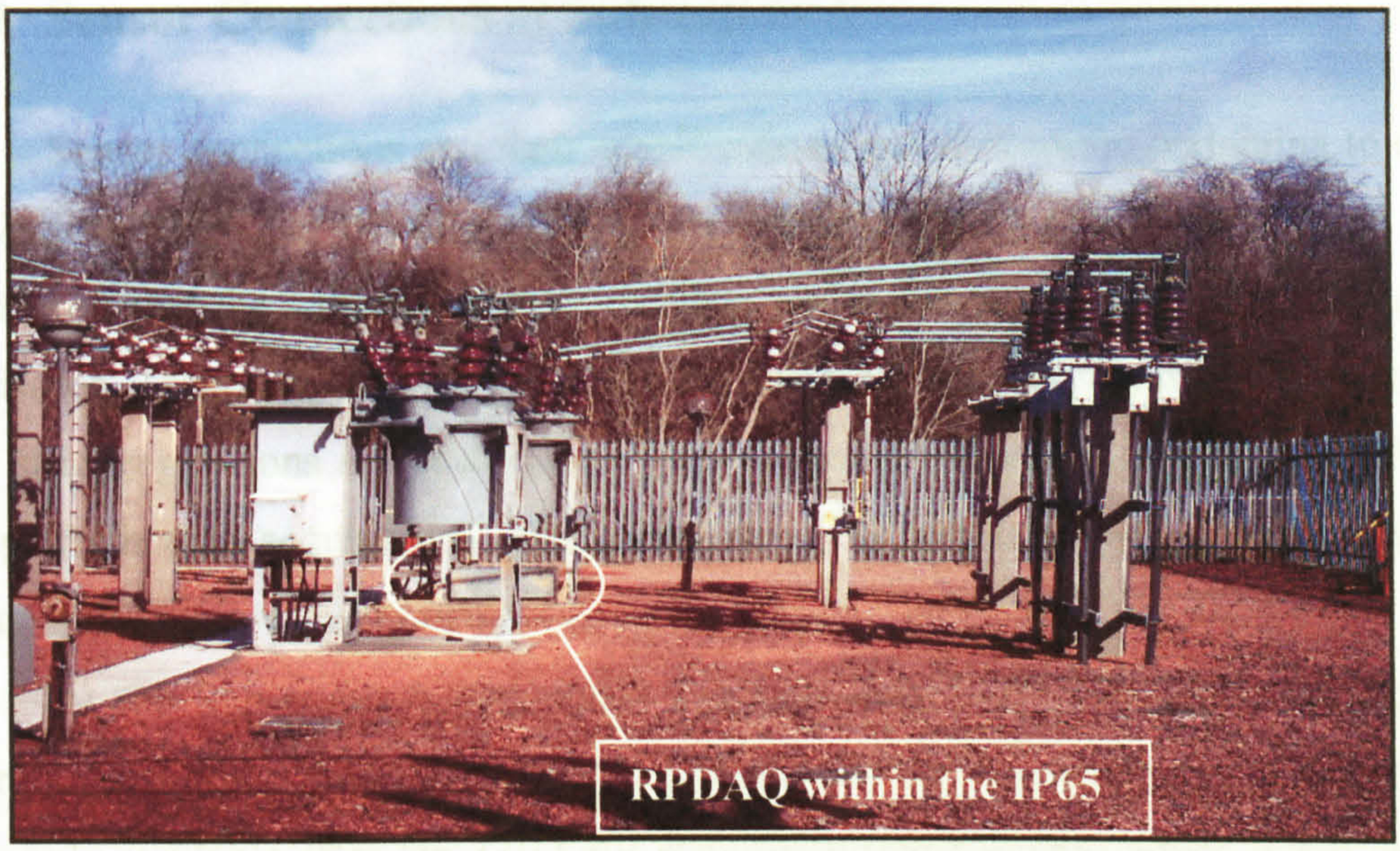

Figure 6.1: Picture of IP65 location in substation switchyard

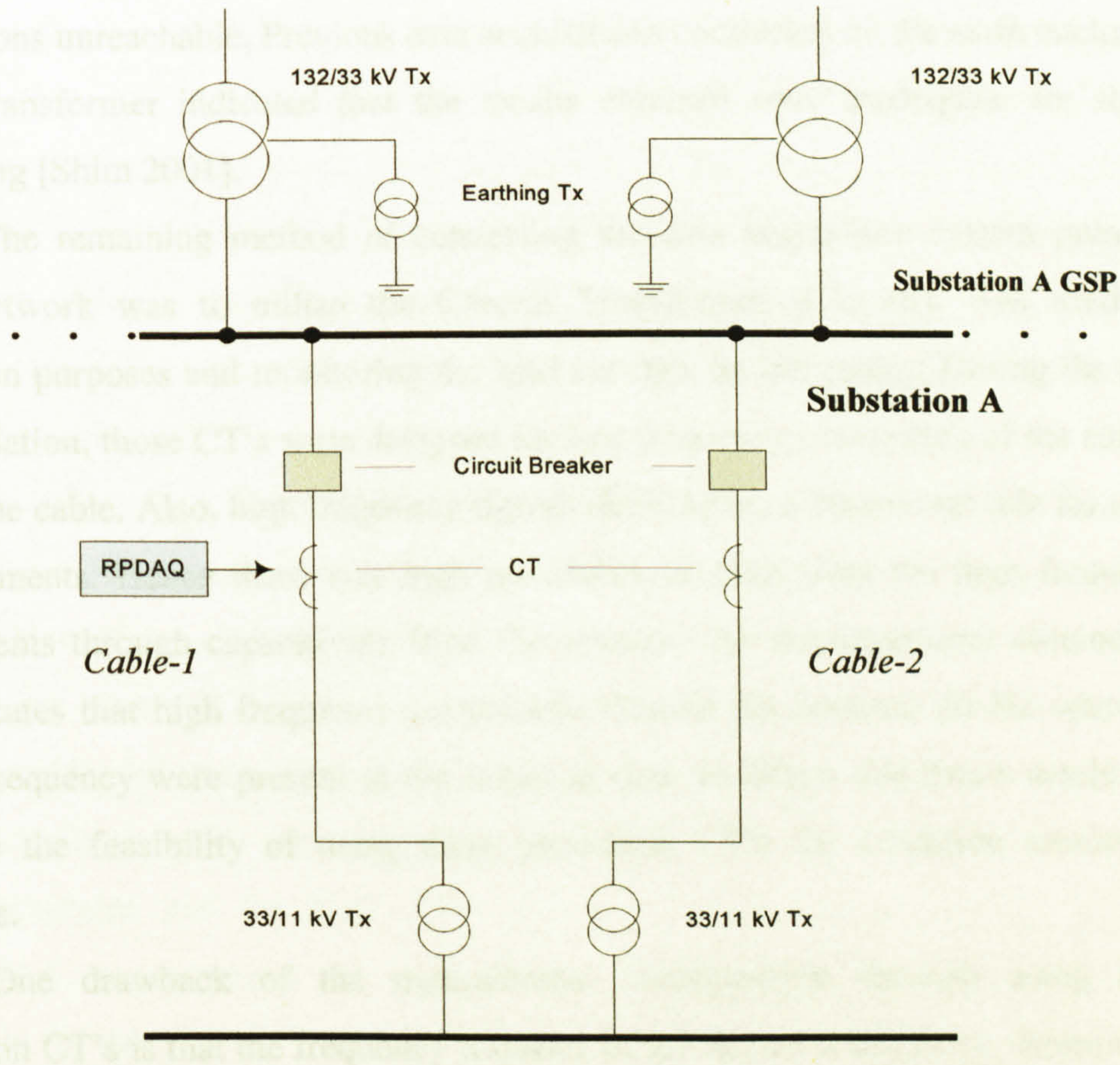

Figure 6.2: Substation A - B 33 kV Cable Network

6.2.1 Sensor Connections at Substation A

Sensor connections and their specifications are vital issues pertaining to data acquisition. They can be connected to accessible parts of a cable, usually at the terminations of the cable. Inductive couplers are quite popular for online PD data acquisition. However, when dealing with live cable networks, the utility companies have strict regulations and restrictions. Hence, for a third party to make connections and perform data acquisitions, permission must be sought. In our case, accessible points to the cable were limited.

At the Substation A end, there was very little possibility of connecting an external sensor onto the cable network. Whilst at the Substation B end, access points were only available after the 33/11 kV step-down transformers; which is not useful for the measurements. The fully enclosed transformer had made the cable connections unreachable. Previous data acquisitions conducted on the earth enclosure of the transformer indicated that the results obtained were inadequate for signal processing [Shim 2001].

The remaining method of connecting the data acquisition system onto the cable network was to utilise the Current Transformer (CT) that was used for protection purposes and monitoring the load currents on the cables. During the time of installation, those CT's were designed for low frequency monitoring of the current within the cable. Also, high frequency signals did not play a significant role for those measurements. Hence there was high possibility of measuring the high frequency components through capacitively from the sensors. The measurements obtained so far indicates that high frequency components beyond the nominal 50 Hz operating power frequency were present in the acquired data. In effect, this thesis would also examine the feasibility of using these protection CT's for condition monitoring purposes.

One drawback of the measurement configuration through using these protection CT's is that the frequency response of the device is unknown. However, if the assumption that the high frequency components have been coupled uniformly from the device, the data acquired through within can be considered valid. If not,

these CT's are can be substituted with proper high frequency CT's. The data acquisition system and the DSP techniques developed in this thesis will still be applicable.

6.2.2 Cable Joints

The knowledge of cable joint configuration is crucial for the understanding and interpretation of PD signals. Continuity between the layers of cable insulation and semi-conductive layers will affect the pulse propagation through the joint. Partial discharge propagation usually travels along the interface layers of the cable, i.e. at the sheaths and the semi-conductive layers [Fouracre 2000]. There are several types of cable joint configurations depending on the particular instances and connection. Some examples are straight joints for three-core to three-core, three-core to single cores, and "T-joints". In the Substation A - B cable network, only straight joints are present. The details of the jointing procedures will not be dealt with in depth, but the actual cable joint diagrams are available in Appendix D. However, the important factor worth noting is that the semiconductor layers of all three phases of the cables are in contact with each other. Hence, there will be a high degree of cross-talk between the cables.

PD cross-talk is the signal coupling between phases or other nearby circuits which induces PD signals into healthy cable phases. During offline testing, usually only one phase of the cable is energized, and PD cross-talk are easily isolated since measurements are made mainly on the tested phase. While under online conditions, all three phases of the cables are energized simultaneously, which makes the interpretation complexity rises. In general, phantom PD's are identified by their lower magnitudes and by their phase relative to the voltage [CIGRE 2002]. Simultaneous measurements of the different phases of the cables will enable justification for this matter.

However, this is not true for all cases as there are physical factors that can affect the strength of the PD signal within each phase. The strength of the PD pulse

will depend on the origin of the source of PD within the cable. In general, the phase closest to the source will have the highest signal amplitude and the furthest will have the smallest signal amplitudes. This will depend on the total electric field concentrations in the void generated from all three phases of the cable. A simple model of the real PD magnitude to the detected apparent charge at the cable terminations is presented in [Wielen 2003]. A calibration pulse with known amplitude is first applied to determine the characteristics and losses of the cable. Then it is used to work out the apparent charge of a discharge occurred within the cable.

6.3 Interpreting the origin of pulse

The complexity of online PD diagnostics is increased by the process of interpreting the origin of the pulse. Unlike offline methods, whereby the circuit breakers are opened to isolate the test cable, the ends of the cables remain connected to the previous configuration of the network. This means that clear open circuited reflections are not produced. Furthermore, pulses measured at the acquisition system may originate from either within or outside of the cable (near-end or far-end). A major challenge is to recognise and isolate these pulses that are not of interest.

6.3.1 Single Ended Systems

For the ideal single ended systems, where the ends of the test section of cable have reflective terminations, if directional couplers were not applied, the conventional method is to determine the delay of the reflected pulse (far-end from measured end). This is further illustrated with the aid of Figure 6.3. Appendix E describes the more complicated behaviour encountered in the substation concerning with the present study.

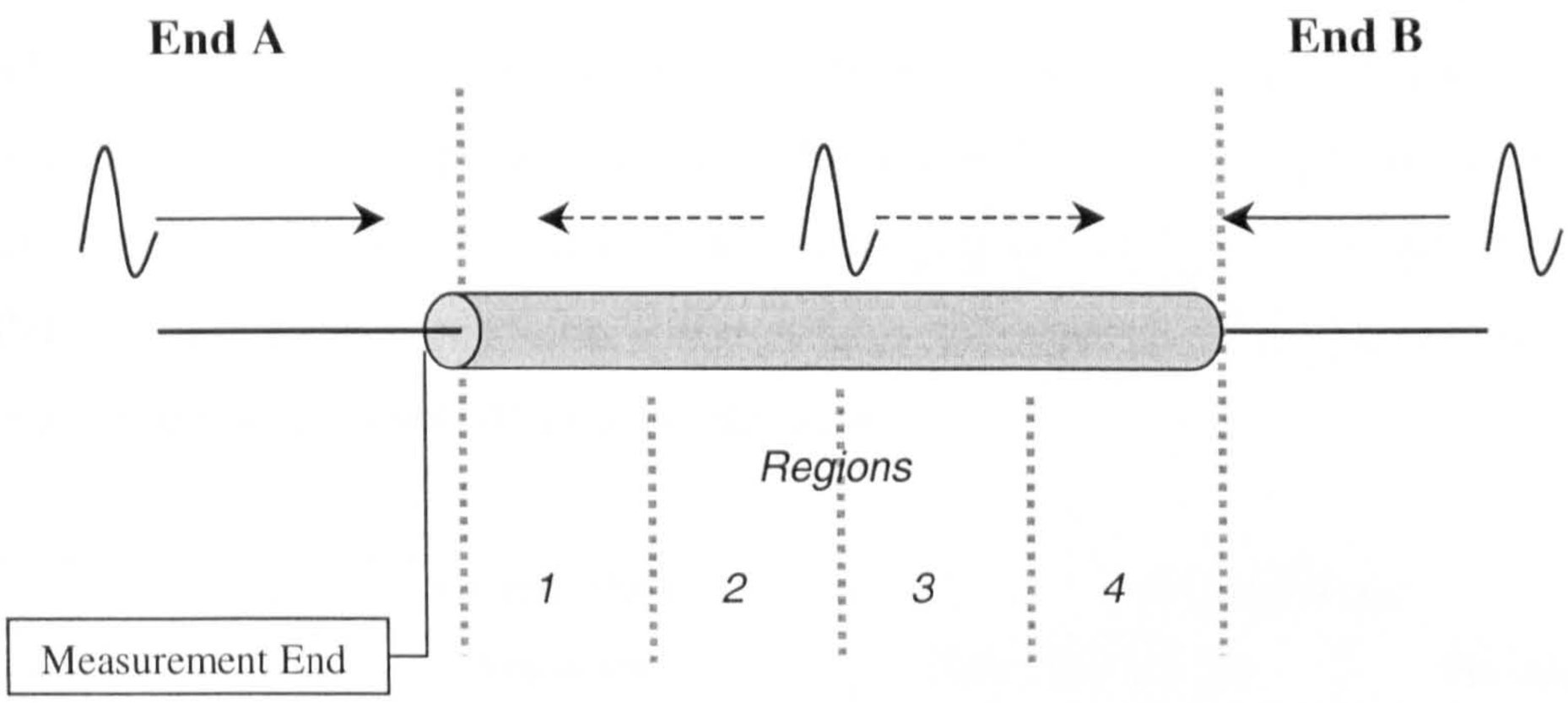

Figure 6.3: Interpreting pulse origin from single ended measurement systems

PD pulses originating outside of the cable can be determined through reflected signals. If measurements are conducted at End A, the reflection of the pulse from End B will take double the time-of-flight of the cable, since it has to travel to the other end and travel back to End A. This is likewise if the measurements were conducted from End B. However, there are several factors that negate this, such as very small amplitude of the reflected signal and a PD occurring within the cable that is located in close proximity to the measured end. To identify the PD pulse that has occurred within the cable, the reflection of the pulse at both ends of the cable will be less than two times the time-of-flight, τ. The pulse origin can be summarized as:

- $\tau_r = 2\tau$ (outside cable) *(6.1)*
- $\tau_r < 2\tau$ (in cable) *(6.2)*

where τ is the time-of-flight and τ_r is the delay time of the reflected pulse. The main challenge for single ended systems remains still in the interpretation of the reflected pulse. Table 6.1 illustrates the general characteristics of a pulse occurring from different sections of a cable. These characteristics will assume that reflection does take place at the far end of the cable. From this table, if a pulse has originated from regions 1, the likelihood of detecting the reflected pulse is small because of the pulse

propagation distance. The pulses occurring from region 2 and 3 will have higher incident pulse amplitudes and chances of detecting reflections are moderate. From region 4, the incident pulse and the reflected pulse will have small amplitudes because of the distance travelled. Hence, these general principles can be used to aid in data interpretation procedures. If the cable can be calibrated with a test pulse, the interpretation process will be greatly enhanced.

	Incident Pulse	**Reflected Pulse**	
Region	***Amplitude***	***Travelled Distance***	***Detection***
1	Very Good, clear defined	1.75L < x < 2L	Low chances
2	Good, clear defined	1.5L < x < 1.75L	Slight possibility
3	Average	1.25L < x < 1.5L	Possible
4	Smallest amplitude	L < x < 1.25L	Best chance

Table 6.1: General characteristics of a pulse and its reflection in a cable

6.3.1.1 Single Ended Location Method

Locating the origin of a PD pulse within a cable using the single-ended TDR method is straightforward. The objective is to obtain the time delay between the incident pulse and the reflection (as described in Section 2.8.1). However, the difficulty of this task is magnified by the fact that prominent reflections are usually not the case, whether for offline or online acquired signals. Significant advantages are obviously present with offline signals because of less noise corruption levels. Interpretation of reflected pulses from mishmash signals tends to be more challenging task. In both cases, a systematic approach has to be adopted to produce efficient and accurate results. Most cable failures are caused by cable joints (52%), followed by non-electrical damages (43%), cable terminations (4%) and cable insulation (1%) [Cigre 2002]. Nominally, the probability of a PD coming from a joint is much higher than any parts of the cable. The faults occurring from cable joints are mainly caused by poor workmanship manufacturing, which eventually leads to PD

activities and permanent breakdowns. From the statistics obtained from many of the experiences and publications in research, cable joints become the prime suspect for the cause of PDs. Therefore important data pertaining the information of cable joint locations are vital. With this information, the process of PD location is then narrowed down and it provides a form of biasing to aid in deciding the PD source.

When computing the time delay from the incident pulse to the reflected pulse, the result is often produced in units of samples. The resolution of which, is determined by the sampling rate. The higher the sampling rate, the better the resolution for time. For illustration purpose, Figure 6.4 depicts an example of simulated TDR signal. With a sampling rate of 100MS/s, the resolution between each sample is 10*n*s in duration. The reflection time, $T_r = S_r / Fs$, where S_r is the reflection in samples, and Fs is the sampling rate. When S_r is 200 samples, with the velocity of propagation, v at 1.68×10^8 ms^{-1} and the length of cable to be 2 km, the origin of the pulse 1.832 km from the measure end of the cable (using equation 2.17). Each deviation in the sample difference is related to $0.5v / Fs$, which amounts to approximately 0.8m of cable per sample for the previous values. This value is high and the errors can become significant for example with an error of 100 samples, the error in location becomes 80 m from the actual location. The errors are mainly caused by inaccurate interpretation from the reflected pulse that will be attenuated and distorted. It also depends on the bandwidth of the analogue system and the transducers. These errors can be avoided by computing averages and by using cable joint markers.

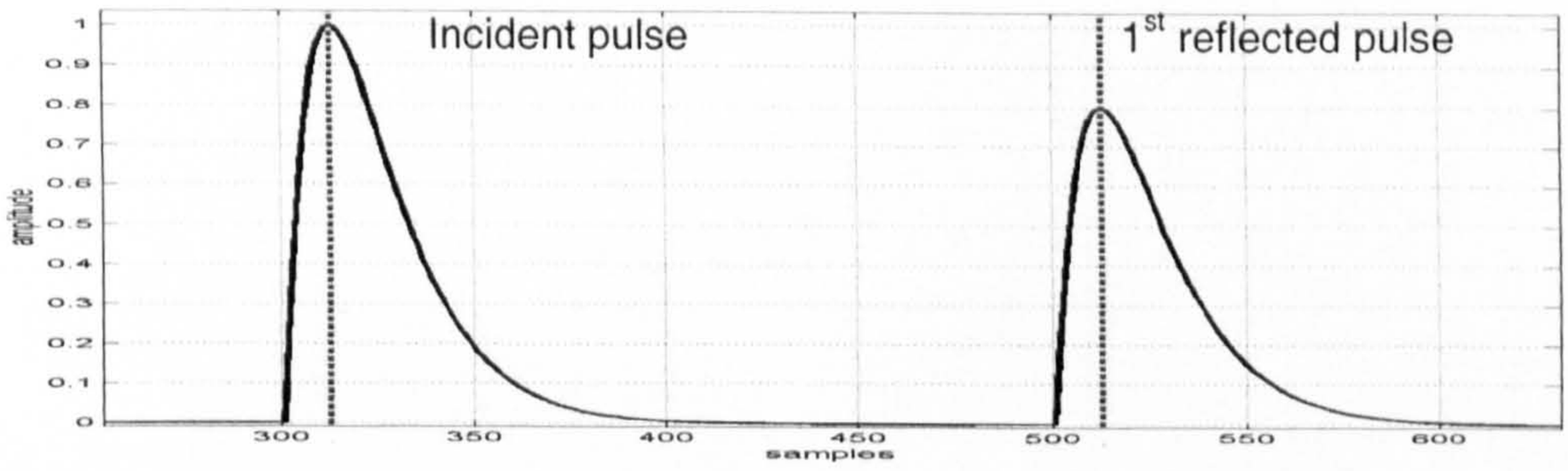

Figure 6.4: Example of TDR location technique.

Cable joint markers are used to aid the interpretation of the reflected signals. These markers are derived from the actual physical location of the cable joints within the cable. Each marker should indicate the possible position of the reflected pulse, if the incident pulse has originated from that particular cable joint. Figure 6.5 depicts an example of cable joint markers used for the same TDR analysis. Here the reflected pulse is in close proximity of J_5, which indicates a high possibility that the PD source has originated from this cable joint.

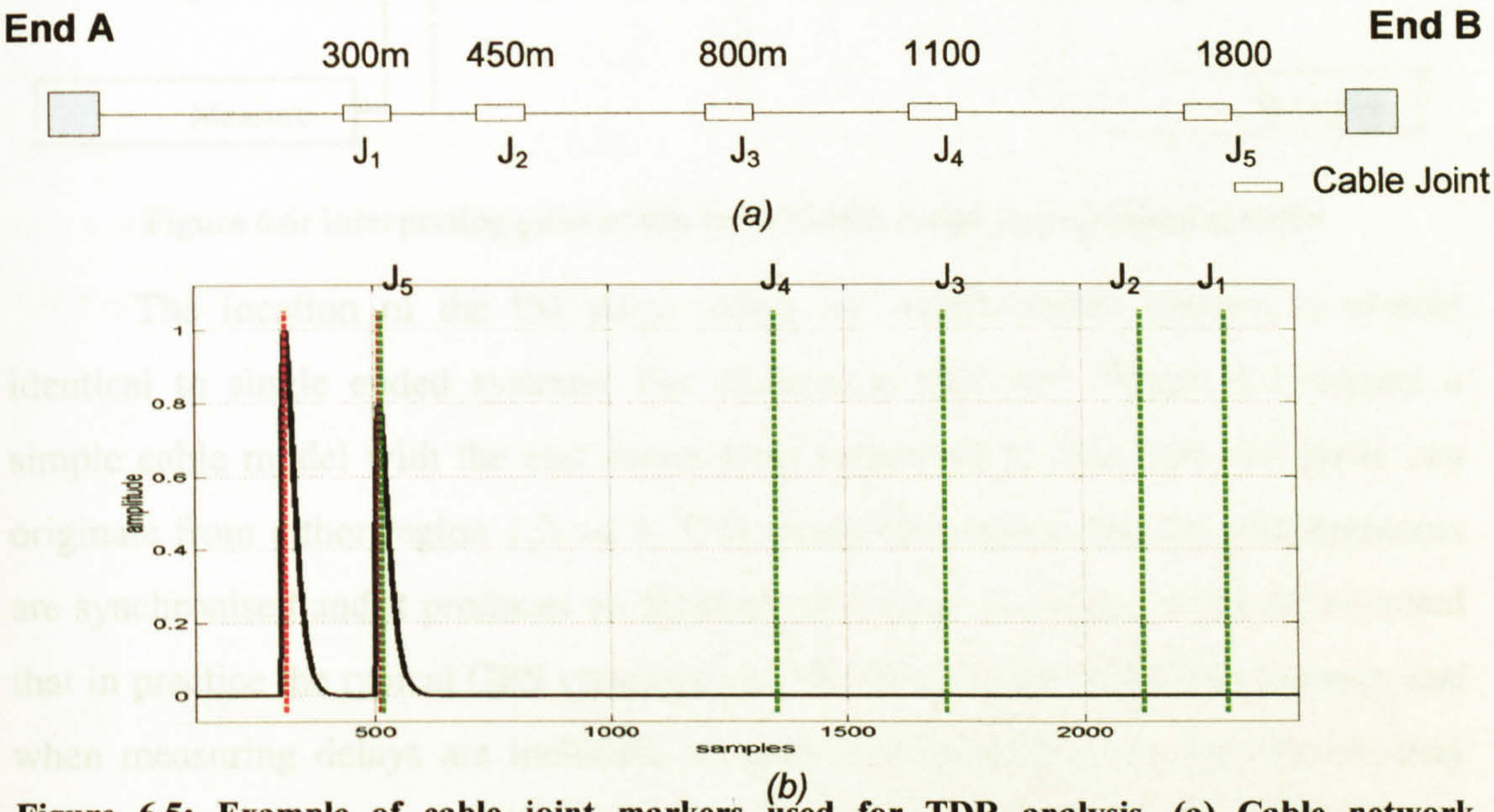

Figure 6.5: Example of cable joint markers used for TDR analysis. (a) Cable network topography indicating the position of cable joints within the cable. (b) TDR signal with cable joint markers added.

6.3.2 Double Ended Systems

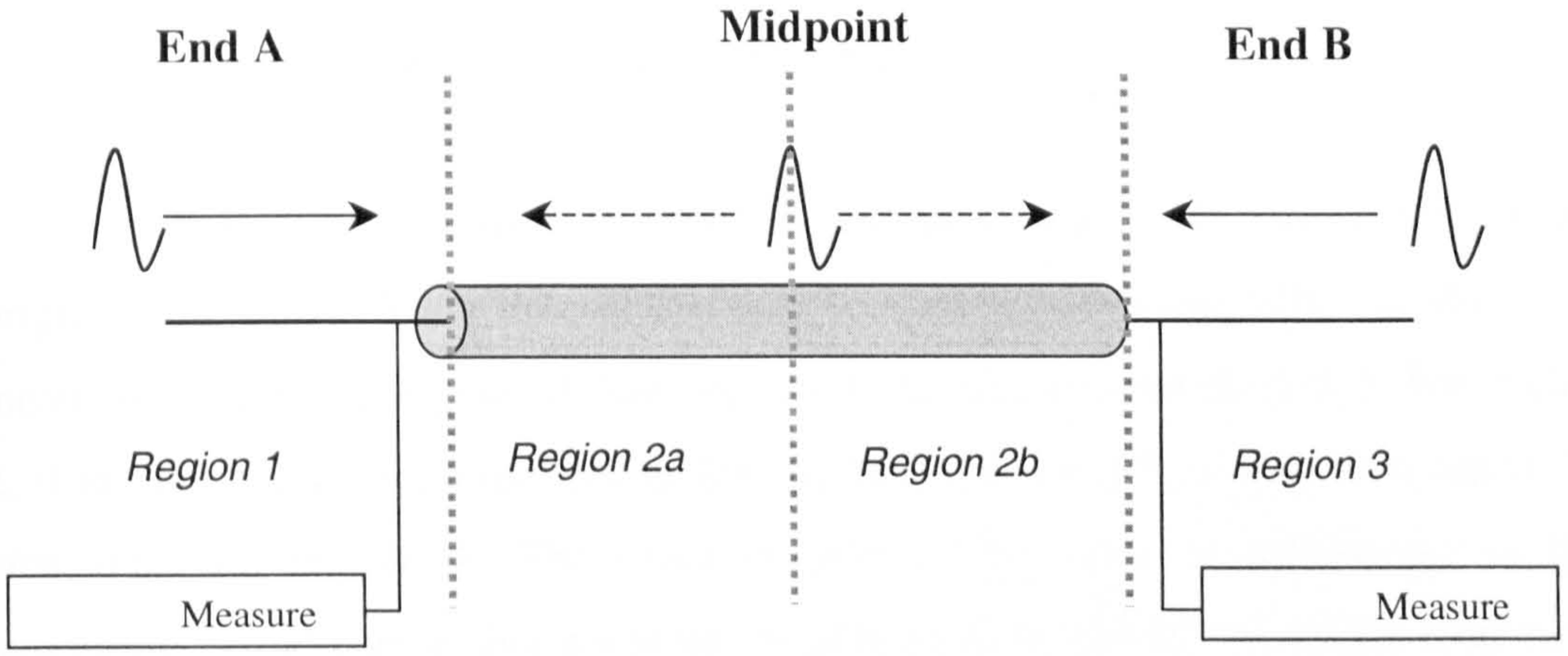

Figure 6.6: Interpreting pulse origin from double ended measurement systems

The location of the PD pulse origin for double-ended systems is almost identical to single ended systems. For illustration purposes, Figure 6.6 depicts a simple cable model with the end connections neglected. In this case, the pulse can originate from either region 1,2, or 3. This example assumes that the measurements are synchronised and it produces an arbitrary start time. However, it should be noted that in practice the typical GPS system gives 10-100 *n*s synchronisation accuracy and when measuring delays are included, accurate synchronisation in this context may not be sufficient. Figure 6.7 illustrates a typical measured signal for this system.

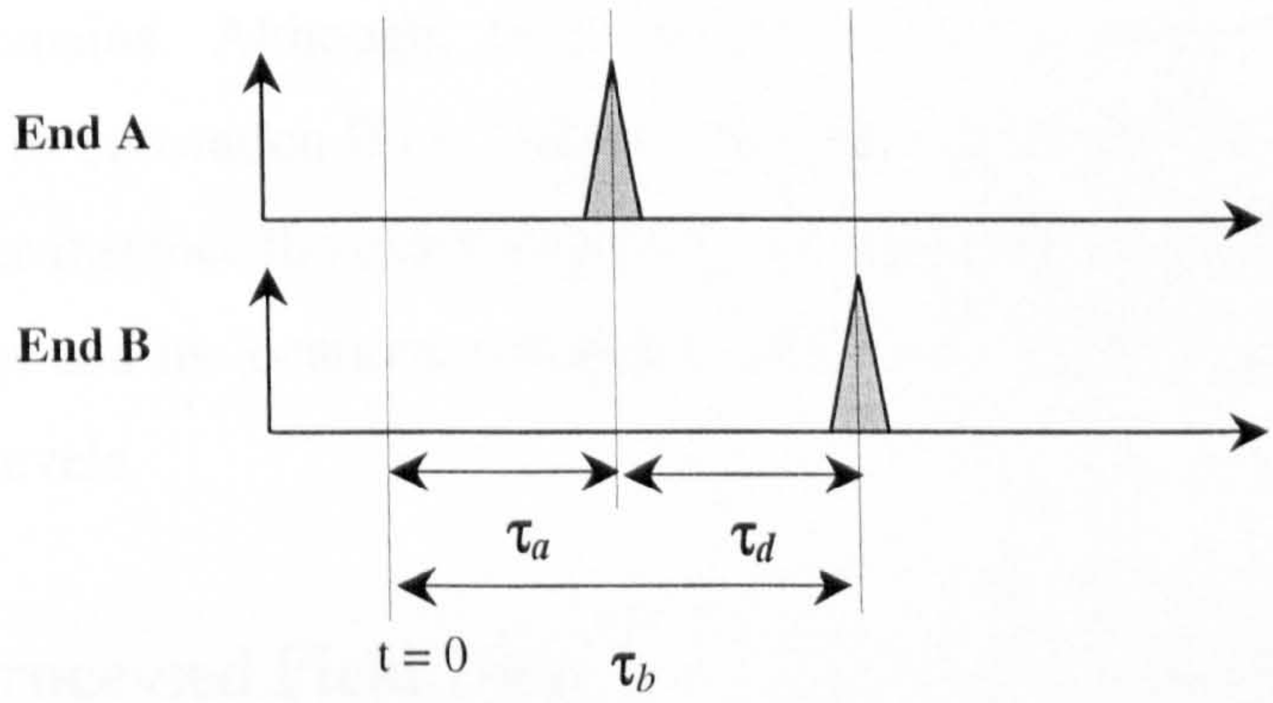

Figure 6.7: Typical example of double ended measured signal

The PD location can be determined by evaluating the time difference between the pulses measured from End A and End B, (t_d). This can be summarized as:

- $\tau_d = \tau$ *(Region 1 & 3)* *(6.3)*
- $\tau_d < \tau$ *(Region 2)* *(6.4)*

In both cases, the time of arrival of the pulse at the ends will determine the origin of the pulse. If the time difference is τ and was measured first at End A, it means the pulse has originated from Region 1 and likewise for Region 3. For region 2, if the pulse was measured first at End A, the pulse has originated from region 2a vice versa for region 2b. The exact location of the pulse is determined by the measuring τ_d and performing a simple calculation to determine the origin relative to any end of the cable. For instance, the location of the pulse relative to End A, x_a, is obtained by:

$$\tau_a = 0.5(\tau - \tau_d) \quad (6.5)$$

$$\chi_a = v\tau_a \quad (6.6)$$

6.4 Substation A Field Data

This section investigates further into actual online data in the time and frequency domains. Although, there are two sets of cable lines linking from Substation A to Substation B i.e. Cable-1 (W1) and Cable-2 (W2), they differed from each other; for instance the exact lengths of the cables [ScottishPower 2003], number of cable joints and its locations within the cables, failure track records and the noise interference levels.

6.4.1 Unprocessed Field Data

In order to compare and evaluate the signal propagation in W1 and W2, a real time simultaneous measurement from the access points is required. By doing this, the actual load conditions and the noise interference level can be correlated. However,

the limitation for us was that there was only one data acquisition system. Hence, the measurement system was switched from W1 and W2 within a 15-minute time frame i.e. the time to transfer the data acquisition system from W1 to W2.

For a general overview of the data from these circuits, Figure 6.8 and 6.9 depicts the data for both W1 and W2 circuits respectively. In those figures, the relative phases of the signal is represented by the dotted lines and the other signal is the actual raw signal measured from the CT outputs (without the 50 Hz signal). From the daily load current profile, it was found that the amplitudes of the noise and pulses vary during the day. From both cable circuits, high noise levels are present. These noises originate from a combination of narrowband RF signals, and wideband noise. However, for online measured signals, sources originating beyond the cable are considered noise. It was found that high levels of transient noise have corrupted the signals measured from both W1 and W2. Transient noise may originate from other HV equipments such as transformers and switchgear. One major challenge of online data interpretation is to extract only useful signal from the raw signal.

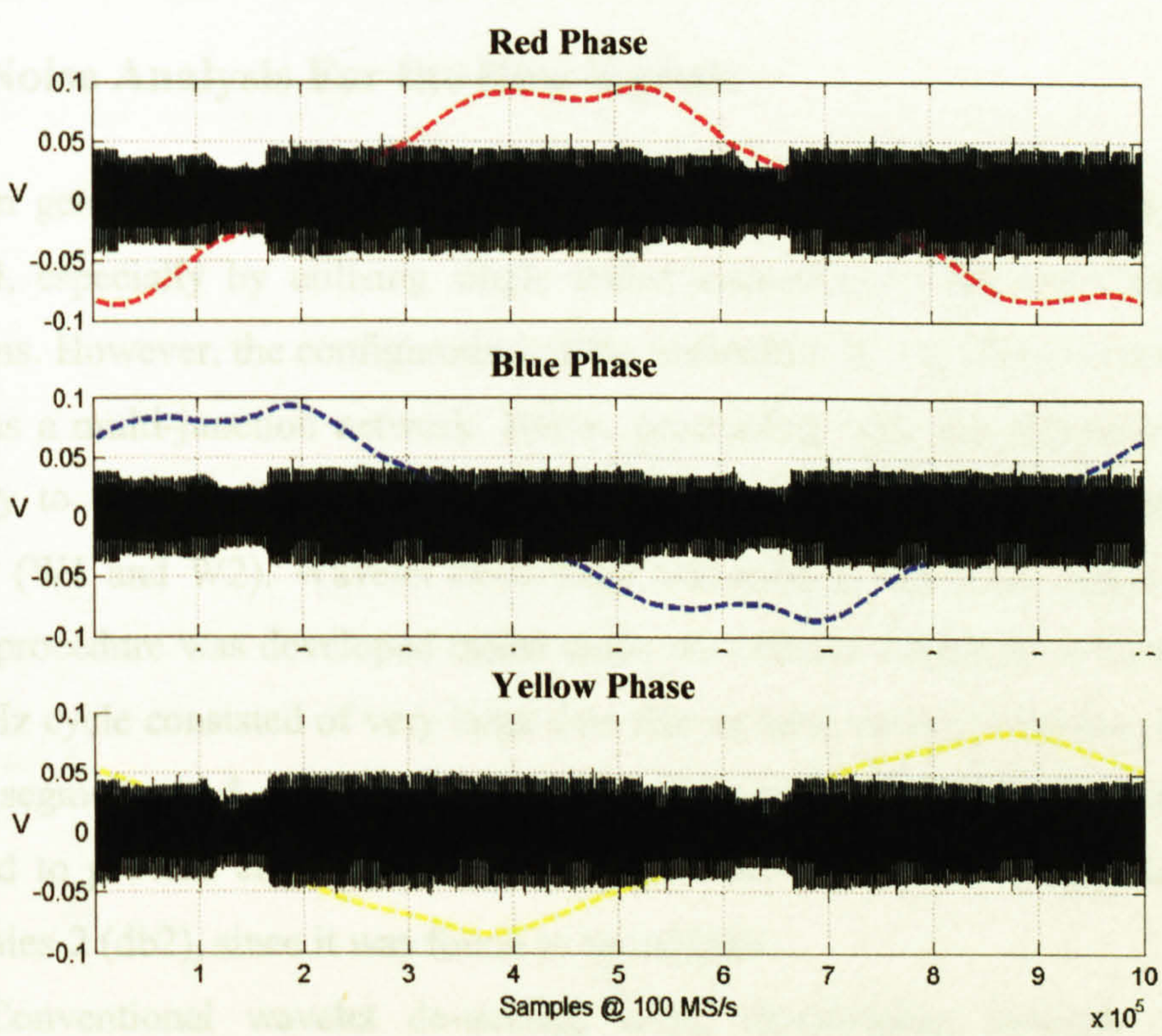

Figure 6.8: RPDAQ data for Cable-1 cable circuit.

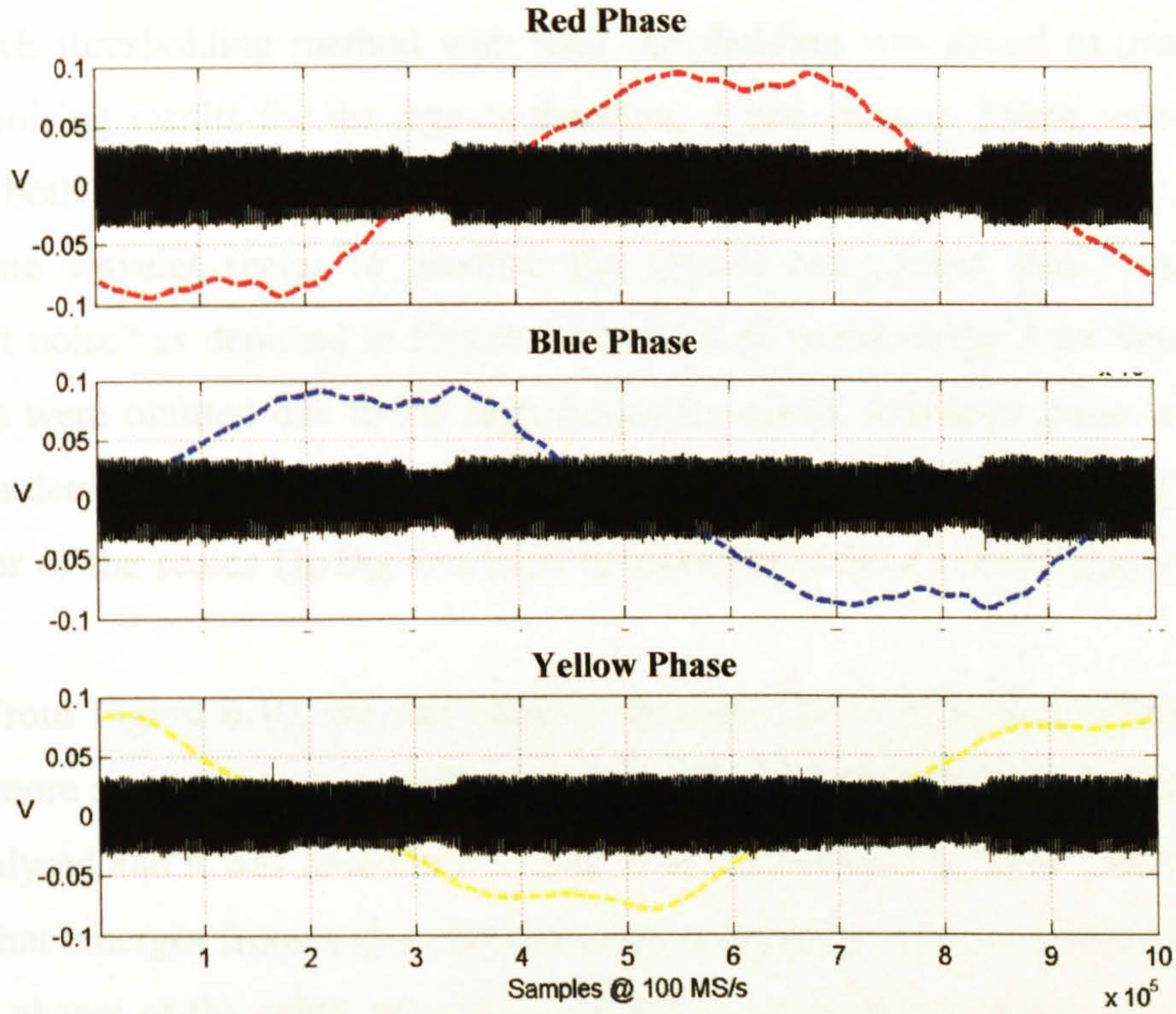

Figure 6.9: RPDAQ data for Cable-2 cable circuit.

6.4.2 Noise Analysis For the Raw Signals

In general, identification of the source of transient signal is difficult to be achieved, especially by utilising single ended measurement systems under online conditions. However, the configuration of the Substation A – B 33kV network can be treated as a multi-junction network. Before proceeding with that discussion, it was necessary to observe the typical characteristics of the signals obtained from each terminal (W1 and W2). Wavelet de-noising was used to clean the signal. The de-noising procedure was developed based under the criteria discussed in Chapter 5. A full 50 Hz cycle consisted of very large data size in total, so it was broken down into smaller segments and separately de-noised. The non-decimated wavelet transform was used to provide consistency. The wavelet filter used for the analysis was the Daubechies-2 (db2), since it was found to be suitable.

Conventional wavelet de-noising using thresholding methods were not suitable for these signals because of the high transient noise interference present. The

HeurSURE thresholding method with hard thresholding was found to produce the best de-noising results for the signals therefore it was chosen. These settings were used for both sets of signals. The thresholding procedure was customized, by using appropriate wavelet scales to produce the signals categorised into "signal" and "transient noise" as depicted in Figure 6.10 and 6.11 respectively. Low detail scales (D_1 - D_3) were omitted due to the high frequency noise. Transient noise was found mainly in details D_1 - D_7, hence the scales D_4 – D_7 were separated (Figure 6.11). The remainder of the scales D_8-D_{10} was used to reconstruct the cleaned "signal" (Figure 6.10).

From Figure 6.10, we can observe that the signal structures obtained from W2 are more and have higher amplitudes than W1. In W2, the other signal structures were analysed and it was found that if continuous measurements were conducted, the pattern that emerges from it does not have any correlation with the inception voltage for all 3 phases of the cable. Also the time difference between each bursts of pulses are consistent. Hence, this structure is considered to be noise that originates from equipment connected to the cable and is not likely PD activity.

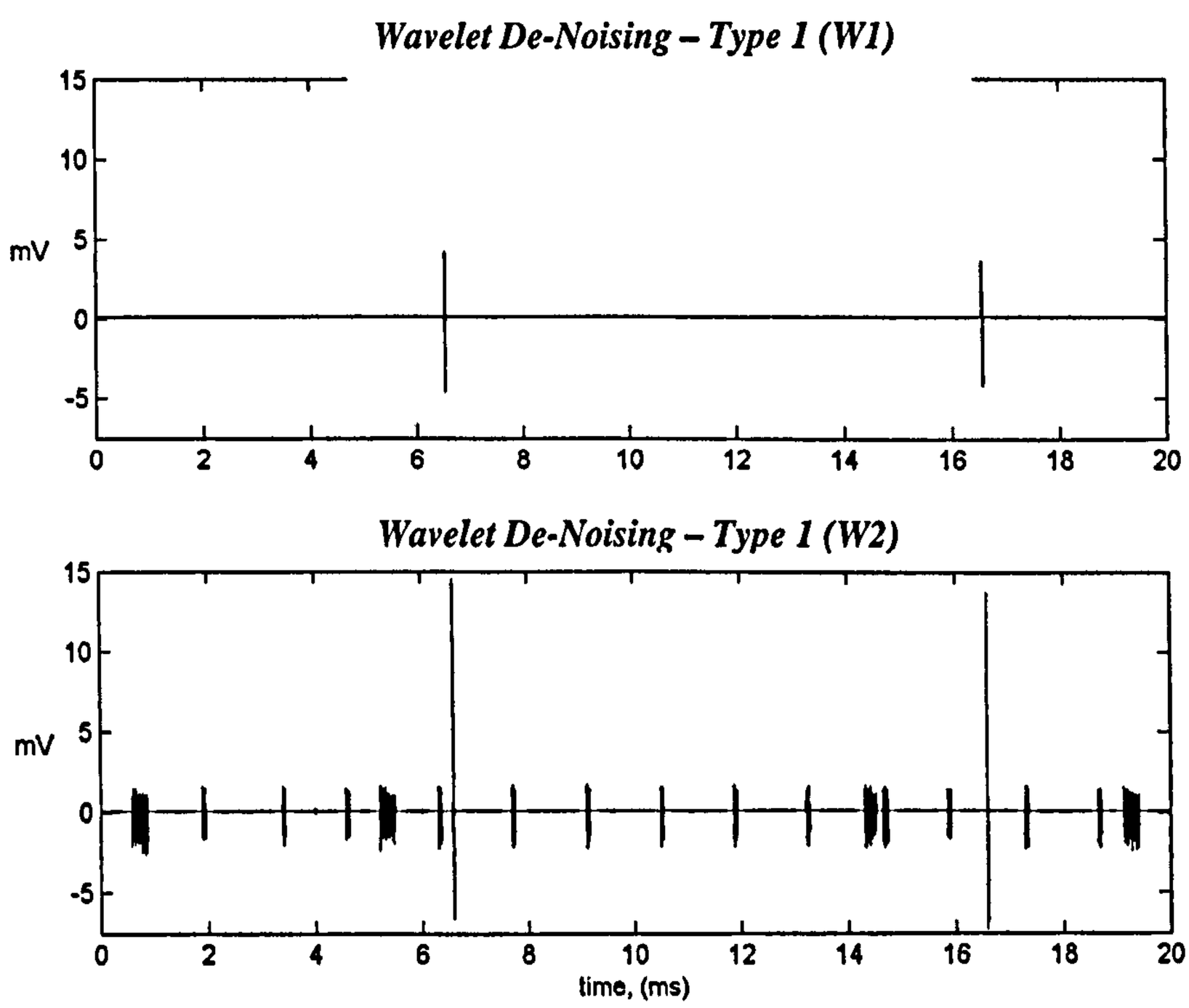

Figure 6.10: De-noised "signal" for W1 and W2

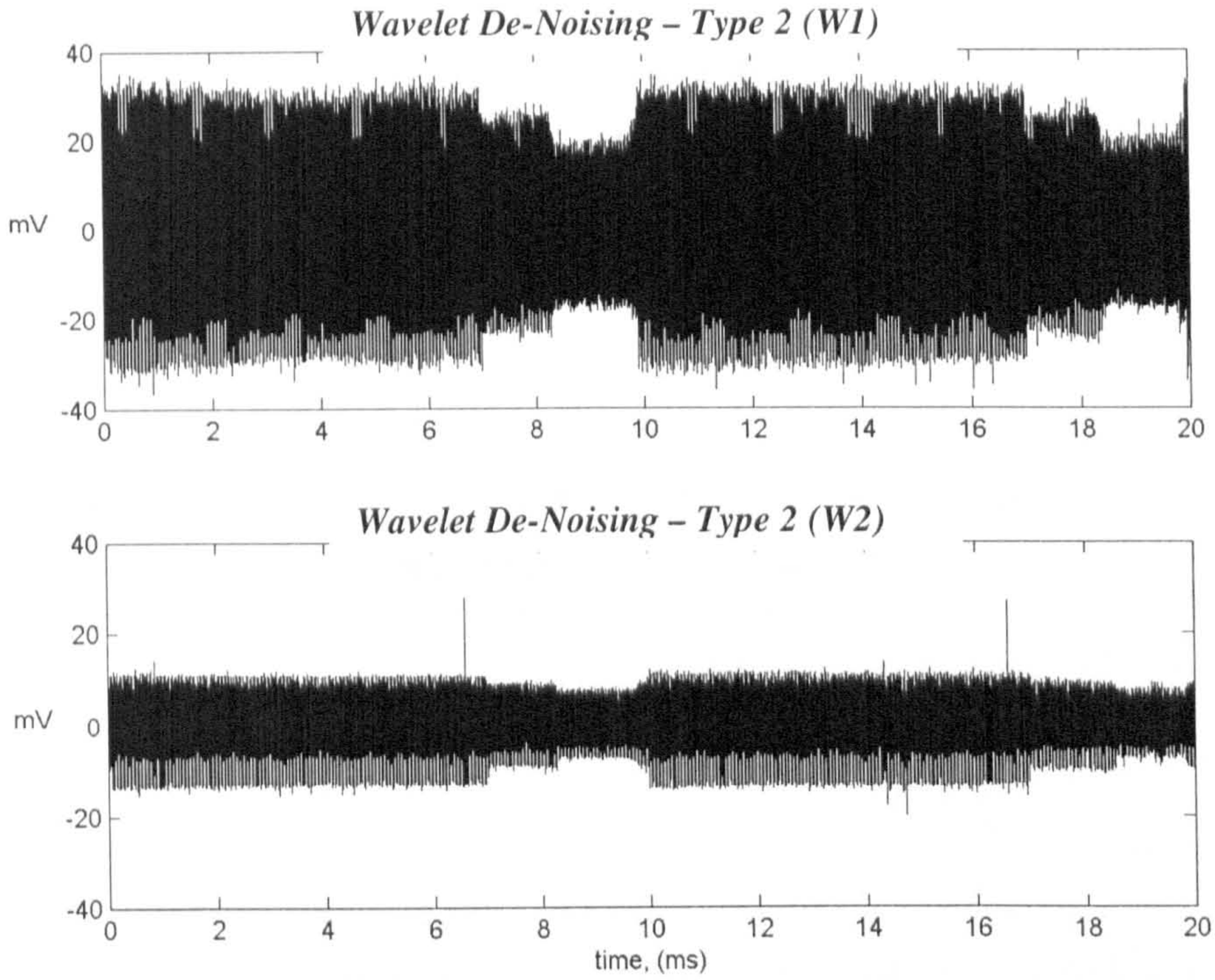

Figure 6.11: Transient noise interference for W1 and W2

However, a prominent signal structure is observed from both cable circuits that occur roughly within the same inception voltage regions. This signal structure has a high probability of being PD activity and for simplicity purposes it shall be referred as PD1 in this chapter. The characteristics of PD1 will are discussed in the coming sections. Note that the amplitude of PD1 is significantly higher in W2 than W1, which suggest that the source is more likely to have come from the cable side of W2.

A zoomed version of the de-noised PD1 is illustrated in Figure 6.12. From the diagram, the pulse at W1 has smaller amplitude and dispersed as the pulse width is extended compared to the pulse in W2.

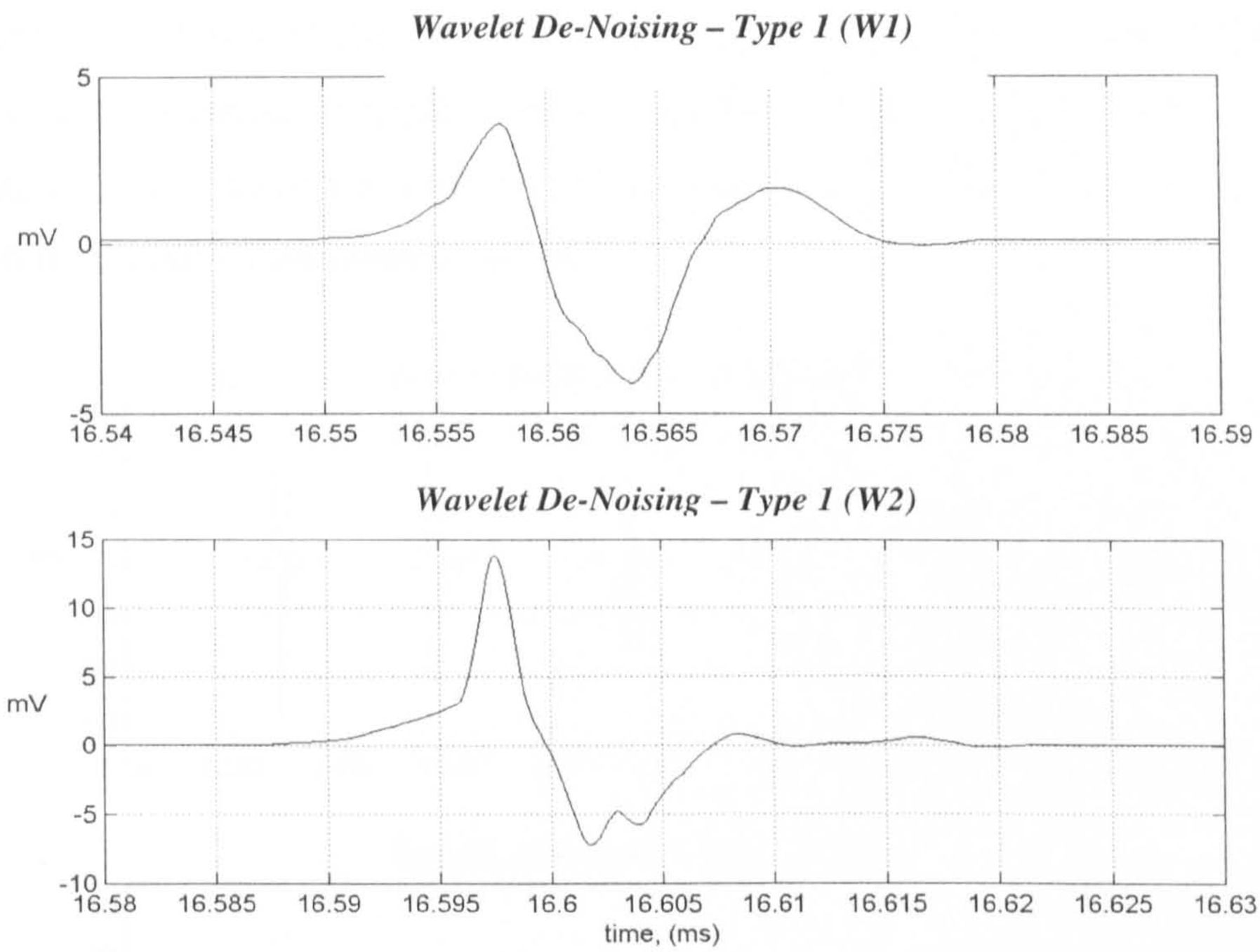

Figure 6.12: Zoomed de-noised PD pulses

In Figure 6.11, the transient noise is isolated through the wavelet de-noising. The amplitude of the noise is higher in W1 than W2. The transient noise is assumed as noise for the moment because it significantly disrupts the chances of detecting other transient like signals within the raw data. The transient noise was found to have same shape and time occurrences throughout the 3-phases of the cables for W1 and W2. Also a distinct pattern is observed in relation to the phase of the voltage. The difference is observed from the amplitudes i.e. high (0-7 *m*s and 10-17 *m*s), medium (7-8.4 *m*s and 17-18.4 *m*s) and low (8.4-10 *m*s and 18.4-20 *m*s). If this transient noise were to be classed as PD activity, observing the correlation of the pulse occurrence with the phase of the voltages it is most likely to originate from the yellow phase of W1 (see Figure 6.8).

The zoomed version of the "high" transient noise is depicted in Figure 6.13. Four distinct pulse shapes are observed in the diagram for W1 and W2 (sequence from the left). The period of occurrence of these shapes is approximately 32 μs, which corresponds to a frequency of 31.25 kHz. Also observed is that pulse 3 has the

same shape as pulse 1 except that it is inversed. This is not true for pulse 4 and pulse 2. The time difference between these pulses is approximately 16 μs, which does not correspond to the time-of-flight, τ, that is 10.48 μs for the length of 1.76 km and the propagation velocity of 1.68×10^8 ms^{-1}. The origin of these pulses were not identified, therefore this pulses are regarded as noise.

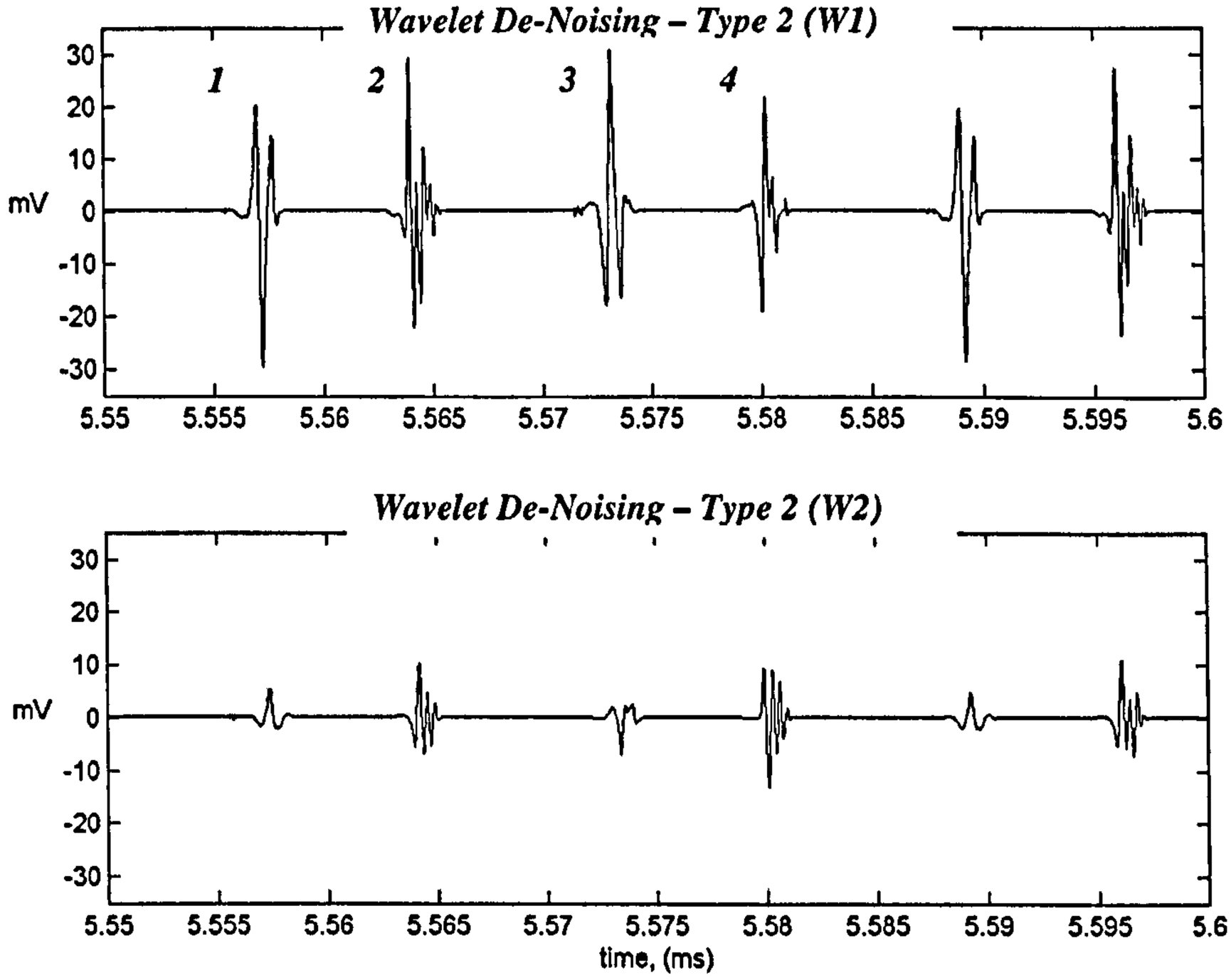

Figure 6.13: Zoomed version of transient noise

Based on the results of the noise analysis, the emphasis was given on the PD1 signal structure in the Cable-2. In the next few sections, the aim is to attempt to characterise the PD1 signal structure.

6.5 Characterisation of PD1 source

6.5.1 Examining the characteristics of PD1 with the load current profiles

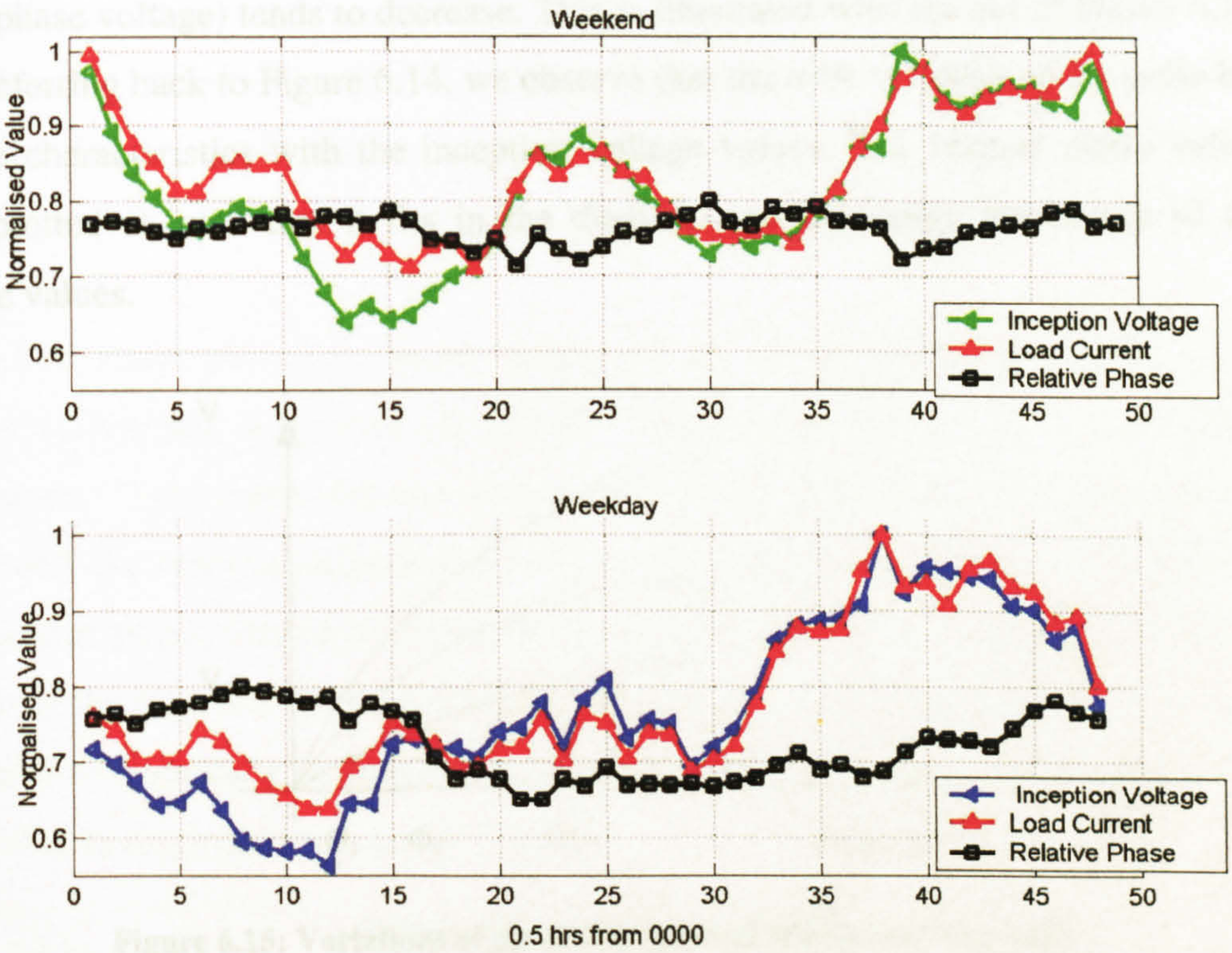

Figure 6.14: Characteristics of PD1 inception voltage with the load current

Load current variations in the cable were discovered to affect the PD activity within the cables. The load current indirectly has the impact on the temperature of the insulation. Hence, as the current loading rises in the cable, the temperature of the insulation rises. Gas voids within the cable begins to experience an increase of the gas pressure (Gas laws). As a result of that, the more electric field stress is required to initiate the PD. Therefore higher inception voltages are required for PD activity. This is illustrated in Figure 6.14, where PD characteristics are categorised by weekday and weekend load profiles. The values of the inception voltage and the load current were normalised. Also included is the PD location relative to the phase voltage. In the figure, the load current peaks and increases during evening time. The

inception voltage also follows the pattern of the load current. However, the relative location to the phase is contrary to that.

This is because as the phase voltage increases in amplitude, at the same inception voltage value (V_1) in the different phase voltages the phase angle (relative to the phase voltage) tends to decrease. This is illustrated with the aid of Figure 6.15. Now referring back to Figure 6.14, we observe that the relative phase of the pulse has inverse characteristics with the inception voltage values. The relative phase values were plotted as such that it fits in the diagram and represents percentage of the voltage values.

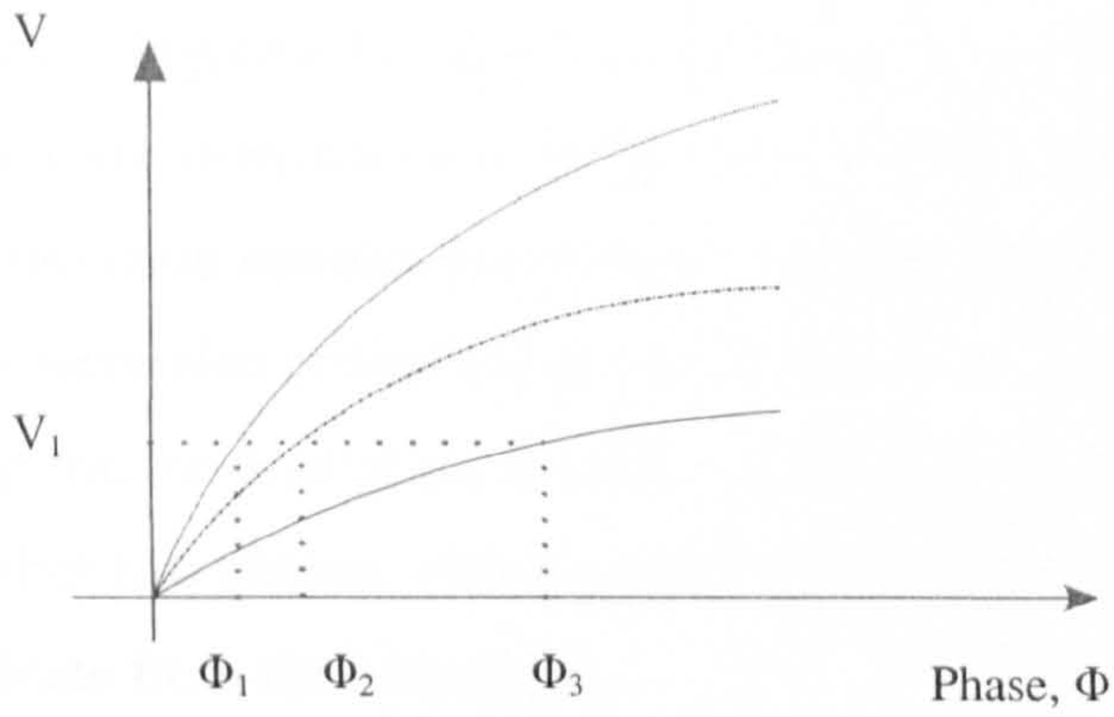

Figure 6.15: Variations of phase voltages and effects on phase angle

6.5.2 Interpreting Origin of Discharge Activity

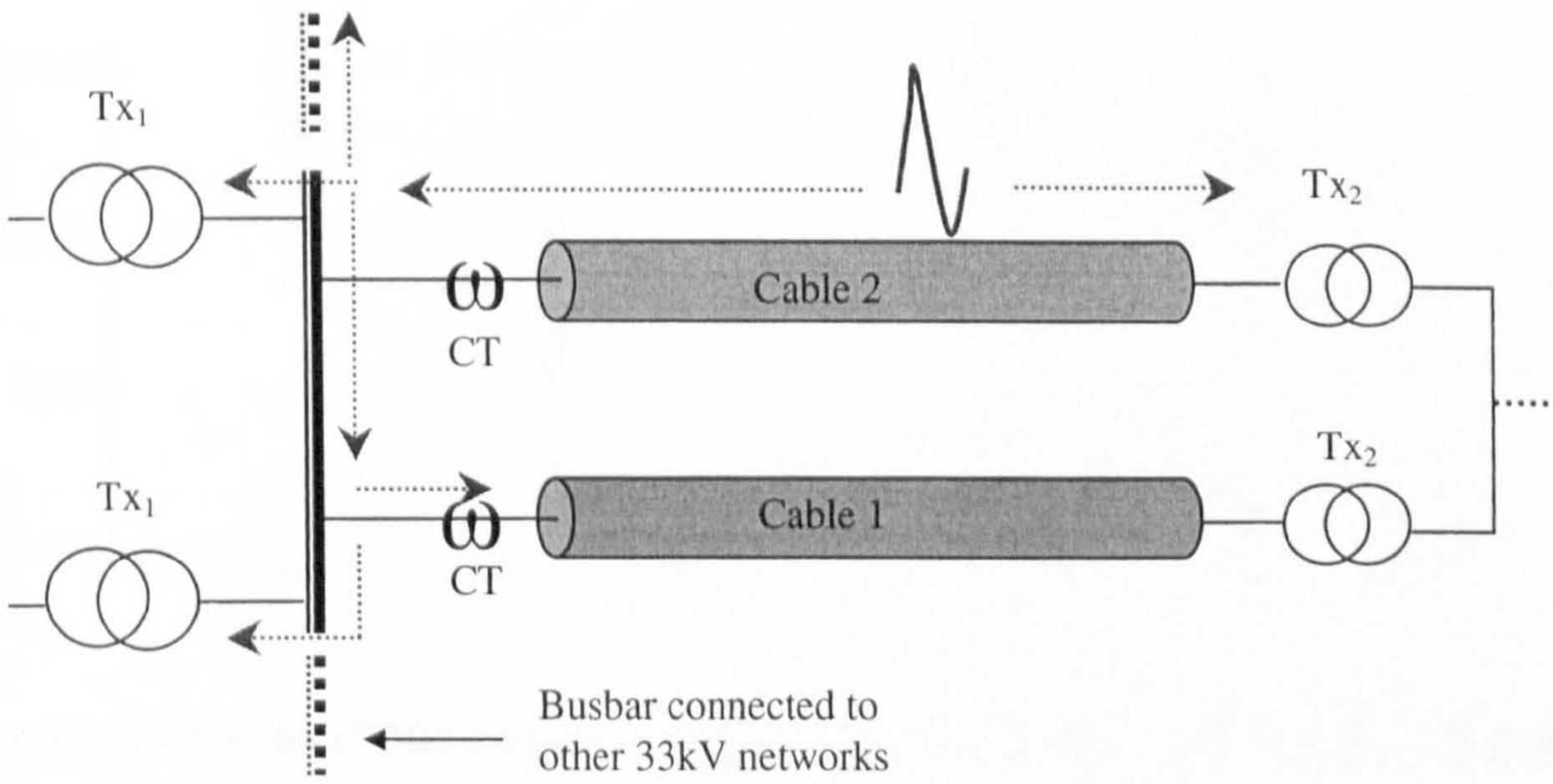

Figure 6.16: Pulse propagation within Substation A cable network

The possibility of PD1 originating from Cable-2 is higher than Cable-1 if the assumption is based on the amplitude of the signal. The pulse propagation in can be illustrated through Figure 6.16, where the pulse reaches the first CT at W2 and then propagates through all available paths. Not long after the pulse would arrive at the CT at W1 and is measured again. One method used to verify the propagation of the pulse can be verified if measurements are simultaneously conducted for W1 and W2. However, due to our limitations the PD origin is only hypothesised based on the amplitude of the discharge pulses, which is assumed to originate from one of the cables.

The scatter plot of the peak voltage values of PD1 against the relative phase voltage is illustrated in Figure 6.17. The PD1 pulses are obtained from 200 cycles per cable phase. These measurements were performed in sequentially in multiple sets of cycles and not continuous consecutively, due to the acquisition system limitation. The measurements were also conducted at the peak time of load current usage in the day. From the diagram, the blue phase has the highest average peak values of 35 mV compared to the other two phases. This suggests that the discharge source has a high probability to originate from the blue phase.

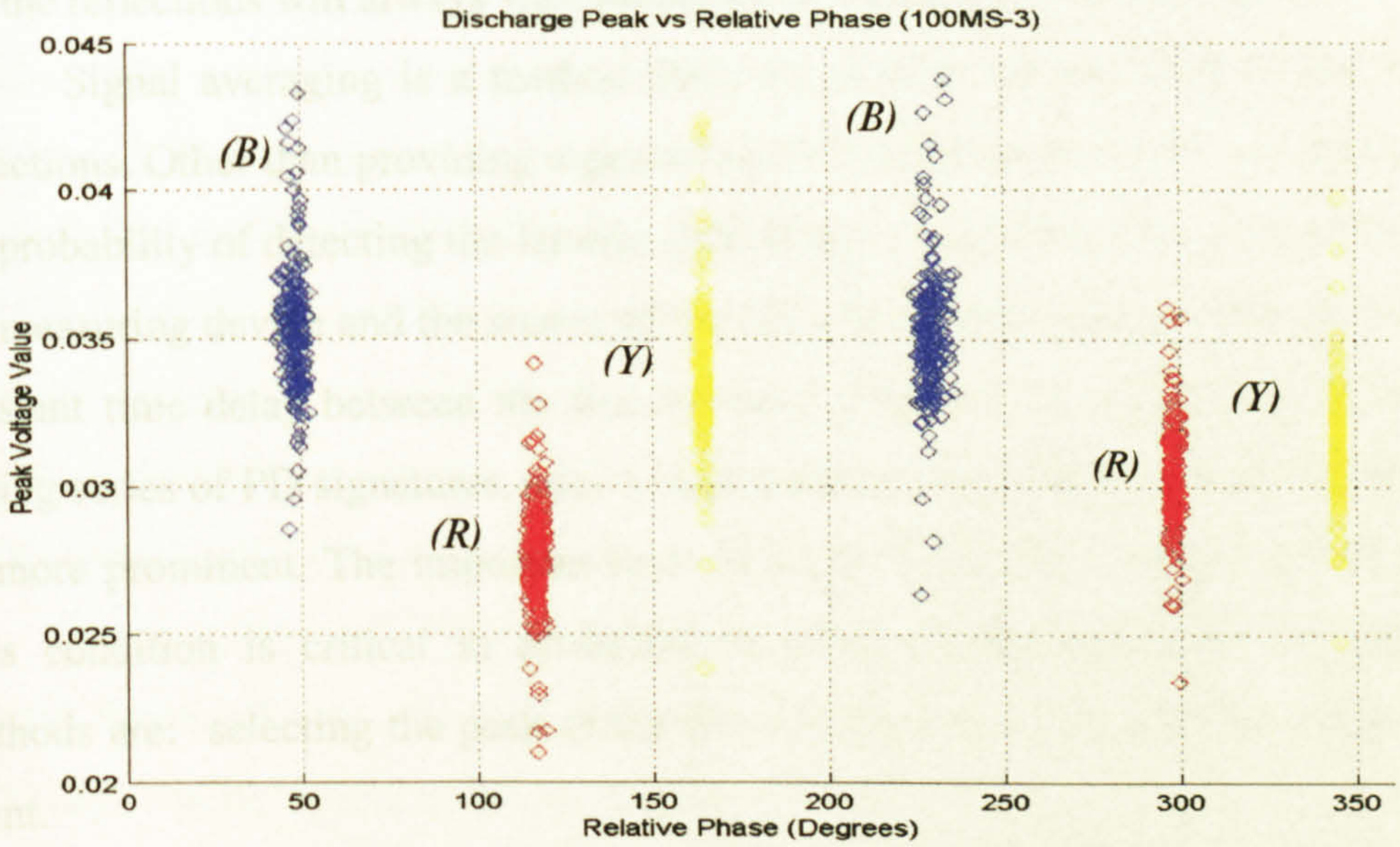

Figure 6.17: Scatter plot of PD1 for peak voltage values against relative phase voltage (Blue (B), Red (R), Yellow (Y))

Also an interesting finding was that when the measurements from all 3 phases are correlated in the time domain, the PD1 pulse was measured at the same time instance. This suggests that there is a high degree of cross-talk within the cable. After examining the physical properties of the cable, we found that the cable has a unique semiconductor layer configuration i.e. it was all intimately in contact with one another. Hence, the PD discharge occurring from one phase would likely to be measured in the other phases. The strength of the discharge will depend on its location relative to the other phases as described in [Wielen 2003].

6.5.2.1 Signal Averaging

PD signatures occur stochastically during each power cycle, with variations in amplitude, time of occurrence relative to the phase, and shape. The first measured incident pulse is usually detectable without problems. However, identifying the far-end reflection may be problematic because of very small reflections. Usually the reflections are too small to be distinguished. If the random processes are accounted for, the reflections will always vary adding to the difficulty of the situation.

Signal averaging is a method that can increase the visibility of the far-end reflections. Other than providing a generalised PD signature from the incident pulses, the probability of detecting the far-end reflections is increased. The distance between the measuring device and the source of the PD will remain constant. This generates a constant time delay between the first incident pulse and the far-end reflection. By adding series of PD signatures, over a large number of pulses the reflected pulse will be more prominent. The important issue in signal averaging is alignment of pulses. This condition is critical in producing accurate results. Examples of alignment methods are: selecting the peak of the first epoch or the zero crossing before signal event.

Figure 6.18Figure 6.18 depicts the normalised signal averaged pulse for the original PD1 signal over for 100 cycles. Pulses shown are for all three phases of the cables including a normalised version of an original PD1 pulse from the red phase.

The advantage of using the averaged PD1 pulse is that the transient noise is clearly diminished. From the diagram, the PD1 pulse shape does not have strong variations and the main pulse shape is consistent from all the phases of the cable.

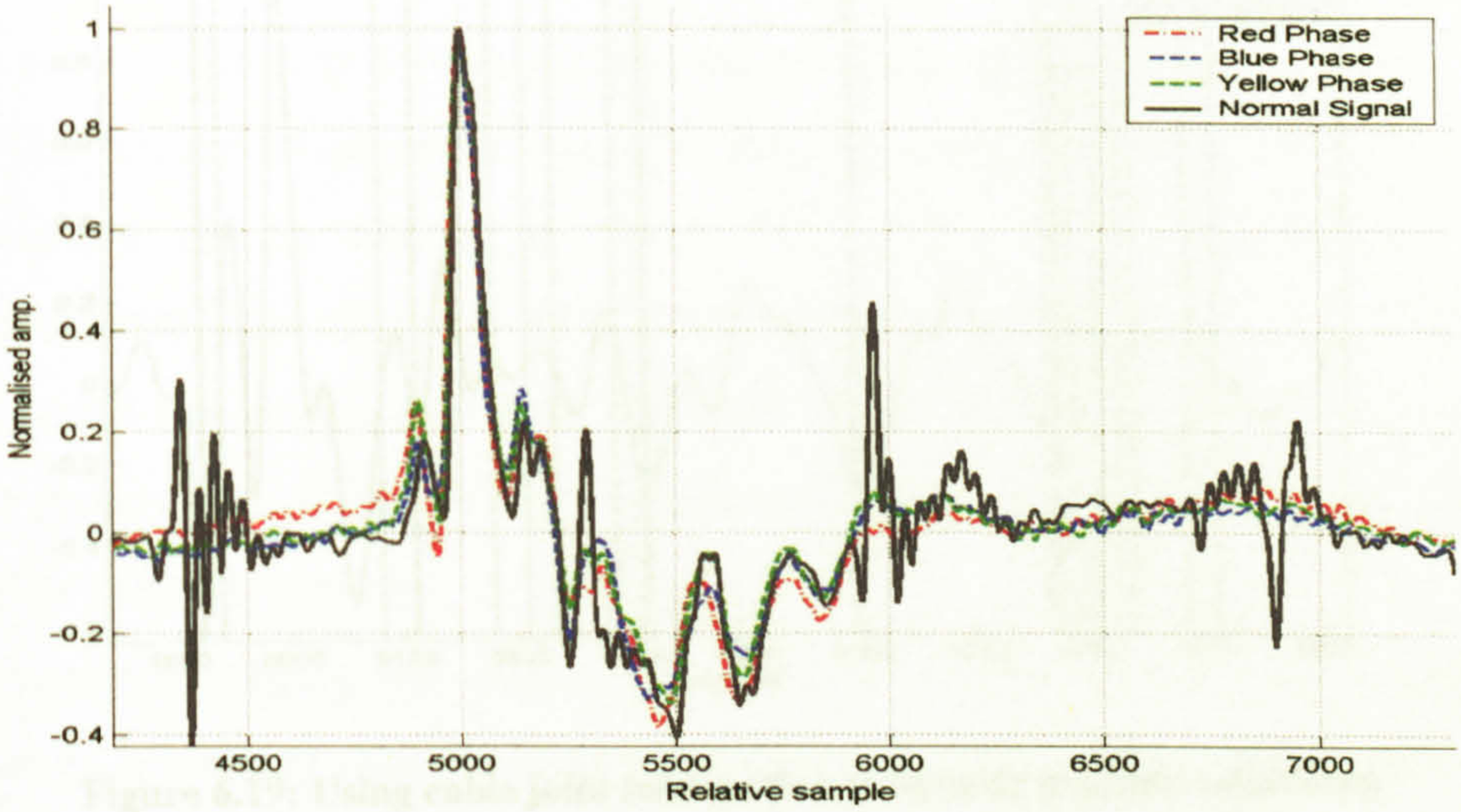

Figure 6.18: Signal averaging for 100 PD1 pulses for 3 phases in W2 cable

The cable joint locations were matched to the averaged PD signal to identify the possible origin of the PD. This was performed by applying the wavelet transform onto the averaged signal. Then the cable joint markers are applied to the appropriate wavelet scale, in this case detail scale 5, as depicted in Figure 6.19. The PD signature has high oscillatory signal structure. Hence, the reflected signal is likely to be superimposed with the main pulse. The interpretation process is difficult because the signal cannot be separated. One method of determining the reflection is though searching matching peaks of the signal. From the results, it was found that the possible reflections could have occurred at locations 85.9%, 76.2%, 67.5% and 58.9% respectively of the cable from the Substation A end.

In previous reports by EA Technology a company that performed diagnostic tests for ScottishPower, the discharge activity was high in the blue and red phase [EATech]. The test was conducted through offline diagnostic techniques i.e. the 0.1 Hz method and the discharge location was identified at 58 – 61% of the cable from Substation A end. Based on these results, the single ended location method was not feasible under online conditions. The noise interference was high and the reflections

were not determined. The alternative to this problem is to utilise double-ended location method. Then problems with identifying pulse reflections will be mitigated.

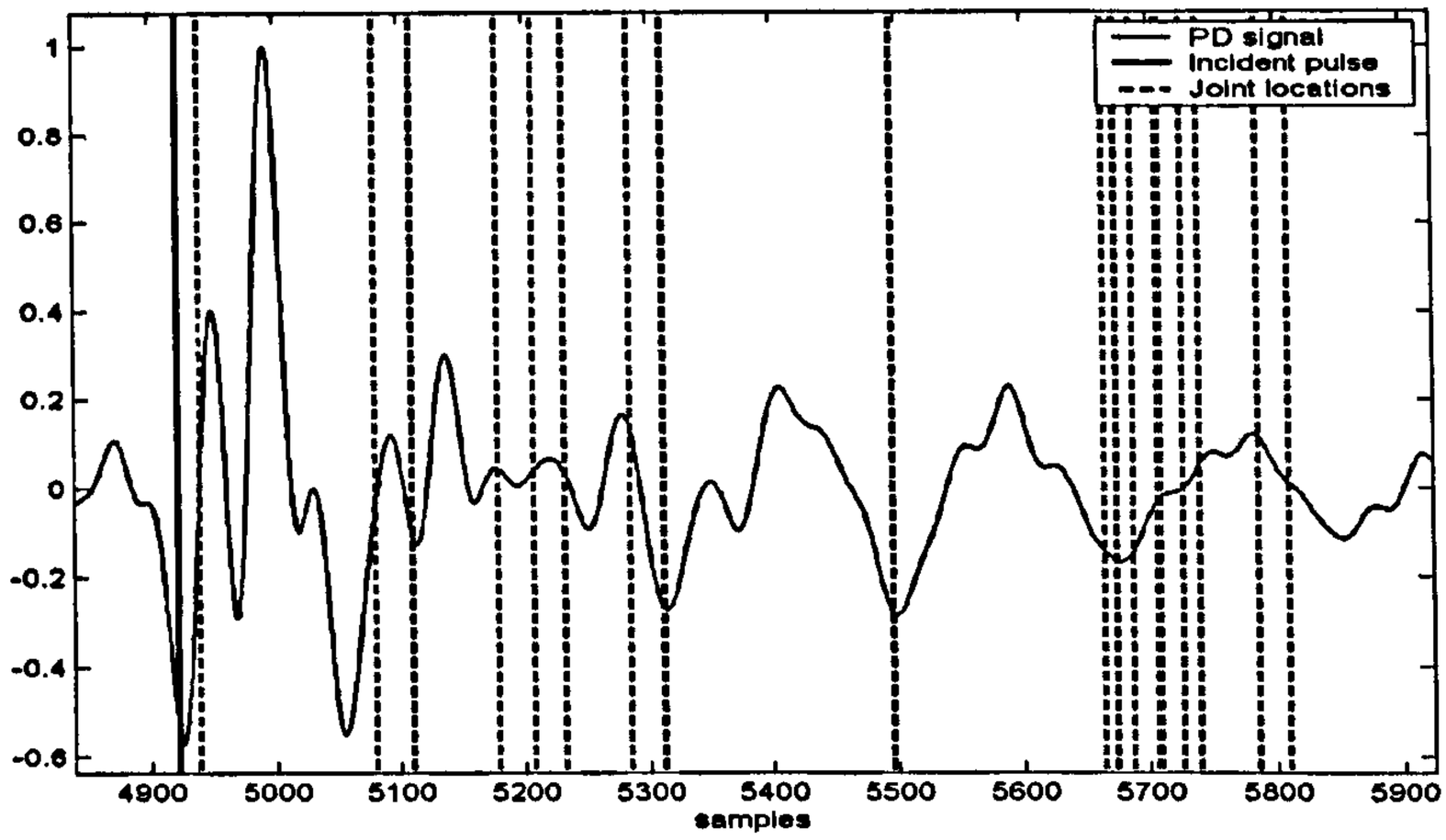

Figure 6.19: Using cable joint information to identify possible reflections

6.6 Conclusions

In this chapter, the investigations were carried out on the field data acquired from the new data acquisition unit developed in Chapter 4. Related aspects crucial for data interpretation were also covered such as the cable network configuration, the cable joints and the sensors utilised during the data acquisition. Cable joints play important role in PD location because it is usually the component that has high probability of containing discharges. Interpretation of pulse origin was also covered in this chapter; these include methods of interpretation for both single-ended and double-ended systems.

These were then applied to the online field data gathered over the period of time. A general overview of the unprocessed data was presented to differentiate the amplitude levels and the differences between the sets of cables. It was found that interpreting online field data were more difficult than expected. The noise levels were high and transient noise was present. Wavelet algorithms developed in Chapter 5 were applied to these signals. The transient noise was successfully reduced at the

expense of removing a many scales of the wavelet decomposition. After this process, the de-noised signals from both Cable-1 and Cable-2 were compared. It was found that certain signal components were had difference amplitudes on the sets of data. Based on the signal amplitudes, the origin of those signal components was assumed. The PD activity was found to be likely to occur from Cable-2 cable.

The characterisation of the PD pulse produced several positive results corresponding to the nature of PD's. The load current characteristics were investigated with regards to the PD pulse amplitude. It was found that as the load current varied the inception voltage of the PD also varied, with inverse relationship with the phase of the voltage source. This suggested that the signal structure has high probability to be PD activity.

Signal averaging was conducted to maximise the possibility of producing a reflection in the signal. The location procedure was carried out using the cable joint markers to highlight the possible locations of the PD from cable joints. Several cable joints were highlighted. However, the overall results were not successful because the method only produces an approximation and without distinct clarity because of the superimposed signals.

From all the conclusions gathered, it was found that online data acquisition using backup protection CT's are not favourable although results showed that high frequency components were captured in the data. Where possible, proper high frequency CT should be used as the main sensor connection for data acquisition. Under online conditions, using single ended measurement systems were found to be disadvantageous because the origin of pulses cannot be distinguished, for instance external pulse coming from beyond the cable. Also problems associated with identifying PD reflections hinder the PD location process. Double-ended systems are more advantageous because it enables the identification of pulse origin and PD reflections are not of importance.

Chapter 7 Summary, Conclusions and Future Directions

This chapter summarises the research work presented in this Thesis, identifies the conclusions that may be drawn and indicates the direction of potential future investigations.

7.1 Summary and Conclusions

(Note: main conclusions are shown below in **bold** type)

In this Thesis, we have focussed on the problems associated with online PD diagnostics for HV underground cables. One of the main problems in this research was the lack of online field data. Another problem that arisen from this was the logistics and conforming to the regulations or protocols of the utility company. The process of acquiring online field data was tedious and many negotiations were performed before an agreement was reached. Followed that are other common problems such as the physical aspects of making online data, the interpretation of data in heavy noise interference environments, and detection and location of PD within the cables. The original contributions developed in this research work include the following: a new online PD data acquisition system for underground HV cables, signal processing tools for enhanced PD detection, and wavelet-based signal processing algorithms for PD location through TDR.

Recent advances in technology in this 21st century have promoted the increase of micro-processing power usage and directly impacted PD diagnostics. Before this, online PD diagnostics were limited by the processing power in terms of speed, memory and storage capacity. In Chapter 2, the basics of PD were presented, which were mainly the physical characteristics of PD and power cables. The various techniques for PD diagnostics were also reviewed. Although online techniques are more favourable, there are still many applications of offline techniques in reality. This is due to the maturity and reliability of the technology. The 0.1 Hz technique is one of the common techniques employed and is effective for PD detection and location for cables. However, the drawbacks of offline techniques are that they are not performed under normal operating conditions and the negative effects of separate cable energisation are not certain.

Online PD diagnostics will involve the synthesising of signals measured either in voltage or current waveforms. Understanding these signals and the conditions of the acquisition configurations will be essential to effectively interpret and characterise the PD activity. This was the aim of Chapter 3, where the guide to PD in the signal realm was presented. This chapter also reviewed the various signal processing techniques that have been applied to PD diagnostics. Wavelet-based algorithms were found to be the widely applied technique by researchers in the field. This was due to the advantages and the effectiveness of PD detection and signal enhancement. The variations of the wavelet implementation were also reviewed.

One of the first conclusions drawn from this study was that there was a need to acquire appropriate examples of online data from practical cable installations.

A new online PD data acquisition system (RPDAQ) was developed during the course of this research. The main motivation for doing this was the need for online field data for experiments. The details and features of the new system were presented in Chapter 4. The system was designed to accommodate the difficulties associated with both the strict health and safety regulations of the utility company and the electrically noisy conditions in which any PD signal was to be detected. Signal conditioning features were included in the hardware sections of the unit and it

was also capable of performing post-processing signal conditioning. However, the post-processing features were not included in the RPDAQ at this initial stage. The overall results of the measured data were validated and compared by using a separate prototype measurement system developed in [Shim 2001]. A database of the online field data was created through the RPDAQ. **It was concluded from the preliminary data that the recorded signals varied with changes in the level of current loading in the cable, as described in the literature.**

Chapter 5 dealt with the wavelet-based PD signal processing algorithms. This chapter included the important factors one should consider before applying the DWT. The methods of PD detection using wavelets were described i.e. the multi-scale edge detection approach and the de-noising approach. **It was concluded that the first approach was the preferred approach because it could be used to identify false peaks within the signal, whereas the de-noising approach had the possibility of removing parts of important information from the PD signal and also generating false peaks.** A comparison of the wavelet implementation types i.e. the commonly known DWT to the decimated DWT and the non-decimated DWT was performed. **It was concluded that by using the non-decimated DWT the shift-invariant property was preserved. This had significant impact on the synthesising of PD signals that are non-stationary while using the TDR approach. By using the conventional DWT approach, the PD signatures generated in the wavelet scales were inconsistent. Robust PD signatures were generated through the non-decimated DWT and the effect of this property was reflected in the more accurate results of the PD location process.** This was demonstrated through simulated data and was applied to the field data. In the simulated data, it was found that the location of the non-decimated wavelet approach was more accurate. However, in the field data this was not demonstrated because the reflection could not be identified. Nevertheless, the PD signatures generated through the non-decimated wavelet approach was shown to be more robust.

A novel kurtosis wavelet-based algorithm was developed as presented in Chapter 5. This novel algorithm was developed to aid the processing of large volumes of data. In order to reduce the processing time of the data, the algorithm

functions to extract segments of the entire signal that may contain PD activity. These segments are then highlighted and the information is reduced to simplified format for a user identification/system as described in Section 5.4. These segments can then be extracted and analysed extensively to verify the presence of PD. The algorithm was applied to both the simulated data and the acquired field data. **It was concluded with both simulated and field data that this novel algorithm performed according to expectations, significantly reducing processing time and hardware requirements, except when the field data contained high transient interference.** A clear example of this limitation is observed with the signals shown in Chapter 6, which contain significant transient noise. It was acquired from the same substation and cables as that shown in Chapter 5. In the later instance, the algorithm failed because most regions in the signal would be highlighted as containing potential PD, which defeats the aim of the algorithm. **It was also concluded, therefore that there is a need for more data from other sets of cables and that such data will provide a better understanding of the general signal characteristics from online measurements.**

Also in Chapter 6, the issues pertaining to online field data interpretation was presented. Important information containing the details of the physical network configuration of the test site and other relevant information were included. These included the sensors that were used for the data acquisition and the typical cable joint configurations. Because cable joints are known to be one of the major sources that cause PD [Cigre 2002], the joint locations were treated as weighting factors to aid the identification of PDs and their location. The approaches to single-ended and double-ended systems with the emphasis on the cable joints were discussed. This chapter also focussed on the field data acquired. The raw form of the data was investigated and the differences of the data obtained from the Cable-1 and Cable-2 were compared. In particular, the noise interference was analysed. It was found that the transient noise level was higher in Cable-1 than Cable-2. **It was concluded that the transient noise had originated from Cable-1 and propagated into Cable-2.** This hypothesis was justified in Section 6.4.2, where the signals showed correlation between one another. However, these measurements were conducted at different

instances in time. Hence, the data is only valid as an approximation. **It was concluded that, in order to fully verify the suggestion of pulse propagation between cables, simultaneous measurements from both Cable-1 and Cable-2 should be performed.**

It was also found that there was potential PD activity that was prominent in Cable-2. This PD signature was detected more prominently in the Cable-2 circuit than Cable-1 (as depicted in Figure 6.12). This PD signature was labelled as PD1 for simplicity purposes. The PD1 characteristics were analysed through the monitoring of its amplitude, inception voltages, and percentage apparent charge against the effects of current loading. **It was found that the characteristics exhibited by PD1 indeed portrayed the characteristics of PD.** Signal averaging was applied onto the PD1 structure over 100 pulses. In theory, the reflection of the PD pulse from the far end should be magnified over many events. However, after applying the cable joint locations as potential sources the possibilities were narrowed down to the 85.9%, 76.2%, 67.5% and 58.9% location of the cable from the Substation A end after applying cable joint markers. **However, it was concluded that the exact position of cable joints that contained PD sources could not be determined with certainty using the present system as currently operated.** However, it must be noted that the utility had hired to diagnose these cables found that PD activity was present at locations 58-61% of the cable from the Substation A end, showing some agreement with the present work.

From the aspect of the sensors, the measurements were limited to only the backup protection CT that the utility had provided. **After conducting the research, it was concluded that wherever possible high frequency CTs should be employed.**

Finally, it was considered that single-ended systems may have major disadvantages for the detection and location of PD for HV cables under online conditions, unless the direction of signal propagation can be determined. This is because the origin of the PD, i.e. whether from the cable or beyond, cannot be accurately determined through a single point of measurement. Furthermore, PD location through this approach will require the detection of PD reflections in the

signal, which is often difficult because of attenuation and superposition of the pulses. Therefore, a means of identifying pulse origin is required and the most suitable alternative is by using dual measurement systems.

7.2 Directions of Future Research

During the course of this research, several aspects of research that prompt future investigations have been discovered. Some of these aspects are the subsequent effects of the contributions made in this thesis.

The usage of advanced digital signal processing tools for PD diagnostics has been reviewed in chapter 3. However, in this thesis we have only focussed primarily towards the application of wavelet-based algorithms and found that by using non-decimated DWT have major advantages especially for PD signature identification. Further exploration into the application of neural networks and fuzzy reasoning should be performed because they are potential tools that can be combined with the wavelet-based techniques developed. We have also developed a new PD data acquisition unit as described in Chapter 4. The next logical step is to develop a unit that will form a general PD diagnostic unit, which enables the acquisition of data from the sensors and includes the signal processing algorithms into the process. Incorporating these algorithms can actually help to reduce the storage required in the acquisition system by extracting only useful signal parts or information.

The focus of the data acquisition and interpretation was towards single-ended systems. This was due to the financial constrains and also it was the initial step in our research on online systems. Double-ended system was not investigated because of the physical limitations of the substation configuration. However, double-ended system has a significant advantage for PD location procedures. Hence, the data acquisition system should be extended to function in double-ended systems mode.

From the aspects of sensors, this research work was restricted to only sensors provided by the utility company. These sensors were the backup protection CT that functions specifically to monitor at power frequencies only. Hence, the reliability of

these sensors to high frequency is unknown. If possible, comparing the data obtained from these sensors and a proper high frequency CT will be beneficial in order to verify the accuracy of interpreting data from the backup protection CT.

In chapter 6, the network configuration of the substation was described. The data acquisition unit was connected on two points of the cable network, which are essentially same points at two parallel sets of cables. Due to some restrictions, those measurements were performed at alternate instances. It was found that the pulses had high possibility of propagating from one set of cables to the other set. This is a difficulty associated to online PD diagnostics since all cables remain in contact. Hence, if possible simultaneous measurements on these points will provide better understanding of the signal propagation and its properties in the network. This may produce useful information, which may be an alternative to double-ended systems.

One of the major difficulties that we have encountered during the course of the research is the arrangements and logistics of making data acquisitions at the substation. Currently, the measurements were performed in the switchyard of the substation where the bus bars and switchgear are located. Here, the strict utility regulation and protocols actually deters access for the data acquisition process. Hence, it is crucial that an alternative is sought. One way is to perform data acquisitions in the control room where access is less strict and in most substations the physical configuration is similar to one another. However, before that can be performed the signals acquired from the control room have to be correlated with the measurements performed in the switchyard.

In terms of acquired data, high volume of data was acquired forming a rich database. However, these data is limited to the set of cables (Cable-1 and Cable-2). Therefore, more data should be acquired from other substations to provide a variation of data and a means of comparison. For instance, in chapter 5 the wavelet-based algorithm that incorporated the kurtosis was not successfully applied to the field data due to the amount of transient natured interference, which may not be the case for other field data.

Appendix A

RPDAQ Connections and Configurations

Appendix A1: RPDAQ connection to CT sensors

The connection of the RPDAQ to the utility backup protection CT is depicted in Figure A1. The RPDAQ is connected in parallel to a measurement device that functions as an alarm for the protection system of the utility. The impedance of this measuring device is very low and usually approximately 5Ω. There input impedance of the RPDAQ has to be significantly higher than the measuring device.

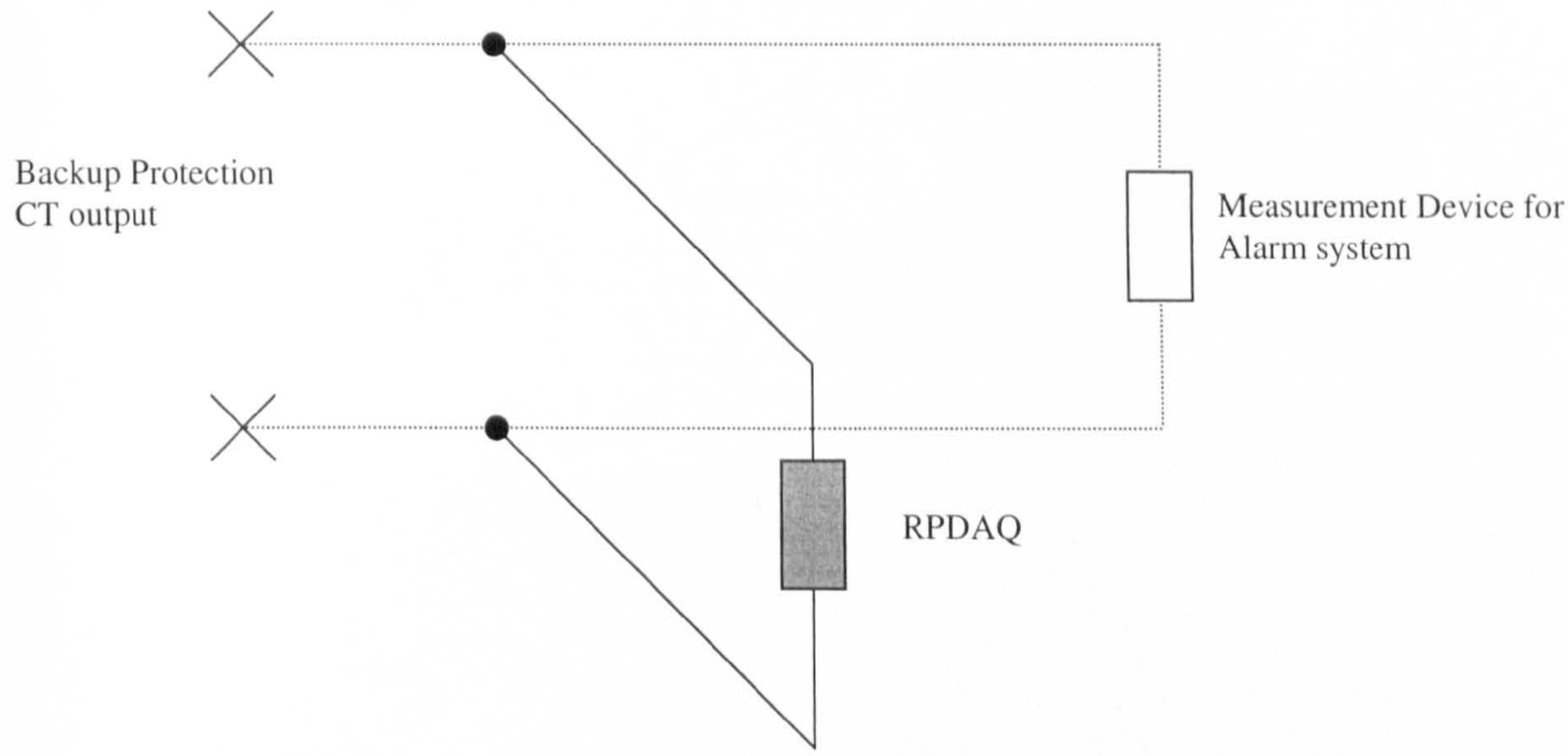

Figure A1: RPDAQ connection configuration

Appendix B

System Components of RPDAQ

Appendix B1: Band-pass filter response

Band-pass Filter Typical performance[*1]

Figure B1 shows a typical response of the band-pass filter with a lower cut off frequency of 25MHz, and upper cut off frequency of 48MHz and a band-pass gain of –22dB.

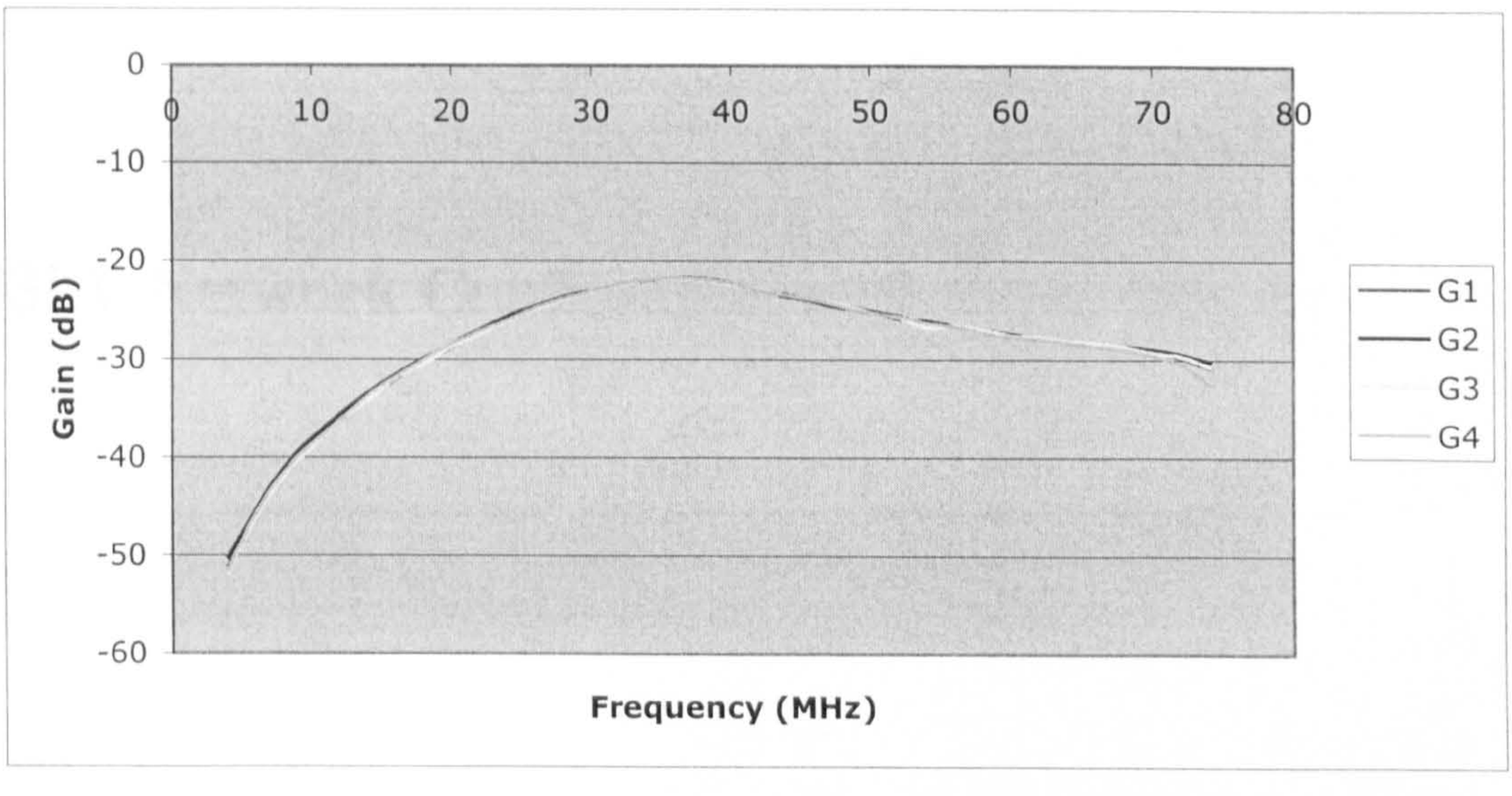

Figure B1 Band-pass filter response

[1] Page 6 of report taken from "Programmable filter for the PD acquisition unit", Progress report, A. Sellars, 2 July 2003.

Appendix C

33kV Network Configuration at Substation A

Appendix C1: Substation network configuration

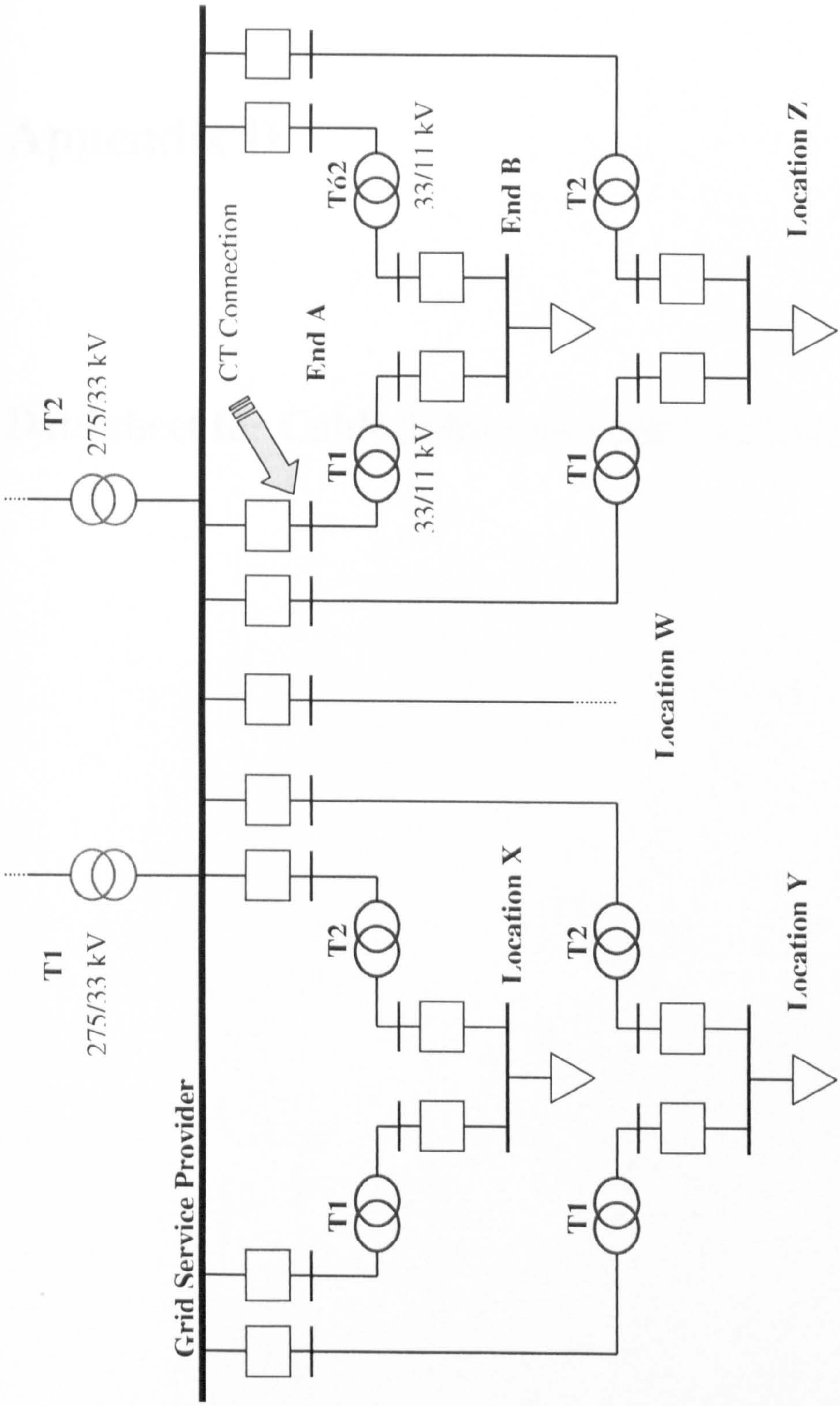

Figure C1: Substation network configuration

Appendix D

Data sheet for Cable Joint and Cable Stripping

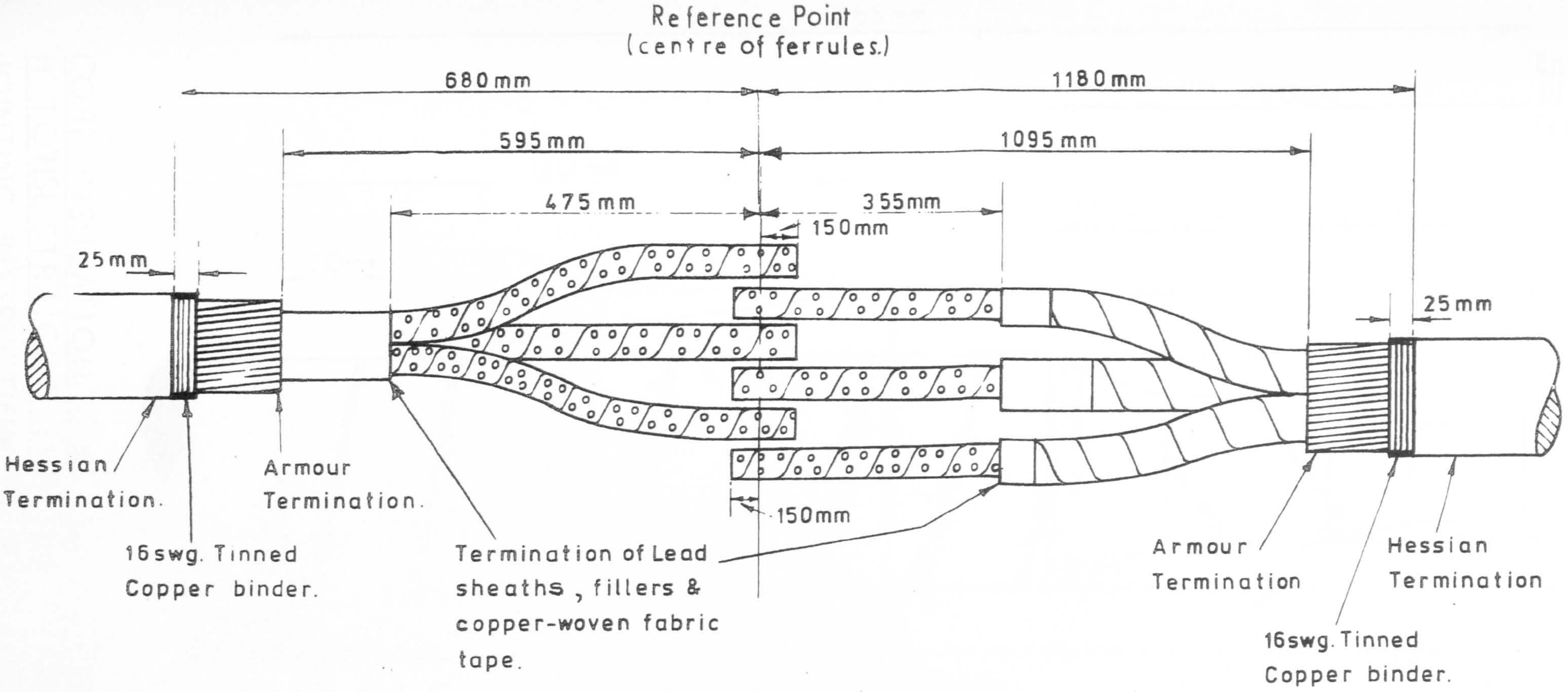

FIG.1.

STRIPPING DIAGRAM FOR 33kV. 'H' TO 'HSL'
STRAIGHT THROUGH JOINT.
Jointing Instruction D3.

MNW.11/13272/A4.

CORE INSULATION DIAGRAM FOR 33 kV
'H' TO 'HSL' STRAIGHT THROUGH JOINT
JOINTING INSTRUCTION No. D3.

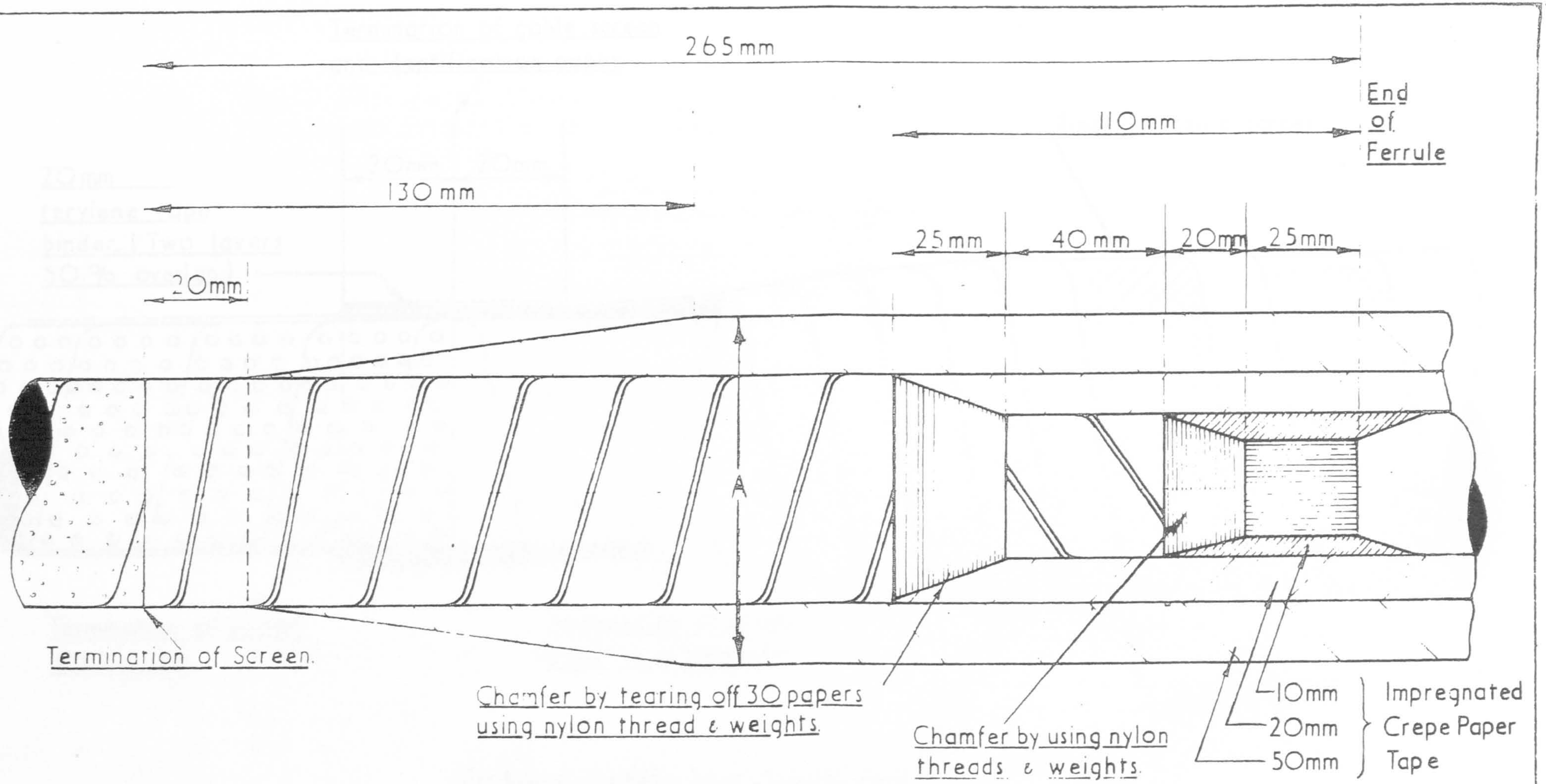

FIG 2.

DIAMETER TAPE MEASUREMENT OVER CREPE PAPER INSULATION		
EQUAL CONDUCTOR SIZE	A mm	UNEQUAL CONDUCTOR SIZES
0.1 in^2	62	0.1 in^2 TO 0.15 or 0.2 or 0.25 or 0.3 or 185 mm^2
0.15 in^2	58	0.15 in^2 TO 0.2 or 0.25 or 0.3 in^2 or 185 mm^2
0.2 or 0.25 in^2 or 185 mm^2 or 0.3 in^2	52	0.2 or 0.25 or 0.3 in^2 TO 185 mm^2
0.4 or 0.5 in^2 or 240 or 300 mm^2	58	0.2 or 0.25 or 0.3 in^2 or 185 mm^2 TO 0.4 or 0.5 in^2 or 240 or 300 mm^2

TINSEL STOCKING SCREEN DETAILS
STRAIGHT - THROUGH JOINT.
33kV 'H' TO 'HSL'.
JOINTING INSTRUCTION No. D3.

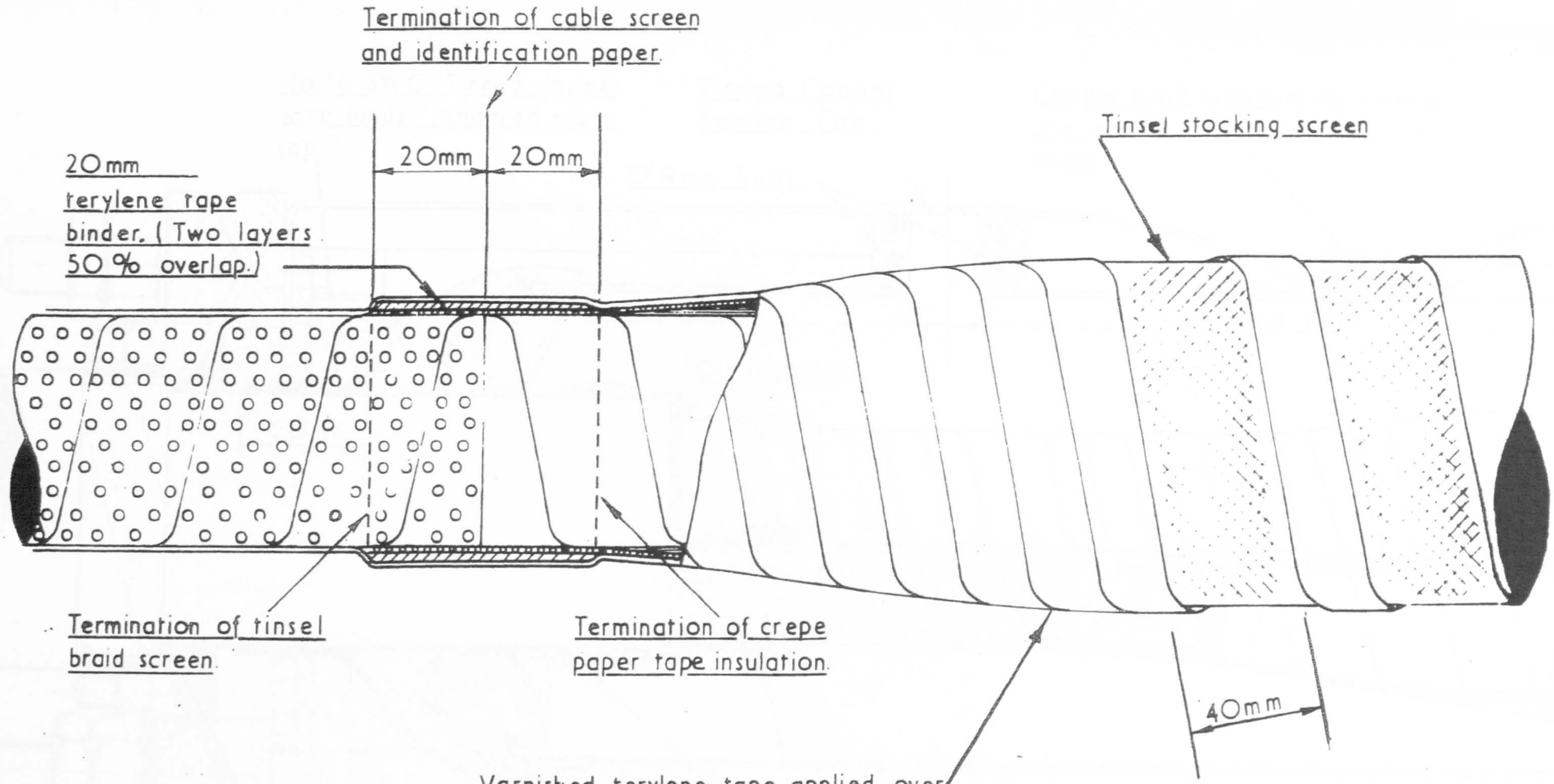

FIG. 3.

GENERAL ASSEMBLY DETAILS 33KV 'H' TO 'HST'

STRAIGHT-THROUGH JOINT ('H' end of Joint)

JOINTING INSTRUCTION No D3.

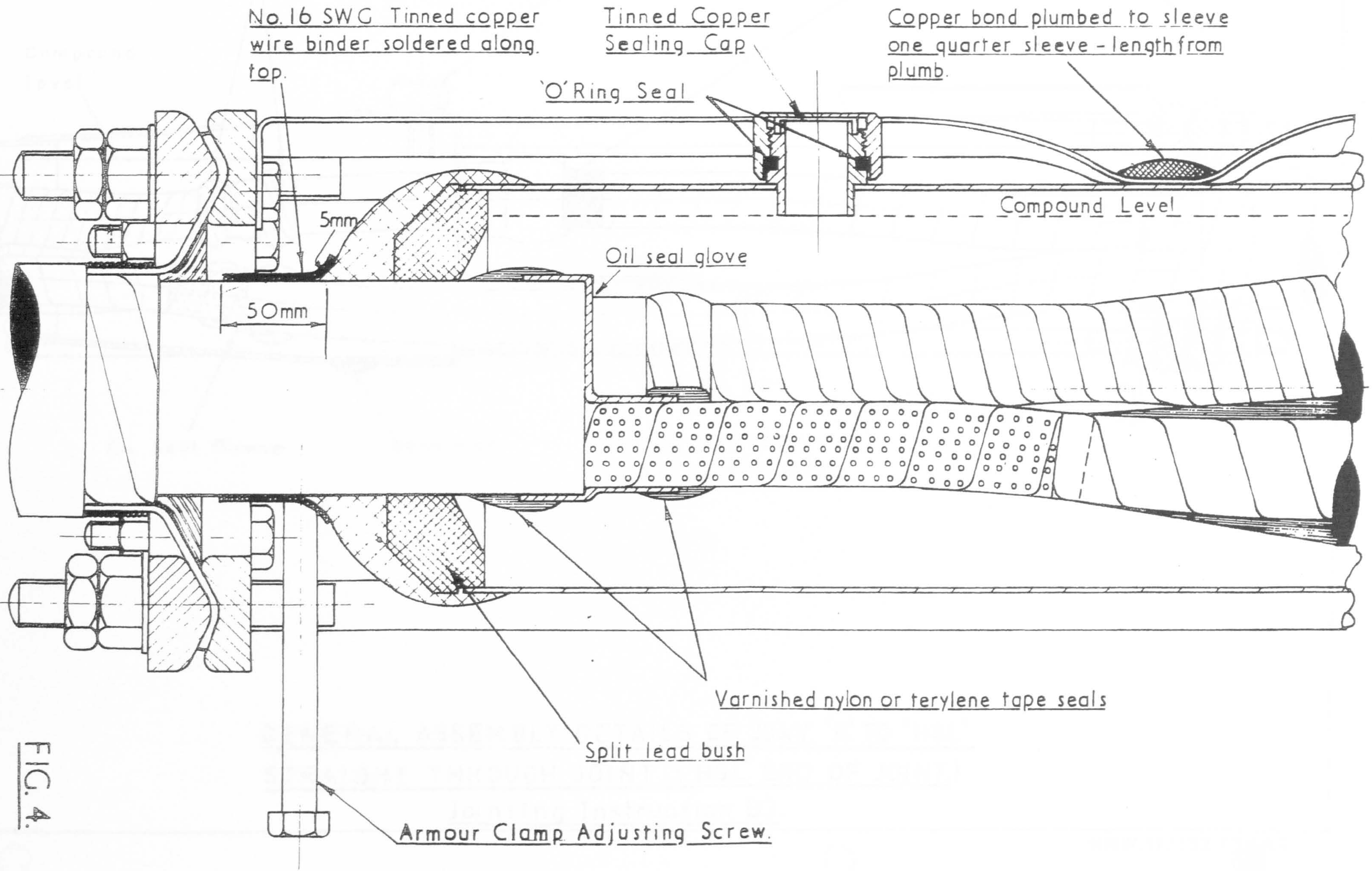

FIG. 4.

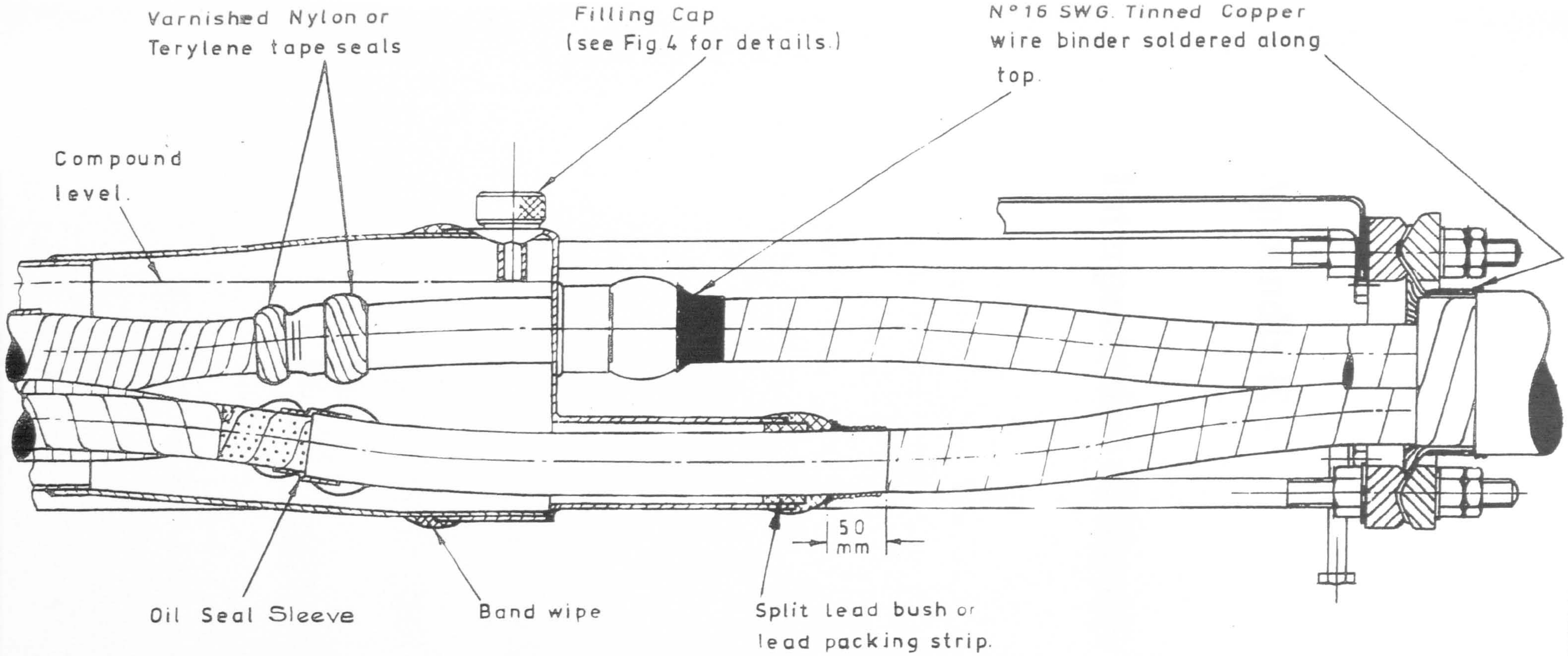

FIG 5

GENERAL ASSEMBLY DETAILS OF 33kV. 'H' TO 'HSL'
STRAIGHT THROUGH JOINT ('HSL' END OF JOINT.)
Jointing Instruction D3.

Appendix E

Interpretation of Signals

Appendix E1: Single-Ended Measurement Systems

This section describes a typical example of a single ended system for HV networks. Generally, the termination of the cable can be terminated with a transformer (or other equipment) or another cable section, each of which would produce different strengths of pulse reflection. For the case of a transformer, open-circuit pulse reflections are usually produced. Figure E1 depicts an example of a typical cable connected to section of a 33 kV busbar. When the pulse occurs, it will propagate towards the ends of the cable. When it reaches the termination with the transformer (T_{x2}), a clear reflection should be obtained. However, when the pulse arrives at the busbar, it will continue to propagate until it reaches the transformer (T_{x1}) and the other cables connected to the busbar. At the transformer (T_{x1}), a clear reflection should be produced. When the pulse arrives at the other cables, a reflection can be produced, which can be approximately 33% of the incident pulse [Clegg 1993].

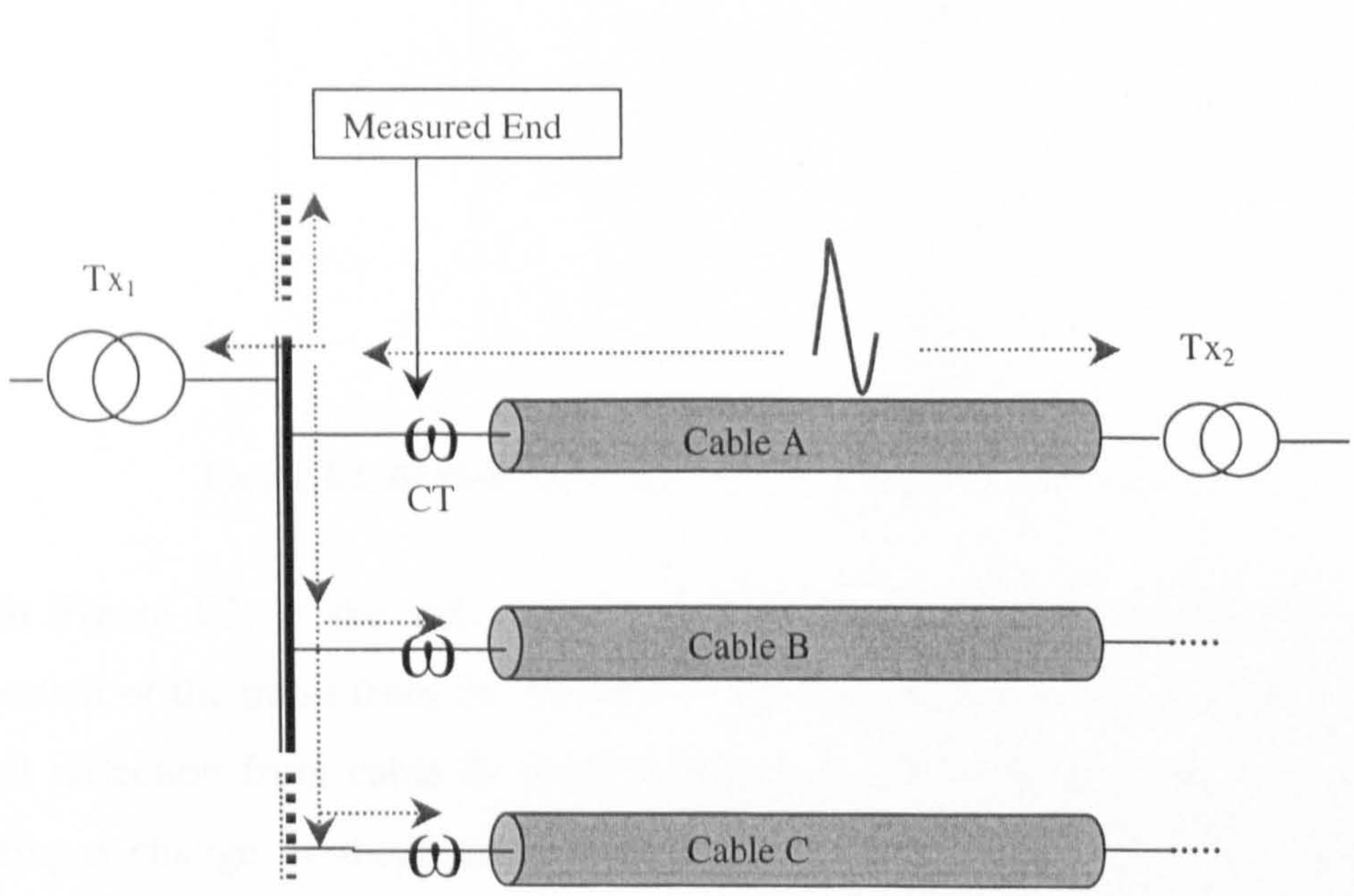

Figure E1: Example of a PD pulse propagation in a 33kV cable network

In this case, interpreting the pulse reflection will more complicated than in the example described in Section 6.3.1. A Bewley lattice diagram for this example is illustrated in Figure E2.

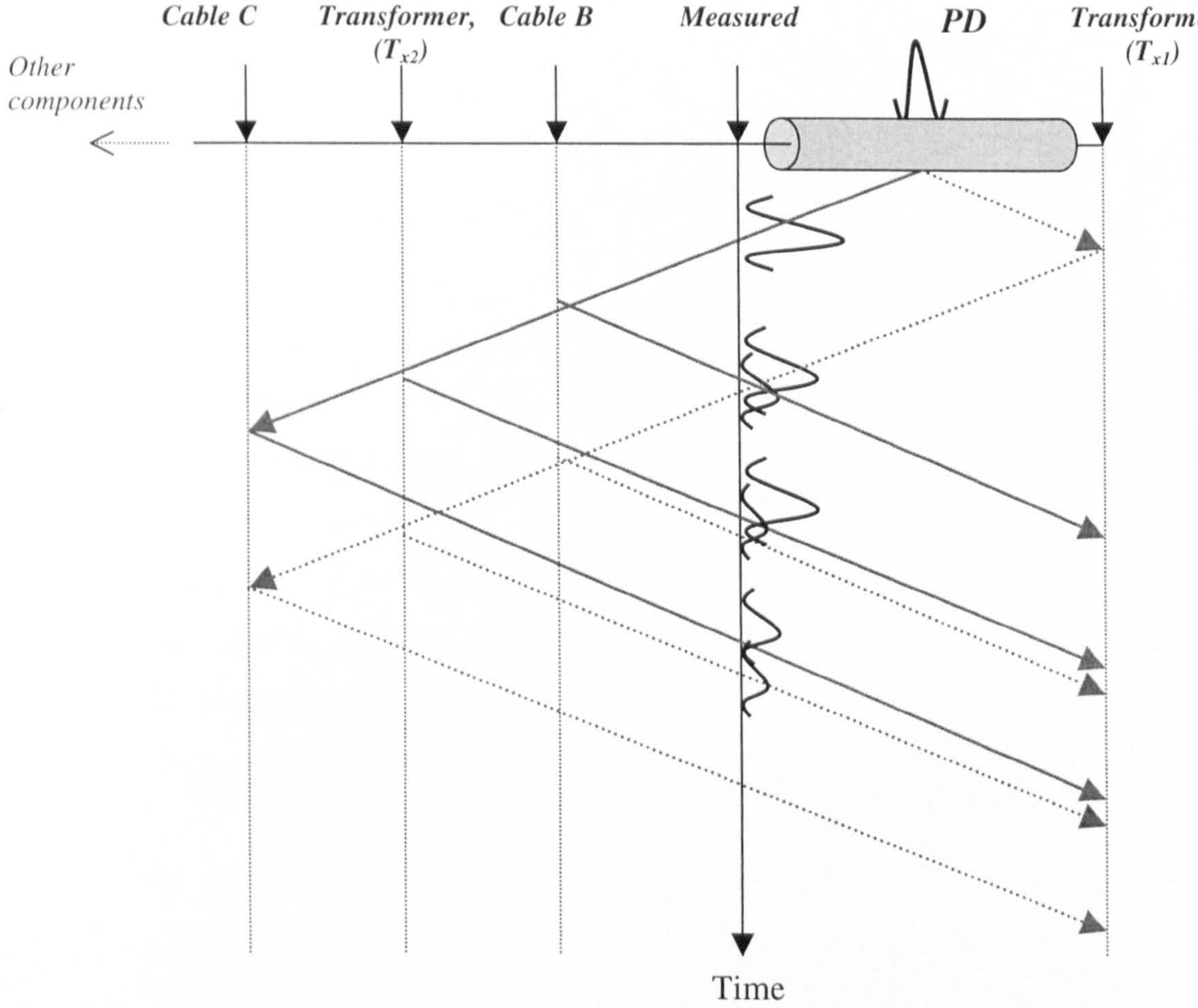

Figure E2: Bewley lattice diagram for example in Appendix E1

From Figure E2, at the axis where the measurements were carried out, the first reflection of the pulse from the far end of the specimen cable has coincided with the small reflection from cable B. Superposition of pulse will take place at this point, causing a change in shape and amplitude of the reflected signal. The outcome of which will depend on the shape of the discharge itself. Hence, in general the interpretation of the reflected PD pulse will depend on the network configuration and also the location of the PD origin. Therefore, the interpretation of the reflected PD

signal will be complicated and depends on individual situations. As mentioned in section 6.3, the cable joint markers can be used to enhance the interpretation process.

Appendix F

Author's Publications and Presentations

(i) GB Patent Application 0316221.3, " Detecting Partial Discharge in High Voltage Cables", **M. H. Foo**, J. J. Soraghan, W. H. Siew, March 2004.

(ii) **M. H. Foo**, J.J.Soraghan, W.H.Siew, "Remote Control Partial Discharge Acquisition Unit", *17th International Conference on Electricity Distribution*, Barcelona, Spain, May 2003.

(iii) **M. H. Foo**, J.J.Soraghan, W.H.Siew, "Practical Application of Discrete Wavelet Transform and Higher Order Statistics for Partial Discharge Analysis", *Symposium on Quality and Security of Electric Power Delivery Systems*, Montreal, Canada, October 2003.

(iv) **M. H. Foo**, J.J.Soraghan, W.H.Siew, "Application of Non-Decimated Discrete Wavelet Transform for Partial Discharge Analysis", *18th International Conference on Electricity Distribution*, Turin, Italy, June 2005.

(v) **M. H. Foo**, J.J.Soraghan, W.H.Siew, "Importance of Shift-Invariant Properties in Wavelet Transforms for PD Analysis", *submitted to IEEE Trans. for Dielectric and Electrical Insulation.*

Bibliography

[Abramovich 1998] F. Abramovich, T. Sapatinas, B. Silverman, "Wavelet Thresholding via a Bayesian Approach", J. R. Statist. Soc. B, Vol. 60(4), 1998, pp715-749.

[Ahmed 1998] N. H. Ahmed, N. N. Srivinas," Online PD Detection in Cables". IEEE Transactions in Dielectrics & Electrical Insulations, Vol 5, No. 2, April 1998, pg 181-188.

[Bartnikas 2000] R. Bartnikas, K. D. Srivastava, "Power and Communication Cables". IEE Press, 2000.

[Bartnikas 2002] R. Bartnikas, "Partial Discharge: Their Mechanism, Detection and Measurement", IEEE Transactions on Dielectrics And Insulation,Vol. 9, No. 5, 2002, pp763-808.

[Baumgartner 1992] R. Baumgartner, B. Fruth, W. Lanz, K. Patterson, "Partial Discharge in Gas Insulated Substations-II", IEEE Electrical Insulation Magazine, Vol. 8, No. 1, Jan/Feb 1992,pp16.

[Baur 2005] Baur, High Voltage Diagnostic and Testing Equipment, http://www.baur.at/en_baur/_products/_overview.htm, 2005.

[Bewley 1951] L. V. Bewley, Travelling Waves on Transmission Systems , John Wiley & Sons Inc. , 1951.

[BICC 1948] British Insulated Callender's Cable, "High Voltage Cables", London : British Insulated Callender's Cables Limited, 1948.

[Boggs 1990a] S. A. Boggs, "Partial Discharge: Cavity-Induced PD in Solid Dielectrics", IEEE Electrical Insulation Magazine, Vol. 6, No. 6, Nov/Dec 1990, pp.11

[Boggs 1990b] S.A. Boggs, "Partial Discharge F– Part II: Detection Sensitivity", IEEE Electrical Insulation Magazine, Sept/Oct 1990, Vol. 6, No. 5, pp35-42.

[Boggs 1996] S. A. Boggs, "Partial Discharge XXII : High Frequency attenuation in shielded solid dielectric power cables & Implications thereof for PD location". IEEE Elec. Ins. Magazine, V0l. 12, No. 1, Jan/Feb 1996.

[Boggs 2000] S. A. Boggs, J.Densley, "Fundamentals of Partial Discharge in the Context of Field Cable Testing" , IEEE Electrical Insulation Magazine, Vol. 16, No. 5, Sept/Oct 2000, pp13.

[Borsi 1995] H. Borsi, E. Gockenbach, D. Wenzel, "Separation of Partial Discharge from Pulse-Shaped Noise Signals with the Help of Neural Networks", IEE Proceedings – Science, Measurement and Technology, Vol. 142, No. 1, 1995, pp69-74.

[Borsi 2000] H. Borsi, " A PD Measuring and Evaluation System Based on Digital Signal Processing", *IEEE Trans. on Dielectrics and Elec. Ins.*, Vol. 7, No. 1, Feb. 2000, pp 21-29.

[Brunt 1994] R.J. Bunt, "Physics and Chemistry of Partial Discharge and Corona, Recent Advances and Future Challenges", *IEEE Trans. on Dielectrics and Elec. Ins.*, Vol 1, No. 5, October 1994, pp 761-784.

[BS3938 1973] British Standards, " Specifications for Current Transformers", 1973.

[Bungay 1982] E. Bungay, I. W. McAllister, " Electric Cables Handbook", Blackwell Science, 1982.

[Burns 1992] N.M Burns, R.M. Eichhorn, C.G. Reid, "Stress Controlling Semiconductive Shields in Medium Voltage Power Distribution Cables", *IEEE Electrical Insulation Magazine*, Vol. 8, No. 5, Sept/Oct 1992, pp.8.

[Candela 2000] R. Candela, G Mirelli, R. Schifani, "PD recognition by means of statistical an fractal parameters and a neural network", *IEEE Transactions on Dielectrics And Insulation*, Vol. 7, Iss. 1, 2000, pp 87-94.

[Canny 1986] J. Canny, "A Computational Approach to Edge Detection", IEEE Trans. Pattern Analysis and Machine Intelligence, Vol. PAMI-8, 1986, pp 679-698.

[Carminati 2001] E. Carminati, L. Cristaldi, M. Lazzironi, A. Monti, "A Neuro-Fuzzy Approach for the Detection of Partial Discharge", IEEE Trans. On Instrumentation and Measurement, vol. 50, no. 5, Oct. 2001, pp 1413-1417.

[Cavallini 2003] A. Cavallini, G. C. Montanari, A. Contin, F. Puletti, "A New Approach to the Diagnosis of Solid Insulation Systems Based on PD Signal Inference", *IEEE Electrical Insulation Magazine,* vol. 19, No. 2: March/April 2003, pp. 23-31.

[Chan 1991] J. C. Chan, P. Duffy, L. J. Hiivala, "Partial Discharge – Part VIII: PD Testing of Solid Dielectric Cable". *IEEE Electrical Insulation Magazine*, 7,No. 5, September/October 1991, p9.

[Chang 1997] G. Chang, B. Yu, M. Vetterli, "Wavelet Thresholding for Image Denoising and Compression", IEEE Transaction on Image Processing, 2000 .

[CIGRE 2002] Cigre TF 15.11/33.03.02, "Knowledge Rules For Partial Discharge Diagnosis in Service", CIGRE, 2002.

[Clegg 1993] B. Clegg, *Underground Cable Fault Location,* McGraw Hill Book Company, London, 1993.

[Coifman 1995] Coifman, R.R.; Donoho D.L. (1995), "Translation Invariant De-noising," *Lecture Notes in Statistics*, 103, 1995, pp 125-150.

[Contin 2002] A. Contin, A. Cavallini, G. C. Montanari, G. Pasini, F. Puletti, "Digital Detection and Fuzzy Classification of Partial Discharge Signals", *IEEE Trans. Dielectrics and Electrical Insulation*, Vol. 9, No. 3, pp. 335-348, June 2002.

[Cotton 1931] H. Cotton, H. Barber, "The transmission and Distribution of Electrical Energy", The English Universities Press Ltd. 1931.

[Daubechies 1994] I. Daubechies, *Ten Lectures On Wavelets*, CBMS, SIAM, 61, 1994.

[Dervos 1990] C.Dervos, P.D.Bourkas, E.A.Kayafas, I.A.Stathopulos: "Enhanced Partial Discharges due to Temperature Increase in the Combined System of a Solid-Liquid Dielectric". *IEEE Trans. on Electrical Insulation*, Vol. 25, No. 3, pp. 469-474, 1990.

[Dissado 1997] L.A. Dissado, S.J. Dodd, J.V Champion, P.I. Williams, J.M. Alison, "Propagation of electrical tree structures in solid polymeric insulation", *IEEE Trans. on Dielectrics and Elec. Ins.*, Vol. 4, No. 3, June 1997, pp. 259–79

[Donoho 1994] D.L. Donoho, I.M. Johnstone, "Ideal Spatial adaptation via Wavelet Shrinkage" Biometrika, Vol. 81, 1994, pp425-455.

[Donoho 1995a] D.L. Donoho, "De-noising by soft-thresholding", IEEE Trans. on Information Theory, Vol. 41, 1995, pp613-627.

[Donoho 1995b] D.L. Donoho, I. M. Johnstone, "Adapting to unknown smoothness via wavelet shrinkage", Journal of the American Statistical Association, Vol. 90, No. 432, December 1995, pp1200-1224.

[Du 1997] Z. Du, P.K. Willett, M.S. Mashikian, "Performance Limits of PD Location Based on Time-domain Reflectometry", IEEE Transactions on Dielectrics and Electrical Insulation. Vol. 4, No. 2, April 1997, pp182.

[EATech 2001] "Commisioning of High Voltage Cables", EA Technology Homepage, www.eatechnology.com

[EATech] EA Technology, "Services Report T2587", property of ScottishPower Plc., U.K.

[Ece 2004] D. G. Ece, O. N. Gerek, "Power Quality Event Detection using Joint 2D Wavelet Subspace", IEEE Trans. On Instruments and Measurement, vol. 53, no. 4, Aug. 2004, pp. 1040-1046.

[ERA 2004] ERA Technology Webpage, www.era.co.uk

[Fouracre 2000] T. Fouracre, "Msc in Electrical Eng. Course Notes:- Solid Dielectric Insulation Materials", University of Strathclyde, Glasgow, UK.

[Gao 1998] H.Y.Gao, "Wavelet Shrinkage De-noising using the Non-Negative Garrote", *Journal of Computational and Graphical Statistics*, 1988, Vol. 4, pp. 469-488.

[Gonen 1988] T. Gonen, " Electric Power Transmission System Engineering", John Wiley & Sons, 1988.

[Gulski 1998] E. Gulski, J.J. Smit, P.N. Seitz, J.C. Smit, "PD Measurements On-site using Oscillating Wave Test System", IEEE International Symposium on Electrical Insulation, Washington DC, USA, June 7-10, 1998.

[Gulski 2000] E. Gulski, F. J. Wester, J. J. Smit, "Advance Partial Discharge Diagnostics of Medium Voltage Power Cables Systems Using Oscillatory Wave Test System", IEEE Electrical Insulation Magazine, Vol 16, No. 2, pg 17, March 2000.

[Guo 1995] H. Guo, "Theory and Application of Shift-Invariant, Time-Varying and Undecimated Wavelet Transforms", MSc. Thesis, Rice University, Houston, Texas, May 1995.

[Hamid 2002] E. Y. Hamid, Z. I. Kawasaki, "Wavelet-Based Data Compression of Power System Disturbances Using the Minimum Description Length Criterion", *IEEE Trans. On Power Delivery*, vol. 14, no. 3, April 2002, pp. 460-466.

[Harrold 1993] R. Harrold, "Partial Discharge – PartXVI: Ultrasonic Sensing of PD within Large Capacitors", IEEE Elec. Ins. Mag., May/June 1993, Vol. 9, No. 3, pp21-28.

[Hassani 2002] M.Hassani, "Underground Cable Diagnostic Utilizing Partial Discharge Technique –2002 Report", Reliability Services, Potomac Electric Power Company, May 2002.

[Hayt 1989] W.H. Hayt Jr., *Engineering Electromagnetics*, McGraw Hill, 1989.

[Heitz 1999] C. Heitz, "A Generalized model for partial discharge processes based on a stochastic process approach", *Journal of Physics: Applied Physics*, vol. 32, 1999, pp. 1012-1023.

[Hotboll 1997] J.T. Hotboll, H. Edin, "PD Detection vs. Loss Measurements at High Voltages with Variable Frequencies", 10th Int. Symp. on HV Eng., Montreal, Canada, 1997.

[Hu 1998] M. Hu, X. Jiang, H. Xie, Z. Wang, "A New Technique for Extracting PD Signals in Online Monitoring with Wavelet Analysis", Proceedings of International Symposium on Electrical Insulating Materials, Toyohashi, Japan, Sept. 1998 pp 677-680.

[Hucker 1995] T. Hucker, H.G. Kranz, "Requirements of Automated PD Diagnosis Systems for Fault Identification in Noisy Conditions", *IEEE Trans. on Dielectrics and Elec. Ins.*, Vol. 3, No. 4, Aug 1995, pp. 544–555.

[Hudon 1995] C. Hudon, R. H. Rehder, "Recognition of Phase Resolved Partial Discharge Patterns for Internal Discharges and External Corona Activity", 5th International Conf. On Conduction and Breakdown in Solid Dielectrics, 1995, pp. 386-392.

[IEC 60270] International Electrotechnical Commission, "High-Voltage Test Techniques", 3rd Ed., 2000.

[Ifeachor 1999] E. C. Ifeachor, B. W. Jervis, "Digital Signal Processing: A Practical Approach", Addison Wesley, England, 1999

[Jansen 1997] M. Jansen, M. Malfait, A. Bultheel, "Generalised cross validation for wavelet thresholding", *Signal Processing*, 1997, Vol. 56, pp 33-44.

[Judd 1998] M. Judd, O. Farish, "A Pulsed GTEM System for UHF Sensor Calibration", IEEE Trans. On Instrumentation and Measurement, Vol. 47, No. 4, August 1998, pp 875-880.

[Kaneiwa 2000] H. Kaneiwa, Y. Suzuoki, T. Mizutani, "Partial discharge characteristics and tree inception in artificial simulated tree

channels", *IEEE Trans. on Dielectrics and Elec. Ins.*, Vol. 7, No. 6, December 2000, pp. 843–848

[KEMA 2004] Kema Webpage, www.kema.com/nl

[Kim 2004] C. S. Kim, T. Kondo, T. Mizutani, "Change in PD pattern with Aging", *IEEE Trans. Dielectrics and Electrical Insulation*, Vol. 11, No. 1, pp. 13-18, Feb 2004.

[Kopf 1995] U. Kopf and K. Feser, "Rejection of narrow-band noise and repetitive pulses in on-site PD measurements", *IEEE Trans. on Dielectrics and Electrical Insulation*, vol. 2, no. 6, Dec. 1995., pp. 1180-1191

[Kreuger 1989] F. H. Kreuger, " Partial Discharges Detection in High Voltage Equipment". Butterworth, 1989.

[Kreuger 1993] F. H. Kreuger, M. G. Wezelenburg, " Partial Discharge Part XVIII : Errors in the location of Partial Discharges in High Voltage Solid Dielectric Cables". IEEE Electrical Insulation Magazine, Vol. 9, No. 6, pg 15, Nov/Dec 1993.

[Kreuger 1995] F.H. Kreuger, *Industrial High DC Voltage*, Delft University Press, 1995.

[Krim 2000] H. Krim, I.C. Schick, "Minimax description length for signal denoising and optimised representation ",*IEEE Trans. Information Theory*, 1999, Vol. 45, No. 3, pp 898-908.

[Lai 1998] L.L. Lai, A.G. Sichanie, "Application of Discrete Wavelet Transform to High Impedance Fault Identification", International Conference on Energy Management and Power Delivery, Vol. 2, 1998, pp559-563.

[LDIC] LDS-6 product specification, LDIC. http://www.ldic.ch

[Lemke] Technology of High Voltage Testing and Measuring Techniques, Webpage, www.ldic.de/englisch/produkte/te/lds6/lds6.html

[Ma 2001] X. Ma, C. Zhou, I. J. Kemp, "Wavelets for the Analysis and Compression of Partial Discharge Data", Proceedings of 2001 Conference on Electrical Insulation & Dielectric Phenomena (CEIDP2001), Kitchener, Ontario, Canada, 14-17 October 2001.

[Ma 2002] X. Ma, C. Zhou, and I. J. Kemp, "Interpretation of Wavelet Analysis and Its Application in Partial Discharge Detection", *IEEE Trans. On Dielecric and Elec. Ins.*, 2002, Vol. 9, pp. 446-457.

[Mallat 1989] S. Mallat, "A Theory for Multiresolution signal decomposition: the wavelet representation", IEEE Trans. Pattern Recognition and Machine Intelligence, July 1989, Vol.11, pp674-693.

[Mallat 1989a] S. Mallat, *A Wavelet Tour of Signal Processing*, Academic Press, 1989.

[Mallat 1992] S. Mallat, S. Zhong, "Characterization of Signals from Multi-scale Edges", *IEEE Trans. on Pattern Analysis and Machine Intelligence*, 1992, Vol. 14, pp. 710-732.

[Mathworks 2000] Mathworks Power System Blockset, http://www.mathworks.com/access/helpdesk/help/toolbos/powersys/pisectionline.shtml

[Matthieu 2003] M. Matthieu, "Moving towards a complete Online Condition Monitoring Solution", Proc. of 17th Int. Conf. On Electricity Distribution, Barcelona, 12-15 May 2003.

[Mayoux 1995] C. Mayoux, C. Laurent, "Contribution of Partial Discharges to Electrical Breakdown of Solid Insulating Materials", *IEEE Trans. Dielectrics and Elec. Ins.*, Vol. 2, No. 4, Aug 1995, pp. 641- 655.

[McAllister 1997] I. W. McAllister, " Partial Discharges in Spherical Voids" , IEEE Transactions of Dielectrics and Electrical Insulation, Vol. 4, No. 4, Aug 1997.

[Meyer 1916] E.B. Meyer, *Underground Transmission and Distribution*, McGraw-Hill, New York, 1916.

[Misiti 1997] M. Misiti, Y. Misiti, G. Oppenheim, J. Poggi, *Wavelet Toolbox For Use with MATLAB,* The Math Works, Inc., 1997.

[Misiti 2000] M. Misiti, Y. Misiti, G. Openheim, J.M. Poggi, *Wavelet Toolbox User's Guide*, The Mathworks, Inc.,2000.

[Montanari 2000] G. C. Montanari, A. Contin, A. Cavallini, "Random sampling and data processing for PD-pulse height and shape analysis", IEEE Transactions on Dielectrics And Insulation 2000,Vol. 7, Iss 1,pp 30-37.

[Morshuis 1993] P.H.F. Morshuis, *Partial Discharge Mechanisms*, Delft University.

[Nagesh 1994] Nagesh , B. I. Gururaj, "Automatic detection and elimination of periodic pulse shaped interference in partial discharge measurements", IEE Proc. on Science, Measurement and Technology, vol. 141, no. 5, Sept. 1994, pp 335-342.

[Nason 1995] G. P. Nason, B. W. Silverman, "The Stationary Wavelet Transform and its Application", Tech. Rep. BS8 1Tw, University of Bristol, 1995.

[Navaneethan 2001] S. Navaneethan, J. Soraghan, W.H. Siew, F. McPherson, P.F. Gale, "Automatic Fault location for underground low voltage distribution networks", IEEE Trans. Power Delivery, Apr 2001, pp346-351.

[Nikias 1993] C. L. Nikias and A. P. Petropulu, "Higher-Order Spectra Analysis", *Prentice Hall,* 1993, pp.16.

[Okubo 2002] H. Okubo, N. Hayakawa, A. Matsushita, "The Relationship Between Partial Discharge Current Pulse Waveforms and Physical Mechanisms", IEEE Electrical Insulation Magazine, Vol. 18, No. 3, May/June 2002, pp39.

[Peschke 1999] E.F. Peschke, R. von Olshausen, "Cable Systems for High and Extra-High Voltage", MCD Verlag, Munich, 1999.

[Pesquet 1996] Pesquet, J.C.; H. Krim, H. Carfatan, "Time-invariant Orthonormal Wavelet Representations," *IEEE Trans. Sign. Proc.*, vol. 44, 8, 1996, pp. 1964-1970.

[Phung 1999] B.T.Phung, Z.Liu, T.R.Blackburn, R.E.James, "Wavelet Transform Analysis of Partial Discharge Signals", Proc. of Australasian Universities Power Engineering Conference 1999 (AUPEC'99), Darwin, Australia, 26-29 September 1999.

[Pillay 1996] P. Pillay, A. Bhattacharjee, "Application of Wavelets to Model Short-Term Power Systems Disturbances", IEEE Transactions on Power Systems,Vol. 11, No. 4, Nov 1996, pp2031-2037.

[Polikar 1998] R.Polikar, "The Wavelet Tutorial Parts I-IV", http://www.public.iastate.edu/~rpolikar/WAVELETS , 1998.

[Powers 1994] W.F. Powers, Jr., "The Basics of Power Cable", IEEE Transactions on Industry Applications, Vol. 30, No. 3, May/June 1994, pp506-509.

[Raja 2002] K. Raja, F. Devaux, S. Lelaidier, "Recognition of Discharge Sources Using UHF PD Signatures", IEEE Electrical Insulation Magazine, Vol. 18, No. 5, Sept/Oct 2002, pp 8

[Ramchandran 1996] K. Ramchandran, M. Vetterli, "Wavelets, Subband Coding, and the Best Bases", Proceedings of the IEEE, Vol. 84, No. 4, April 1996, pp541-560.

[Ravier 1998] P. Ravier and P. Amblard, "Combining an adapted wavelet analysis with fourth-order statistics for transient detection", *Signal Processing*, Issue 70, pp115-128, 1998.

[Robinson] Robinson Electronic Instruments, " E.R.A. Discharge Detector Model 3 System Manual", EIRE Electronics Limited.

[Russworm 2000] D. Russwurm, "On-Site Partial Discharge Monitoring using Differential Lemke Probe LDP-5 and its Accessories", HV Testing and Monitoring Workshop, Virginia, Sept. 2000. pg8.1-8.11.

[Salama 2000] M.M.A. Salama, R. Bartnikas, "Fuzzy logic applied to PD pattern classification", IEEE Transactions on Dielectrics And Insulation 2000,Vol. 7, Iss 1,pp 118-123.

[Santoso 1997] S. Santoso, E.J. Powers, W.M. Grady, "Power Quality Disturbance Data Compression using Wavelet Transform Methods", IEEE Transactions on Power Delivery, Vol. 12, No. 3, July 1997, pp1250-1257.

[Satish 2003] L. Satish, B. Nazreen, "Wavelet-Based De-noising for Partial Discharge Signals Buried in Excessive Noise and Interference", IEEE Transactions on Dielectrics And Insulation 2000,Vol. 10, Iss. 2, pp 354-367.

[Setaredhan 1998] S. K. Setadrehan, "Echocardiographical Cardiac Function Assessment and Wall Motion Visualisation Using Fuzzy Logic and The Wavelet Transform", Ph.D Thesis, University of Strathclyde, 1998.

[SheikhAkbari 2005] SheikhAkbari, "Fuzzy Multi-scale based Image and Video processing with applications", Ph.D Thesis, University of Strathclyde, 2005.

[Shim 1999] I. Shim, J.J. Soraghan, W.H. Siew, F. McPherson, K. Sludden, P.F. Gale, "Locating Partial Discharge in High Voltage Cable Networks", *1999 Annual Report Conference on Electrical Insulation and Dielectric Phenomena*, Vol. 1, pp210-213.

[Shim 2000a] I. Shim, J.J. Soraghan, W.H. Siew, 2000, "Digital Signal Processing Applied to the Detection of PD : An Overview", *IEEE EI- Mag., 2000,* vol.16(3), pp 6-12.

[Shim 2001] I. Shim, "Signal Processing Techniques for Partial Discharge Detection and Mapping in High Voltage Underground Cable Networks", Ph.D Thesis, University of Strathclyde, 2001.

[Shim 2001a] I. Shim, J.J. Soraghan, W.H. Siew, "Noise Reduction Technique for online PD detection and location in High Voltage (HV) Cable Networks" *Institute of Physics:*

Measurement Science & Technology, Vol. 11, No. 12, pp1708-1713.

[Shukla 2003] P. Shukla, "Complex Wavelet Transforms and Their Applications", MPhil. Thesis, University of Strathclyde, U.K., 2003.

[Smith 2002] K. N. Smith, R. A. Perez, "Locating Partial Discharge in a Power generating system using Neural Networks and Wavelets", Annual Report Conference on Electrical Ins. and Dielectric Phenomena, 2002. pp. 458-461.

[SP Dist 2003] Scottish Power Distribution Ltd., "Distribution Long Term Development Statement for SP Distribution Ltd.", Nov. 2003.

[Steennis 2001] E.F. Steennis, R. Ross, N. van Schaik, W. Boone, D.M. van Aartrijk, "PD Diagnostics of Long and Branched Medium Voltage cables", *Proc. Of The IEEE 7th Int. Conf. on Solid Dielectrics*, pp. 27-30, 2001.

[Steiner 1992] J. P. Steiner, P. H. Reynolds, W. L. Weeks, "Estimating the Location of Partial Discharges in Cables", IEEE Transactions on Electrical Insulation, Vol. 27, No.1, Feb 1992, pp 44.

[Strang 1996] G. Strang, T. Nguyen, *Wavelets and Filter Banks*, Wellesley-Cambridge Press, 1996.

[Swaffield 2004] D. J. Swaffield, P. L. Lewin, Y. Tian, G. Swen, S. G. Swingler, "Characterisation of Partial Discharge Behaviour in Liquid Nitrogen", Conference Record of the 2004 IEEE International Symposium on Electrical Insulation, Indianapolis, IN USA, 19-22 September 2004, pp. 135-138.

[TF21.05 2002] Task Force 21.05, "Experiences with AC Tests", Electra, No. 205, Dec. 2002, pp. 2-12.

[Tian 2003] Y.Tian, P.L. Lewin, A.E. Davies, S.J. Sutton, S.G. Swingler, "Partial Discharge Detection in Cables Using VHF Couplers", IEEE Trans. Dielectrics and Elec. Ins., Vol. 10, No. 2, April. 2003.

[Trinh 1995] N. Giao Trinh, "Partial Discharge XIX : Discharge in Air, Part 1: Physical Mechanisms", IEEE Electrical Insulation Magazine, Vol. 11, No.2, March/April 1995, pp23-29.

[Tu 2002] Y. Tu, Z. D. Wang, P. A. Crossley, "Partial Discharge Pattern Recognition based on 2-D Wavelet Transform and Neural Network Techniques", *IEEE Power Engineering Society Summer Meeting*, Chicago, USA, July 2002.

[Turner] M. Turner, "OWTS® - a New Method for Diagnosis of Installed Medium Voltage Power Cables",

[Veen 2003] J. Veen, P.C.J.M van der Wielen, "The application of match-filtering to PD detection and localisation", *IEEE Electrical Insulation Magazine,* vol. 19, No. 5: Sept –Oct 2003, pp. 20-26.

[Vetterli 1995] M. Vetterli, J. Kovaevid, "Wavelets and Subband Coding", Englewood Cliffs, NJ, Prentice Hall, 1995.

[Vonglahn 1995] P. Vonglahn, R.J. Vanbrunt, "Continuous Recording and Stochastic Analysis of PD", *IEEE Transactions on Dielectrics and Electrical Insulation*, Vol. 2, Iss. 2, 1995, pp590-601.

[Walton 2003] C. Walton, "PD Monitoring – A Critical Tool for Condition-Based Assessment", Transmission & Distribution World, Dec 2003, pg 38-46.

[Webb 2002] M. Webb, M. Lomax, "Experiences with continuous partial discharge monitoring", *3rd AVO New Zealand International Technical Conference*, Methven, New Zealand, 15-17 October 2002

[Webber 1986] H. J. Weber, " Partial Discharge Measuring Techniques, Tettex Instruments.

[Werle 2002] P. Werle, A. Akbari, H. Borsi, E. Gockenbach, "Enhanced Online PD Evaluation on Power Transformers using Wavelet Techniques and Frequency Rejection Filter for Noise

Suppression", IEEE Internation Symposium on Electrical Insulation, Boston, MA U.S.A., April 2002, pp. 195-198.

[Wester 2003] F. Wester, E. Gulski, J. Smit, E. Groot, M. Van Vliet."Sensitivity aspects of online PD Diagnosis of MV Power Cables", Proc. of 17th Int. Conf. On Electricity Distribution, Barcelona, 12-15 May 2003.

[Whalen 1971] A.D.Whalen, "Detection of signals in noise", Academic Press, New York, 1971.

[Wielen 2003] P.C.J.M van der Wielen, E. F. Steenis, P.A.A.F. Wouters, "Fundamental Aspects of Excitation and Propagation of Online Partial Discharge Signals in Three-phase MV Cable Systems", *IEEE Transactions in Dielectrics & Electrical Insulations*, Vol 10, No. 4, August 2003, pg 678-688.

[Wielen 2003a] P.C.J.M van der Wielen, J. Veen, P.A.A.F. Wouters, "Evaluation of Different Types of Sensors and Their Positioning for Online PD Detection and Localisation in Distribution Cables", Nordic Insulation Symposium, June 11-13, 2003.

[Wielen 2004] P.C.J.M. van Der Wielen, J. Veen, P.A.A.F Wouters, E.F. Steenis, "Time Based Alignement of PD Signals Measured at Multiple Cable Ends", *Proc. of IEEE Int. Conf. on Solid Dielectrics*, 2004.

[Wilkinson 1996] W.A. Wilkinson, M.D. Cox, "Discrete Wavelet Analysis of Power System Transients", *IEEE Transactions on Power Systems*, Vol. 11, No. 4, November 1996, pp2038-2044.

[Yang 2003] L. Yang, M. D. Judd, "Recognising Multiple Partial Discharge Sources in Power Transformers Using Wavelet Transforms", IEE Proceedings of Science Measurement and Technology, vol. 150, iss. 3, May 2003, pp. 119-127.

[Zaengl 2003] S. Zaengl, "Applications of Dielectric Spectroscopy in Time and Frequency Domain for HV Power Equipment", IEEE

Electrical Insulation Magazine, Vol. 19, No. 6, Sept/Oct 2003, pp 9.

[Zu 1997] Z. Zu, P. K. Willett, M. S. Mashikian, "Performance Limits of PD Location Based on Time-domain Reflectometry", *IEEE Trans. on Dielectrics and Electrical Insulation*, vol. 4, no. 2, April 1997, pp. 182-188.